ISSN 1831-9424

European Commission

JRC CONFERENCE AND WORKSHOP REPORT

ESReDA | European Safety, Reliability & Data Association

# Advances in Modelling to Improve Network Resilience: Proceedings of the 60th ESReDA Seminar

*Hosted by the University Grenoble Alpes, Grenoble, France, 4-5 May 2022.*

Remenytė-Prescott, R., Sanderson, K., Kopustinskas, V., Simola, K.

2022

Joint Research Centre

EUR 31164 EN

**EU Science Hub**
https://joint-research-centre.ec.europa.eu

JRC130275

EUR 31164 EN

PDF ISBN 978-92-76-55142-3 ISSN 1831-9424 doi:10.2760/503700 KJ-NA-31-164-EN-N

Luxembourg: Publications Office of the European Union, 2022



How to cite this report: Remenytė-Prescott, R., Sanderson, K., Kopustinskas, V., Simola, K., *Advances in Modelling to Improve Network Resilience: Proceedings of the 60th ESReDA Seminar*, Publications Office of the European Union, Luxembourg, 2022, doi:10.2760/503700, JRC130275.

# Contents

## Abstract

These proceedings are the outcome of the 60th ESReDA seminar “Advances in Modelling to Improve Network Resilience” that took place at the Université Grenoble Alpes in France, on 4-5 May in 2022. A broad spectrum of resilience topics were covered, with sessions addressing Resilience Evaluation, Infrastructure Resilience to Natural Hazards, Resilience of Infrastructure Networks, Resilience of Utility Networks and Resilience of Transport Networks and Smart Cities. The seminar attracted a good mix of academic and industrial participants from many European and overseas countries, and provided a platform for stimulating discussion and debate on resilience techniques and their applications in practice.

The editorial work for this volume was supported by the Joint Research Centre of the European Commission in the frame of JRC support to ESReDA activities.

# Foreword

**European Safety, Reliability & Data Association**

**(ESReDA)**

European Safety, Reliability & Data Association (ESReDA) is a European Association established in 1992 to promote research, application and training in Reliability, Availability, Maintainability and Safety (RAMS). The Association provides a forum for the exchange of information, data and current research in Safety and Reliability.

The contents of ESReDA seminar proceedings do not necessarily reflect the position of ESReDA. They are the sole responsibility of the authors concerned. ESReDA seminar's proceedings are designed for free public distribution. Reproduction is authorized provided the source is acknowledged.

ESReDA membership is open to organisations, privates or governmental institutes, industry researchers and consultants, who are active in the field of Safety and Reliability. Membership fees are currently 1000 EURO for organisations and 500 EURO for universities and individual members. Special sponsoring or associate membership is also available.

For more information and available ESReDA proceedings please consult:

http://www.esreda.org/

# 1 Introduction

We would like to thank everyone for attending and contributing to the 60th ESReDA seminar, "Advances in Modelling to Improve Network Resilience", held at the Université Grenoble Alpes in France, on 4-5 May in 2022. We hope that the seminar provided a platform for stimulating discussion and debate and that participants were able to take the opportunity to form new, collaborative links and share their knowledge of resilience techniques and their applications in practice, with like-minded engineers and scientists.

We would also like to thank the local organising committee in Grenoble, chaired by Julien Baroth, Christophe Berenguer, Nour Chahrour, Jean-Marc Tacnet and Sylvie Perrier, for making this in-person seminar a very enjoyable and memorable experience in the calendar of events, supported by ESReDA.

The seminar's proceedings contain 20 papers (17 full papers and 3 extended abstracts), with authors spread across academia and industry. A broad spectrum of resilience topics is covered, with sessions addressing Resilience Evaluation, Infrastructure Resilience to Natural Hazards, Resilience of Infrastructure Networks, Resilience of Utility Networks and Resilience of Transport Networks and Smart Cities.

The seminar has attracted a good mix of academic and industrial participants from many European and overseas countries. There were authors from universities in France, UK, Spain, Switzerland, Netherlands, Belgium, Sweden, Norway, Latvia, China, Malaysia and USA. Industrial contributors to research work for companies included MAD-Environnment, Consultant RiskLyse, Compagnie National du Rhône, IMdR, Resallience by Sixense and Orange in France; European Commission Joint Research Centre (JRC) and ISPRA (Istituto Superiore per la Protezione e la Ricerca Ambientale) in Italy; Ingeman in Spain, the Austrian Institute of Technology, and Agifer in Romania.

We wish to thank the Technical Programme Committee for their efforts during the review process of the contributions, and all the authors during the presentations and the final stages of paper preparation. We look forward to future opportunities for collaboration and hope to see you at future events.

The editorial work for this report was supported by the Joint Research Centre of the European Commission in the frame of JRC support to ESReDA activities. A special thanks is due to A. Liessens (JRC) for the editorial work.

Dr Rasa Remenytė-Prescott

Kate Sanderson

University of Nottingham

Dr. Vytis Kopustinskas

Dr. Kaisa Simola

European Commission, Joint Research Centre (JRC)

# 2 Conference papers

## Keynote Lecture by Anne Barros:

## Modelling to Improve Resilience Networks: What about interdependent critical?

Anne Barros, Ecole CentraleSupélec, University of Paris-Saclay, France,

anne.barros@centralesupelec.fr

**Abstract:**

In 2020 the chair in Risk and Resilience of Complex Systems at CentraleSupélec (Paris), began a research project activity dedicated to the modelling and the resilience analysis of interdependent infrastructures. The partners involved in the project are EDF (French national power supplier), Orange (French Telecom operator), SNCF (French national railways operator). The objective is to define use cases encompassing at least two networks, one for the physical transportation system, one for its power supplier and one for the telecom services and to address the following research questions: which kind of decisions can be optimized in relation with safety and business continuity, what are the relevant performance indicators for such decisions and what are the suitable modelling techniques?

First, and as an introduction to the ESReDA seminar, a taxonomy of resilience analysis will be presented. Then a review of recent advances in modelling for interdependent infrastructures will be presented with a special focus on interdependent electrical and telecom networks. Lastly, the need for developing optimization techniques to design the optimal coupling of interdependent infrastructures will be illustrated and discussed, with a special focus on interdependent electrical and railway networks.

**Biography:**

Anne Barros, PHD, is professor in reliability and maintenance modelling at Ecole CentraleSupélec, University of Paris-Saclay, France. Her research focus is on degradation modelling, prognostics, condition based and predictive maintenance. She got a PHD then a professorship position at University of Technology of Troyes, France (2003-2014) and spent five years as a full-time professor at NTNU, Norway

(2014-2019). She is currently heading a research group and holding an industrial Chair at CentraleSupélec with the ambition to improve reliability assessment and maintenance modelling methods for complex systems.

## Keynote lecture by Philippe Sohouenou:

# Resilience Performance Assessment (RPA): A framework and decision-making tool to evaluate and follow the resilience of infrastructures and territories

Philippe Sohouenou, RESAILLIENCE, Philippe.sohouenou@resallience.com

**Abstract:**

With climate change, the impacts of natural hazards (such as floods, snow events and landslides) on infrastructures and territories could worsen. Hence, strengthening the resilience of infrastructures and territories to natural hazards is more critical than ever before. To reach this objective, decision-makers need operational tools to evaluate and follow the resilience of infrastructures and territories. The Resilience Performance Assessment (RPA) is an innovative solution that provides a holistic approach combining visualization of both current and future climate change impacts. The RPA also allows the formulation of detailed recommendations and a costs-benefits assessment to estimate the resilience performance of projects and policies aiming at improving resilience and avoiding GHG emissions.

**Biography:**

Dr Philippe SOHOUENOU is Project manager and Transport resilience lead at RESALLIENCE, an international consultancy dedicated to the adaptation of cities, territories and infrastructures to climate change. He has over five years of experience developing modelling techniques to help transport operators and public authorities predict and optimise the design, maintenance and operation of their infrastructures.

Philippe graduated with a master's degrees in Civil Engineering from ESTP Paris (France) and the University of Nottingham (UK) in 2016. He pursued his PhD at the University of Nottingham (2017-2021), where he focused on road network resilience modelling. His PhD was funded by the EU as part of a Marie Skłodowska-Curie Training Network called SMARTI (Sustainable Multi-functional Automated Resilient Transport Infrastructures).

Philippe contributed to the Project Group on Resilience Engineering & Modelling of Networked Infrastructure of ESReDA (European Safety, Reliability & Data Association)(2018-2021). He notably interned at VINCI as an assistant project engineer (2015) on tram construction projects and worked on asset management projects for SNCF (the owner and manager of the rail infrastructure in France) as a civil engineer (2017.

# A Simulation Approach for Evaluating Interventions to Improve the Resilience of Transport Networks Against Climate-Induced Hazards

Hossein Nasrazadani, Bryan Adey and Saviz Moghtadernejad, ETH Zurich, nasrazadani@ibi.baug.ethz.ch, adey@ibi.baug.ethz.ch, moghtadernejad@ibi.baug.ethz.ch

Alice Alipour, Iowa State University, alipour@iastate.edu

## Extended Abstract

Transport networks in some areas are subject to climatic hazard events that heavily disrupt their functionality, which neccisitates transport infrastructure mangers to constantly make decision on executing interventions to improve the resilience of their network against disruptive events. In order to make fully risk-informed decisions on selecting the best candidate intervention, have a quantitative evaluation of both their direct and indirect benefits is crucial. In this evaluation, or in a broader sense, planning resilience enhancing interventions, three factors, among others, are significantly important: 1) the complex spatiotemporal nature of climatic hazards, 2) the complext spatiotemporal behavior of transport networks, and 3) the uncertainties that exist in various aspects of resilience, from hazards to impact and recovery. This study proposes a simulation approach to quantitatively assess the effect of interventions in improving the resilience of transport networks subject to climatic hazards, including heavy rainfall, flooding and landslides, taking into account these three factors. The proposed simulation approach serves as a decision support tool to assist transport infrastructure managers to assess the resilience of their network under multiple scenarios of hazard events, and investigate the effect of various interventions to improve the resilience.

The proposed simulation approach is based on a unifying modeling framework that is composed of a set of interacting probabilistic models, each representing part(s) of the system, i.e., hazards, physical and functional performance of transport networks, and direct and indirect consequences. Additionally, the proposed approach features models that capture the effect of interventions on each of the models in the underlying modeling framework. Next, through the generation of a host of random scenarios in a Monte-Carlo simulation scheme, interventions are evaluated based on their contribution to reducing direct and indirect consequences with respect to the baseline condition, i.e., the one with no intervention. Each scenario represents a random realization of the spatiotemporal evolution of the hazards and transport networks, during the hazard period, and throughout the post-hazard restoration period. The advancement of the proposed simulation approach over previous studies in modeling and evaluating resilience enhancing interventions is threefold: capturing the effect of uncertainties in hazard events on the effectiveness of interventions with the aid of stochastic scenario development, modeling the spatiotemporal evolution of hazards and transport networks, and quantifying the effect of interventions on both direct and indirect consequences during hazard period and restoration phase.

The proposed simulation approach is based on the risk assessment methodology developed by Hackl et al. (1) and Heitzler et al (2), yet improves upon that by incorporating the effect of interventions on enhancing resilience. Simulation has been also previously used by other studies to model complex infrastructure systems, which showed promising benefits (3,4). The proposed simulation approach in this study, including its underlying modeling framework, is schematically depicted in Figure 1. It is composed of five categories of events, including a set of communicating models represented by rectangular boxes that are color-coded with respect to their related events. These events are generically titled as source, hazard, object, network, and societal. Source events include two models: rainfall, which produces spatiotemporal patterns of precipitation, followed by runoff, which produces discharge values of water inflow to the river. Hazard events include the flood model, which produces time series of inundation maps, and the landslides model, which

produces the amount of mudflow for triggered landslides. Object events are those that model the impact of hazard events on the physical and functional performance of roads and bridges, and estimate the restoration needs to recover from those impacts. This includes those that model the physical damage to roads due to inundation and mudflow blocking, and bridges due to scouring, followed by their consequent effect on speed limit and capacity of individual roads and bridges. The collective performance of roads and bridges as the transport network is then captured through the network model. Societal events capture the impacts of the hazard events on the society using two models: restoration, which models the execution of post-hazard restoration interventions, and traffic, which models the spatiotemporal flow of passengers within the transport network. Lastly, the direct and indirect costs of societal events are compiled in their respective category, based on which the resilience of the network is evaluated, denoted by $\mathcal{R}$. For a more detailed overview of the introduced models, please refer to Hackl et al. (5).

**Figure 1.** Schematic overview of considered events and models in the proposed simulation approach

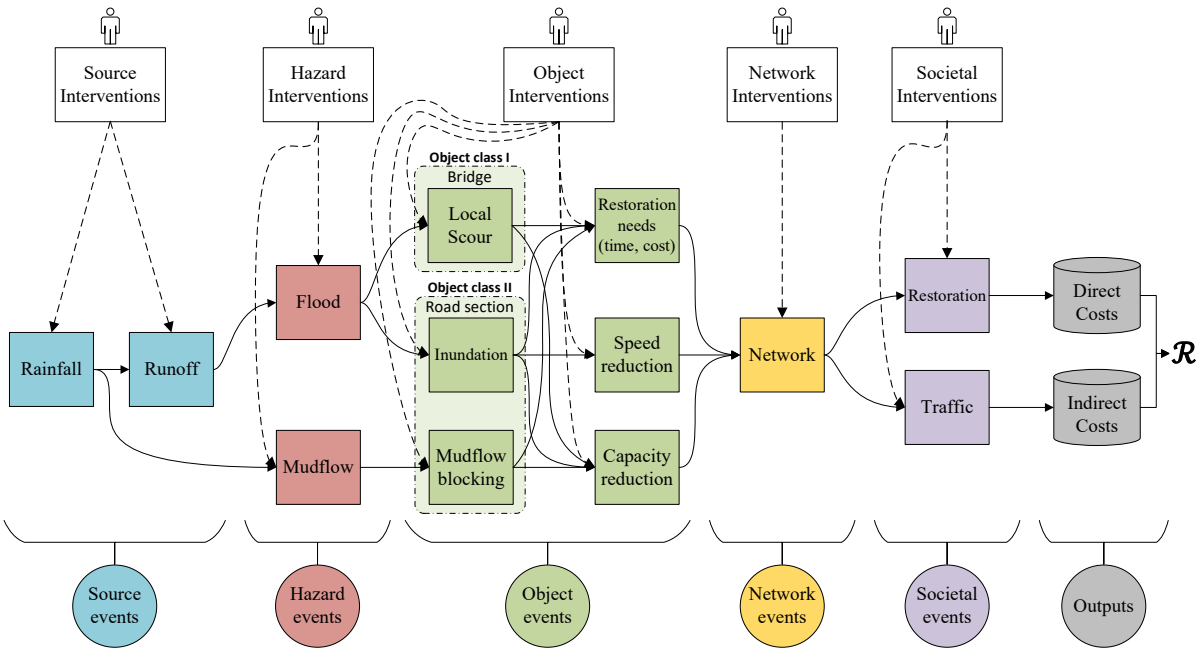


Additionally, the proposed methodology features intervention models, represented by actor boxes in Figure 1, which capture the effect of interventions on the considered events. Therefore, there are accordingly five categories of interventions: source interventions, e.g., changing land use to reduce surface runoff; hazard interventions, e.g., flood protection walls or stormwater retention basins; object interventions, e.g., stabilizing road pavements; network interventions, e.g., closing roads in the floodplain; and societal interventions, e.g., diverting traffic flow to the outside of the floodplain. Once all models are in place, through the generation of numerous scenarios, under baseline condition as well as all candidate interventions, the resilience of the network is assessed using the sum of direct and indirect costs. In this study, direct costs include the costs of executing post-hazard restoration interventions, and indirect costs, include the monetized losses due to additional travel time and loss of connectivity.

The proposed methodology was applied to a transport network, including roads and bridges, located in the region of Chur in the south-eastern part of Switzerland. The region has been historically suffering from flooding in the Rhine River, as well as landslides (6). The Rhine River flows into the region from the southwest part and exists from the northeast. Under scenarios of heavy rainfall, it is expected that the river discharge increases as it flows more toward the downstream due to excessive runoff. For a more detailed description of the case study, please refer to Hackl et al. (1). In this study, the resilience of the considered transport network is intended to be evaluated, and then

improved under flood scenarios with return periods of 50, 100, 250, 500, and 1000 years. For each flood intensity, 100 scenarios were generated, which due to the uncertainty in their source events, lead to a significant variability in the impact they have on the transport network.

Six candidate interventions, including three flood protection walls and three stormwater retention basins, have been considered and their effects on reducing the direct and indirect costs have been evaluated. Figure 2 shows the geographic overview of the area of study, the investigated transport network, and the candidate interventions. Other parameters describing the candidate interventions, including the length and height of flood protection walls, and the volume and average depth of stormwater retention basins are provided in Table 1. For a more detailed description of the flood protection wall model and stormwater retention basin model, please refer to (7,8).

**Figure 2.** Geographic overview of the area of study vs. candidate flood protection walls and stormwater retention basins

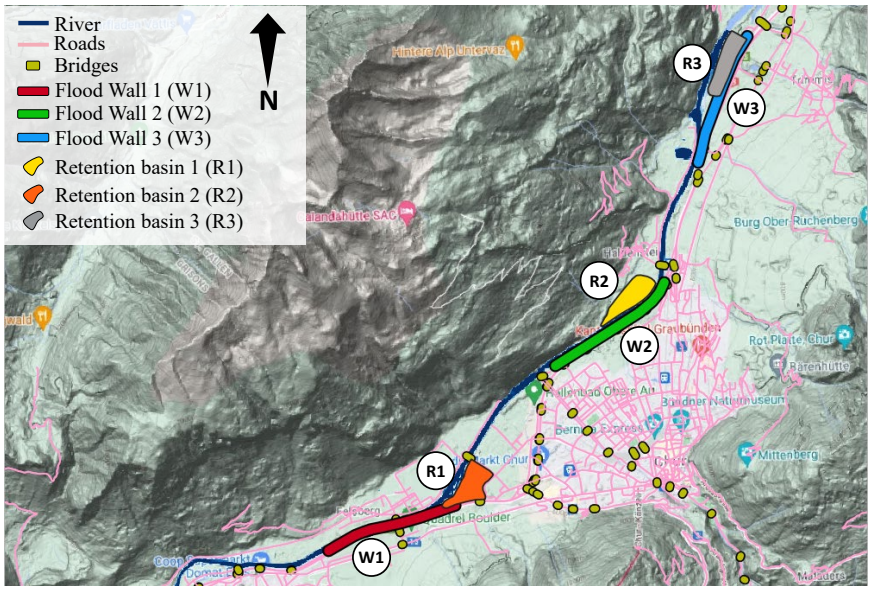


**Table 1.** Overview of the parameters describing the candidate interventions

| | Length (m) | Height (m) | Volume ($10^3$ $m^3$) | Average depth (m) |
|---|---|---|---|---|
| Flood Wall 1 | 2007 | 2.0 | – | – |
| Flood Wall 2 | 2062 | 2.0 | – | – |
| Flood Wall 3 | 2014 | 2.0 | – | – |
| Retention Basin 1 | – | – | 984.4 | 4.15 |
| Retention Basin 2 | – | – | 990.3 | 4.34 |
| Retention Basin 3 | – | – | 977.3 | 4.28 |

Figure 3 shows the output of the proposed simulation approach for a randomly generated scenario in the application of this study at two time steps, which represents how the system evolves over time and space. Each time step of a scenario starts with a spatially distributed precipitation field, producing a map of flood inundation, as well as mudflow blocking. It is then followed by assessing the damages to the roads and bridges, and evaluating their capacity to maintain traffic. Lastly, traffic is redistributed through the network based on its performance. Each scenario ends with an estimation of the incurred direct and indirect consequences.

**Figure 3.** Sample output of the implemented simulation approach for the application of this study

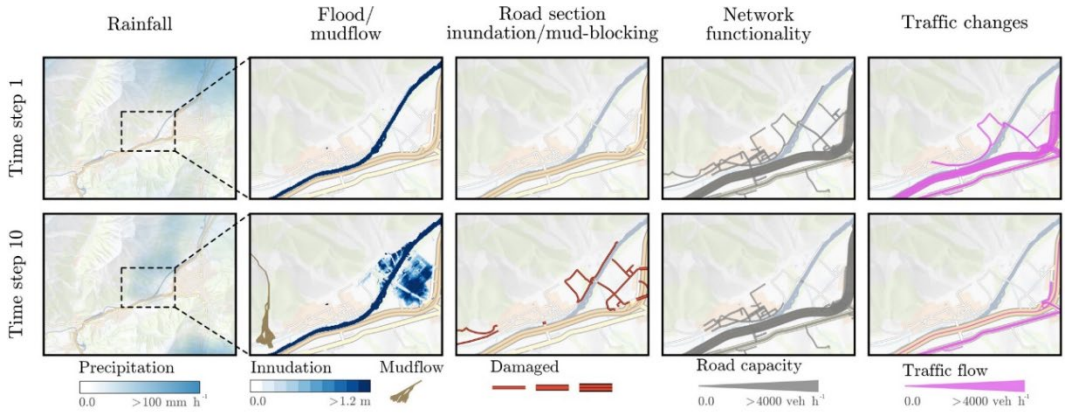


*Source*: Hackl et al. (1)

Figure 4a shows the mean total costs, i.e., the sum of direct and indirect costs, for all candidate interventions with respect to the baseline condition. It is noted that each point in this graph is the average of 100 randomly generated scenarios. This figure suggests an expected increasing trend in total costs, yet more interestingly, shows a gradual decline in the rate of increasing total costs. Figure 4b shows the mean total cost reduction under the implementation of each candidate intervention over different return periods. It is observed that Flood Wall 3 and Retention Basin 3 are the most effective interventions in improving the resilience of the transport network of interest. The main explanation for this observation is the location of these two candidate interventions, which are more towards the downstream, where flooding is more likely and severe, as opposed to Flood Wall 1 and Retention Basin 1, which were shown to be the least effective. Another reason is that Flood Wall 3 and Retention Basin 3 protect a highway in that area which plays a key role in maintaining the connectivity within the network. The results of this analysis assist infrastructure managers to make resilience-informed decisions to improve the infrastructure networks.

**Figure 4**. (a) mean total costs, and (b) mean total cost reduction for each candidate intervention, with respect to the baseline condition

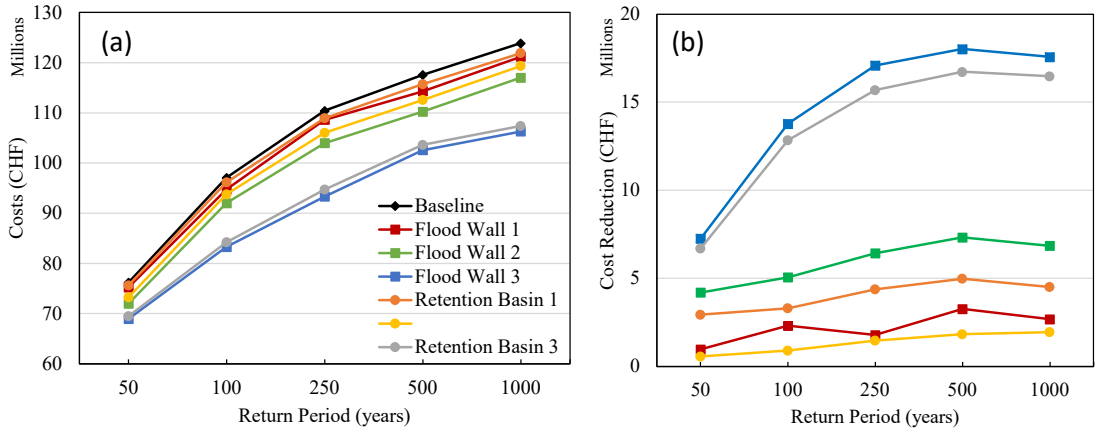

## References


1. Hackl J, Lam JC, Heitzler M, Adey BT, Hurni L. Estimating network related risks : A methodology and an application in the transport sector. Nat Hazards Earth Syst Sci. 2018;18:2273–93.
2. Heitzler M, Lam JC, Hackl J, Adey BT, Hurni L. A simulation and visualization environment for spatiotemporal disaster risk assessments of network infrastructures. Int J Geogr Inf Geovisualization. 2017;52(4):349–63.
3. Nasrazadani H, Mahsuli M. Probabilistic Framework for Evaluating Community Resilience: Integration of Risk Models and Agent-Based Simulation. J Struct Eng. 2020;146(11):04020250.
4. Zhang N, Alipour A. Two-Stage Model for Optimized Mitigation and Recovery of Bridge Network with Final Goal of Resilience. Transp Res Rec. 2020;2674(10):114–23.
5. Hackl J, Heitzler M, Lam JC, Adey BT, Hurni L. Novel indicators for identifying critical INFRAstructure at RISK from Natural Hazards, Deliverable D4.2, Final Model, Methodology and Information Exchange. Zurich, Switzerland: ETH, Zurich, Switzerland; 2016.
6. Fuchs S, Bründl M. Damage Potential and Losses Resulting from Snow Avalanches in Settlements of the Canton of Grisons, Switzerland. Nat Hazards. 2005;34:53–69.
7. Nasrazadani H, Adey BT, Heitzler M, Moghtadernejad S, Alipour A. Evaluating resilience enhancing interventions for transport networks subjected to floods using simulations: example of flood protection wall. In: 3rd International Conference on Natural Hazards & Infrastructure. Athens, Greece; 2022.
8. Nasrazadani H, Adey BT, Moghtadernejad S, Alipour A. A simulation-based methodology to assess resilience enhancing interventions for transport systems: A retention basin example. In: 32nd European Safety and Reliability Conference (ESREL). Dublin, Ireland; 2022.

# Improving power system frequency response with a novel load shedding method

Antans Sauhats, RTU, sauhatas@eef.rtu.lv, Andrejs Utans, RTU, utan@eef.rtu.lv, Dmitrijs Guzs, RTU, mailto:dgpostbox@gmail.com, Laila Zemite, RTU, Laila.Zemite@rtu.lv

## Abstract

*The life of the modern society relies completely on electricity supply and that is why electrical grid have always been considered a life-critical infrastructure. The likelihood of various extreme events, classical, weather-related and modern, man-made threats, has been increased dramatically in recent decades. Along with that, power systems are undergoing radical, renewable energy source (RES)-related transformations which affects both, the structure of the generation sources and the dynamical behaviour of the system after it was exposed by a disaster event. System dynamic behaviour during transients is under control of various automated systems intended to preserve/restore major system parameters (frequency and voltage) at acceptable level. Adequate response on a dynamical processes happening during system transition from a steady-state to a degraded, but stable one, is vitally important because it directly affect the remaining operational capacity of the system and its' ability to recover faster.*

*This paper addresses the problem of preventing significant decline of the system frequency provoked by a large imbalance of power. Novel rapid Load Shedding (LS) Method based on monitoring of synchronous condensers' power injection will be presented. Unlike traditional, frequency-measuring-based Under Frequency LS (UFLS), new method is based on synchronous condensers power injection measuring immediately after contingency. The load will be shed without waiting for triggering of the operation of traditional UFLS. Rapid LS approach allows to achieve much better frequency profile for the same power imbalance/load shed. The method is the most efficient for networks with high penetration of non-inertial RES and with synchronous condensers providing significant part of the system inertia.*

## 1 Introduction

The topic of climate change and the ongoing efforts to combat it and to reduce anthropogenic greenhouse gas emissions have resulted in several high-level policies aimed at reducing the usage of fossil fuels with a massive roll-out of renewable energy generation capacities. A massive replacement of traditional generation sources in favour of non-synchronous RES is expected to bring a number of challenges which, if not taken into account, may adversely affect the resilience of power system. Even grids, which were considered reliable and resilient for many decades, may lose this property as a result of RES penetration-related structural changes. One of the most important problem is maintaining power system stability after it was exposed by an extreme event. Frequency stability of AC power systems is a corner-stone of secure and reliable operation of any modern power system. Maintaining generation/demand balance, especially when power system has been exposed by a major disturbance, is a prerequisite for providing system survivability. From the resilience view point, system ability to avoid complete collapse is crucial, because, to a large extent, it defines how much efforts will it take to recover and how quickly this could be done [1].

In this article we would like to draw attention to frequency stability-related issues. Historically, power system operation principles were based on an assumption that power generation facilities do not experience the shortage of the primary fuels. Electrical power is produced by means of rotating synchronous machines which are fully controllable. Traditional synchronous generators store a large amount of kinetic energy in their rotating masses and therefore, have significant mechanical inertia. When the power balance is suddenly disturbed, the synchronous machines, due to their electro-mechanical coupling

with a grid, provide the grid with stored kinetic energy and thus, resisting to abrupt change of the grid frequency. Generator's rotational inertia slows down the frequency variations, decrease the rate of change of frequency (ROCOF), thus limiting the frequency drop and giving a time to respond for a primary frequency regulation. A comprehensive overview of the frequency instability phenomenon and frequency instability-related problems can be found in [2].

Modern wind turbines and photovoltaic-based electricity generation systems are non-synchronous and have no direct coupling with grid and thus, do not provide the inertial response similar to traditional generators. These peculiarities are expected to bring a number of challenges as reduction of total system inertia, increasing rate of change of frequency, decreasing number of generation units providing primary and secondary frequency regulation resulting in reduced frequency stability margin [3,4]. Therefore, we have to revise several, system resilience-related aspects, under the scope of existing and future planned transformations.

The remaining part is organized as follow: first theory, method and the principles of the proposed approach are described, then the case studies are portrayed, finally the conclusions are made.

# 2 Frequency stability

The importance of the frequency stability cannot be overestimated due to system frequency being a paramount parameter for any alternating current (AC) power system. Frequency deviation from its nominal value directly reflects a presence of imbalance between generated and consumed power. The most unfavourable and even dangerous scenario is a sudden loss of a large power generating plant or tripping of high voltage interconnector importing significant amount of power. System ability to cope with immediate imbalance and prevent frequency decline to unacceptable level will depend upon two main factors, namely, available system inertia and system capability quickly regain the power balance. Equation (1) which is a form of swing equation [5] clearly shows that the change in system frequency $d\omega/dt$ is inverse proportional to the total system inertia $H_{tot}$ in MWs, so that decreasing inertia level will lead to a faster fall in frequency for the same power imbalance $\Delta P$:

$$\frac{d\omega}{dt} = \Delta \mathrm{P} \frac{\omega_{syn}}{2H_{tot}} \tag{1}$$

In attempt to improve $d\omega/dt$ one can either increase the available system inertia $H_{tot}$— by adding more synchronous machines (as for example synchronous condensers), by imitating inertial response (synthetic inertia for inverter-based RES) or reducing the imbalance $\Delta P$ as quickly as possible. Power balance cannot be regained instantly due to generator governor response time delay (1-3 s) and therefore, immediately after event, frequency decline will be limited solely by inertial response of the synchronous machines. After all the kinetic energy stored in rotational mass have been released, frequency fall could be stopped only by decreasing power imbalance, progressively reducing it to zero. Power imbalance can be diminished either, by increasing generated power or decreasing load. In case the primary frequency regulation does not respond quickly enough or in the absence of power reserve, a certain amount of load need to be shed in attempt to avoid complete frequency collapse.

# 3 Classic/Static UFLS and Its Challenges

Under-frequency load shedding (UFLS) is a classic and commonly accepted measure used to counteract a potential frequency collapse following a serious loss-of-generation incident. The UFLS is typically triggered when the activation of available frequency reserves does not provide sufficient frequency stabilization. UFLS is usually defined by a list of loads with matching frequency thresholds which are disconnected from the grid by frequency relays when the grid frequency reaches any of the predetermined thresholds in the list. The main

disadvantage of such "static" UFLS schemes is their inability to adapt fixed thresholds and the amount of load to be shed by each step to continuously varying load/generation profiles and to severity of power imbalance.

Traditional UFLS schemes can be enhanced by more sophisticated UFLS schemes and concepts proposed and described in the literature [6–10]. A semi-adaptive UFLS scheme can use a triggering method utilizing static frequency and ROCOF thresholds instead of a frequency-only approach. An adaptive UFLS scheme can adopt triggering methods employing a dynamic combination of frequency and ROCOF. Another type of dynamic UFLS schemes use algorithms including calculating the system inertia values or the total power imbalance of the system and use these for load shedding triggering together with frequency and ROCOF threshold values [8, 9].

Despite the advantages of the adaptive approaches over the classic one, the disadvantages of the adaptive UFLS schemes are well known and described [11]. A still ongoing search for new methods or concepts for UFLS is explained by the complexity of using Equation (1) in adaptive approaches due to the complexity of a real power system with many generators, each with own moment of inertia. The frequency in a multi-machine power system becomes a local parameter during the transient power imbalance oscillations and the Equation (1) is then describing the behaviour of each generator separately. Generators might oscillate at different rates and, therefore, frequency gradient is not homogeneous at different nodes of the system. As a result, to estimate the disturbance $\Delta P$, knowledge of the frequencies and inertia of many generators in the power system is required. A comprehensive overview of the ROCOF-based power imbalance estimation-related problems and frequency gradient measurement-related issues is given in [12, 13].

A search for improved UFLS approach for low-inertia power systems is the main motivation for authors of this paper and therefore a novel method, intended to improve the system frequency response will be presented here. This article is a continuation of the authors' work that was presented in [14].

# 4 Rapid LS principle

An unexpected disconnection of a large generator in the power system causes a deceleration of all synchronously rotating machines, namely, synchronous generators, synchronous condensers and motors. In the process of decelerating of rotating masses of the elements of the power system, the kinetic energy accumulated in them is transformed into electric energy and injected into the electrical network. As result of this injection (inertial response) the balance of generated and consumed electrical energy is maintained immediately after the transient. Within a few seconds delay after disturbance, generator's governors start to react on the frequency decline trying to restore the frequency rated value (primary frequency control). Additionally, diminishing of the frequency causes a decrease in the power consumption of the frequency dependent load. However, the initial period of the considered transient process is mainly determined by the imbalance of active power $\Delta P$ at the beginning of the process and the inertia of the system. Consequently, we can assert that the volume of the disconnected power $\Delta P$ at the very beginning of the process prior to primary frequency control is compensated by the injection of the active power by each element of the power system possessing inertia [14]:

$$\Delta \mathrm{P} = \sum_{a=1}^{S} \Delta P_{SC\_a} + \sum_{b=1}^{G} \Delta P_{G\_b} + \sum_{c=1}^{L} \Delta P_{L\_c} \qquad (2)$$

where $\Delta P_{SC\_a}$, $\Delta P_{G\_b}$ and $\Delta P_{L\_c}$ are active power injections of every synchronous condenser (SC), synchronous generator and frequency dependent load (for example electric motors) present in the power grid; where $S, G, L$ are the total numbers of synchronous condensers, synchronous generators and frequency dependent loads in the power grid. To stop the change in frequency, it is enough to restore the balance of generation and consumption by disconnecting, for example, a load equal to $\Delta P$. Estimates of the volume of this load can be carried out on the basis of measuring all $\Delta$P's included in Equation (2). However, in real power systems, due to the large number of elements, this path is unacceptable. Moreover,

in case the system has significant frequency reserve, the amount of load needed to be shed to stop frequency decline may be smaller than the measured $\Delta P$.

All of the existing UFLS schemes use frequency measurements in one or another manner. The load shedding is activated only after frequency value reaches the first (highest) threshold within a list of thresholds of UFLS system. If it were known what amount of load could be safely shed before the first UFLS threshold is reached, then the frequency profile could be improved significantly, comparing with a typical, UFLS operation-based frequency profile. Several frequency profiles depending on time "t" when the load have been shed (LS) are shown in Figure 1.

**Figure 1.** Frequency response: LS at 0.6 s, LS at 1.0 s, LS at 1.5 s and standard UFLS in 4 steps.

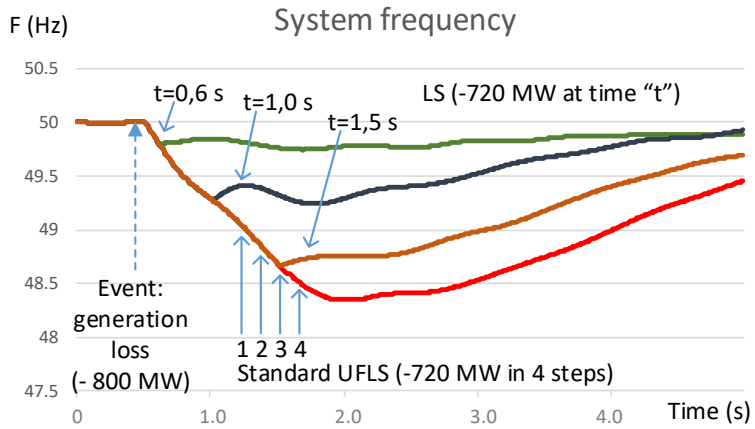


Frequency responses clearly shows that, for the same amount of disconnected load (720 MW), the frequency nadir can be greatly improved if the LS action is activated earlier than the standard multi-step UFLS. Referring Equation (2), when any of the active power injections $\Delta P_{SC\_a}$, $\Delta P_{G\_b}$ or $\Delta P_{L\_c}$ is measured immediately after imbalance event, then the same amount of load could be shed before the frequency reaches the first threshold of UFLS.

We would like to propose a principle of much faster triggering of LS than that of the conventional UFLS—a principle which allows to trigger (not to be confused with activate) LS up to 200 ms from the moment of the contingency without usage of either frequency or ROCOF measurements. The principle is based on the monitoring of the active power injections of the SCs. Our hypothesis is following: active power injection of a SC contains information on the instantaneous shortfall of a major generation unit and the expected fall in frequency. SC active power injections can therefore be used as a set off for rapid LS activation. Execution of such rapid scheme of LS substantially reduces the ROCOF and the value of frequency nadir, thus greatly reducing the risk of frequency limit violation.

It should be noted that the new method is not intended to replace the traditional UFLS system but will serves as valuable addition to already existing UFLS schemes. Furthermore, it is supposed that the load which will be disconnected by rapid LS method is a non-critical load, for example, pump motors of the pumped-storage hydro plant. The schematic representation of the proposed LS principle is seen in Figure 2.

**Figure 2.** Schematic of the proposed LS principle.

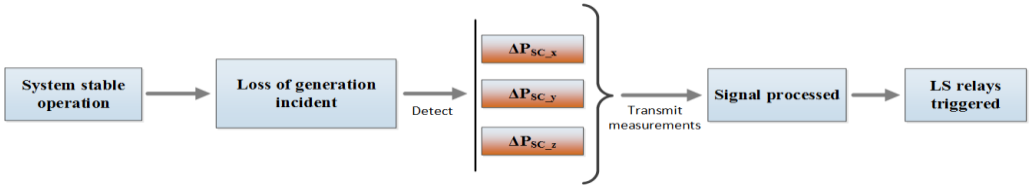


*Source:* [14], 2021.

# 5 Rapid LS evaluation methodology

In order to assess the efficiency of the rapid LS principle, dynamic simulations are usually executed and the results are investigated. The authors of this paper will test the proposed LS approach through executing dynamic simulations on a specific model depicting the Baltic power system (Figure 3).

**Figure 3.** Schematic of the 330 kV Latvian network in island mode of operation.

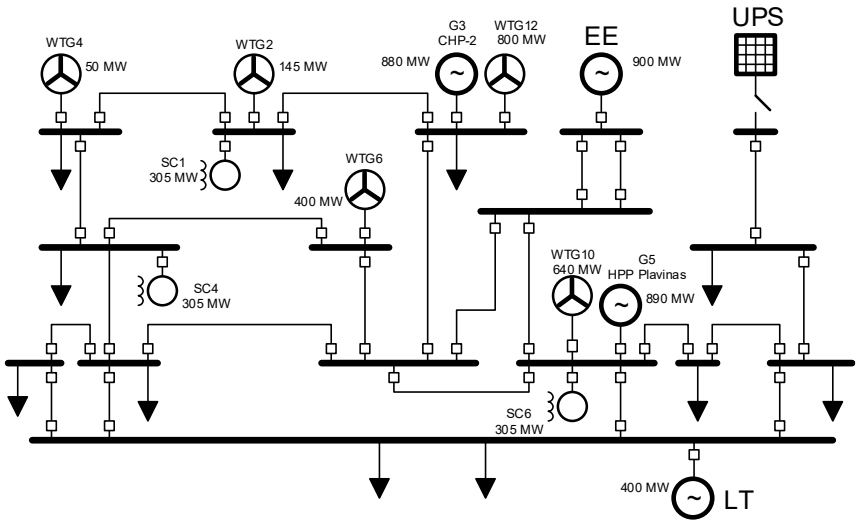


The Baltic region has been selected as a case study due to two major reasons.

First being the major structural changes in the Baltic power grid upcoming in 2025 [15]. Nowadays, Baltic and the Unified Power System of Russia (UPS) power systems are inter-connected with nine high capacity AC interconnectors and frequency stability is not an issue in today's situation due to the size of the UPS power system providing near unlimited frequency reserve. The power system of Baltic States will be disconnected from the synchronous area of UPS and new synchronous interconnection with the European Network of Transmission System Operators (ENTSO-E) synchronous power system will be established [15]. The upcoming synchronous connection between the Baltic and the ENTSO-E power systems is to succeed through a single double-circuit high-capacity synchronous interconnector. Planned or unplanned outages of this interconnection, with UPS system already disconnected, will result in the operation of Baltic states' power grid in an island mode. During this mode of operation, the Baltic power system is only to rely on its own inertia and frequency reserves which are radically lower comparing with today's situation.

The second reason is an accelerated commissioning of new offshore wind parks intended to compensate a gradual decommissioning of the outdated oil shale-fired energy blocks. Wind power generators are non-synchronous so they do not contribute to the system inertia. Besides that, an intent to use the wind parks at full power significantly lowers the frequency containment reserves.

Due to aforementioned reasons the total system inertia and the availability of frequency reserves is expected to decline. This will negatively affect the frequency stability margin of the Baltic grid and may negatively affect the resilience of the system.

To mitigate these developments and to safeguard frequency stability of the Baltic power grid Baltic TSOs have agreed to make investments in three synchronous condensers rated ca. 305 MVA each—totalling nine synchronous condensers planned in the Baltic power grid by 2025 [16]. Synchronous condenser (SC) is a synchronous generator without a prime mover and therefore it is not a source of active power in a classic manner but will provide an additional inertia for the system [17].

Latvian grid has connections with Estonian (EE) and Lithuanian (LT) networks that have been modelled with aggregated loads and equivalent generators. The UPS grid, which nowadays provides near unlimited frequency reserves, is disconnected to simulate grid operation in island mode. To prove the concept, we will perform power grid dynamic simulation case studies presenting a range of scenarios: from today's situation with little non-synchronous renewable generation of considerable size to a scenario with non-synchronous renewable generation supplying significant part of the electricity demand. Synchronous condensers (SC1, SC4, SC6) have been added to the network model and some alternative scenarios with wind parks (WTG10, WTG12) replacing a major traditional power plants (CHP-2, HPP Plavinas) have been considered (Figure 3).

Parameters of the modelled, conventional six-step UFLS are given by the Table 1. Each step disconnects a certain percentage of total load (Pload_UFLS_n, %, MW) with time delay of 0.3 s after threshold has been reached. Transient stability package ETAP 12.5 was used to evaluate the system frequency behaviour in response to loss-of-generation event.

**Table 1.** Conventional UFLS parameters.

| | **Load Shedding Step Number, n** | | | | | |
|---|---|---|---|---|---|---|
| | **1** | **2** | **3** | **4** | **5** | **6** |
| **Freq. threshold, Hz** | 49.0 | 48.8 | 48.6 | 48.4 | 48.2 | 48.0 |
| **Pload_UFLS_n, %,(MW)** | 5,(120) | 5,(120) | 10,(240) | 10,(240) | 10,(240) | 10,(240) |

The algorithm of the proposed rapid LS (RLS) method is described below and illustrated in Figure 4. Real power of synchronous condensers (SC1, SC4, SC6 in Figure 3) continuously measured and the total power of all SCs: $P_{\Sigma} = \sum_{i=1}^{n} P_{SC\_i}$ is calculated. Signal is low-pass filtered and averaged for a 50 ms window to remove transient process-induced spikes.

After power change $\Delta P_{\Sigma 1} > \Delta P_{min}$ has been detected, with a time delay 0.2 s the amount of load $LS1 \geq \Delta P_{\Sigma 1}$ is disconnected. The amount of load $LS1$ is chosen to be closest to a discrete step(s) of the conventional UFLS (Table 1). Load disconnection is initiated by transmitting a trip command to the frequency relays, assigned to the step(s) of the conventional UFLS. Referring Figure 4, for $\Delta P_{\Sigma 1} \cong 220\ MW$ the amount of load $LS1 = P_{\text{load\_UFLS\_1}} + P_{\text{load\_UFLS\_2}} = 120\ MW + 120\ MW = 240\ MW$ , therefore, trip command will be send to the frequency relays of the 1st and 2nd step of UFLS. Load $LS1$ disconnection resulted in SCs power change $\Delta P_{\Sigma 2}$. Then an approximate remaining imbalance can be calculated:

$$\Delta P_{rem} \cong \frac{LS1 \cdot \Delta P_{\Sigma 1}}{\Delta P_{\Sigma 2}} - LS1 \quad (3)$$

If the remaining imbalance exceed the amount of load assigned to the next step of the UFLS, then, with a time delay 0.2 s, load $LS2 = P_{load\_UFLS\_n}$ is disconnected ($LS2 = P_{load\_UFLS\_3} = 240\ MW$ in Figure 4).

**Figure 4.** Synchronous condensers response on a loss-of-generation event.

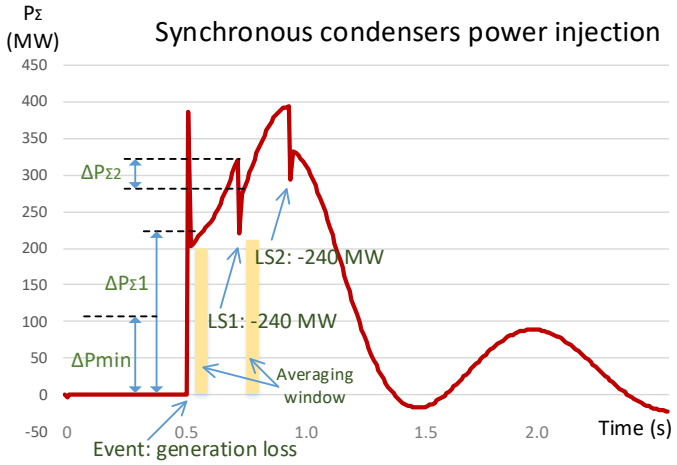


The value of $\Delta P_{min}$ is determined by simulating the loss-of-generation events for which conventional UFLS is not triggered for all feasible network regimes. For the Latvian network model (Figure 3), an imbalance of 300 MW will not trigger UFLS and, for this case, the SCs' active power injection does not exceed $\Delta P_{min} \leq 100\ MW$.

# 6 Case study

An overview of the test case set scenario parameters in the different modelled scenarios for the network model presented in Figure 3 is seen in Table 2.

**Table 2.** Grid element parameters for different modelled scenarios, MW/*MWs in italic*.

| Scenario | Gen. Loss event | CHP-2 | HPP | EE | LT | WTG12 | WTG10 | WTG2 +WTG4 +WTG6 | Post-conting. system inertia |
|---|---|---|---|---|---|---|---|---|---|
| **A** | CHP-2 | 800 | 800 | 500 | 350 | x | x | 290 | *13080* |
| **B** | HPP | 800 | 800 | 500 | 350 | x | x | 290 | *15500* |
| **C** | CHP-2 | 800 | x | 650 | 350 | x | 640 | 290 | *10500* |
| **D** | WTG12 | x | x | 650 | 350 | 800 | 640 | 290 | *10500* |
| **E** | WTG10 | 800 | x | 650 | 350 | x | 640 | 290 | *15500* |

x = generation source not in operation.

## 6.1 Scenario A

An outage of CHP-2 synchronous generation of 800 MW is simulated at t = 0.5 s and the rapid LS is activated according to the proposed algorithm. The active power response of

SCs and the system frequency response resulting from both, conventional UFLS and rapid LS action can be seen in Figure 5.

**Figure 5.** Synchronous condensers and system frequency response scenario A.

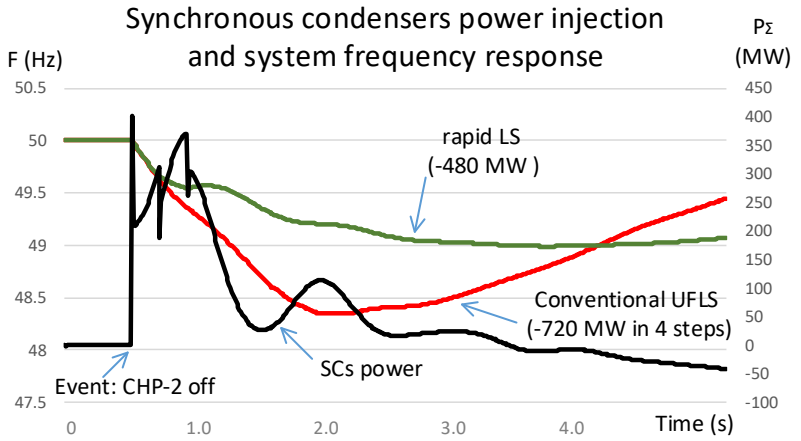


At time t=0.7 s the RLS algorithm triggers frequency relays of the 1st and 2nd step of the UFLS disconnecting 240 MW. An approximate remaining imbalance (Equation 3) is calculated $\Delta P_{rem} \cong 710\,MW$ that exceed the 3rd step of UFLS, therefore, at time t=0.9 s frequency relays of the 3rd step are triggered disconnecting additional 240 MW. In contrast, the conventional UFLS system disconnects 720 MW of load in 4 consequent steps.

## 6.2 Scenario B

An outage of HPP Plavinas synchronous generator of 800 MW is simulated at t = 0.5 s. The active power response of SCs and the system frequency response resulting from both, conventional UFLS and rapid LS action can be seen in Figure 6.

**Figure 6.** Synchronous condensers and system frequency response scenario B.

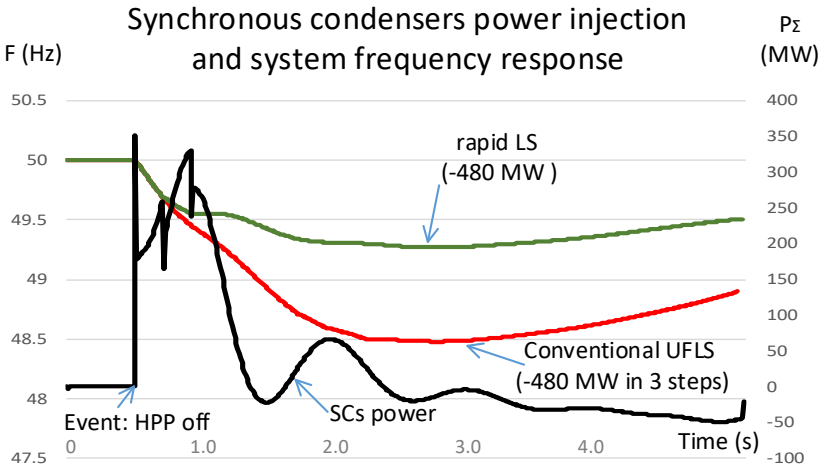


The amount of disconnected load is the same for both cases, but the rapid LS provides much better frequency profile with a lower ROCOF and higher frequency nadir.

## 6.3 Scenario C

An outage of CHP-2 synchronous generation of 800 MW is simulated at t = 0.5 s. Comparing with scenario A, the system inertia is reduced due to replacement of the HPP Plavinas with a non-inertial wind power generator WTG10. The rapid LS disconnects 480 MW by triggering frequency relays of the 1st, 2nd (at t= 0.7 s) and 3rd (at t=0.9 s) step of the UFLS system. Rapid LS actions did not stop frequency decline and therefore, at t=4.2 s, the 4th step of the conventional UFLS disconnects additional 240 MW of load (Figure 7). The total amount of load that has been disconnected is 720 MW. In contrast, conventional UFLS disconnects 960 MW of load in 5 steps.

**Figure 7.** Synchronous condensers and system frequency response scenario C.

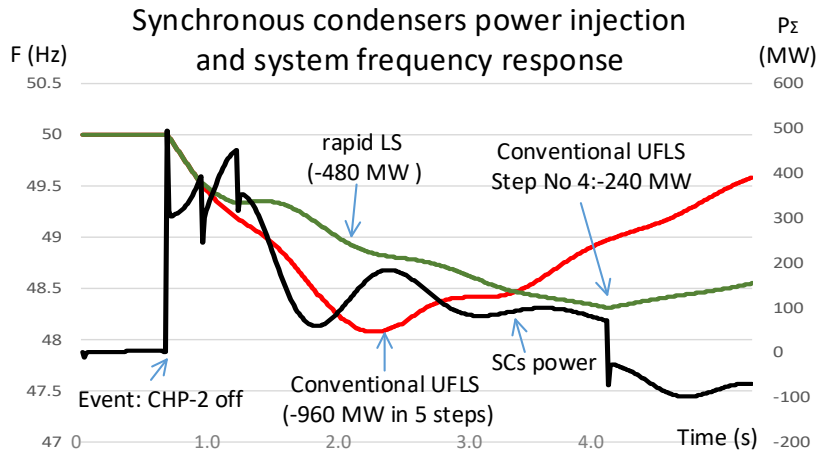


## 6.4 Scenario D

In this scenario two inertial generation sources CHP-2 and HPP Plavinas have been replaced with non-inertial one WTG12 and WTG10. System inertia is reduced compared with scenarios A and scenario B. An outage of WTG12 is simulated resulting in instant deficit of 800 MW. Rapid LS algorithm triggers 1st and 2nd step of the UFLS at t=0.7 s disconnecting 240 MW of load. At t=0.7 s the 3rd step was triggered resulting in 480 MW of total disconnected load. In contrast, conventional UFLS disconnects 720 MW of load in 4 steps (Figure 8).

**Figure 8.** Synchronous condensers and system frequency response scenario D.

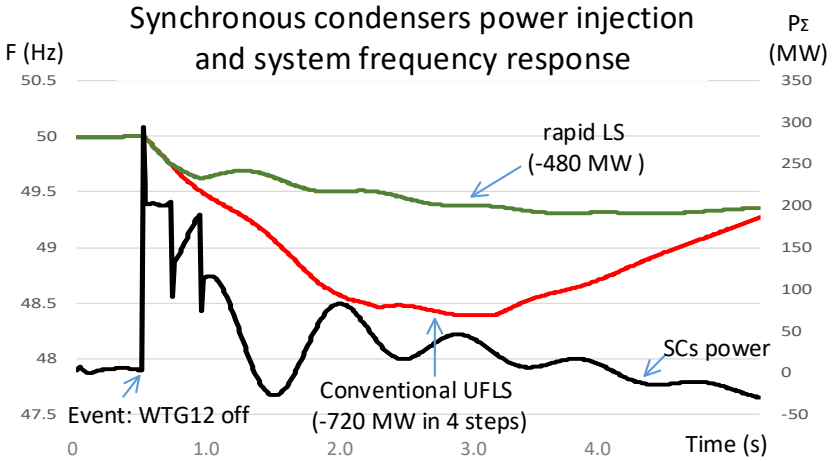

## 6.5 Scenario E

In this scenario HPP Plavinas has been replaced with non-inertial WTG10. An outage of WTG10 is simulated resulting in instant deficit of 640 MW. Rapid LS algorithm triggers 1st step of the UFLS at t=0.7 s disconnecting 120 MW of load and at t=0.9 s the 2nd step was triggered resulting in 240 MW of total disconnected load (Figure 9). Conventional UFLS disconnects same amount of load in 2 steps but the frequency nadir is lower and with a higher ROCOF.

**Figure 9.** Synchronous condensers and system frequency response scenario E.

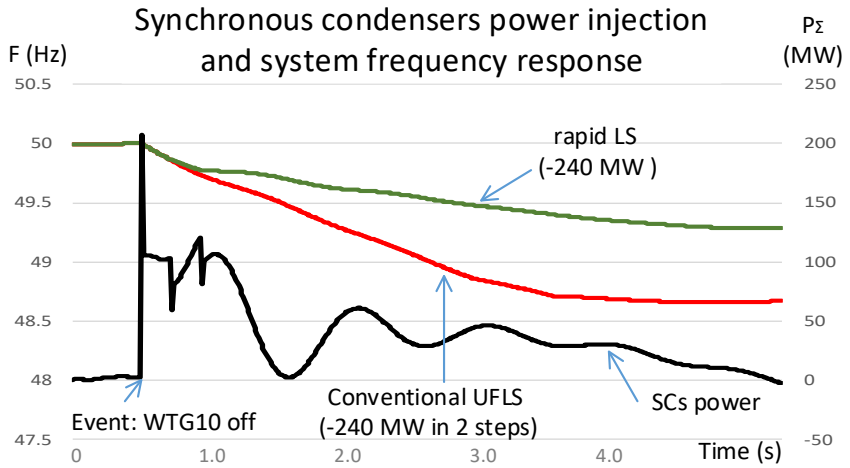


Numerical results for all scenarios are summarized in Table 3.

**Table 3.** Disconnected load and frequency nadir for different modelled scenarios.

| Scenario | Power deficit, MW | Disconnected load, MW, RLS / UFLS | Freq. nadir, Hz, RLS / UFLS | Gen. loss event | Total post-contingency inertia, MWs |
|---|---|---|---|---|---|
| **A** | 800 | 480 / 720 | 49.0 / 48.3 | CHP-2 | 13080 |
| **B** | 800 | 480 / 480 | 49.27 / 48.5 | HPP | 15500 |
| **C** | 800 | 720 / 960 | 48.3 / 48.07 | CHP-2 | 10500 |
| **D** | 800 | 480 / 720 | 49.3 / 48.4 | WTG12 | 10500 |
| **E** | 640 | 240 / 240 | 49.3 / 48.65 | WTG10 | 15500 |

Summarizing the results of the case studies one can conclude that an addition of the rapid LS principle to already existing UFLS system significantly improves the frequency profile resulting from a major loss-of-generation incident. For all considered cases the ROCOF improves (decreases) and the frequency nadir is higher for the same amount of disconnected load. In three cases (case A, C and D) the better frequency response was achieved even with smaller amount of disconnected load.

# 7 Conclusions

The simulations showed that SCs actively counteract frequency disturbances caused by tripping of generation by injecting considerable amounts of active power into the grid. These injections are observed almost instantly, are of considerable size and are well measurable. The test case set simulations show that the proposed rapid LS method significantly improves the post-contingency frequency response and, in some cases, the amount of load that need to be disconnected to provide acceptable frequency response is smaller comparing with UFLS-only-based load shedding. The rapid LS principle demonstrate its efficacy for both, systems with regular inertia and systems with lowered inertia. Several different automation concepts can be used to implement the proposed LS method in practice. The SC active power injection measurements can trigger a SCADA based LS algorithm which will calculate the amount of load shedding needed and activate the load shedding relays. The function of measuring the active power can be assigned to the terminals of microprocessor based relay protection or phasor measurement unit-based wide area measurement system. The value of the threshold $\Delta P_{min}$, exceeding which the rapid LS should be activated, is a matter of detailed simulations using practical topology of the grid the novel LS method is intended to be used for.

## Acknowledgements

This research is supported by the Ministry of Economics of the Republic of Latvia, project "Future-proof development of the Latvian power system in an integrated Europe (FutureProof)", project No. VPP-EM-INFRA-2018/1-0005 and by the Latvian Council of Science, project "Management and Operation of an Intelligent Power System (I-POWER)" (no. lzp-2018/1-0066).

## References

1. Guzs, D., Utans, A., Sauhats, A. (2021) Evaluation of the resilience of the Baltic power system when operating in island mode. Proceedings of the 31th European Safety and Reliability Conference, pp. 1876-1883, https://doi.org/10.3850/978-981-18-2016-8_056-cd.
2. Dixon, A. (2019) Modern Aspects of Power System Frequency Stability and Control, Elsevier Inc., https://doi.org/10.1016/C2017-0-03431-6.
3. Dreidy, M., Mokhlis, H., Mekhilef, S. (2017) Inertia response and frequency control techniques for renewable energy sources: A review. Renew. Sustain. Energy Rev., vol. 69, pp. 144–155, https://doi.org/10.1016/j.rser.2016.11.170.
4. Tielens, P., van Hertem, D. (2012) Grid Inertia and Frequency Control in Power Systems with High Penetration of Renewables. In: Proeceedings of the Young Researchers Symposium in Electrical Power Engineering, Delft, The Netherlands, 16–17 April 2012.
5. Machowski, J., Bialek, J.W., Bumby, J.R. (2008) Power System Dynamics, 2nd ed., John Wiley & Sons: Aachen, Germany, 2008; p. 171.
6. Delfino, B., Massucco, S., Morini, A., Scalera, P., Silvestro, F. (1989) Implementation and comparison of different under frequency load-shedding schemes. In: Proceedings of the 2001 Power Engineering Society Summer Meeting. Conference Proceedings (Cat. No.01CH37262), New York, NY, USA, 16–18 October 1989, IEEE: Piscataway, NJ, USA, 2001, vol. 1, pp. 307–312.
7. Rudez, U., Mihalic, R. (2010) Comparison of adaptive UFLS schemes in modern power systems. In: Proceedings of the 2010 IEEE Electrical Power & Energy Conference, San Diego, CA, USA, 22–26 July 2012, IEEE: Piscataway, NJ, USA, 2011, pp. 233–238.

8. Ben Kilani, K., Elleuch, M., Hamida, A.H. (2017) Dynamic under frequency load shedding in power systems. In: Proceedings of the 2017 14th International Multi-Conference on Systems, Signals & Devices (SSD), Marrakech, Morocco, 28–31 March 2017, IEEE: Piscataway, NJ, USA, 2017, pp. 377–382.
9. Zare, F., Ranjbar, A., Faghihi, F. (2019) Intelligent topology-oriented load shedding scheme in power systems. In: Proceedings of the 2019 27th Iranian Conference on Electrical Engineering (ICEE), Yazd, Iran, 30 April–2 May 2019, IEEE: Piscataway, NJ, USA, 2019, pp. 652–656.
10. Jianjun, Z., Dongyu, S., Dong, Z., Yang, G. (2018) Load Shedding Control Strategy for Power System Based on the System Frequency and Voltage Stability. In: Proceedings of the 2018 China International Conference on Electricity Distribution (CICED), Tianjin, China, 17–19 September 2018, IEEE: Piscataway, NJ, USA, 2018; pp. 1352–1355.
11. Rudez, U., Mihalic, R. (2017) Trends in WAMS-based under-frequency load shedding protection. In: Proceedings of the IEEE EUROCON 2017-17th International Conference on Smart Technologies, Ohrid, Macedonia, 6-8 July 2017, IEEE: Piscataway, NJ, USA, 2017; pp. 782–787.
12. Rudez, U., Mihalic, R. (2011) Analysis of Underfrequency Load Shedding Using a Frequency Gradient. IEEE Trans. Power Deliv. 2011, vol. 26, pp. 565–575, https://doi.org/10.1109/tpwrd.2009.2036356.
13. Frigo, G., Derviskadic, A., Zuo, Y., Paolone, M. (2019) PMU-Based ROCOF Measurements: Uncertainty Limits and Metrological Significance in Power System Applications. IEEE Trans. Instrum. Meas. 2019, vol. 68, pp. 3810–3822, https://doi.org/10.1109/tim.2019.2907756.
14. Sauhats, A., Utans, A., Silinevics, J., Junghans, G., Guzs, D. (2021) Enhancing Power System Frequency with a Novel Load Shedding Method Including Monitoring of Synchronous Condensers' Power Injections. Energies 2021, vol. 14, pp. 1490. https://doi.org/10.3390/en14051490.
15. European Commision. The Baltic Power System Between East and West Interconnections, JRC Science for Policy Report; European Commision: Brussels, Belgium, 2016.
16. AS Augstsprieguma Tīkls. Latvian TSO. Riga, Latvia, https://ast.lv/en.
17. Payerl, C. (2020) Introduction to ABB Synchronous Condenser Offering—A Solution to Improve Grid Strength, IEEE: Piscataway, NJ, USA, 2020.

# Definition and nature of resilience

MERIAN Yves, Institut pour la maîtrise des risques (IMdR), yves.merian@orange.fr

## *Abstract*

*There are a lot of definitions of resilience for organizations, generally based on the notions of "absorbing" and "adapting" and sometimes "preparing" and "restoring". But they can differ about the state to be achieved by the organization after the disruption. What is the outcome for an organization: return to the previous state (the "normal situation") or transform (going to a "new normality")? Clarify the appropriate definition of resilience for organizations is a key issue to understand the concept and its nature.*
*Resilience is a broad concept, covering both technical and socioeconomic systems, showing various schemes and two faces (individual and collective), appearing as a goal for risk management which encompasses numerous disciplines.*
*It is finally a relative notion for which methods of evaluation are a real challenge.*

## Introduction

There are a lot of definitions of resilience for organizations. They are generally based on the notions of "absorbing" and "adapting" and sometimes "preparing" and "restoring". But they can differ about the state to be achieved by the organization after the disruption. Survival is not sufficient. Restoring the existing state is sometimes essential and a beautiful result. But in some situations, return to the previous state with no modifications can be a mistake. This is a key issue to well understand the concept. Clarify the appropriate definition of resilience for organizations is the first step of this paper.

The point of the definitions leads to reveal the nature of resilience: diversity of situations; goal of risk control with a need to go beyond crisis management and integrate different disciplines often used in isolation, showing both faces – individual for its own benefit and collective through mutual relationships.

Finally, to give confidence as an operational tool, resilience needs to be both managed and measured. How to do it? That is a challenge because of its relative – not absolute - nature.

These issues, general for all organizations, address notably critical infrastructures and territories considered as relying on interdependent actors and networks..

This work is based on comparison of existing definitions of resilience, analysis of international standards, lessons learnt from crisis management, emergency management, business continuity management, and post-crisis management. Diagrams are provided to illustrate the principles.

# 1. Definition(s) of resilience

Definitions of resilience for organizations are generally based on the common use of the notions of "absorbing" and "adapting" and also "preparing" and "restoring". They can differ about the state to be achieved by the organization after the disruption: restoring the previous state (the "normal situation") or modify to a "new normality". This is a key issue to well understand the concept of resilience and apply it in an appropriate way.

## 1.1. Original definitions and extension

### 1.1.1. Original definitions

There are two main original definitions according to the entities.

Definitions of resilience for a material (an inanimate object) (from latin resilire, bounce)
- ability of a material to resist to pressures and recover its initial structure
- in physics, the capacity of a material receiving an impact to recover its initial state.

Definitions of resilience for a person (a living entity)
- capacity to live, succeed, develop in spite of adversity
- capacity of a person to adapt, following a trauma
- psychological phenomenon which consists for an individual affected by a trauma to acknowledge the traumatic event so as to not or no more live in misfortune and to rebuild on a socially acceptable manner.

For Jean-Paul Louisot, the definition for a material – capacity to find its initial shape after having been compressed or having received shocks, physical or thermal – gives the notion to find the initial state, whereas the definition for a child – ability to continue to develop despite an unfavorable and traumatic social and family environment – has not the purpose to find the initial state, but to continue its development in an unfavorable context.

### 1.1.2. extension to organizations and society

The point is: what is the outcome for an organization: return to the previous state (the "normal situation") or transform (going to a "new normality")? Opinions differ spontaneously on that issue.

André Lannoy outlines that restoring the existing state is essential and is already a beautiful result. The UK report notes that "resilience refers to emotional and psychological resilience as well as physical or material resilience. Jean Pariès proposes a kind of compromise for socioeconomic systems: evolution is a condition for the resilience of a living entity, but evolution relies partly on maintaining a certain order and partly on change and innovation.

In fact, both ways are acceptable depending on the context. In the case of the maintenance of an equipment, the possibility to return to the previous state – restore a bridge as if it was new– would be the best solution. But, after a flood, a process of "build back better" (BBB) should be systematically examined and return to the previous state without modification could be a mistake.

## 1.2. Clarification

### 1.2.1. official definitions

The French White Paper on defense and national security (2008) defines resilience as:
**resilience**
capability of public authorities and the (national) society to respond to a major crisis and rapidly restore normal functioning.

The United Nations Office for Disaster Risk Reduction (UNDRR) gives a detailed definition of resilience:
**resilience**
ability of a system, community or society exposed to hazards to resist, absorb, accommodate, adapt to, transform and recover from the effects of a hazard in a timely and efficient manner, including through the preservation and restoration of its essential basic structures and functions through risk management.
Note that this definition uses both aspects: (a) transformation and (b) preservation of basic structures and functions.

ISO gives only a short definition of resilience in its standard on vocabulary (ISO 22300):
**resilience**
ability to absorb and adapt in a changing environment
But, it is more explicit in another article of this standard, dedicated to urban resilience: ability of any urban system (…) to positively adapt and transform (…) while facilitating (…) development**.**

### 1.2.2. proposition

The idea is:

- to give a definition for both technical systems (inanimate) and socioeconomic systems (partly living)
- to complete the ISO definition, based on "absorb and adapt", to explicit the possible outcomes depending on the concrete cases. It becomes:

Proposition

**Resilience**
ability to absorb and adapt in a changing environment (dealing with shocks or chronic stresses), with the view of
either restoring the previous state as near as possible to continue to operate
or restoring basic functions and transforming to continue to develop and prosper.

## 2. Nature of resilience

According to the proposed definition, resilience (a) has different aspects end (b) is not a discipline, but a goal for the organization.

### 2.1. Diversity

Traditionally, a lack of resilience is schematized by a diagram where an organization is prevented to continue to deliver its products and services at the nominal level and where the delivery is interrupted or drastically reduced (fig. 1 and fig. 2 case 1 - fall in activity). The challenge is to recover quickly, before the impacts are intolerable.

**Fig. 1** Base type of disruption

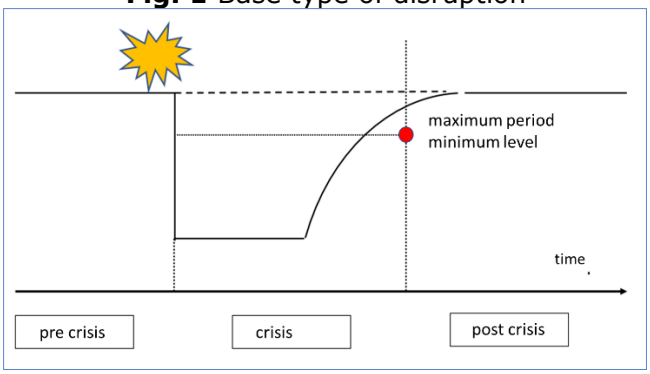


There are other key situations of disruptions (fig. 2): in case 2, a pressure in demand can exceed the capacity of the organization (supposed to be engaged; e.g. the hospitals during the COVID crisis peaks); in case 3, the organization cannot meet a deadline (for example, delayed timetable of school examinations). These situations can occur simultaneously in one organization (activity reduced and boosted in different areas).

**Fig.2**: different types of situations for resilience

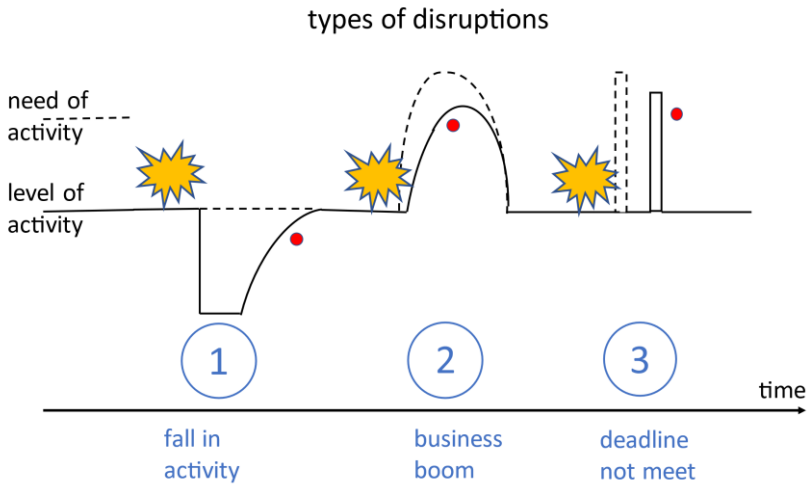


Crises are not always punctual and simple; they can have different profiles: shocks or chronic stresses, repetition (waves of crisis), cascading effects, long duration (fig. 3).

**Fig. 3**: rhythm of crises

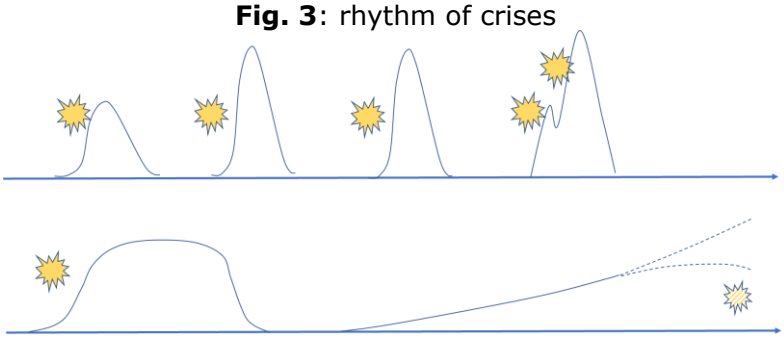

## 2.2. An essential goal for risk management

### 2.2.1. A general goal

Resilience can be considered as a major purpose for risk management. It focuses on consequences (of occurred threats or missed opportunities) and then on solutions and action. So, it has a positive meaning, better to mobilize actors and people, when risk is perceived as more negative. All risks are considered. In the diagram below (fig. 4), they are classified in three categories according to key factors belonging to (a) market and regulation, (b) disruptions and disasters (risk of natural, technological or human origin) and (c) policy of the organization.

**Fig. 4**: Links between risk and resilience

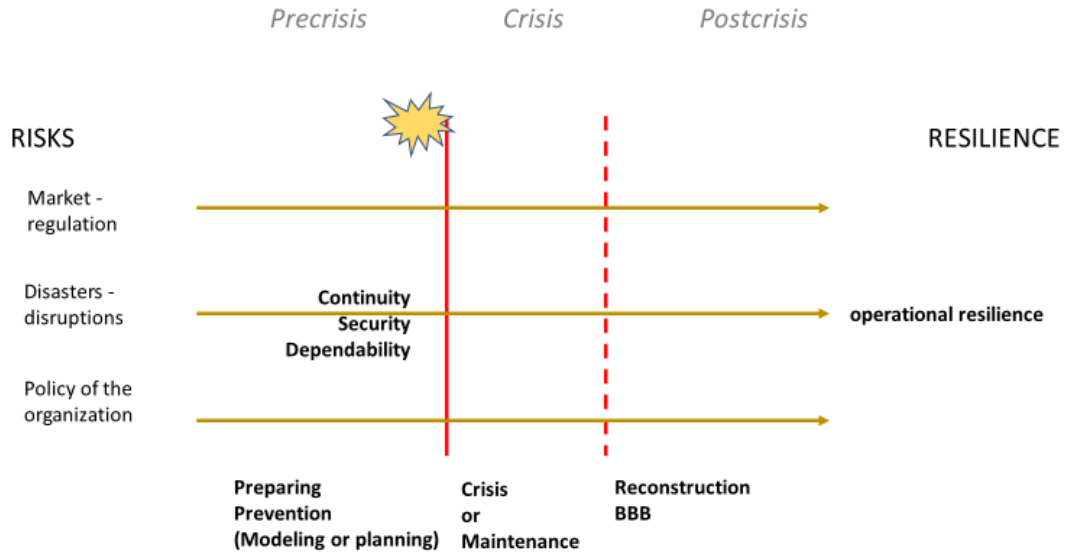


Resilience is not the unique purpose of risk management. Performance is another one. Resilience and performance are sometimes in conflict, namely because of the cost of redundances needed, and sometimes complementary. It is important to note that resilience has its own limits, and that "too much resilience kills resilience".

Operational resilience is part of resilience which addresses the risk of disruptions. It is a broad approach which can be considered as an extension of business continuity and encompasses continuity, dependability, security, crisis management (partly), prevention and reconstruction.

In case of disruptions, continuity and security are often mixed and have to be treated successively or simultaneously and to be balanced when there are dilemmas, as it was showed by the COVID crisis. In France, in case of disasters, emergency management - through the ORSEC mechanism - and business continuity management are few interconnected. Risk reduction needs to go beyond crisis management and encompass prevention (in precrisis period) and reconstruction (in postcrisis period).

### 2.2.2. Both individual and collective

Resilience needs a balanced cooperation with the ecosystem.

Resilience is often considered from the point of view of the entity alone and as an autonomous process; but in fact interactions with the ecosystem, between entities, are very important to enhance resilience, for several reasons:

- as vaccines against covid, resilience is a protection for itself but also for other interested parties;
- any organization has to receive information and aid from other parties in case of disruptions,
- grouping entities in a supply chain, sector or territory can improve individual and collective resilience through appropriate interactions.

The capacity of a person to develop after a trauma requires social interactions with an external supportive network (Boris Cyrulnik). The French white paper on defense and security states that resilience concerns not only the public authorities, but also the economic actors and the whole society. As crisis experience showed, cooperation is useful or essential between train and bus, between electricity and telecommunication, between hospitals (when a hospital is overloaded by covid patients).

For the supply chain, ISO 22318 urges organizations (a) to obtain visibility on their supply chain and design it, and (b) to examine the capacity of their critical suppliers in case of disruption and, if appropriate, to agree with them a formalized commitment. This principle of cooperation is extended in the context of urban resilience as follows (ISO 22300 article 3.1.284 Note 2 to entry): "Urban resilience is dependent upon the individual and collective resilience of the separate components of a complex urban system. Although a city, town or community within an urban area can individually demonstrate enhanced resilience within its respective boundaries, urban resilience encompasses the broader geographic scope of urban agglomeration."

The following diagram (fig. 5) gives a simplified description of the actors to be mobilized inside a territory for collective resilience - a central leader, the critical organizations operating in the area, including critical infrastructures, and people. External relationship with other actors, networks or territories, namely intermunicipal or in proximity, are also be built to both promote positive cooperation and avoid negative dependencies (fig. 6).

**Fig. 5**: internal actors for the resilience inside a territory

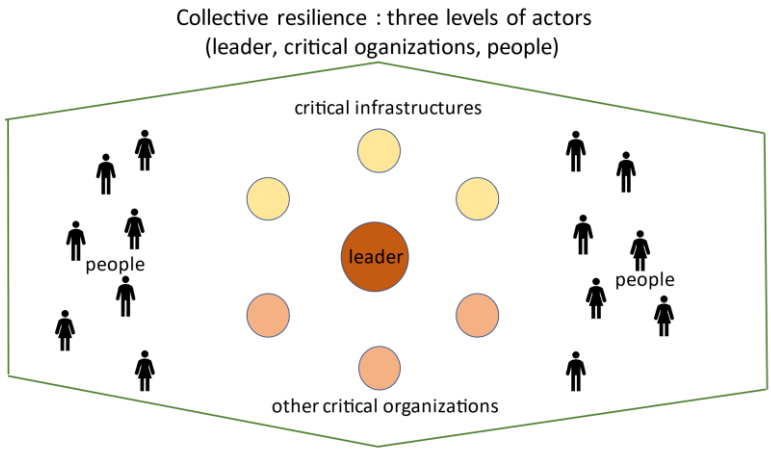


**Fig. 6** interconnexions between interdependent infrastructures

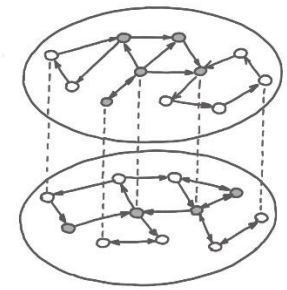

# 3. Resilience building

According to the title of the UK report, resilience should be built. A new project of ISO standard seems to establish this idea. There are two issues: can resilience be managed? if yes, can it be evaluated?

## 3.1. Resilience foundation

A material is more or less resilient by intrinsic characteristics, which are permanent.

An object using such material can be resilient by design and by conditions of utilization. Technical systems may require protection and maintenance methods, as well as introduction of innovation, during a life cycle.

Socioeconomic organizations are complex and combine both aspects (inanimate and living). Core elements of resilience management can be aggregated as a structured and reflective framework.

**Table 1** aggregated elements for foundation of resilience management

| | |
|---|---|
| Prepared | Preparedness relies on ability to have tolerance to uncertainty and on elaboration of flexible plans, based on lessons learnt from crisis, emergency and business continuity management. These plans should cover preparation, prevention, crisis management and reconstruction, including BBB. |
| Adaptive | adaptability to change needs in peculiar redundancy, which generates costs; cost issue should be more understood (resilience is not an underperformance) and modelized in an acceptable way. |
| Integrated | resilience mobilizes a diversity of disciplines, skills and actors; it is a major challenge to obtain horizontal and vertical exchanges by avoiding siloes (isolations) and developing fluent communication between levels (namely between leadership, concerned persons and people). |
| Durable | it is necessary to take into account the cycle of life (for technical matters), the scarcity and saturation of physical resources, the duration of the adverse effects. |
| Transparent | Transparency and trust are necessary to some extent.<br>This requires an appropriate culture of resilience. |

For the foundation of resilience management, training of the teams is essential.

Complexity needs to simplify the approach to be practicable. The idea is to prepare generic approaches as a decision-making aid. This should encompass the ability to (a) assess risk situations, (b) elaborate plans proposing adequate solutions and (c) make appropriate decisions. Concerning the decisions, it is necessary to pay attention to the numerous biases and to possible absurd decisions (MOREL Christian).

## 3.2. Resilience evaluation

It is necessary to evaluate the level of resilience of an organization. But it can be difficult and uncertain. To what extent is resilience measurable?

Resilience is a broad concept, not measurable for an organization as for a material.

For a material, resilience can be measured precisely by tests (e.g. Charpy impact test).

For an organization, when based on technical aspects, resilience can be measured quantitively in terms of efficiency, robustness and cost, with a multi criteria approach (e.g. transportation by bus of passengers trapped in a stopped train; program of maintenance of assets).

When human factors are more sensible, resilience measure is more qualitative and relative (not absolute). Thus, ISO recommends that an urban system's capability for resilience should be measured and analyzed through qualitative and quantitative data (ISO 22300 article 3.1.284).

A lot of issues are to be examined: measure the result or the effort (the frame), choose a method to collect and analyze information (data, indicators); accept to add an opinion to the measure …

A key point is the way to conduct the evaluation. We can distinguish three major categories:

- internal assessment ("experience feedback") through report and lessons learnt
- notation (e.g. FM Global resilience index)
- questionnaire and dialogue (cf. ISO 22318 example), with possible reference to a collective label.

At this stage, the use of questionnaire enabling dialogue between an organization and some partners seems to be a interesting practice.

---

**Bibliographical references**

French government (2008) The French White Paper on defense and national security, site http://archives.livreblancdefenseetsecurite.gouv.fr
UK HOUSE OF LORDS (2021), Preparing for Extreme Risks: Building a Resilient Society
UNDRR (2022), site https://www.undrr.org/terminology/resilience
ISO 22300 Security and resilience – Vocabulary (2021)
ISO 22316 (2017) Security and resilience — Organizational resilience — Principles and attributes
ISO 22318 Security and resilience – Business continuity management systems — Guidelines for supply chain continuity management (2021)
CEN/TS 17091 Crisis management - Guidance for developing a strategic capability (2018)
LOUISOT Jean-Paul (2021) La résilience : objectif stratégique au cœur de l'ERM
PARIES Jean (2021) Gestion des risques & Covid 19 : la résilience organisationnelle, Institut pour une culture de la sécurité industrielle (ICSI)
MOREL Christian (2002, 2012, 2018) Les décisions absurdes (tomes I, II, III)

# Real-time Monitoring of Gas Pipelines with Leak Detection and Localization via a Receding Horizon Observer

Didier Georges, Univ. Grenoble Alpes, CNRS, Grenoble INP*, GIPSA-lab, F-38000 Grenoble, France, didier.georges@grenoble-inp.fr

*Institute of Engineering & Management / Univ. Grenoble Alpes

## Abstract

*The paper is devoted to some preliminary results on the design and application of a Receding Horizon Observer (RHO) for the real-time leak detection and monitoring transient mass flux and pressure distributed along long gas pipelines. The RHO, already used for the monitoring of chemical industrial processes for example, is based on the repeated co of a least-square inverse problem taking advantage of new sensor measurements obtained at each sampling time. It is shown that the effective detection and localization of a single leak and the estimation of the transient states of the gas dynamics can be performed in real-time using a RHO based on a reduced-order model and a limited number of mass flow rate sensors. The simulation results demontrate the potentiality of the proposed approach when applied to a 100 km-long gas pipeline. Future challenges are also considered in the paper regarding the optimal location of sensors and the application of the approach to gas pipeline networks.*

## 1 Introduction

Gas transportation networks are large-scale infrastructures exposed to the risk of leaks. Leaks can be caused by malicious acts or by material aging and pipe corrosion. They can lead to catastrophic events, such as explosions and fires, resulting in direct fatalities or human injuries, and financial losses, but they can also significantly contribute to increased global warming through the release of methane gas into the atmosphere. For these reasons, it is essential to be able to detect and localize leaks quickly to take the necessary maintenance measures.

Many research works have been devoted to the problem of leak detection in gas networks in the last decades, using both hardware or software-based methods [1]. Recently, various probabilistic or Machine Learning techniques have been developed to detect and localize leaks in gas networks, mainly when equilibrium state of the pipeline (no use of a dynamical model of the gas networks) [5,6,7,8].

The approach proposed in this paper is original in the sense that it allows to detect and localize a leak in real-time, while ensuring the permanent estimation of the pressure and the mass flux distributed in the pipeline at the same time, in realistic situations where the gas demand always varies. Indeed, many approaches rely on the assumption that the system is at an equilibrium. Since the occurrence of a leak drastically changes the dynamics of the pipeline, it is important to estimate the state of the system under the faulty situation. The Receding Horizon Observer (RHO) or Moving Horizon Observer (MHO) design has been mainly applied to industrial process monitoring and less often to large scale infrastructures or environmental applications (see [2]).

It will be shown in the paper that a limited number of mass flux sensors are needed to ensure observability properties, i.e., effective monitoring of transient states, and detection/localization of a potential leak. The proposed approach relies on the appropriate spatial discretization of the well-known distributed dynamical model governing both pressure and mass flux throughout the pipeline. It is also noticeable that, to the best of my knowledge, this paper is the first application of a nonlinear RHO for the real-time monitoring of gas pipelines.

The paper is now organized as follows: Section 2 presents the partial differential equations governing gas pipeline dynamics and the proposed discretized model used in the rest of

the paper. Section 3 is devoted to the observability analysis of the discretized model. The formulation of the RHO and its numerical computation are discussed in section 4. Section 5 is devoted to computational simulations demonstrating the potential of the proposed approach. Section 6 considers future challenges. Finally, the last section considers some conclusions and perspectives for future works.

# 2 Modeling

## 2.1 Gas pipeline dynamics

The dynamics of compressible gas within a pipeline with slow transients (without waves, or shocks), in the presence of a leak located at position $x_l$ and magnitude $C$ are given by the following one-dimensional Euler equations:

$$\partial_t \rho(x,t) + \partial_x \phi(x,t) = -\Delta(x - x_l) C \sqrt{\rho}(x,t), \tag{1a}$$

$$\partial_t \phi(\mathrm{x,t}) + \partial_x \left(\frac{\phi(\mathrm{x,t})^2}{\rho(\mathrm{x,t})}\right) + a^2\, \partial_x \rho(\mathrm{x,t}) + \rho(\mathrm{x,t}) g \sin\theta = -\frac{\lambda}{2D} \frac{\phi(\mathrm{x,t})|\phi(\mathrm{x,t})|}{\rho(\mathrm{x,t})}. \tag{1b}$$

The Eq. (1a) and (1b) denote the mass and momentum balance equations, respectively. The variables $\rho, \phi$ represent the gas density and mass flux, respectively. These two variables are defined on the domain $[0, L] \times [0, T]$, where L represents the pipeline length. $\Delta(x - x_l)$ is the characteristic function of the leak located at $x_l$. This characteristic function is here given by a Gaussian function of the form $\Delta(x - x_l) = e^{-\frac{||x - x_l||^2}{2\sigma}}$, where $\sigma$ denotes a dispersion coefficient, here assumed to be fixed. $C$ represents the magnitude of the leak (depending on the width of the leak hole). $\theta$ is the pipe angle with respect to the horizontal position. $a$ is the speed of sound in the gas for a constant temperature. $D$ is the diameter of the pipe. $\lambda$ is the coefficient of friction of gas on the pipe walls. $g$ denotes the acceleration of gravity.

Boundary conditions are needed to ensure well posed-ness of the problem. Here it is assumed that the pressure is constant at the upstream/source end of the pipe: $P(x = 0, t) = a^2 \rho(x = 0, t) = P_0$ thanks to a compressor. At the downstream end, the mass flux is given by a transient withdrawal d(t): $\phi(x = L, t) = d(t)/S$, where *S* is the cross-sectional area of the pipe.

## 2.2 Reduced-order discretized model

The choice is made here to derive a reduced-order finite-dimensional model by discretizing the PDEs (1a) and (1b), using a first-order approximation of the spatial operator $\partial_x$ (method of lines) on a spatial one-dimensional grid of N+1 nodes:

$$\dot{\rho}_l + \frac{(\phi_i - \phi_{i-1})}{dx} = -\Delta(x_i - x_l) C \sqrt{\rho_i}, i = 1, \ldots, N, \rho_0 = P_0/a^2, \tag{2a}$$

$$\dot{\phi}_l + \frac{1}{dx}\left(\frac{\phi_{i+1}^2}{\rho_{i+1}} - \frac{\phi_1^2}{\rho_i}\right) + a^2 \frac{(\rho_{i+1} - \rho_i)}{dx} + \rho_i g \sin\theta = -\frac{\lambda}{2D} \frac{\phi_i |\phi_i|}{\rho_i}, i = 0, \ldots, N-1, \phi_{\mathrm{N}}(t) = d(t)/S, \tag{2b}$$

where the index $i$ denotes the variable evaluated at the node $i$ of the grid corresponding to the position $x_i$ in the spatial domain.

The Eq. (2a) and (2b) define a set of *2N* nonlinear ordinary differential equations with the inputs $d(t)$, and $P_0$, that can be integrated by using a Runge-Kutta method for instance.

# 3 Observability analysis

The question is here to discussed the conditions required in terms of measurements to ensure both observability of the leak parameters $C$ and $x_l$, and the states (densities/pressures and mass fluxes) at each node of the grid.

The reduced-order system (2a) - (2b) is now denoted as

$$\dot{X}(\mathrm{t}) = F(\mathrm{X(t)}, \mathrm{u(t)}, \theta), \quad y = H\big(X(t)\big), \tag{3}$$

where $X$ is the vector of the 2N state variables of (2a) and (2b), $H$ is the measurement operator depending on the sensor's location and nature, $\theta$ is the vector of the leak parameters $(C, X)$, and $u$ is the vector of inputs, namely the 2 boundary conditions $(P_0, d(t))$.

The observability property of nonlinear systems has been extensively studied in the last 50 years. Observability of dynamical systems is closely related on the indistinguishability of initial states or parameters. Several criteria have been proposed to characterize the observability property of nonlinear systems. In particular the observability rank condition $\dim dO(H)|_X = 2N$, where $dO(H)|_X$ is the set of $d\Psi(X)$ with $\Psi \in O(H)$, and $O(H)$ is the observation space of system (5) containing the components of $H$ and closed under Lie derivation defined by $L_F H = \frac{\partial \Psi}{\partial X} F$(see for instance [3]). This criterion is a direct extension of Kalman's observability rank condition for linear systems. Using this criterion and formal calculus, it can be shown that the full state observability and identifiability of $\theta$ are obtained when the mass flux states of the reduced system (3) are all measured. It can be noticed that other combinations of sensors could be used, such as replacing one mass flux sensors by a pressure sensor placed at the downstream end of the pipeline.

# 4 Receding Horizon Observer design

## 4.1 RHO formulation

A RHO consists in solving a data assimilation problem using a sliding window of measurements. $N_0$ defines the size of the measurement window. At each time $k$, the following nonlinear regression problem is solved, that provides a new update of some unknown parameters $\theta$ and the state estimate at time $k - N$ :

$$\min_{\theta, X(k-N_0)} \frac{1}{2} \sum_{l=k-N_0}^{k} \| y(l) - H_l\big(X(l)\big) \|^2_{R^{-1}} + \frac{1}{2} \| \theta - \theta^{k-1} \|^2_{B^{-1}} + \frac{1}{2} \| X(k-N_0) - X(k-N_0)^g \|^2_{B^{-1}}, \tag{4}$$

subject to the dynamics of reduced-order system (3) now discretized in time,

where $X(k-N_0)^g$ denotes an initial guess that can be for instance the vector obtained at time $k-1$. $B$ is symmetric positive-definite matrix of regularization.

The existence of a solution to the problem (4) requires that the observability is ensured thanks to an adequate choice of the sensors, as discussed in the previous section, and $N_0$ large enough.

## 4.2 Numerical computation

The solution of this nonlinear constrained optimization problem (4) requires the use of an iterative descent method. In this paper, the quasi-Newton method, that is very effective to solve medium-size nonlinear optimization problems, was successfully implemented. The cost function in Eq. (4) is now denoted as $J(v)$, where $v$ is the vector of the decision variables. The well-known Newton method consists in first approximating the cost function using a second-order Taylor's series expansion:

$$J(v_k + \Delta v) \approx J(v_k) + \nabla J(v_k)^T \Delta v + \frac{1}{2}\Delta v^T H(v_k)\Delta v. \quad (5)$$

Secondly, the necessary conditions for optimality are given by

$$\nabla J(v_k + \Delta v) \approx \nabla J(v_k) + H(v_k)\Delta v = 0. \quad (6)$$

Then the updated solution $x_{k+1}$ is computed by inversion of the Hessian matrix $H(x_k)$

$$v_{k+1} - v_k = \Delta v = -H(v_k)^{-1}\nabla J(v_k). \quad (7)$$

The main drawback of the direct Newton method is the need for a costly inversion of the Hessian matrix at each iteration. Approximation of the inverse of the Hessian matrix is the key idea of quasi-Newton approaches. They all consist in determining a sequence of approximate positive-definite inverses $B_k$ of the Hessian matrix such $B_{k+1} = argmin \|B - B_k\|_V$, where $\|.\|_V$ denotes the norm induced by a positive-definite matrix $V$. The update of $B\_k$ is given by the following expression in the case of the well-known BFGS method:

$$B_{k+1} = B_k + \frac{y_k y_k^T}{y_k^T \Delta v_k} - \frac{B_k \Delta v_k (B_k \Delta v_k)^T}{\Delta v_k^T B_k \Delta v_k}, \quad (8)$$

where $y_k = \nabla J(v_{k+1}) - \nabla J(v_k)$.

# 5 Application to a test case

The test case consists in a 100 km-long horizontal pipeline of cross-sectional diameter 0.5 m [9]. The gas is supplied at the source node at a pressure of 943 psi. The gas is withdrawn at the other extremity with the mass flow rate $68(1 + 0.1\sin(8\frac{\pi t}{T})$ kg/s, where T corresponds to 24 hours. The Fig. 1 shows a scenario with a leak occurring during a one-day period. The simulation model is based on a 51 nodes grid leading to a 100-state model (2a) – (2b).

**Figure 1.** 24-hour simulation of the pipeline dynamics with a leak occurring at location 35 km, at time t=1 hour, and when the leak is fixed after 10 hours.

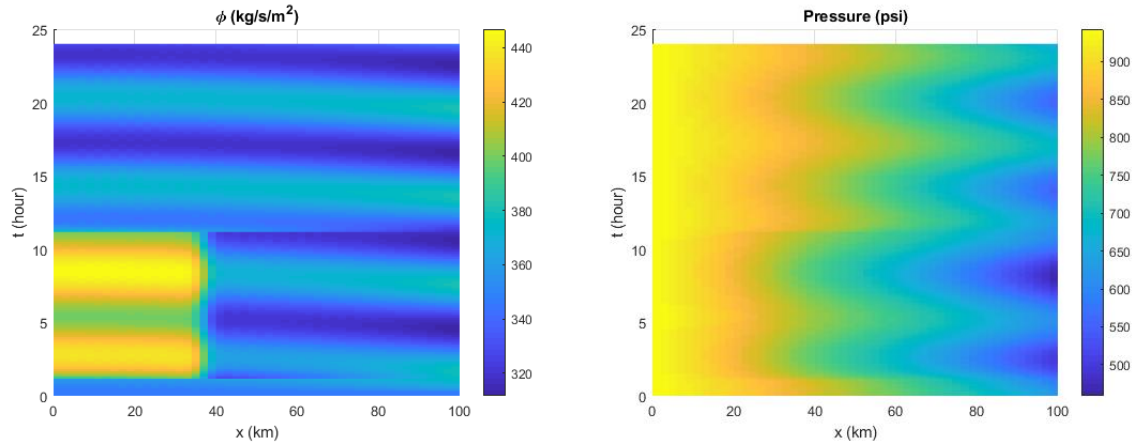


The question is now to experimentally determine the minimum requirements in terms of both model size and measurements to attain the goals of leak detection and state monitoring. An additive Gaussian noise with variance 1 is added to all the measurements. All the tests are performed with a sampling period of 1 minute. The horizon $N_0$ is chosen here to be equal to $N + 1$, where $N$ is the number of grid nodes.

Fig. 2 presents 4 results of leak detection starting with only 4 states until 20 states. It can be shown that a reduced model with 8 states and 4 mass flux sensors is needed to ensure an accurate detection and localization of a leak located at 35 km for this 100km-long pipeline. The RHO is also able to detect that the leak is repaired after a certain time. A 4-state model is however not sufficient to ensure a good localization of the leak. With $N_0 =$

5 (with the 8-state reduced model), the leak is detected with a delay of 10 minutes only. More generally, the leak can be detected with a delay of $(N+1)T_s$ minutes, where $T_s$ is the sampling period. Fig. 3 demonstrates that the effective estimation of the transient states can be performed while estimating the leak at the same time, with a precision in the leak localization better than 1 km.

**Figure 2.** Top left: N=2 (4-state reduced model); top right: N=3 (6-state reduced model); bottom left: N=4 (8-state reduced model); bottom right: N=10 (20-state reduced model);

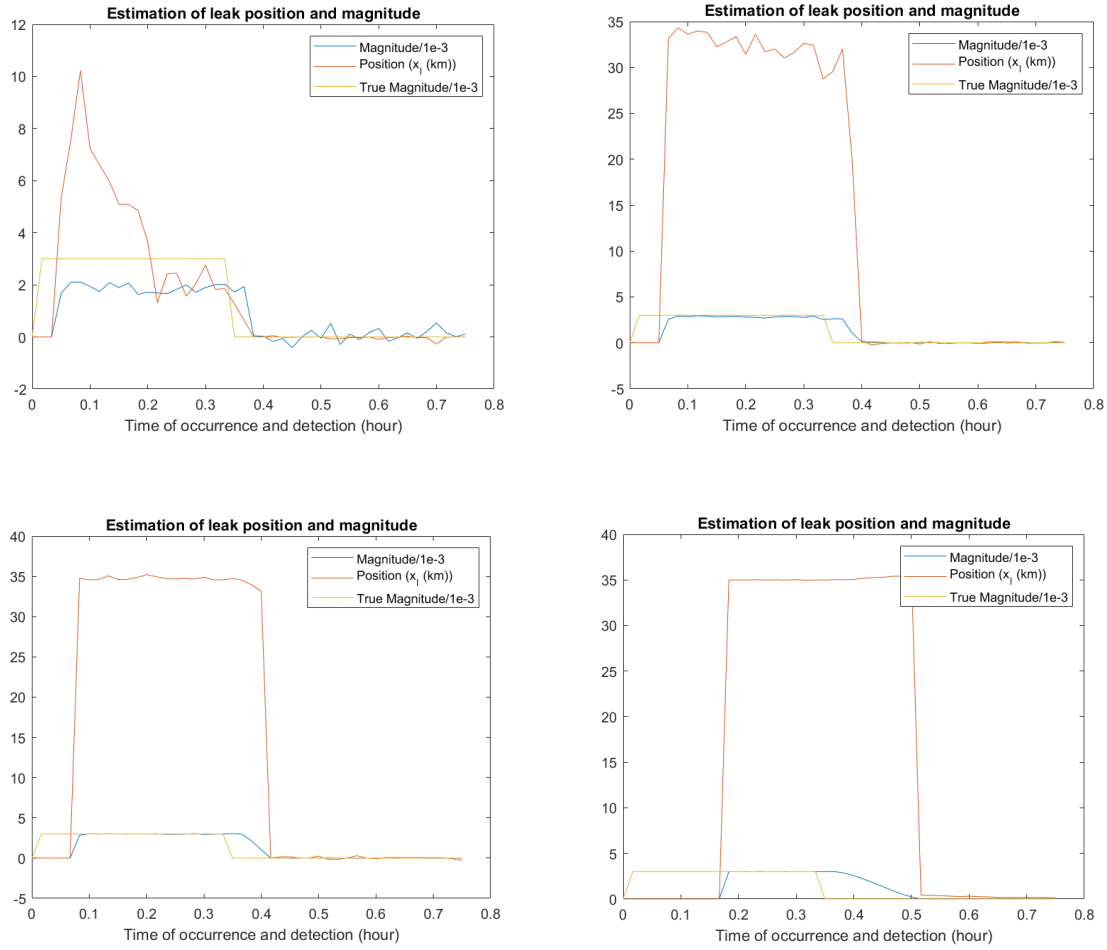


**Figure 3.** Estimation of the transient state with the RHO for the 20-state reduced model

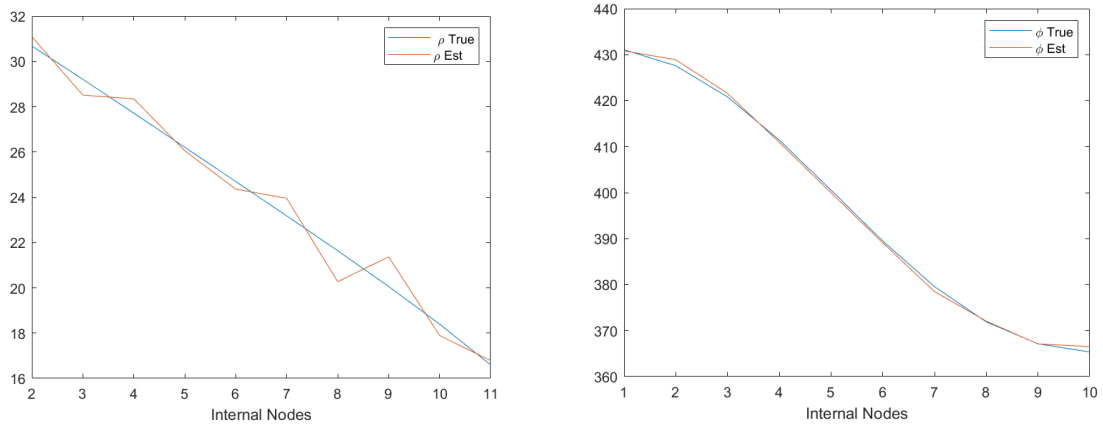

# 6 Future challenges

## 6.1 Optimal sensor location

In fact, the uniform distribution of sensors along a pipeline is certainly not the best configuration to ensure the optimal estimation in the sense of the maximization of an observability index.

Observability here refers to the sensitivity of the measurement outputs to both the initial states and the parameters of the leak on a given time interval *[0,T]*. Indeed, an unobservable component will show a sensitivity equal to zero. In order to determine unobservable components, it is convenient to introduce an index based on a Fisher sensitivity matrix [2] defined as follows:

$$W = \int_0^T (\partial_\Phi y(t))^T R^{-1} \partial_\Phi y(t) dt, \tag{9}$$

where $\partial_\Phi y(t)$ denotes the sensivity of the measurement output vector with respect to the components $\Phi = (\mathrm{X}_0^{\mathrm{T}}, \theta^{\mathrm{T}})^{\mathrm{T}}$ (the initial states and leak parameters) to be estimated, that can be computed by integrating the additional sensitivity system:

$$\frac{d}{dt}\left(\partial_{\mathrm{X}_0} X(t)\right) = \partial_X F(X(t), u(t), \theta)\partial_{X_0} X, \partial_{X_0} y(t) = \partial_X H(X(t), X_s)\partial_{X_0} X(\mathrm{t}) \tag{10a}$$

$$\frac{d}{dt}\left(\partial_\theta X(t)\right) = \partial_X F(X(t), u(t), \theta)\partial_\theta X + \partial_\theta F(X(t), u(t), \theta), \partial_\theta y(t) = \partial_X H(X(t), X_s)\partial_\theta X(\mathrm{t}) \tag{10b}$$

Matrix *R* is the covariance matrix of the measurement noise affecting the sensors. $X_s$ here denotes the vector of sensor locations to be determined.

The number of eigenvalues of matrix *W* equal to zero gives the number of unobservable components. An observability index $I_O(X_s)$ can then be defined by

$$I_O(X_s) = \log\left(\det(\mathrm{W})\right). \tag{11}$$

The optimal sensor location problem will then consist in finding a sensor configuration $X_s$ that maximizes $I_O(X_s)$.

## 6.2 Gas pipeline networks

A direct but simplistic application of the here-proposed monitoring approach to a network of pipelines would consist in duplicating the RHO for each pipeline, that will be certainly not optimal in terms of sensors needed for the monitoring of the whole system and considering the fact that the occurrence of simultaneous leaks in all the pipelines is highly unlikely. Indeed, it seems preferable (this is still to be confirmed) to consider the monitoring of the network at a whole and to try to take advantage of the mesh structure of the network to reduce the number of sensors needed to ensure the monitoring of the transient states and the detection of a number of simultaneous leaks fixed a priori.

A gas pipeline network can be modelled by using a connected graph $G = (V, E)$, where V and E represent the set of $M_J$ junctions (vertices) and the set of $M_p$ pipelines connecting the junctions (edges). In addition, the network topology is defined by an incidence matrix A. Each junction has dynamics given by 2 PDEs of the form (1a)-(1b):

$$\partial_t \rho_i + \partial_x \phi_i = -\Delta\left(x - x_l^i\right) C_i \sqrt{\rho_i}, \tag{12a}$$

$$\partial_t \phi_i + \partial_x \left(\frac{\phi_i^2}{\rho_i}\right) + a^2\, \partial_x \rho_i + \rho_i g \sin\theta_i = -\frac{\lambda_i}{2D_i}\frac{\phi_i|\phi_i|}{\rho_i}, i = 1, \ldots, M_p. \tag{12b}$$

For simplification purpose and without restriction, compression units are not considered.

The vertices of the graph allow to define the boundary conditions of each set of two PDEs by using the first Kirchhoff law (conservation of mass at each junction). A set of $2M_p$ boundary conditions can then be denoted as

$$B\left(\bar{\phi}(\bar{0},t), \bar{\phi}(\bar{L},t), \rho_{sn}(0_{sn},t), p_0(t), \bar{d}(t)\right) = 0, \tag{13}$$

where $\bar{\phi}(\bar{0},t)$ denotes the vector of the upstream mass fluxes, $\bar{\phi}(\bar{L},t)$ is the vector of the downstream mass fluxes, $\rho_{sn}(0_{sn},t)$ is the gas density at the slack node, $p_0(t)$ is the pressure at the slack node, and $\bar{d}(t)$ is the vector of the gas demands.

Model (12a-12b-13) generalizes the model of a single pipeline given by (1a)-(1b). The optimal sensor location problem defined in the previous section is obviously more complicated since it requires the solution of a highly combinatorial problem. In the same way, the RHO application requires to solve a large-scale problem and an effective model reduction appears to be crucial.

# 7 Conclusions

In this paper, the application of a Receding Horizon Observer based on the repeated solution of an optimal inverse problem was proposed for the goal of real-time leak detection and localization together with the estimation of transient values of the gas density and mass flux distributed along a long gas pipeline. It was shown that the effective detection of a leak and the monitoring of the transient states of the gas dynamics can be performed using such a nonlinear Receding Horizon Observer based on a finite-difference reduced-order dynamical model and a limited number of mass flow rate sensors. In particular, a 8-state reduced model appears to be sufficient to ensure the effective detection and localization of a single leak. Furthermore, the approach is compatible with real-time requirements even under MATLAB and produces satisfactory results in terms of accuracy in the leak localization. The approach was successfully tested on a 100 km-long gas pipeline using synthetic data. Future work will consider the use of real data, the optimal configuration of sensors, the multi-leak detection problem, and the extension of this approach to pipeline networks.

## Acknowledgments

The author would like to thank anonymous reviewers for useful remarks and suggestions.

## References

1. Murvay, P.-S., and Silea, I. (2012), A survey on gas leak detection and localization techniques, *Journal of Loss Prevention in the Process Industries 25 (2012), pp. 966-973.*
2. Georges, D. (2020), Towards Optimal Architectures for Hazard Monitoring Based on Sensor Networks and Crowdsensing, *IDRiM 2019 Conference Special Issue, Journal of Integrated Disaster Risk Management, Vol 10, Issue 1, 2020*, *https://doi.org/10.5595/001c.17963*.
3. Besançon, G. (Ed.) (2007). Nonlinear Observers and Applications, *Lecture Notes in Control and Information Sciences 363, Springer-Verlag, berlin Heidelberg.*

4. Rao, C.V.; Rawlings, J.B.; Maynes, D.Q (2003), Constrained State Estimation for Nonlinear Discrete-Time Systems: Stability and Moving Horizon Approximation*, IEEE Transactions on Automatic Control. 48 (2): 246–258, doi:10.1109/tac.2002.808470.*
5. Gupta, P., Zan T., Wang, M., Sauwels, J., and Ukil, A. (2018), Leak detection in low-pressure gas distribution networks by probabilistic methods, *Journal of Natural Gas Science and Engineering 58, pp. 69-79, https://doi.org/10.1016/j.jngse.2018.07.012*.
6. Kim, J., Chae, M., Han, J., Park, S., and Lee, Y. (2021), The development of leak detection model in subsea gas pipeline using machine learning, *Journal of Natural Gas Science and Engineering 94, https://doi.org/10.1016/j.jngse.2021.104134*.
7. Pérez-Pérez, E.J., Lopez-Estrada, F.R., Valencia-Palomo, G., Torres, L., and Puig, V. (2021), Leak diagnosis in pipelines using a combined artificial neural network approach, *Control Engineering Practice 107.*
8. Quy, T.B., Kim, J.-M. (2021) Real-Time Leak Detection for a Gas Pipeline Using a k-NN Classifier and Hybrid AE Features. *Sensors 2021, 21, 367*, *https://doi.org/10.3390/s21020367*.
9. Sundar, K., A. Zlotnik (2019), State and Parameter Estimation for Natural Gas Pipeline Networks Using Transient State Data, *IEEE Transactions on Control Systems technology, Vol. 27, Issue: 5, pp. 2110-2124. https://doi.org/10.1109/TCST.2018.2851507*.

# Bayesian updating and reliability analysis for nuclear containment buildings

Donatien Rossat, Université Grenoble Alpes, CNRS, Grenoble INP, 3SR & Electricité de France (EDF/DIPNN/DT) – donatien.rossat@univ-grenoble-alpes.fr

Julien Baroth, Université Grenoble Alpes, CNRS, Grenoble INP, 3SR – julien.baroth@univ-grenoble-alpes.fr

Matthieu Briffaut, Université de Lille, CNRS, Centrale Lille, LaMcube – matthieu.briffaut@centralelille.fr

Frédéric Dufour, Université Grenoble Alpes, CNRS, Grenoble INP, 3SR – frederic.dufour@univ-grenoble-alpes.fr

Alexandre Monteil, Electricité de France (EDF/DIPNN/DT) – alexandre.monteil@edf.fr

Benoît Masson, Electricité de France (EDF/DIPNN/DT) – benoit.masson@edf.fr

Sylvie Michel-Ponnelle, Electricité de France (EDF/R&D) – sylvie.michel-ponnelle@edf.fr

## Extended abstract

Double-walled reactor buildings of French 1300-1450 MWe nuclear power plants constitute large reinforced and prestressed concrete structures, whose integrity plays a crucial role in their serviceability and the safety of their surrounding environment. In particular, the leak tightness of the inner containment wall is periodically evaluated through pressurization tests, and compared to a regulatory leak threshold which should not be exceeded. Leak tightness of nuclear containment buildings (NCB) may evolve over time under the action of operating loads, and complex multi-physical processes related to aging, such as drying, creep and shrinkage. Today, a wide range of models aiming at describing the thermo-hydro-mechanical and leakage (THML) behaviour of concrete has been developed in the literature. This enabled to devise deterministic computational strategies aiming at accurately assessing the behaviour of NCB at structural scale. Such strategies are based on several parameters, describing material properties, loading and numerical parameters. Nevertheless, due to intrinsic variability or a lack of knowledge, such parameters may be sensibly uncertain.

Besides, aging large concrete structures such as NCB are carefully monitored: observations of their delayed mechanical behaviour are continuously collected over time, whereas observations of their leakage rate are collected during pressurization tests. Then, such observation data may be used in order to infer input parameters, and eventually reduce their uncertainties. In this perspective, Bayesian inference offers a probabilistic framework which allows to update uncertainties of input parameters, by combining a prior state of knowledge to observation data of the system response.

Then, a Bayesian updating framework suitable for aging large concrete structures is presented. The proposed framework is based on a complex THML modelling strategy [1] involving several uncertain parameters. Such a modelling strategy is based on chained finite element calculations aiming at assessing the thermal, hydrous, mechanical and leakage behaviour of concrete at structural scale. The whole THML computational chain may be seen as a deterministic function $M : D_{\boldsymbol{X}} \subseteq \mathbb{R}^d \rightarrow D_{\boldsymbol{Y}} \subseteq \mathbb{R}^n$, which maps a set of input parameters $\boldsymbol{x} \in D_{\boldsymbol{X}}$ to a response $\boldsymbol{y} = M(\boldsymbol{x}) \in D_{\boldsymbol{Y}}$. The response of the THML model includes several physical variables of interest such as temperature, strains or leakage rate of the structure. The uncertain parameters of the model $M$ are modelled by a random vector $\boldsymbol{X}$

with density $\pi(\boldsymbol{x})$. The latter summarizes the degree of knowledge in the input parameters, and is usually known as the *prior* density in the framework of Bayesian inference [2].

Then, provided that a prior density has been elicited for the uncertain inputs $\boldsymbol{X}$, the uncertainties of the model response $M(\boldsymbol{X})$ induced by the uncertainties of $\boldsymbol{X}$ can be quantified, through a first prior uncertainty propagation step. To that end, random sampling techniques (such as Monte Carlo or Quasi-Monte Carlo approaches) may be used. Nevertheless, such approaches are computationally intractable, since a single call to the THML model requires a non-negligible cost (~10 minutes per call). Then, Polynomial Chaos Expansions (PCE) surrogate models [5,6] are constructed, in order to provide an approximation $\widehat{M} \approx M$ of the model by a truncated series expansion of multivariate polynomials, which are orthonormal with respect to the prior density. Such an approximation may subsequently be used for computing low-order moments of the THML response (i.e. mean or variance), and more generally for estimating the distribution of the model outputs. In particular, one is interested in estimating the probability that the structural leakage rate $Q = Q(\boldsymbol{X})$ of the structure exceeds a regulatory threshold value $q_*$, which writes:

$$P_f = \mathbb{P}(Q > q_*) = \int_{D_{\boldsymbol{X}}} \mathbf{1}_F(\boldsymbol{x})\pi(\boldsymbol{x})\mathrm{d}\boldsymbol{x} \tag{1}$$

where $F = \{\boldsymbol{x} \in D_{\boldsymbol{X}} : Q(\boldsymbol{x}) > q_*\} \subset D_{\boldsymbol{X}}$ is the so-called *failure event,* and $\mathbf{1}_F$ denotes the indicator function of $F$. A wide class of Structural Reliability (SR) methods enable to estimate failure probabilities (1), including Monte Carlo simulation, Line Sampling, and Subset Simulation (SuS) [4].

Then, let $\boldsymbol{y} \in D_{\boldsymbol{Y}}$ be observed data related to the structure's response (such as delayed strains or leakage rate), namely a realization of random observables $\boldsymbol{Y}$. Bayes' rule enables to derive the expression of the *posterior* density of input parameters [2], namely the conditional density of $\boldsymbol{X}$ knowing $\boldsymbol{Y} = \boldsymbol{y}$:

$$\pi(\boldsymbol{x}|\boldsymbol{y}) = \frac{\pi(\boldsymbol{x})L(\boldsymbol{x};\boldsymbol{y})}{C} \tag{2}$$

where $L(\boldsymbol{x};\boldsymbol{y})$ is the so-called *likelihood function*, which stems from an assumed probabilistic model linking observations and the model outputs, and $C$ is a normalization constant known as *model evidence*:

$$C = \int_{D_{\boldsymbol{X}}} L(\boldsymbol{x};\boldsymbol{y})\pi(\boldsymbol{x})\mathrm{d}\boldsymbol{x} \tag{3}$$

The posterior density (2) summarizes all available information about parameters $\boldsymbol{X}$ once observation data have been collected and analyzed. It represents an updated state of knowledge, which stems from the combination of the prior state and noisy observation data.

For computational purposes, the posterior density (2) and the model evidence (3) are determined in the so-called BuS (Bayesian updating with Structural reliability methods) [2,3], which reformulates classical Bayesian inference into a SR problem. Such an equivalent SR problem may be solved by using a modified version of the SuS algorithm [3], which enables to draw samples from the posterior distribution (see Figure 1) as well as estimating the model evidence (3). The obtained posterior samples may subsequently propagated through the THML model for performing new predictions of the THML response of the studied structure (see Figure 2).

Then, following [2], a posterior SR analysis may be conducted (see Figure 3), in order to estimate the posterior failure probability defined by:

$$P_{f|\boldsymbol{y}} = \mathbb{P}(Q > q_* \mid \boldsymbol{Y} = \boldsymbol{y}) = \int_{D_{\boldsymbol{X}}} \mathbf{1}_F(\boldsymbol{x})\pi(\boldsymbol{x}|\boldsymbol{y})\mathrm{d}\boldsymbol{x} \tag{4}$$

The above probability is estimated through a two-stage SuS algorithm. This probability expresses an updated quantification of the risk of exceeding a regulatory leakage threshold valuer, after collecting information about the physical behaviour of the structure.

Then, the proposed approach is illustrated through an application to a full-scale operating NCB. Results underline that the proposed approach enables to reduce uncertainties of input parameters throughout the structure's life, and may be used for providing decision aid in the framework of the maintenance of containment structures.

**Figure 1.** Posterior input parameters of the THML model – Univariate and bivariate marginals.

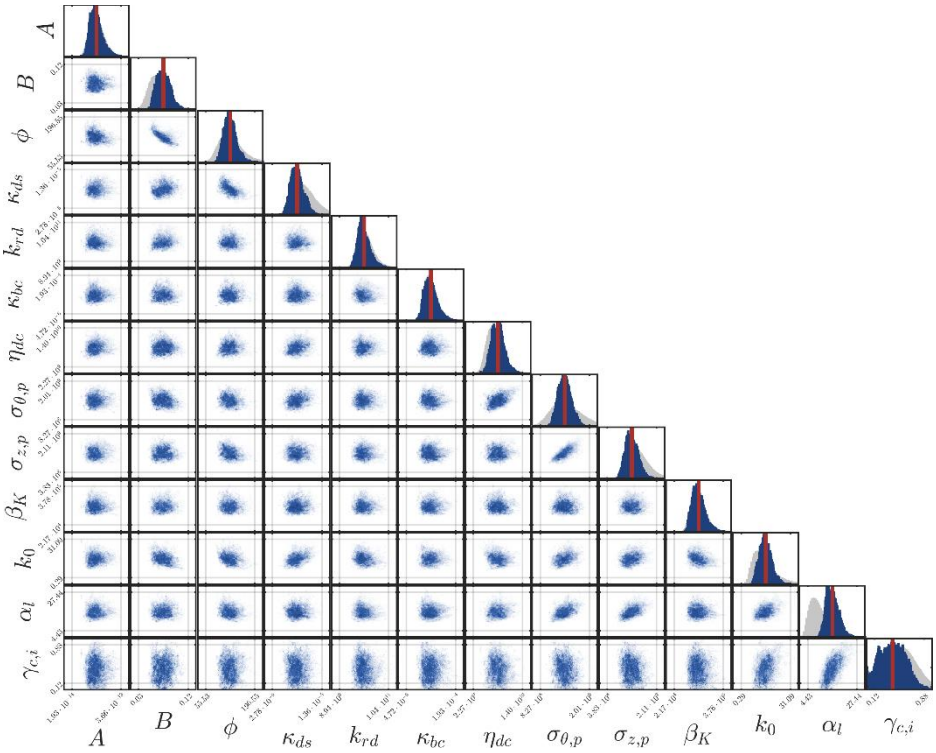


**Figure 2.** Prior (left) and posterior (right) predictions of the time evolution of tangential strains of the NCB standard zone.

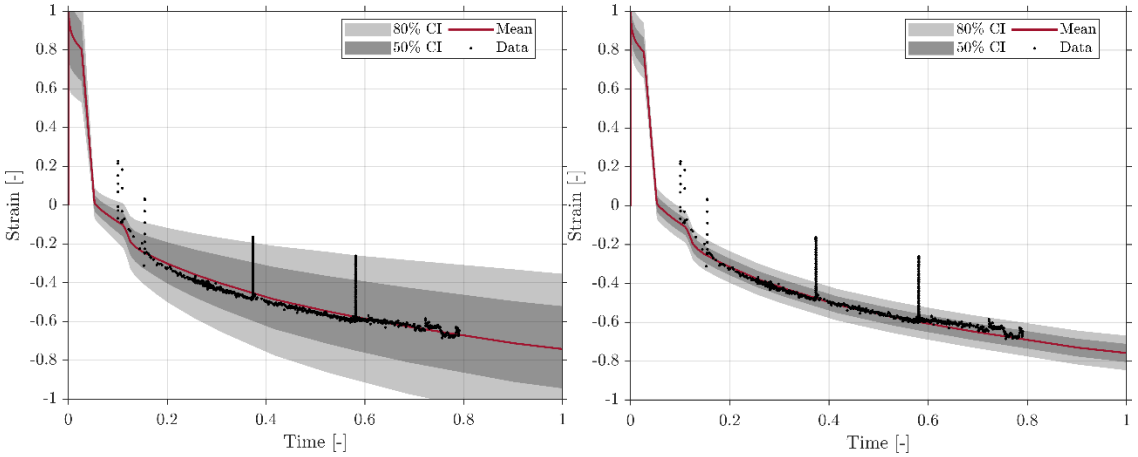

**Figure 3.** Empirical CDFs of the structural leakage rate, for several coating repair works scenarii.

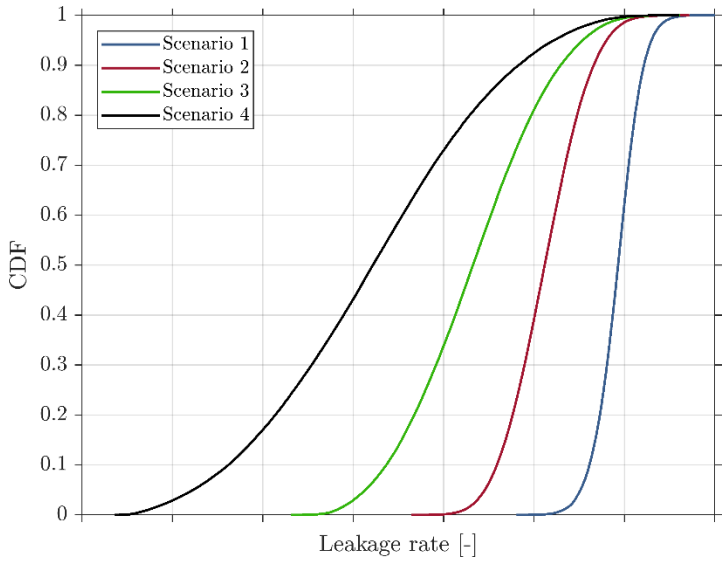


## References


1. Bouhjiti, D. E.-M.; Boucher, M.; Briffaut, M.; Dufour, F.; Baroth, J. & Masson, B. Accounting for realistic Thermo-Hydro-Mechanical boundary conditions whilst modeling the ageing of concrete in nuclear containment buildings: Model validation and sensitivity analysis. *Engineering Structures*, 2018, 166, 314-338, https://doi.org/10.1016/j.engstruct.2018.03.015

2. Straub, D.; Papaioannou, I. & Betz, W. Bayesian analysis of rare events. *Journal of Computational Physics*, 2016, 314, 538-556, https://doi.org/10.1016/j.jcp.2016.03.018

3. Betz, W.; Papaioannou, I.; Beck, J. L. & Straub, D. Bayesian inference with Subset Simulation: Strategies and improvements. *Computer Methods in Applied Mechanics and Engineering*, 2018, 331, 72-93 https://doi.org/10.1016/j.cma.2017.11.021

4. Au, S.-K. & Beck, J. L. Estimation of small failure probabilities in high dimensions by subset simulation. *Probabilistic Engineering Mechanics*, 2001, 16, 263-277, https://doi.org/10.1016/S0266-8920(01)00019-4

5. Ghanem, R. & Spanos, P. Stochastic finite elements - A spectral approach. *Springer Verlag*, 1991, https://doi.org/10.1007/978-1-4612-3094-6

6. Blatman, G. & Sudret, B. Adaptive sparse polynomial chaos expansion based on Least Angle Regression. *Journal of Computational Physics*, 2011, 230, 2345-2367, https://doi.org/10.1016/j.jcp.2010.12.021

# Simulation Supported Bayesian Network Approach for Performance Assessment of Complex Infrastructure Systems

Mohsen Jafari Songhori, Claudia Fecarotti, and Geert-Jan van Houtum, Department of Industrial Engineering and Innovation Science, Eindhoven University of Technology, P.O. Box 513, 5600 MB Eindhoven, The Netherlands, mj2417@gmail.com, c.fecarotti@tue.nl, G.J.v.Houtum@tue.nl

## 1 Introduction

With increasing traffic demand, aging infrastructure, and higher user expectations, bridge network managers seek tools & approaches by which they can maintain the normal service performance of bridge networks.

In order to achieve such a goal, decision makers of a bridge network can take different actions to improve their system performance. For instance, they can change traffic flow and distribution of loads on some bridges. Alternatively, they can invest on improving structural health monitoring of a subset of bridges. While often such tasks can improve a bridge network performance, with a limited budget, infrastructure system managers need to choose only a subset of (instead of all) of them.

Relevantly, decision makers can largely benefit from a modelling tool that enables them to conduct scenario-based analyses, and assess (aggregated) system level performance consequences of bridge level repair & reinforcement decisions. Similarly, their decisions are likely to be improved if they can also evaluate system level consequences of road level traffic decisions (e.g., changing intensity of traffic flow on a road by opening/closing some lanes). In this line of thought, this paper presents a modelling tool that facilitates these system level assessment of bridge network performance.

## 2 Contribution and novelty

From problem definition aspect, our work considers both infrastructure owner's cost and user cost (i.e., travel time) within a bridge network. Therefore, our approach is likely to provide a more precise picture of the state of the infrastructure system (i.e., bridge network) than other studies which use only either of those measures, or focus only on connectivity aspect of an infrastructure system (Gehl et al, 2018). Moreover, in order to calculate travel costs, this work takes the Markov Chain Traffic Assignment (MCTA) approach developed in (Salman and Alaswad, 2018) to model traffic dynamics and calculate the expected travel time based on the availability bridges.

With regard to modelling perspective, this paper proposes a new methodology to model a bridge network system. That is, we base our method on the recently introduced concept of a Simulation Supported Bayesian Network (SSBN) (El-Awady and Ponnambalam, 2021). With SSBN, simulation is used as a source information to build the desired BN model of a system.

As monitoring of actual conditions of bridges can be difficult (Orcesi and Cremona, 2010), our method (which is based on SSBN and uses simulation to build the desired Bayesian Network model of a system) can be suitable for such systems. Lastly, we take the previously built Bayesian Network (BN) model for bridge networks by (Wang et al, 2020), and improve it by considering economic dependencies among bridges.

## 3 Methodology

In this paper, we define a bridge network as a transportation road network in which bridges (each located on a road) are the only components that deteriorate and can fail. In addition, we mainly discuss steps and illustrate results of applying our methodology on

a small scale bridge network shown in Figure 1, and we refer to it as "the focal bridge network" or "the system". Two key aspects of the proposed method are *system decomposition & integration of simulation results into a BN* model. By conducting the decomposition process, we develop three layers of system resolution. Initially, we label the whole system level as layer L = 0 (see Figure 1). Next, the system as a whole is broken down into the road sections (which on each, one bridge is located). The road sections collectively form layer L = 1. Lastly, for each of those road sections, bridge maintenance features (e.g., maintenance advised rate according to the asset management strategies of the bridge network owner) are recognised, and placed at the last layer, layer L = 2.

**Figure 1.** The focal bridge network & its corresponding three layers of system resolution.

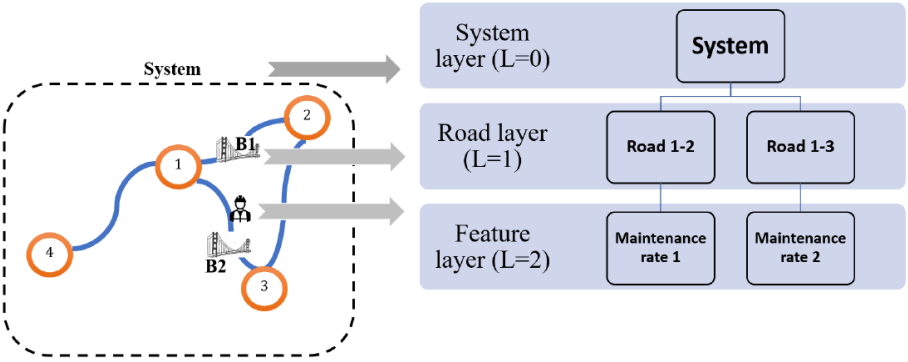


In addition to system decomposition, integration of simulation results into a BN model enables us to analyse dependence of system-level (layer L = 0) performance variables on feature variables at the last layer, layer L = 2. Such integration involves three processes. At first, we define random variables at each layer $L \in \{0,1,2\}$. As shown in Figure 2, at layer L = 0, two performance random variables are total costs & expected travel time. In the next layer, layer L =1, the corresponding random variables are road costs & availability. On the last layer, maintenance rates are the variables of interest.

In the second process, at each layer $L \in \{1,2\}$, we add directed arcs from a random variable to a related random variable at layer L = 1 if the corresponding system part of the former is dependent on that of the latter in the system resolution. For instance, in Figure 1, the costs & availability of road 1-2 depend on the maintenance rate 1, and therefore, in Figure 2, we elaborate arcs from the defined random variable "maintenance rate 1" to "road 1-2 cost" & "road 1-2 availability".

In the third process, we use the results of the simulation experiments to materialize the conditional dependencies among the random variables identified in the second process. That is, we conduct simulations for each random variable at layers $L \in \{0,1\}$, their results are used to elaborate conditional dependence of the corresponding random variables (e.g., conditional dependence of "road 1-2 availability" on "maintenance rate 1" in Figure 2).

Overall, the methodology consists of the following two steps: (1) *Step 1*- model bridge network and evaluate availability & maintenance costs of road section with bridges (via using a Markov Chain model for state evolution of bridges), (2) *Step 2*-analyze travel time and costs of the whole system by:

- (a) Estimating system level maintenance costs and expected travel time by means of simulation based on input from step 1,
- (b) Building the BN of the transportation network. The simulation results from steps 1 & 2-a are used to build the BN model, including its structure and the conditional probability tables.

**Figure 2.** The BN structure of the focal bridge network in three layers which have direct correspondence with system resolution layers..

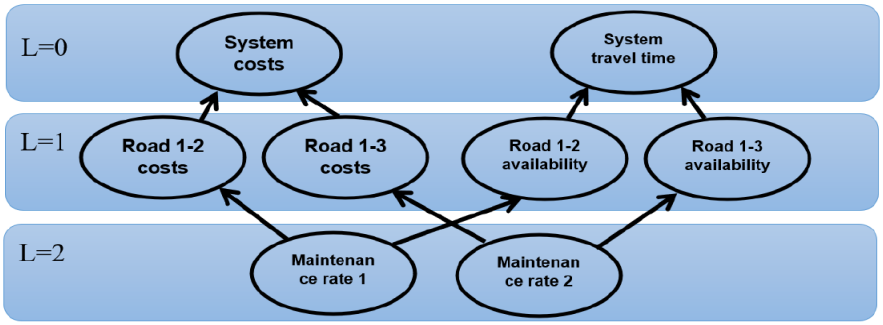


# 4 Discussion

The presented approach can be used by infrastructure managers as a scenario-analysis tool to support decisions related to maintenance of bridges. For its applicability to large scale networks, we adapt it as follows. We add an additional step to the methodology which uses MCTA & the recently developed KDA algorithm (Berkhout and Heidergott, 2019) to identify subnetworks which can be considered as independent according to their traffic dynamics. In the BN model this change will translate into an additional layer between the "system" layer (whole network, currently layer L = 0) and the road sections layers (currently L = 1).

## References


1. Berkhout, J., & Heidergott, B. F. (2019). Analysis of Markov influence graphs. *Operations Research*, 67(3), 892-904.
2. El-Awady, A., & Ponnambalam, K. (2021). Integration of simulation and Markov Chains to support Bayesian Networks for probabilistic failure analysis of complex systems. *Reliability Engineering & System Safety*, 211, 107511.
3. Gehl, P., Cavalieri, F., & Franchin, P. (2018). Approximate Bayesian network formulation for the rapid loss assessment of real-world infrastructure systems. *Reliability Engineering & System Safety*, 177, pp. 80-93.
4. Orcesi, A. D., & Cremona, C. F. (2010). A bridge network maintenance framework for Pareto optimization of stakeholders/users costs. *Reliability Engineering & System Safety*, 95(11), 1230-1243.
5. Salman, S., & Alaswad, S. (2018). Alleviating road network congestion: Traffic pattern optimization using Markov chain traffic assignment. *Computers & Operations Research*, *99*, pp. 191-205.
6. Wang, J., Fang, K., Li, S., & He, S. (2021). Bayesian network-based vulnerability assessment of a large-scale bridge network using improved ORDER-II-Dijkstra algorithm. *Structure and Infrastructure Engineering*, 17(6), 809-820.

# Applying deep reinforcement learning to improve the reliability of an infrastructure network

Jose Carlos Hernandez Azucena, Henley Wells, Haitao Liao, Kelly Sullivan and Edward A. Pohl, Department of Industrial Engineering, University of Arkansas, epohl@uark.edu

## Abstract

*Maximizing connectivity is one of the most critical requirements in constructing an infrastructure network. In practice, the goal could only be achieved after completing a sequence of possible actions. This work examines an infrastructure network needing reliability improvement concerning all-terminal reliability. Given the initial structure, the objective is to maximize the network's all-terminal reliability by adding edges under several practical constraints, such as the total budget and available types of edges for each step. To solve the complex optimization problem, the potential of using Deep Reinforcement Learning (DRL) is investigated in this work. To allow for quick testing and prototyping of the DRL method, a computational environment is developed by integrating OpenAI-Gym and Stable Baselines. Specifically, a Proximal Policy Optimization (PPO) agent capable of sequentially deciding the addition of new edges in a connected network is created first, and the network structure evolves as appropriate edges are added subject to the total budget that constrains the number and types of available edges at each decision-making epoch. Technically, the proposed computational environment recurrently formulates and evaluates the network's all-terminal reliability by computing the corresponding reliability polynomial. To facilitate the implementation of DRL in solving such problems, different methods are explored with the help of a permanent database that stores previously observed network states without recalculating their polynomials. Numerical examples for given initial structures are provided to illustrate the potential of using DRL in achieving reliability improvements for infrastructure networks.*

# 1 Introduction

Infrastructure networks, such as highways, communication networks, power networks, and water networks, play an essential role in our daily activities. Unfortunately, natural disasters and malicious attacks pose serious threats to these infrastructure networks. Historically, many failures in infrastructure networks occurred which have caused issues for many people. One well-known example is the 2003 Northeast blackout that affected fifty million people in the United States and Canada [1]. Another failure in infrastructure networks include the levee failure in Louisiana during Hurricane Katrina [2]. The levees in Louisiana were not adequately prepared to handle the water from Hurricane Katrina, thus, they breeched due to the pressure and caused much of New Orleans to flood. Clearly, these examples show how essential it is to ensure infrastructure networks are reliable.

To quantify the reliability of an infrastructure network, one essential task is to investigate the connectivity of components in the network. Mathematically, the problem can be formulated as an all-terminal network reliability problem. In practice, quite a few infrastructure networks can be modelled as an all-terminal network, such as highways, communication networks, power networks and water networks. To calculate all-terminal network reliability, numerous methods have been used. These methods provide either an exact value or an estimate of the reliability. Ball et al. [3] summarizes exact methods for calculating network reliability such as exponential time exact algorithms for general networks and polynomial time exact algorithms for restricted classes of networks, as well as other methods such as bounds on network reliability, and Monte Carlo simulation. Gaur et al. [4] also detailed many different network reliability methods including state enumeration, minimal cut, and neural networks, and they discussed the limitations of each method. Technically, cut enumeration entails enumerating the minimal subsets of links whose failure causes the network to fail. This method is an exact method and very useful for small networks, but it reaches its computational limitations very quickly. Monte Carlo

simulation (MCS) methods choose a random sample of states to explore and estimate the network reliability as the proportion of sampled states in which the network is functioning properly. Karger [5] found one of the flaws of the MCS approach is that it is very slow when the probability of failure is very low. Cardoso et al. [6] studied Monte Carlo simulation in conjunction with neural networks to investigate the structural reliability of different structures. MCS only allows one network structure to be calculated at a time, so it can be very time consuming to calculate the reliability. As a solution, they combined neural networks with MCS which allowed them to save computational time and obtain more precise reliability measurements.

Srivaree-ratana et al. [7] used an Artificial Neural Network (ANN) to estimate network reliability. In their study, they trained the ANN using a set of network topologies and link reliabilities. They then used the ANN to estimate the network reliability based on the link reliabilities and the topology in finding the optimal network topology by simulated annealing. They demonstrate that their approach performs well empirically through comparisons to an exact approach as well as to an upper bound derived from a polynomial time algorithm. However, the disadvantages of their method are that the training of ANN needs to be performed first for a topology of a fixed number of nodes and optimal network design can be carried out only for this topology. It would be more useful to develop a method that finds the optimal network via reliability evaluation and learning without such limitations.

In this paper, a new method based on Deep Reinforcement Learning (DRL) along with the use of a reliability polynomial is proposed for maximizing the all-terminal reliability of a network under the constraints on total budget and available types of edges for each step. To demonstrate the use of the proposed method, the initial structures of example networks are in the form of all nodes being connected in series. It is worth pointing out that although this paper focusses on maximizing the all-terminal reliability of a network by adding additional links, the proposed method can be extended to solve network design problems with the flexibility of adding additional nodes.

The remainder of this paper is organized as follows. Section 2 describes the reliability model for an infrastructure network and the method of calculating all-terminal reliability using a reliability polynomial. Section 3 introduces the proposed DRL method for network reliability improvement and elaborates on several important computational issues. Section 4 provides numerical examples to illustrate the use of the proposed method in improving infrastructure network reliability. Finally, we summarize our results and draw conclusions in Section 5.

# 2 Reliability model for an infrastructure network

An infrastructure network can be described by a network model, which in its simplest form is a collection of nodes connected by edges. Chartrand [8] formally defines a general network using the notation $N = (V, E, w)$, where $V$ is the set of nodes (e.g., $v_1$, $v_2$, …, $v_n$) and $E$ is the set of edges (e.g., $e_{1,2}$, …, $e_{i,j}$, …, $e_{n-1,n}$) with the corresponding weights given in w. In this paper, the weights of the edges are the corresponding reliability values. Moreover, networks can either be directed or undirected. In this work, an infrastructure network is modelled as an undirected network, and reliability improvement decisions are made with respect to the network's all-terminal reliability.

## 2.1 All-terminal reliability of a network

The probability that a network is performing its intended function at a given point in time is known as its reliability. Specially, the two-terminal reliability of a network is the probability of having at least one operational path between the source and end nodes. Consider the simple undirected network shown in Figure 1. The network has four nodes and five links with corresponding reliability values. If node 1 and node 4 are the source and end nodes, respectively, and the nodes are perfectly reliable, the two-terminal

reliability of the network can be calculated by considering three possible paths: for path 1-3-4, the reliability is $R_1 = 0.85(0.8) = 0.68$; for path 1-4, the reliability is $R_2 = 0.95$; for path 1-2-4, the reliability is $R_3 = 0.9(0.75) = 0.675$. Since the three paths are in parallel, the two-terminal reliability of the network is simply $R = 1 - (1 - R_1)(1 - R_2)(1 - R_3) = 0.9948$.

**Figure 1.** An example of simple series-parallel network.

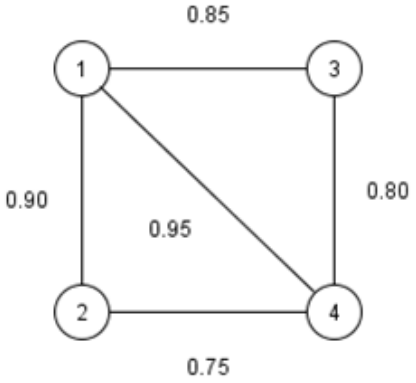


Unlike two-terminal reliability problems, all-terminal reliability problems are interested in that every node in the network is connected to every other node, and the reliability is defined as the probability that the network is fully connected. Consider an *n*-node network (*V*, *E*, *w*) with edge topology $X = [x_{1,2}, \ldots, x_{i,j}, \ldots, x_{n-1,n}]$ with $x_{i,j} = \{1$, if edge $e_{i,j}$ is present; 0, otherwise$\}$. Let $p(x_{i,j})$ be the reliability of edge $e_{i,j}$. Then, the all-terminal reliability of the network can be expressed as [7]:

$$R = \sum_{X' \in \Omega} \left[\prod_{(i,j) \in X'} p(x_{i,j})\right] \left[\prod_{(k,l) \in (X \setminus X')} (1 - p(x_{k,l}))\right] \quad (1)$$

where $\Omega$ consists of all operational states (i.e., edge subsets $X' \subseteq E$ that connect all nodes in the network). For example, to calculate the all-terminal reliability of the network in Figure 1, we can simply calculate the probabilities of all network configurations where all nodes remain connected even if one or more edges fail. Then, after adding all the probabilities together, we obtain the all-terminal network reliability to be 0.9414. Clearly, it becomes more difficult to calculate all-terminal reliability for complex networks with more nodes and edges [9].

## 2.2 Reliability polynomial for all-terminal reliability evaluation

The all-terminal reliability of a network can be expressed as a function of the edge reliabilities. This expression is a property arising from the network topology, and it is often known as the reliability polynomial of the network. For a network *N*, when all edges have identical and constant reliability of *r*, the all-terminal reliability is equivalent to [10]:

$$RP(r) = r^{n-c}(1 - r)^{m-n+c} T(1, (1 - r)^{-1}) \quad (2)$$

where *n* is the number of nodes, *m* is the number of edges, and *c* is the number of connected components. *T* is the Tutte Polynomial of the network, a property arising from the network topology, defined as [11]:

$$T(x, y) = \sum t_{i,j} x^i y^j \quad (3)$$

where $t_{i,j}$ represents the number of spanning trees of the network whose internal activity is *i* and external activity is *j*. The summation is over all the subgraphs in the network [11].

### 2.2.1 Basic method

While this polynomial can be computed using Equation (2) for the identical reliability case, our algorithmic procedure keeps track of the individual link reliabilities. The resulting expression of the all-terminal reliability is an equation that takes the link reliabilities as arguments.

Using an algorithmic procedure to create a symbolic representation of this polynomial, we can automate the algebraic expression for any arbitrary network *N*. This allows for computing the polynomial once per every network configuration. It is enough for any specific edge reliability values to replace the appropriate variables in the reliability polynomial to calculate the all-terminal reliability. As computing time grows with the number of edges, in our experiments, we limit our networks to at most 10 nodes and 20 edges with no parallel edges between any two nodes.

For the network topology presented in Figure 1, the reliability polynomial that represents the all-terminal reliability if all the identical links are identical is:

$$RP(r) = 4r^5 - 11r^4 + 8r^3 \tag{4}$$

For a more general case with nonidentical links, the reliability polynomial is:

$$\begin{aligned} RP(\{r_{12}, r_{13}, r_{14}, r_{24}, r_{34}\}) = {} & 4r_{12}r_{13}r_{14}r_{24}r_{3,4} - 2r_{12}r_{13}r_{14}r_{24} - 2r_{12}r_{13}r_{14}r_{34} \\ & + r_{12}r_{13}r_{14} - 3r_{12}r_{13}r_{24}r_{34} + r_{12}r_{13}r_{24} \\ & + r_{12}r_{13}r_{34} - 2r_{12}r_{14}r_{24}r_{34} + r_{12}r_{14}r_{34} \\ & + r_{12}r_{24}r_{34} - 2r_{13}r_{14}r_{24}r_{34} + r_{13}r_{14}r_{24} \\ & + r_{13}r_{24}r_{34} + r_{14}r_{24}r_{34} \end{aligned} \tag{5}$$

By substituting the link reliability values as shown in Figure 1 into this equation, we arrive at the same network reliability value of 0.9414 as we obtained earlier.

### 2.2.2 Computational Algorithm

---

**Algorithm 1.** Recursion-based Reliability Polynomial
RecursiveReliabilityPolynomial($N$) :
1 : *Input* ← $N$ ={*V* = {1,2,3,…,*n*}, *E* = $\{e_{ij}\}$, $R = \{r_{ij} = p(x_{ij})\}$}
2 : **If** $N$ is not connected:
3 : **Set** *Output* ← 0
4 : **Else If** |*V*| > 0 :
5 : **Set** $e_{kl}$ ← First element in *E*
6 : **Set** $N_{contracted}$ ← $N$ with $e_{kl}$ contracted
7 : **Set** $N_{deleted}$ ← $N$ with $e_{kl}$ removed
8 : **Set** $RP_{contracted}$ ←RecursiveReliabilityPolynomial($N_{contracted}$)
9 : **Set** $RP_{deleted}$ ←RecursiveReliabilityPolynomial($N_{contracted}$)
10 : **Set** $\mathrm{RP}_N \leftarrow r_{kl} * RP_{contracted} + (1 - r_{kl}) * RP_{deleted}$
11 : **Set** *Output* ← $RP_N$
12 : **Else** :
13 : **Set** *Output* ← 1
14 : **end**
23 : **Return** *Output*

---

We have tested computing the polynomial using recursive and enumerative methods. The recursive methods rely on finding the subgraphs by contracting or removing edges in the network and applying the same procedure to each substructure until reaching disconnected or fully connected states while keeping track of the symbolic multiplications. The

enumerative methods list all the possible states on which the edges can be configured, remove the ones that result in a disconnected network, and apply the appropriate operations on the reliability variables to obtain the polynomial.

**Algorithm 2.** Enumeration-based Reliability Polynomial

```
Input ← N = {V={1,2,3,…,n}, E ={e_ij},  R = {r_ij = p(x_ij)}}
Set n_nodes ← |V|
Set n_edges ← |E|
Set PossibleStates ← ∏_{i=1}^{n_edges} {0,1}_i = {0,1}_1 × {0,1}_2 × … × {0,1}_{n_edges}
Set FeasibleStates ←{Combination ∈ PossibleStates such that ∑Combination ≥ (n_nodes − 1)}
Set Terms ← {Empty Set}
For each Combination in FeasibleStates :
    N_temp ← N ={V = {1,2,3,…,n}, E={e_ij if S_ij is 1}, R ={r_ij = p(x_ij)}
    If N_temp is connected :
        Set Result ← 1
        For each S_ij in Combination :
            If S_ij is 1 :
                Result ← r_ij*Result
            Else If State is 0 :
                Result ← (1-r_ij)*Result
            end
        end
    Else :
        Set Result ← 0
    end
    Append Result to Terms
end
Set Output<-∑Terms
```

In Algorithm 2, the *PossibleStates* are composed of arrays of zeros and ones that denote if the corresponding edges present or not. Each of these arrays is considered a *Combination* and each combination is composed of states $S_{ij}$ that represent if the edge is included in the configuration or not. As a connected network needs at least $n_{nodes} - 1$ edges, we filter those combinations that are guaranteed to lead to disconnected configurations before evaluation.

The recursive algorithm is based on a similar approach designed for the case with identical links [12]. We have modified this procedure to account for the individual edge reliability values. The final algorithm keeps track of the individual edges. We use the enumeration-based version to validate our results. To further exploit reusing these polynomials, we use a NoSQL database based on MongoDB [13] to store the precomputed representations. To account for the potentially large equations, we also use GridFS for a distributed storage of files [14].

# 3 Reliability improvement using deep reinforcement learning

ANNs are based on the biological neural networks within the human body. Just like the brain, the components of ANNs work together in parallel and series to learn based on experiences. This learning occurs using a training set which is a set of inputs with known, target outputs.

In sequential decision-making, ANN can be used to create functional maps from system states or observations to the best action among a finite set of possible actions. In general, when the decision system is trained in a loop that assigns rewards to any of the actions taken, and the system learns the mapping from actions and observations to rewards, this is known as Reinforcement Learning (RL). When the function mapping the relationship between actions, observations, and rewards is an ANN, it is known as Deep Reinforcement Learning (DRL) [15].

## 3.1 Problem Formulation

For reliability improvement, this takes the form of deciding the best next edge to add to an infrastructure network to maximize the all-terminal reliability. When it is also possible to choose the quality of the new edges, the decision space grows. By considering cost constraints on the decision problem, the edge quality affects the reliability value and the added cost of the decision. Then, a finite sequence of edge decisions that will maximize the all-terminal reliability exists. Mathematically, the problem can formulated as follows:

$$\max_{\boldsymbol{A_t}|\boldsymbol{O_t}} \mathcal{R}_t = Log\left(R_{network,t}\right) - Log\left(1 - R_{network,t}\right) + \lambda \mathcal{R}_{t-1} \tag{6}$$

$$\boldsymbol{A_t} = [x_{ij}, q_{ij}] \tag{7}$$

$$\boldsymbol{O_t} = [\boldsymbol{x_{ij}}, c_{ij}, C_{t-1}] \tag{8}$$

$$r_{ij} = p(x_{ij}, q_{ij}) \tag{9}$$

$$\boldsymbol{s.t.} \sum_i \sum_j c_{ij} x_{ij} = C_t \leq B \tag{10}$$

On each decision step $t$, the agent decides which set of actions $\boldsymbol{A_t}$ will maximize the reward $\mathcal{R}_t$ given the observations from the environment $\boldsymbol{O_t}$. The reward is a function of the current all-terminal reliability and the value on the previous time step, discounted by a factor $\lambda$. The actions include the new edge to add, $x_{ij}$, and its quality level $q_{ij}$. Observations include the edges already in the network, the cost associated with each edge in the network, $c_{ij}$, and the total cost of the network at the previous time step $C_{t-1}$. The budget constraint keeps the current cost of the network $C_t$ within the the budget, $B$.

The current implementation uses the log-odds of the system being connected for the reward function: a transformation of the all-terminal reliability. It is worth pointing out that our initial experiments used the all-terminal reliability. We found more consistent performance using the negative log of the unreliability, and after further experiments, this led to using the log-odds of the system being connected. For actions, the options are the links not yet in the network and the quality level, with discrete options defining the edge reliability value. For the observations, the states, we propose the network topology, the cost of each link in the network, and the total cost of the current configuration. A cost constraint defines the budget for the added links limiting the number and quality of the added edges.

## 3.2 Implementation Framework

For the implementation, we base our training environment on the OpenAI-Gym framework [16]. This provides the basic elements to train and test DRL models. As there is a common interface for the models to train on, this allows for quick prototyping and testing.

Stable Baselines [17] is a set of DRL models that can be tested using the OpenAI-Gym interface. This grants access to a collection of algorithms that can be explored using an appropriate training environment. Each model is a different agent that can learn from the tuples of observations, actions, and rewards: striving to maximize the defined rewards while adjusting to the conditions posed by the environment, such as conditions for stopping and feasible actions.

### 3.2.1 Training Environment

An environment requires four basic elements: observations, rewards, actions, and a way to evolve. The current environment starts with a path network with *n* nodes, and the *n-1* links all have a reliability value of $r_0$, this makes the initial all-terminal reliability ${r_0}^{n-1}$. Then, the possible actions are $(n^2 - n)/2 - (n - 1)$ link options to add, with $q_{ij} = 1,2 \ldots m$, $m$ is the number of quality levels, with $r_{ij} = 1 - (1 - r_0)^{q_{ij}}$, which is equivalent to considering each

quality level to having $q_{ij}$ basic links in parallel. This translates into each link cost as $c_{ij} = q_{ij}$.

On each decision step, a DRL agent observes the state of the network, the connected links, the cost of each link, and the total cost. Then, it can choose one of the links to add, and one of the quality levels, if it is within budget. After adding the link, the reliability is computed from the corresponding polynomial and the different edge probabilities and the agent receives the associated reward. If the budget has not been exhausted, and there are feasible edges that can be added, the next decision step proceeds; otherwise, the episode stops.

## 3.3 Selected model

For our experiments, we work with a variant of Proximal Policy Optimization (PPO) [18]. PPO is a DRL model that explores decision policies in sets of actions that tries to balance the exploration of new decision policies with the optimization of a surrogate objective function. Specificly, it is a Policy Gradient method that limits itself to exploring points in a neighboring policy space by taking small incremental steps when the actions lead to an advantageous increase in rewards but is clipped, restricted to a neighboring range, when a disadvantageous direction is found [18]. This is designed to avoid stalling the decision in regions difficult to escape.

The variant used is a Maskable Proximal Policy Optimization (M-PPO) [19], an algorithm that considers the feasibility constraints posed by the training environment. For the formulated problem, this is equivalent to restricting the action space only to those links that are not yet in the network and are within budget. The M-PPO model uses a validity mask, a vector that keeps track of the valid actions, and operates it with the probability of taking a given action before updating the weights on each training step. This is useful to ensure the agent only learns to take feasible action and, for our problem of interest, guarantees that the network reliability increases on every decision step.

# 4 Numerical examples

Experiments for different network configurations are conducted in this section. The results presented correspond to networks with $n$=7 and $n$=10 nodes. $r_0 = 0.8$, and there are $m$=3 levels of edge reliability: 0.8, 0.96, and 0.992. The budget is set on $B$=5, so at most five links can be added.

**Figure 2.** Results for the 7-node network with $B$=5.

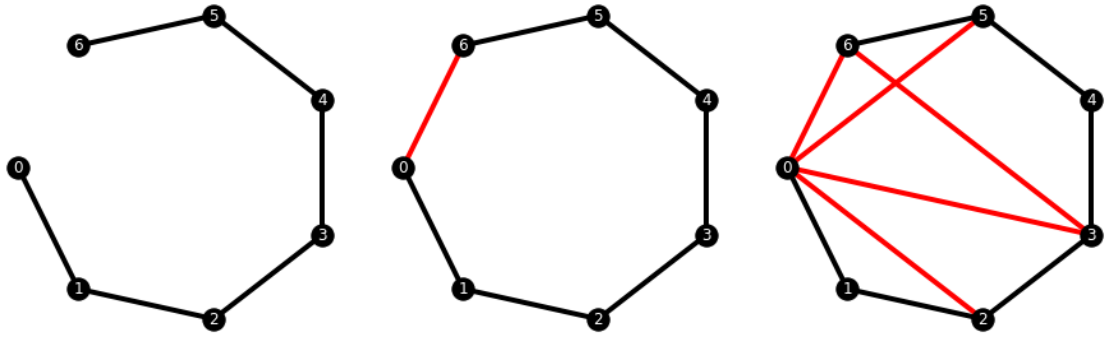


(a) (b) (c)

Figure 2 shows the results for $n$=7. The first network (a) is the original configuration. The black edges represent the original n-1 edges in the path network. The red edges represent those with $q_{ij}$=1. For this case, the DRL agent only chose to add red links: it chose to maximize connectivity versus edge quality. The second network (b) is the configuration after one decision step and the third network (c) is the configuration at the final step. The

all-terminal reliabilities are 0.26, 0.58, and 0.88 respectively. With the current approach, training the DRL agents while evaluating the reliabilities with no precomputed polynomials takes around 1.35 hours for 6144 training episodes of this experiment. This leads to an average of 0.8 seconds per training episode. The number of episodes was an arbitrary choice and further experiments are needed to decide the appropriate number of training steps, as well as to quantify the learning progress on the model. Further comparisons with baselines, such as total enumeration, are required to identify the optimality gap of the current approach.

**Figure 3.** Results for the 10-node network with $B$=5.

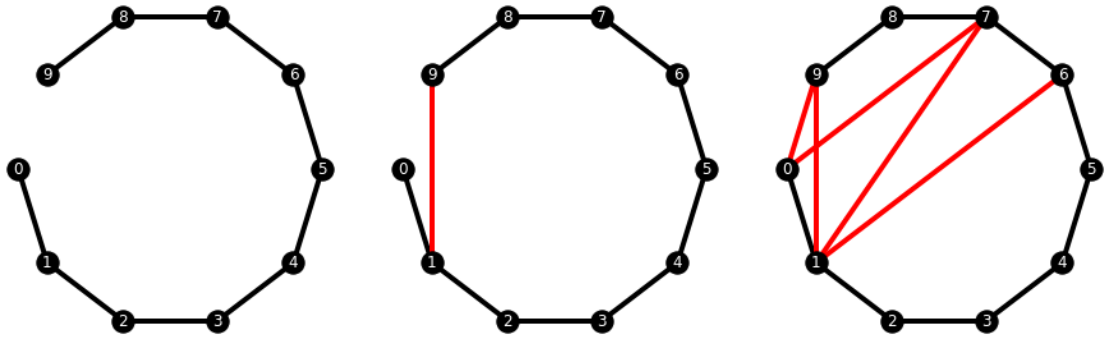


Figure 3 shows the results for $n$=10. The first network (a) is the original configuration. Again, for this case, the DRL agent only chose as many low-quality links as possible: maximizing connectivity. The second network (b) is the configuration after one decision step, and the third network (c) is the configuration at the final step, exhausting the budget. The all-terminal reliabilities are 0.1342, 0.3490, and 0.6722 respectively. With the current approach, training the DRL agents while evaluating the reliabilities with no precomputed polynomials takes around 4.36 hours for 6144 training episodes of this experiment. This leads to an average of 2.56 seconds per training episode. Similar to the previous experiment, more informed decisions about the number of episodes and procedures to performance are required.

# 5 Conclusions

The DRL method proposed in this paper enables reliability improvements of infrastructure networks. As a promising alternative to total enumeration and evolutionary optimization methods, the proposed method along with the use of reliability polynomial take advantage of machine learning capability in finding the best design of a general network with respect to all-terminal reliability. The polynomial computation is exact and challenging to scale, but as it only has to be computed once per network topology, it can be reused for different edge reliability values. This, combined with the permanent NoSQL database, allows for faster training of the DRL agents. The M-PPO model for network reliability improvement is a data-driven approach that learns to solve the sequential decisions for the network topology while considering constraints on the feasible actions. For the experiments considered, it learns to optimize the choice of edges, maximizing connectivity, and quickly improving the all-terminal reliability of the networks of interest.

For future research directions, the computed polynomial can be used to generate datasets mapping network topologies and individual edge reliabilities to all-terminal network reliability. These datasets can then be used to train surrogate models capable of approximately estimating the network reliability. The DRL agents can also be used to sequentially improve the network reliability in scenarios where each link can degrade over time and eventually fail and become disconnected. The objective is now to maximize the

network reliability while managing the new and degrading edges. For further complexity, we can include inspections, maintenance, and repairs of links among the set of actions. We are optimistic that DRL agents can handle this type of maintenance problem and be competitive in comparison with traditional process control methods.

## Acknowledgements

This research was sponsored in part by the Test Resources Management Center (TRMC) Science of Test Consortium.

## References

1. History.com Editors (2009) Blackout hits Northeast United States. Retrieved from: *https://www.history.com/this-day-in-history/blackout-hits-northeast-united-states*.
2. Pruitt, S. (2020) How Levee Failures Made Hurricane Katrina a Bigger Disaster. Retrieved from *https://www.history.com/news/hurricane-katrina-levee-failures.*
3. Ball, M. O., Colbourn, C. J. and Provan, J. S. (1995) Network Reliability. *Handbooks in Operations Research and Management Science*, vol. 7, pp. 673-762.
4. Gaur, V., Yadav, O. P., Soni, G. and Rathore, A. P. (2021) A Literature Review on Network Reliability Analysis and Its Engineering Applications. *Journal of Risk and Reliability*, vol. *235*(2), pp. 167-181.
5. Karger, D. R. (1999) A Randomized Fully Polynomial Time Approximation Scheme for the All-terminal Network Reliability Problem. *SIAM Journal on Computing,* vol. *29*(2), pp. 492-514.
6. Cardoso, J. B., de Almeida, J. R., Dias, J. M. and Coelho, P. G. (2008) Structural Reliability Analysis using Monte Carlo Simulation and Neural Networks. *Advances in Engineering Software,* vol. *39*(6), pp. 505-513.
7. Srivaree-ratana, C., Konak, A. and Smith, A. E. (2002) Estimation of All-terminal Network Reliability using an Artificial Neural Network. *Computers & Operations Research,* vol. *29*(7), pp. 849-868
8. Chartrand, G. (1977) *Introductory Graph Theory.* Courier Corporation.
9. Provan, J. S. and Ball, M. O. (1983) The Complexity of Counting Cuts and of Computing the Probability that a Graph is Connected. *SIAM Journal on Computing*, vol. 12(4), pp. 777-788.
10. Godsil, C. and Royle, G. (2001) Algebraic Graph Theory. *New York: Springer-Verlag*, pp. 354-358.
11. Biggs, N. L. (1993) "The Tutte Polynomial." Ch. 13 in Algebraic Graph Theory, 2nd ed. *Cambridge, England: Cambridge University Press*, pp. 97-105.
12. Dougherty, R. (2016) Reliability Polynomial Calculation. Retrieved from: *https://codereview.stackexchange.com/questions/131709/reliability-polynomial-calculation*
13. MongoDB, Inc. (2022). How to Use MongoDB in Python. Retrieved from *https://www.mongodb.com/languages/python*
14. MongoDB, Inc. (2021). MongoDB Manual: GridFS. Retrieved from: *https://www.mongodb.com/docs/manual/core/gridfs*
15. Arulkumaran, K., Deisenroth, M. P., Brundage, M., & Bharath, A. A. (2017). Deep reinforcement learning: A brief survey*. IEEE Signal Processing Magazine*, 34(6), 26-38.
16. Brockman, G., Cheung, V., Pettersson, L., Schneider, J., Schulman, J., Tang, J., & Zaremba, W. (2016). Openai gym. *arXiv preprint arXiv:1606.01540*.

17. Raffin, A., Hill, A., Ernestus, M., Gleave, A., Kanervisto, A., & Dormann, N. (2019). Stable baselines3. Retrieved from: *https://github.com/Stable-Baselines-Team/stable-baselines3-contrib*
18. Schulman, J., Wolski, F., Dhariwal, P., Radford, A., & Klimov, O. (2017). Proximal policy optimization algorithms. *arXiv preprint arXiv:1707.06347*.
19. Huang, S., & Ontañón, S. (2020). A closer look at invalid action masking in policy gradient algorithms. *arXiv preprint arXiv:2006.14171*.

## List of abbreviations and definitions

| | |
|---|---|
| ANN | Artificial Neural Network |
| DRL | Deep Reinforcement Learning |
| M-PPO | Maskable Proximal Policy Optimization |
| NoSQL | Not Only Structured Query Language |
| RL | Reinforcement Learning |
| PPO | Proximal Policy Optimization |

# Improved Modeling of Fault Propagation, Isolation, and Fast Service Restoration in Smart Grids

Youba Nait Belaid[1,2], Yi-Ping Fang[2], Zhiguo Zeng[2], Patrick Coudray[1], Anthony Legendre[1], Anne Barros[2]

[1] Electricité de France R&D, 7 Boulevard Gaspard Monge, 91120 Palaiseau, France
[2] Risk and Resilience of Complex Systems, Laboratoire Génie Industriel, CentraleSupélec, Université Paris-Saclay, 3 Rue Joliot Curie, 91190 Gif-sur-Yvette, France
(e-mail: youba.nait-belaid@centralesupelec.fr)

## Abstract

*Power network operators monitor the performance of grid assets through well-established Supervisory Control and Data Acquisition (SCADA) systems. Modeling the operation of these ever-sophisticated industrial control systems raises many challenges as involved smart grid components are from the power domain and information and communication technologies (ICTs) domain. The fault localization, isolation, and service restoration (FLISR) function reveals many of the complexities brought by cyber-physical interdependencies in the network. The present work proposes a detailed analysis of the FLISR function taking into account the availability of the telecommunication service. Overhead and underground lines endowed with different types of switches are considered in order to replicate important behaviors in real systems. The general problem is solved under a Mixed Integer Linear Programming (MILP) formulation that aims to enhance the primary response of the system to external events, participating to the system resilience expressed in terms of supplied load. Results stress the importance of considering the telecom service availability for the FLISR function, while highlighting the need for effective first line response to exogenous events in smart grids.*

## 1 Introduction

Smart grids have a wide range of applications that use various communication technologies. The FLISR function in the distribution grid is chosen to investigate the power-telecom coupling during crisis management situations, where localizing and isolating faults then restoring power supply to customers is critical [1]. The FLISR function intervenes when damages are identified as permanent after initial reclosing cycles involved in protection mechanisms. Fault detectors (FDs) and remote-controlled switches (RCSs) are the main enablers of the remote service restoration [2], as the FDs transmit all suitable faults-related measurements to the control center, and the RCSs are used as decision levers to execute the commands issued by the control center. RCSs can in some cases open automatically as a response to a fault, which is typically the case at the upstream of feeders where RCSs are called circuit breakers (CBs) because their opening shuts off the whole feeder. Manual switches are nonetheless more present in power lines and require field intervention crews to operate them on-site [3].

Placement of RCSs and distribution service restoration problems are extensively studied in the literature [4–6]. We extend these studies here to integrate the impact of ICTs. Thereby, the main contributions of this work sum up to:

- Include the automatic response in the grid service restoration model
- Consider the ICT availability
- Study the deployment of new RCSs based on the state of the telecom points (TPs and related characteristics of coverage, battery storage, and redundancy of access.

## 2 System Model

The MV distribution level of the power grid is considered in this work. The distribution grid is represented as a graph, where nodes are the high-voltage to medium-voltage (HV/MV) substations an the MV buses, and edges are the power lines. A hierarchical graph captures the telecom domain of the grid, with edges representing communication links, while the control center is the top-level node, access points at the intermediate level, and connected grid assets (HV/MV substations, circuit breakers, RCSs) at the lowest level. FDs are considered perfect in this study as the focus is on the impact of ICTs and RCSs.

Interdependencies between the two domains are captured by considering ICT points as loads from the perspective of the electrical system, while electrical substations and switches are clients from the ICT perspective. Figure 1 summarizes the interactions between different components of the same domain or different domains, with three main actions: power supply, telecom service, and repair/manual switching.

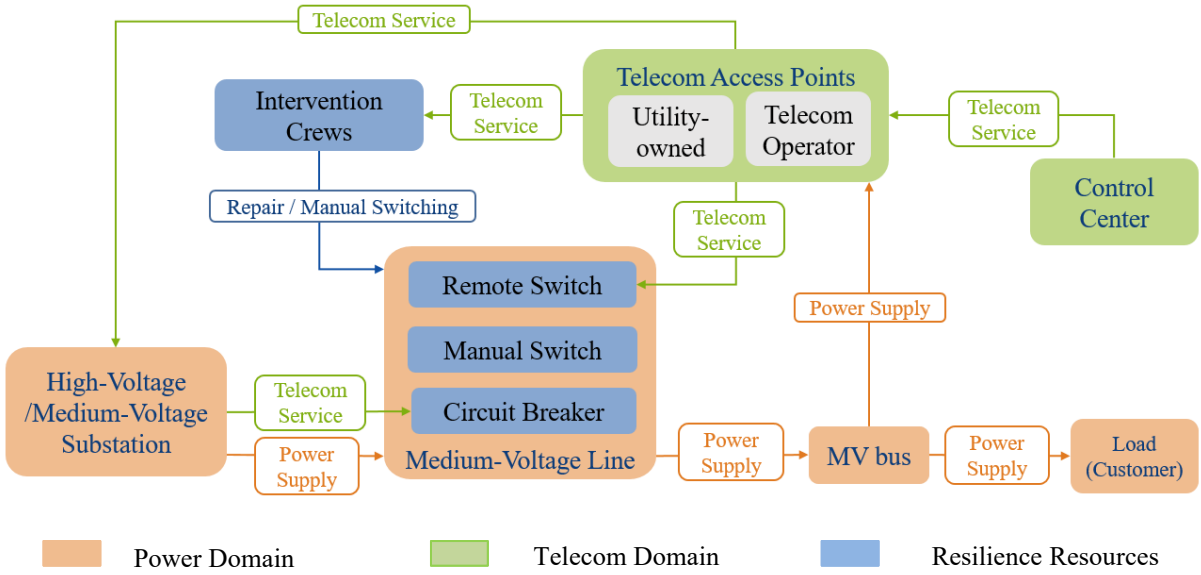


**Figure 1**. Interactions in the proposed model

Since RCSs can be operated both remotely and manually, they are more advantageous, and their proportion in the network is mostly determined by cost-benefit analyses due to increased expenses. The problem can be decomposed into four phases:

- **Pre-event phase (Anticipative new-RCS deployment):** In this phase, a new resilience-based deployment of RCSs is considered to determine proactively the manual switches to upgrade with the remote connection functionality, and which technology to use among: 1) T: utility-owned assets and 2) R: telecom operator service.
- **Automatic isolation:** Scenarios of damages include in the current work faults in power lines and TPs. The first response of the distribution grid is the automatic opening of CBs of affected feeders to protect HV/MV substations. In underground networks, medium voltage to low voltage (MV/LV) substations are directly placed on the mainstream, and RCSs are commonly integrated into the substations. Overhead networks contain more derivations, and RCSs are placed on the lines.
- **Remote isolation:** The initial affected zone isolated by automatic devices is wide and can be reduced using RCSs. In this phase, RCSs are opened wherever they allow to isolate some nodes from faulted zones.

- **Fast service restoration:** At this point, some loads can be restored. An evaluation of the power flow conditions is conducted, and decisions on the state of switches are made. The output of this last phase of the fast reconfiguration stage will be taken by the operator during the deployment of latent restoration resources (e.g. repair crews, mobile distributed generators), which are not considered here.

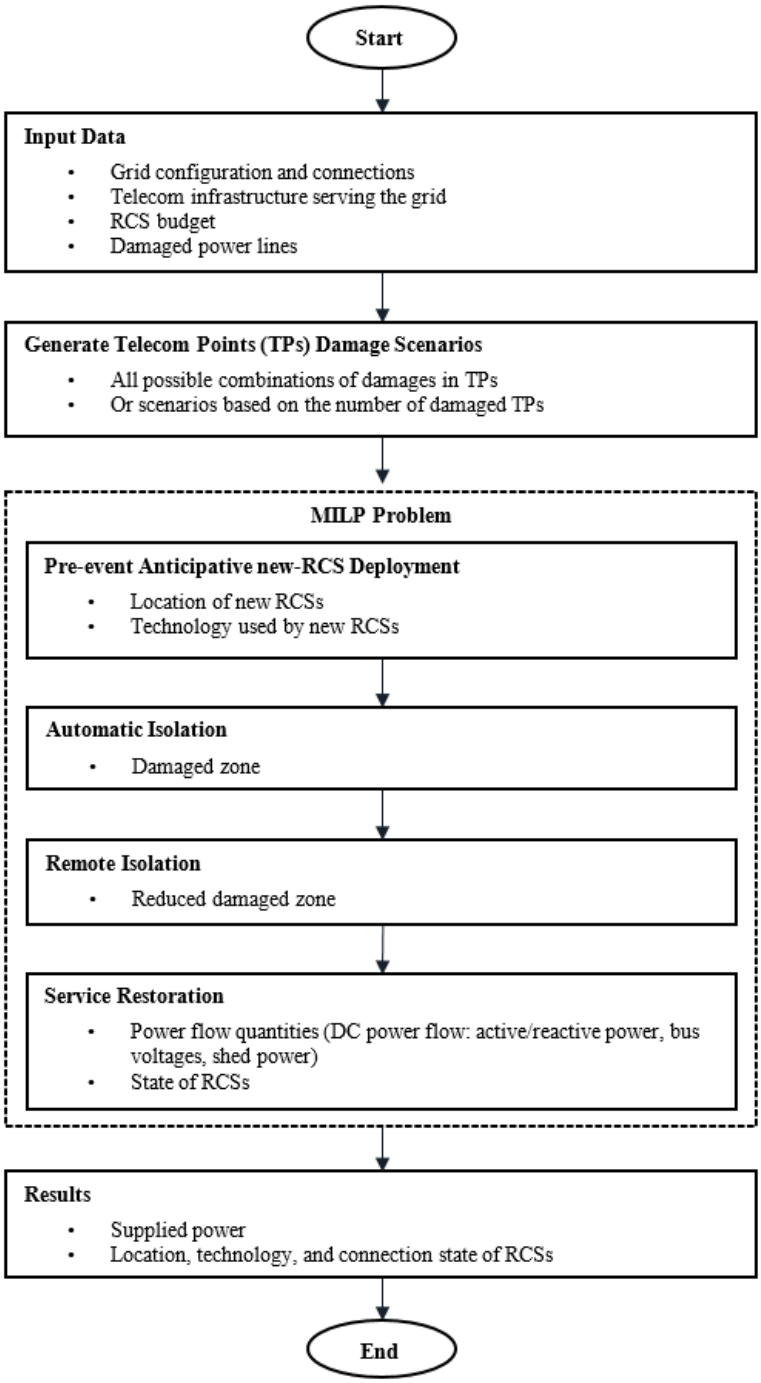


**Figure 2**. Flowchart of the proposed approach

Figure 2 outlines the quantities related to each phase that are computed through the formulated MILP optimization. The objective is chosen to maximize the supplied power through RCS operation.

# 3 Simulation and Results

A case study of 36 power nodes is set based on the IEEE 12-node test feeder to demonstrate the effectiveness of the proposed approach. Capacitors, transformers, and regulators are simplified/ignored in compliance with the study objectives. A per-phase analysis is conducted in the constructed generic medium-size 20kV nominal voltage unbalanced distribution network of total 1305 kW demand. Figure 2 shows the buses served by each feeder, and the interconnections between feeders using tie-switches (dashed lines representing normally-open switches).

Each time step represents one phase in Figure 2. Nodes 1, 2, and 3 represent the HV/MV substations, and the blue nodes are the MV buses, which not only supply power to electrical loads, but also energize TPs of two wireless technologies: telecom operator-owned {T1, T2, T3, T4, and T5}, and utility-owned {R1 and R2}. Assets of technology T have coverage radius of 2.8 km and battery capacity of 3 hours, while for technology R the coverage radius is 3.5 km and battery capacity 5 hours. We can say that R has better coverage and battery storage, while T offers better options in terms of redundancy.

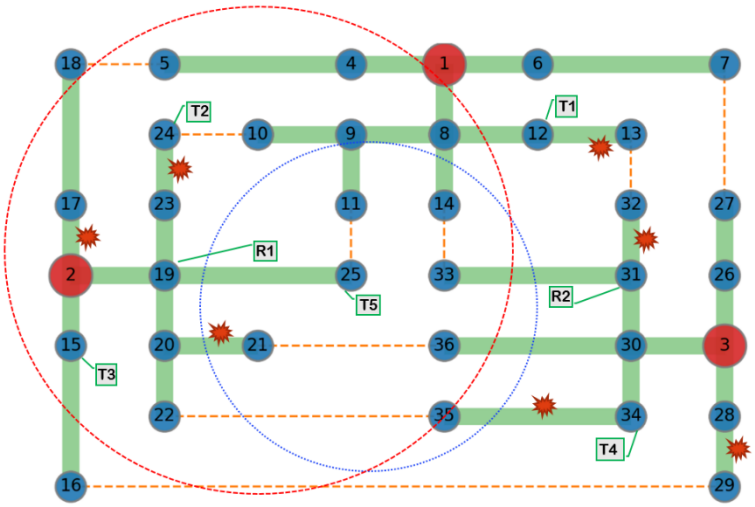


**Figure 3**. Test case

Table 2 summarizes the initial type of switch in each power line. A line or a TP has a binary state, either damaged or safe. Then, a scenario of 7 physical damages in power lines is considered. All the possible 128 combinations of failures in TPs are inspected, constructing a scenario-based evaluation where each scenario is assigned with an equal probability of 1/128. This straightforward stochastic optimization attempts to cope with the uncertainty around damaged TPs. The propagation of damages in overhead and underground lines is well described in the compact MILP formulation.

**Table 1**. Percentage of supplied power at each phase with varying number of damages in telecom points; Budget B=3

| Number of telecom damages | 0 | 1 | 2 | 3 | 4 | 5 | 6 | 7 |
|---|---|---|---|---|---|---|---|---|
| Pre-event phase | 100% | | | | | | | |
| Automatic & Remote Isolation phases | 29.5% | | | | | | | |
| Restoration Phase | 50.96% | 40.23% | 33.77% | 30.79% | 29.91% | 29.61% | 29.5% | 29.5% |

**Result 1.** As we consider a single fault scenario in electrical lines as shown in Figure 1, the damage scenarios are categorized based on the number of affected TPs (Table 1). Damages in TPs clearly affect the ability to restore power supply to customers. Table 1 also shows that if a given threshold of affected TPs is attained, no restoration would be possible even that some points are still available. In this case, the budget for new-RCS deployment was fixed to B=3, meaning only three manual switches could be upgraded to RCSs.

**Result 2.** Table 2 illustrates that, when the number of damages is fixed to 3 and the budget (B) for new-RCS deployment is varied, the supplied power increases with increasing B from 0 to 5. However, when the budget is increased further, no gain is achieved in terms of supplied power. This suggests that beyond an optimal number of RCSs, restoration is no longer possible with RCSs, corroborating that most of the time only a limited recovery is carried out during fast reconfiguration.

**Table 2**. Supplied power considering new-RCS deployment with varying budget (B); Number of telecom damages = 3

| | Initial setup (B=0) | B=1 | B=2 | B=3 | B=4 | B=5 | B=6 | B=13 |
|---|---|---|---|---|---|---|---|---|
| Circuit Breakers | 1-4, 16, 1-8, 2-15, 2-17, 2-19, 3-26, 3-28, 3-30 | | | | | | | |
| Remote Controlled Switches (RCS) | 22-35, 14-33, 15-16, 31-33, 10-24, 5-18, 21-36, 11-25, 26-27, 13-32, 7-27, 16-29, 9-11, 4-5 | 17-18 {R1} | 8-12 {T1,T4} | 19-23 {T2,T3, T4} | 30-31 {T1,T5}, 30-34 {R2}, ~~19-23~~ | 19-23 {T2,T3, T4} | 8-9 {T1,T3, T4} | All lines are RCS |
| Manual Switches | 8-9, 20-22, 12-13, 20-21, 30-31, 6-7, 31-32, 19-23, 9-10, 30-34, 30-36, 23-24, 31-32, 17-18, 28-29, 8-12, 8-14, 34-35, 19-25 | ~~17-18~~ | ~~8-12~~ | ~~19-23~~ | ~~30-31, 30-34,~~ 19-23 | ~~19-23~~ | ~~8-9~~ | |
| Supplied Power (%) | 29.5 | 30.16 | 30.63 | 30.79 | 30.94 | 31.1 | 31.1 | 31.1 |

**Result 3.** The newly equipped lines with RCS are shown in green (Table 2) for the different budgets. The present approach helps to establish a priority between the lines which should be upgraded. The telecom technology used is also specified, inside the curly brackets. By closely inspecting the setup of the network, the lines which can possibly be served by one T point and one R point (17-18, 30-34), tend to choose the R point as it has more resilience in terms of battery storage. At the same time, lines which are in the covered vicinity of one R point and multiple T points, choose rather the T technology for the offered redundancy of access.

# 4 Conclusion

This work provides a resilience-based optimization for fast restoration using remote controlled switches. The objective is to maximize the total power delivered during a failure event, while identifying the optimal scheme (location, technology) for new RCSs. The uncertainty around damages in TPs is partially accounted for through scenario-based optimization. Results suggest that fast restoration is stopped even when some telecom points are still available, and there exists a threshold beyond which increasing the RCS deployment budget brings no more benefit. The chosen technology for each upgrade is linked to battery storage and connection redundancy.

Many extensions are under exploration for this work, such as the adjustment of probabilities on different scenarios of TP failures and the investigation of more than just one power line failure scenario. In addition, the impact of the power supply failure to telecom points is considered by including the capacity of batteries into the objective function, but other options can be tested. Finally, the improvement to the overall restoration brought by the enhancement of fast reconfiguration will be quantified.

## Acknowledgement

This work is funded by EDF/Orange/SNCF in the framework of the Chair on Risk and Resilience of Complex Systems (CentraleSupélec, EDF, Orange, SNCF).

## References

1. Liu J, Qin C, Yu Y. Enhancing Distribution System Resilience With Proactive Islanding and RCS-Based Fast Fault Isolation and Service Restoration. IEEE Trans Smart Grid. 2020 May;11(3):2381–95.

2. Heidari Kapourchali M, Sepehry M, Aravinthan V. Fault Detector and Switch Placement in Cyber-Enabled Power Distribution Network. IEEE Transactions on Smart Grid. 2018 Mar;9(2):980–92.

3. Chen B, Ye Z, Chen C, Wang J. Toward a MILP Modeling Framework for Distribution System Restoration. IEEE Transactions on Power Systems. 2019 May;34(3):1749–60.

4. Zidan A, Khairalla M, Abdrabou AM, Khalifa T, Shaban K, Abdrabou A, et al. Fault Detection, Isolation, and Service Restoration in Distribution Systems: State-of-the-Art and Future Trends. IEEE Transactions on Smart Grid. 2017 Sep;8(5):2170–85.

5. Carvalho PMS, Ferreira LAFM, da Silva AJC. A decomposition approach to optimal remote controlled switch allocation in distribution systems. IEEE Transactions on Power Delivery. 2005 Apr;20(2):1031–6.

6. Abiri-Jahromi A, Fotuhi-Firuzabad M, Parvania M, Mosleh M. Optimized Sectionalizing Switch Placement Strategy in Distribution Systems. IEEE Transactions on Power Delivery. 2012 Jan;27(1):362–70.

# Study of a degrading system with stochastic arrival intensity subject to condition-based maintenance

Lucía Bautista, Department of Mathematics, Universidad de Extremadura, Spain
luciabb@unex.es

Inma T. Castro, Department of Mathematics, Universidad de Extremadura, Spain
inmatorres@unex.es

Luis Landesa, Department of Computers and Communications Technology, Universidad de Extremadura, Spain llandesa@unex.es

## Abstract

*A condition-based maintenance strategy is proposed for a degrading system. The system deterioration is reflected through multiple degradation processes that start at random times following a shot-noise Cox process. Their growth is modelled according to a homogeneous gamma process and the combined process of initiation and growth of the degradation processes is obtained. The system failure is defined as the time instant at which a degradation process exceeds a certain failure threshold fixed previously. The state of the system is checked at periodic times and a preventive or corrective replacement of the system is performed if necessary. Finally, a sequence of costs for the different maintenance tasks is imposed and the total expected maintenance cost is optimized by minimizing the time between inspections and the preventive threshold.*

## 1 Introduction

Condition-based maintenance (CBM) has been widely used in maintenance planning and reliability. Since it is based on the monitorization of the operating condition of a system, the development of new technologies and sensors has considerably increased its utilization. However, early preventive replacements may result in a high cost, and in some systems is difficult to implement CBM.

The non-homogeneous Poisson process (NHPP) has been widely used to model the arrival intensity of new degradation processes. However, since modelling the arrivals with a NHPP assumes that the intensity is a deterministic function, it is not very suitable in certain cases. For example, considering a system subject to external shocks, these shocks can accelerate the initiation or arrival of new degradation processes to the system. When shocks affect the arrival intensity, this phenomenon is better captured by a process with a stochastic intensity such as the Cox process. Degradation processes involving stochastic intensity has been employed in systems working on a dynamic environment, when the system suffers an abrupt increment on the failure rate or loads are induced on the system, causing crack problems. Cox processes also have applications in the fields of seismology, mathematical finances or, more recently, in epidemiology.

The motivation of the work is to find an optimal CBM policy for a system affected by several deterioration processes that arrive and grow independently. Instead of continuous monitoring, a periodic monitoring of the system is implemented. The state of the system is checked at certain times, and the necessary maintenance actions are performed.

## 2 Objectives

The main objectives of the work are:

1. Propose a deterioration model for a system subject to multiple degradation processes.
2. Describe the arrival and growth of the degradation process with a combined process.
3. Describe the main characteristics of the Cox process.
4. Obtain expressions for the expected number of arrivals and the intensity of the process.
5. Develop a CBM model introducing preventive replacements and periodic inspections.
6. Analyse the influence of the maintenance policy on the expected cost rate.
7. Optimise the model parameters and the expected cost rate.

## 3 Framework of the model

We assume that the multiple degradation process that affect the system start at random times and grow independently of one another. The stochastic process chosen for the intensity is a Cox process, also called doubly stochastic Poisson process. It is a generalization of the Poisson process, in which the intensity is itself another stochastic process.

The intensity of the process can be expressed as:

$$\lambda^*(t) = \lambda_0 + \sum_{i=1}^{N(t)} exp(-\delta(t - T_i)) \qquad (1)$$

where $N(t)$ is the counting process associated to the homogeneous Poisson process. Times $T_i$ are the corresponding arrival times of the initiation process and $\lambda_0, \delta > 0$ are constants.

Given the intensity and conditioning on the number of arrivals, the expectation can be obtained as:

$$E[\lambda^*(t)] = \lambda_0 + \frac{\mu}{\delta}(1 - \exp(-\delta t)) \qquad (2)$$

where $\mu$ is the rate parameter of the initial Poisson process $T_i$.

The expected number of arrivals upon time t can also be calculated as:

$$E[N^*(t)] = \int_0^t E[\lambda^*(u)]\, du = \lambda_0 t + \frac{\mu\, t}{\delta} + \frac{\mu}{\delta^2}(\exp(-\delta t) - 1) \qquad (3)$$

Now, the deterioration growth model assumed for these degradation processes is the gamma process, which is appropriate for modelling degradation that involve independent and non-negative increments. This continuous-time stochastic process has independent gamma distributed increments. The density function of a gamma distribution with shape parameter $\alpha > 0$ and scale parameter $\beta > 0$ is given by:

$$f_{\alpha,\beta} = \frac{\beta^\alpha}{\Gamma(\alpha)} x^{\alpha-1} \exp\{-\beta x\}, \quad x > 0, \qquad (4)$$

with

$$\Gamma(\alpha) = \int_0^\infty t^{\alpha-1} e^{-t} dt \qquad (5)$$

The system is failed when the deterioration level of one of the multiple degradation processes exceeds the failure threshold, previously fixed.

# 4 Maintenance policy

The system is inspected periodically each T time units to check its deterioration state. We set two different degradation thresholds, the preventive threshold, and the corrective threshold to check the system state. The following actions are performed:

1) If the degradation levels of the processes do not exceed the preventive threshold, the system is in a good condition, and it is left as it is.
2) If the deterioration level of one of the multiple degradation processes exceeds the preventive maintenance threshold but not the corrective one, a preventive replacement (PM) is performed, which consists of the replacement of the system by a completely new one.
3) If the system is failed at an inspection time, a corrective replacement (CM) is performed, and the system is also replaced by a new one.

# 5 Methods

To obtain the optimal expected cost of the system maintenance process, we will minimize the cost by optimizing two parameters: the preventive threshold (M) and the time between inspections (T). The renewal-reward theorem provides the following expression of the asymptotic cost rate:

$$C(T,M) = \frac{E[C]}{E[R]} \qquad (6)$$

where $E[C]$ is the expected cost in a replacement cycle and $E[R]$ is the expected time to a replacement. The expected cost rate can be developed as:

$$C(T,M) = C_c \sum_{k=1}^{\infty} P_c(kT) + C_p \sum_{k=1}^{\infty} P_p(kT) + C_I E[N_I] + \sum_{k=0}^{\infty} C_d E_d(kT,(k+1)T) \qquad (7)$$

where $E[N_I]$ is the expected number of inspections, $\mathrm{E_d(kT,(k+1)T)}$ is the expected number of downs of the system during the interval $(kT,(k+1)T)$ and $P_c(kT)$, $P_p(kT)$ are the probabilities of performing a preventive or a corrective replacement at inspection time $kT$, respectively. $C_c$ is the cost due to corrective replacements, $C_p$ is the cost due to preventive replacements, $C_I$ is the cost per inspection and $C_d$ is the cost due to downtimes of the system.
A grid with different values for the time between inspections T and the preventive threshold M is built to optimize the cost with Monte-Carlo method.

# 6 Results

A numerical example is study to implement the previous maintenance policy.

The intensity of the corresponding Cox process modelling the arrival of new processes is given by the formula:

$$\lambda(t) = 1 + \sum_{i=1}^{N(t)} e^{-0.5(t-T_i)}$$

$N(t)$ is the number of Poisson processes in the system at time t. We assume that the rate

parameter is $\mu = 2$. These processes determine the arrival times $T_i$ which allow to calculate the intensity $\lambda(t)$ of the main process.

The degradation processes grow according to a gamma process with parameters $\alpha = 1.1$ and $\beta = 1.4$. The corrective threshold is L=10 and the preventive one, M=7.
The following costs due to maintenance actions are assumed in this example:

$$C_p = 100, \qquad C_c = 200, \qquad C_I = 50, \qquad C_d = 60$$

All the costs are expressed in monetary units, except the cost due to downs of the system, which is expressed in monetary units per time unit.

The optimal values obtained with Monte-Carlo method are $T_{opt} = 6.3333$ and $M_{opt} = 6.1429$, with an expected cost rate of 35.3005 monetary units per unit time.

# 7 Conclusions and further work

A combined model of initiating events arriving to the system following a Cox process and evolve following a gamma process has been studied. A PM policy has been implemented, as well as a CBM policy. The analysis is completed through the optimisation of two parameters of the model: the time between inspection T and the value of the preventive threshold M.

Although we assume that the initiation times follow a Cox process, the work can be extended to a non-Cox process such as a Hawkes process. The main characteristic of this process is that it is a self-exciting process: each arrival of a degradation process increases the rate of future arrivals for some period. Also, different degradation patterns and dependencies between the processes can be considered.

# 8 Acknowledgements

This research was supported by Junta de Extremadura (Project GR21057) and European Union (European Regional Development Funds).

## References

1. Alaswad, S. & Xiang, Y. (2017) A review on condition-based maintenance optimization models for stochastically deteriorating system. *Reliability Engineering & System Safety* 157, 54–63.
2. Bautista B.L., Torres, C.I., Landesa, P.L. (2021) Cox processes in system degradation modelling. In K. Kołowrocki et al. (Eds.), *Safety and Reliability of Systems and Processes, Summer Safety and Reliability Seminar 2021*. Gdynia Maritime University, Gdynia, 7-16.
3. Bertoin, J. (1996) Lévy processes. *Cambridge University Press*.
4. Caballé, N., Castro, I.T., Pérez, C.J., Lanza-Gutiérrez, J.M. (2015) A condition-based maintenance of a dependent degradation threshold-shock model in a system with multiple degradation processes. *Reliability Engineering & System Safety* 134, 89–109.
5. Castro, I.T., Caballé, N., Pérez, C.J. (2015) A condition-based maintenance for a system subject to multiple degradation processes and external shocks. *International Journal of Systems Science* 46(9), 1692–1704.
6. Castro, I.T., Landesa, L. (2019) A dependent complex degrading system with non-periodic inspection times. *Computers & Industrial Engineering* 133, 241–252.
7. Cha, J.H., Finkelstein, M. (2017) On Some Shock Models with Poisson and Generalized Poisson Shock Processes. *ICSA Book Series in Statistics*, 67–79.
8. Huynh, K.T., Grall, A., Bérenguer, C. (2017) Assessment of diagnostic and prognostic condition indices for efficient and robust maintenance decision-making of systems

subject to stress corrosion cracking. *Reliability Engineering & System Safety* 159, 237–254.
9. J.M. van Noortwijk. (2009) A survey of the application of gamma processes in maintenance. *Reliability Engineering & System Safety* 94(1), 2-21.
10. Ross, S.M. (2014) Introduction to Probability Models. *Elsevier, Rome*.
11. Wu, S., Castro, I.T. (2020) Maintenance policy for a system with a weighted linear combination of degradation processes. *European Journal of Operational Research* 280; 124–133.

## List of abbreviations and definitions

| | |
|---|---|
| CBM | Condition Based Maintenance |
| PM | Preventive Maintenance |
| CM | Corrective Maintenance |
| NHPP | Non-Homogeneous Poisson Process |

# Practical risk and resilience assessment: a methodology for implementation of Mountain Risk Management and Prevention Strategy (STePRiM)

Tacnet, J.-M., Grenoble Alpes University, INRAE, jean-marc.tacnet@inrae.fr

Carladous S., Sassus, F., French National Forest Office, simon.carladous@onf.fr, francois.sassus@onf.fr

Ripert, E., Lagleize, P. , Community of municipalities Pyrénées Haut-Garonnaises, eva.ripert@ccphg.fr, patrick.lagleize@ccphg.fr

Stephan, A., Calmet, C., Ministry of Ecological Transition, Directorate of risk prevention, ariane.stephan@developpement-durable.gouv.fr, catherine.calmet@developpement-durable.gouv.fr

Gili, V., Departmental Directorate of Territorries of Haute-Garonne, vincent.gili@haute-garonne.gouv.fr

## Abstract

*Mountain territories are highly exposed to natural phenomena which threaten people, assets and infrastructures. Those phenomenona induce both direct consequences (damage) on objects but also indirect consequences due to critical infrastructures failures. For instance, road closures due either to rockfalls, floods, snow avalanches, landslides will have long-term, remote, economic, social consequences which somehow characterize the territory resilience.*

*To reduce risk, local authorities, State, infrastructures managers combine structural and non-structural measures such as protection measures, land use control plans, preventive information. In this context, challenging decision-making issues appear to define and choose the best measures and strategies for a given territory.*

*The French ministry for Ecological Transition (directorate for risk prevention) (MTE/DGPR), responsible for risk management, has designed and proposed a new innovative framework to help local authorities choosing and also funding their risk management strategies in mountain areas (STePRiM : Mountain Risk Management and Prevention Strategy ). It consists in a first step of risk diagnosis followed by a step of prioritization between possible options. Due to large scale assessment, detailed and complex risk and resilience analysis cannot be done for all sites.*

*A specific, incremental methodology is required. This paper describes a practical methodology and emphasizes constraints and requirements for practical resilience analysis. Based on the example of CCPHG, it first recalls how risk and resilience concepts are communicated with technical experts and stakeholders. It then describes how direct and indirect risks are addressed in a consistent but pragmatic way. Results are provided in order to be used and connected with the decision-aiding processes involving stakeholders and considering their preferences and priorities.*

## 1 Introduction

Mountains risks induce direct material, human and indirect consequences on exposed people and assets. Those risks have specific geophysical and socio-economic characteristics. Mountain geography, due to its slope and relief strongly influences and triggers intense and most often rapid phenomena such as rockfalls , landslides, torrential debris flows, snow avalanches, earthquakes, glacier outburst, tsunamis in lakes (1). In a context of climate change, specialists anticipate an increase in the number of events occurrence or intensity of phenomena especially in mountains (2).

## 1.1 Risk management

In the context of natural phenomena, risk is classically defined as a combination of hazard and vulnerability, which is somehow equivalent to the combination of frequency and severity in an industrial, technological context. Hazard combines the intensity and frequency of phenomena. Direct vulnerability is the estimated nature of the physical damage and its value (for each element at risk) reulting from a combination of spatial exposure and potential losses. Natural risk reduction strategies are based on both non-structural measures, e.g., risk zoning maps, preventive information and protective structures, aiming at reducing causes and mountain natural phenomena effects on exposed elements, which may be severely damaged because of, e.g., debris flow impacts, overflowing, scouring, deposition for torrential floods (Figure 1).

**Figure 1.** Risk is reduced through non-structural and structural measures (e.g. in the context of torrential risks).

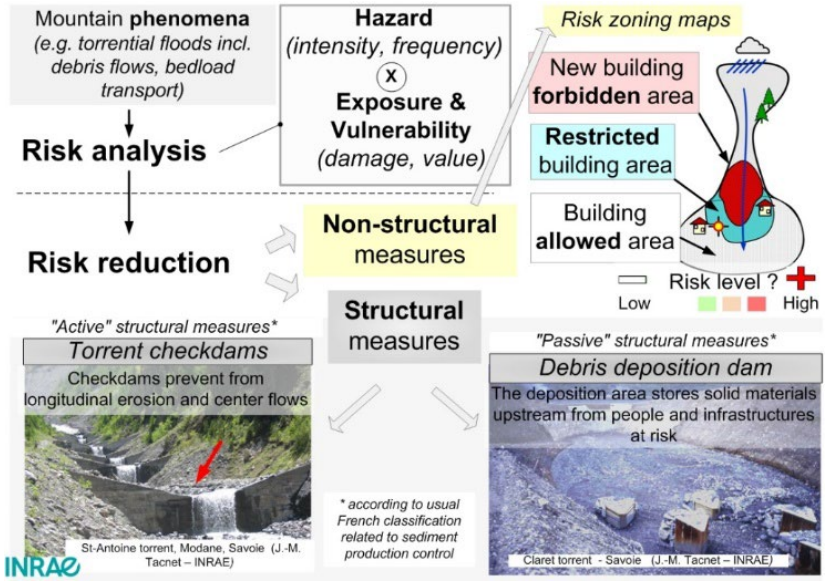


*Source:* adapted from (Tacnet et al.,2014)

Critical infrastructures (energy, water, communication and transport networks) failures (3) have major consequences on territories in human and economic terms: they cut off logistical supply circuits, the transmission of information and access to essential services (security, health) (Figures 2 a,b).

**Figure 2.** Damage to transport infrastructures due to torrential floods.

(a) Montfort, January 2022 (Dept. 38, France *Source:* J.-M Tacnet/INRAE

(b) Saorge, October 2020, Alex storm (Dept. 06, France) Source : ONF/RTM

For roads, direct vulnerability concerns users, vehicles and infrastructures (road itself, bridges…) whereas indirect vulnerability analysis focuses on the remote or delayed damage associated with the loss of the linking function of a critical infrastructure.

**Figure 3.** Indirect vulnerability analysis relates to consequences of loss of linking function of a critical infrastructure.

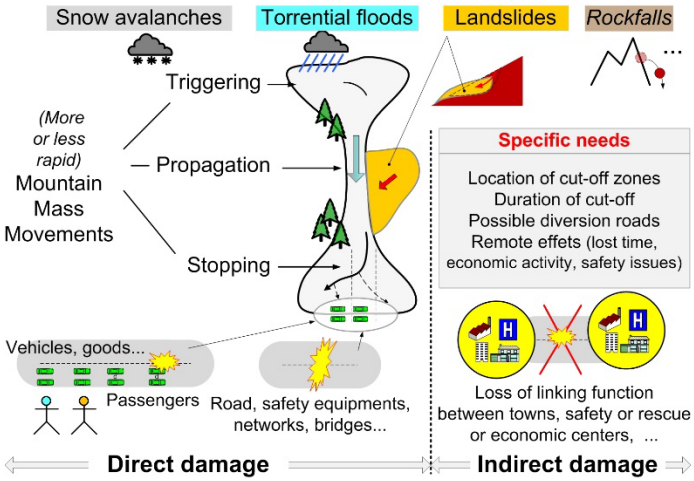


*Source:* adapted from (4)

Quantitative multi-risk assessment have been widely addressed with very detailed and advanced methods (5,6) including climate changes issues (2). Advanced methods (e.g. based on graph theory) do exist to analyze networks resilience (7) with specific studies for roads exposed to natural hazards and calculate costs due to cut-offs (8). Networks structural properties and indicators such as betweeness or centrality allow to identify accessibility of a territory and critical nodes, roads (9,10) with links to decision-aiding specific issues (11). However, despite of their high interest, they may remain difficult to implement in practice in engineering and operational context due to required skills and data.

## 1.2 The STePRiM : a new integrated risk management framework

Mountain risks affect spatially constrained areas in terms of availability of safe buildable areas. Mountains risks is also specific due to the nature of land use and agricultural, touristic development which lead to constraints in terms of accessibility. Promoted by the MTE/DGPR, the STePRiM is an emerging framework based on official specifications document (1). It is put in place in collaboration between French State, its technical services and local authorities. This new system complements the natural risk prevention plans (PPR)[1] which remain the main tool for considering risks into land-use control and planning. All French mountain areas are concerned, i.e. the Alps, Pyrénées, Corsica, the Massif Central, the Jura, Vosges and overseas territories.

The StePRiM aims to increase the territory's resilience through its sustainable development. The aim is to define a strategy, which is translated into an operational programme broken down in actions to achieve reasonable objectives and corresponding to improvement of knowledge and awareness of risks, risk forecasting and monitoring, warning and crisis management, consideration of risks in urban planning, reduction of vulnerability and protection works. It addresses mountain (multiple) risks management in a collective partnership with all stakeholders of the territory including public authority (State, local elected representatives) and also civil society and infrastructures managers. Its objective is to initiate and encourage pilot approaches for natural risks integrated management in

[1] https://www.ecologie.gouv.fr/prevention-des-risques-naturels

mountain areas [2]. The objective of this paper is to present a part of the implementation process of the STePRiM methodology focusing on the assessment of indirect vulnerability and risks linked to the failure of critical road networks exposed to natural phenomena. It first describes the STePRiM framewok and then proposes an application to a test-case recently implemented in Pyrénées mountains.

# 2 Methodology and results

## 2.1 Building the methodology for StePRiM implementation

The STePRiM aims to increase the territory's resilience through its sustainable development. The aim is to define a strategy, which is translated into an operational programme broken down in actions to achieve reasonable objectives and corresponding to: improvement of knowledge and awareness of risks, risk forecasting and monitoring, warning and crisis management, consideration of risks in urban planning, reduction of vulnerability and finally protection works. Figure 4 shows the overall proposed methodology.

**Figure 4.** Overall methodology for the definition of the STePRiM including the progressive passage from risk analysis (diagnosis) to risk management (establishment of the strategy, prioritisation of actions, decision-making process).

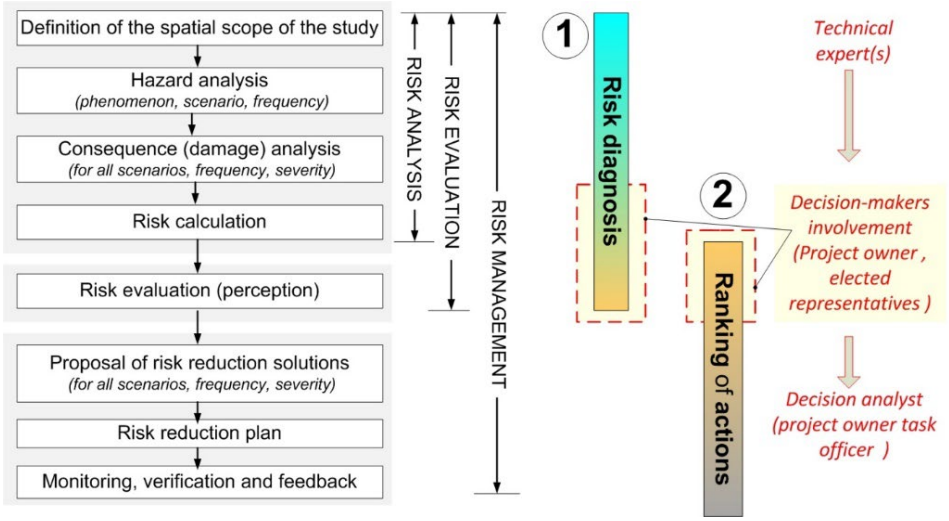


whereas

*Source:* Methodological STePRiM framework (12)

It addresses mountain (multiple) risks management in a collective partnership with all stakeholders of the territory including public authority (State, local elected representatives) and also civil society and infrastructures managers. Its objective is to initiate and encourage pilot approaches for the integrated management of natural risks in mountain areas[3]. The STePRiM methodology is based on three essential steps corresponding to 1) risk diagnosis, 2) protection and mitigation devices analysis and finally 3) the proposal and selection, proritization of actions, solutions over the territory. The STePRiM process is somehow original in that it combines technical analysis and decision support phases with local stakeholders over a wide territory to build a risk management strategy (Figure 5). It also extends the more common, traditional only analysis of local, direct effects of phenomena on directly impacted objects and activities. The STePRiM starts with the assessment of classical risk components (hazard, vulnerability and exposure). While risk

[2] (e.g.) http://risknat.org/girn-alpes/index.html , https://www.bafu.admin.ch/bafu/fr/home/themes/dangers-naturels/info-specialistes/gestion-integree-des-risques.html

[3] (e.g.) http://risknat.org/girn-alpes/index.html , https://www.bafu.admin.ch/bafu/fr/home/themes/dangers-naturels/info-specialistes/gestion-integree-des-risques.html

assessment is done statically at a given time, the STePRiM approach also considers the resilience by taking into account the temporal aspect related (e.g.) to indirect damage due networks cut-offs or through the assessment of efficacy, reliability and maintainibility of protection works (Figure 6).

**Figure 5.** The StePRiM approach embeds risk analysis and evaluation at a wide territorial scale.

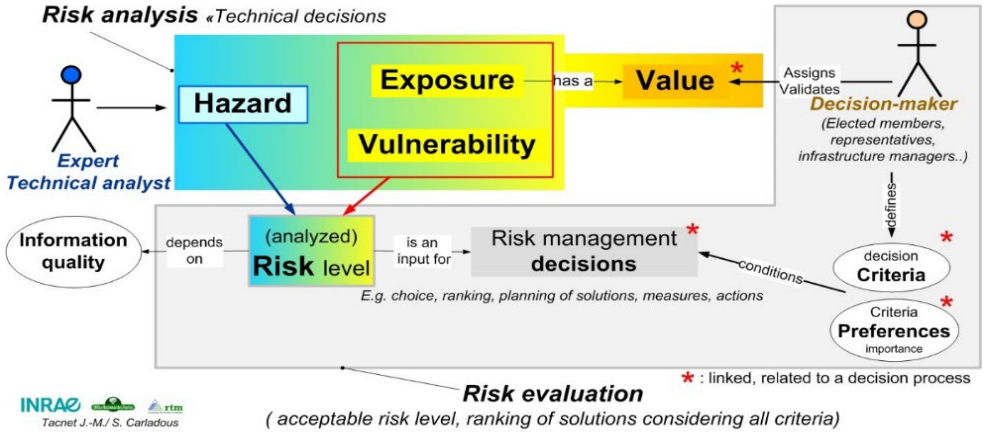


*Source:* Methodological STePRiM framework (12)

**Figure 6.** Core concepts of risk and resilience.

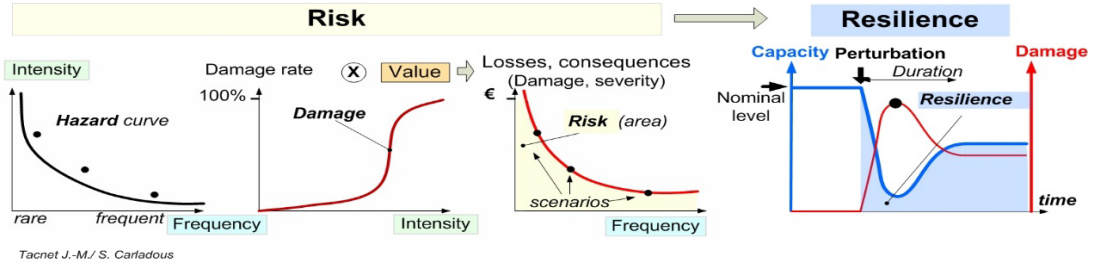


*Source:* STePRiM framework (12) adapted from Tacnet et al., in (13)

Three types of damage (direct material, direct human and indirect) are therefore considered in the approach for each type of stakes (dwelling, persons), phenomenon (landslide, rockfalls, floods etc.) and scenario. Both of them can be assessed either quantitatively (monetary in euros) or qualitatively using scores, notes (0 to 1, 1 to 10) or, finally, using verbal forms (low, medium, high damage) (Figure 7).

**Figure 7.** Principles of the simplified methodology for analysing direct multiple risk

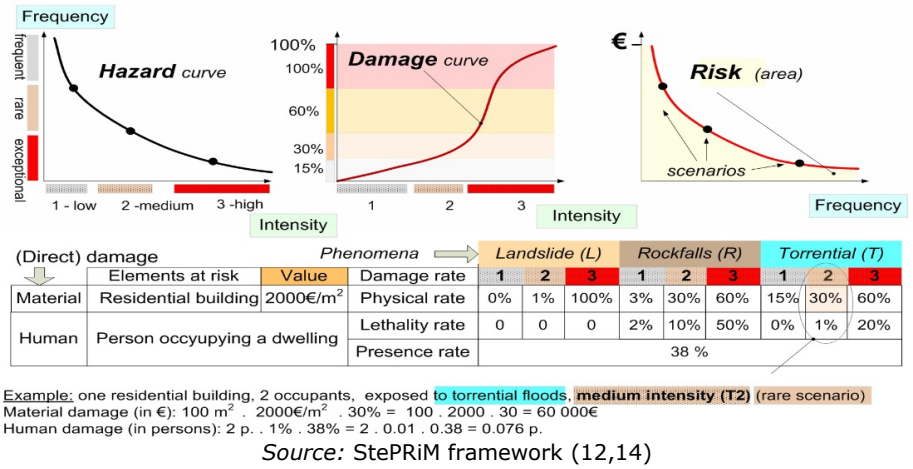


| (Direct) damage | | | Phenomena | Landslide (L) | | | Rockfalls (R) | | | Torrential (T) | | |
|---|---|---|---|---|---|---|---|---|---|---|---|---|
| | Elements at risk | Value | Damage rate | 1 | 2 | 3 | 1 | 2 | 3 | 1 | 2 | 3 |
| Material | Residential building | 2000€/m² | Physical rate | 0% | 1% | 100% | 3% | 30% | 60% | 15% | 30% | 60% |
| Human | Person occyupying a dwelling | | Lethality rate | 0 | 0 | 0 | 2% | 10% | 50% | 0% | 1% | 20% |
| | | | Presence rate | 38 % | | | | | | | | |

Example: one residential building, 2 occupants, exposed to torrential floods, **medium intensity (T2)** (rare scenario)
Material damage (in €): 100 m² . 2000€/m² . 30% = 100 . 2000 . 30 = 60 000€
Human damage (in persons): 2 p. . 1% . 38% = 2 . 0.01 . 0.38 = 0.076 p.

*Source:* StePRiM framework (12,14)

Direct damage may either be tangible, material (destruction of buildings, infrastructure, vehicles) or intangible, immaterial (death, injured people, environmental damage). Tangible indirect damage corresponds, for example, to loss of operations or accessibility. Intangible indirect damage (not addressed in StePRiM framework) may correspond to psychological disorders, effects on socio-cultural heritage and environmental damage.

When dealing with a territorial approach, the problematic concerns also the determination of vulnerability and indirect risks linked to critical infrastructures failures. This vision is not classically embedded in risk management plans and therefore extends the more traditional analysis of local, direct effects of phenomena on directly impacted issues. The application below describes its principles but also emphasizes new needs and challenges.

## 2.2 Application area and practical issues

The Community of municipalities Pyrénées Haut-Garonnaises (CCPHG)[4] is located in South-West of France. Its area is 631 $km^2$ located in the Pyrenees mountain range with a population of 15,545 (25 hab./$km^2$). It gathers 76 municipalities with two thirds of them being in mountainous areas exposed to landslides, rockfalls, plain and torrential floods, snow avalanches, wildfires. To build a strategy for risk reduction, understanding territorial and socio-economic features, in relation with the transport network structure, is essential. The Montréjeau area is dependent on the Saint-Gaudens area, which generates a lot of commuting. On the other hand, the area of Bagnères-de-Luchon is relatively autonomous (80% of the people living in this area work there) (Figure 8-b). 81% of jobs are located in the tertiary economy making this area the first one in terms of development of tertiary activities are most developed). This illustrates the importance of the tourism economy based on mountain activities (ski resorts, hiking…) and also thermal baths (Figure 8-b). The north piedmont area is very well served with the motorway nearby. The train lines also allow to reach main cities of Toulouse, Tarbes, Pau... However, mountainous geography of this territory makes travel, mainly by private cars, difficult. The railway line has been closed since 2014, and its reopening is planned in the coming years after a major overhaul. The Pique and Garonne valleys are well served with a national road accessing to Spain. As soon as one leaves the main roads, access is more complicated (15).

On this basis, the goal is to estimate the indirect damage caused by the cutting of roads by natural phenomena: it requires to know cut-off zones and the value of lost time and the remote impacts on economic activities (tertiary, industrial activities…). Several advanced, detailed analysis exist to assess networks disruption and resilience (7) but in practice, when working on a wide territory, the analyst may face some difficulties. Several data, to be broken down by type of phenomenon, are indeed necessary to make this analysis :
- Normal and increased travel times (resp. $T_{nominal}$ and $T_{deviation}$) are needed. They may be difficult to calculate, hence the idea of using real traffic data. Getting traffic on the different routes (comparing sources based on vehicle counts and data from GPS providers databases is an option, which appears possibly costly) ;
- Cut-off times (real or estimated) according to the nature of the phenomena and their magnitude are also important. Analysing real events constitutes a reference (to avoid the risk of misinterpreting data corresponding to an accident, for example). In our context, the approach has consisted in designing standard tables to determine the duration of cut-off considering to several criteria;
- Identification of possible diversion routes may not be obviouss (this can be obtained either by using "shortest path" type algorithms or from data) (9–11).

The section below shows hows direct and indirect consequences have been addressed based on available information and implementation constraints. Direct material exposure and human damage are first adressed (section 2.3.1). Indirect damage is calculated in section 2.3.2. Expert assessments are formalized in simplifed tables to support this process.

[4] https://cc-pyreneeshautgaronnaises.fr/

## 2.3 A simplified methodology to calculate direct and indirect damage

### 2.3.1 Direct material exposure and human damage on roads

**Direct material exposure** associated with road traffic as showed in tables is calculated as follows (numerical values are given as examples) :
- Average daily traffic (**AvT**) in vehicles/day: 200
- Average speed (**AvS**) in km/h: 50
- Time between 2 vehicles (**TimeV**) in s: (24h/day.3600s/h)/AvT = (24.3600)/200= 432
- Spacing between 2 vehicles (**SpaceV**) in m: (TimeV.AvS.1000 m/km) / 3600 s/h = (432. 50. 1000) / 3600 = 6000
- Length of exposed road section (ExpoL) in m: 300
- Direct material exposure rate (number of vehicles on exposed road section) (**DMER**): ExpoL/SpaceV=300 /6000= 0.05

**Figure 8.** Global territorial socio-economic analysis.

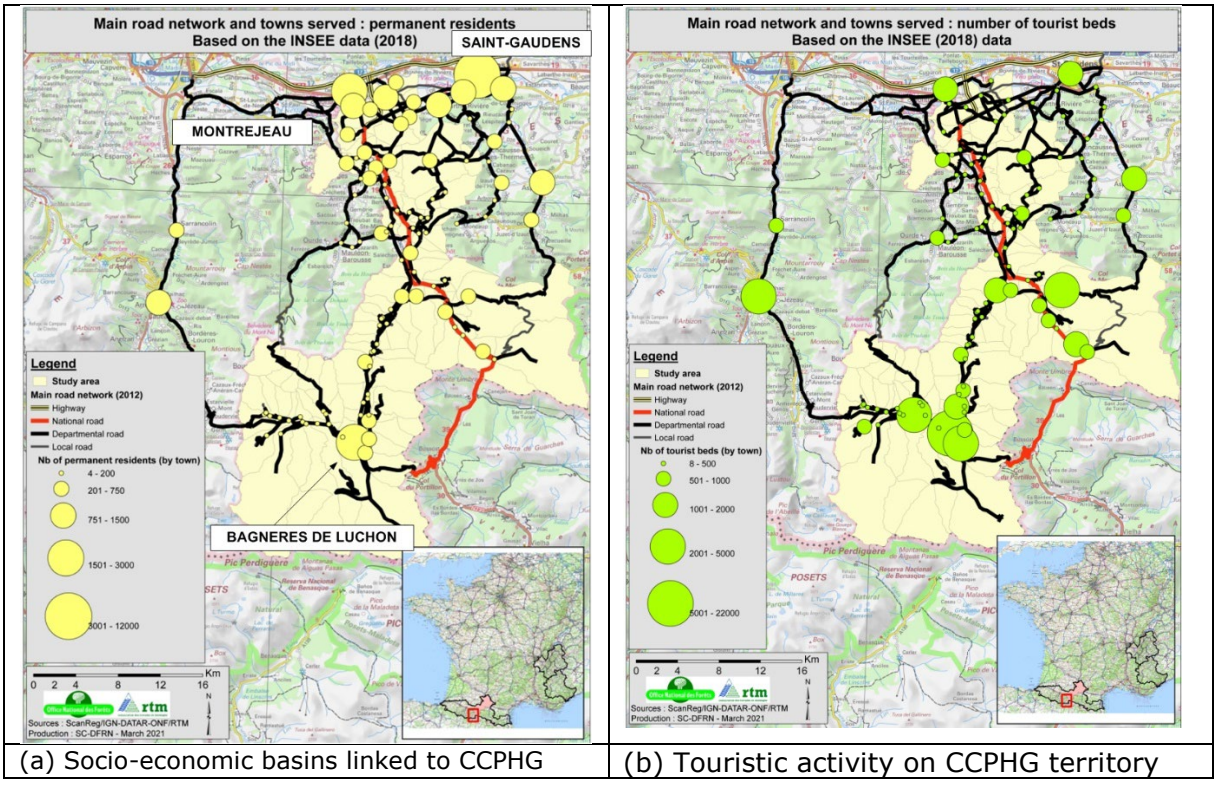


(a) Socio-economic basins linked to CCPHG

(b) Touristic activity on CCPHG territory

**Direct human damage** as showed in table 4 is calculated as follows (numerical values considering a high intensity avalanche event is given as an example) :
- Average human exposure rate (**AvHER**) in persons/vehicle: 1.8
- Letality rate (**LetalR**): 0.1 or 10% (considering vehicle protecting effect, possible rescue)
- Direct material exposure (DMER): 0.05 (5%)
- Reach probability (ratio between phenomenon range and length of exposed road section)(**ReachProba**) : 0.6 (60%)
- Direct Human Damage (on road) (**DHD**) in persons = AvHER . LetalR .DMER . ReachProba= 1.8 . 0.1 . 0.05 . 0.6 = 0.0054

### 2.3.2 Indirect damage on roads

Several levels of analysis of road networks exist depending on whether the problem corresponds to a planning phase (construction of a new road, a new equipement in relation

with existing networks capacities) or the dynamic operation phase (traffic monitoring and management, analysis of travel times with or without interruptions, management of diversions). Here, we only consider a simplified process to contribute to assessment of the indirect vulnerability associated with the loss of the linking function of a critical road infrastructure. The goal is to first assess where are the cut-off zones and then, secondly, the level of consequences and the cost to economic activities associated with a traffic interruption. The overall approach follows the same logical path as that classically implemented for the analysis of direct damage : identification of hazards (phenomena cutting roads), exposure (traffic), damage (duration, costs). The steps are implemented in the context of road networks for each phenomenon, each scenario associated with a given frequency and intensity:

- Identification of the threat: Where are the roads that can be cut? By what? How often? With what intensity? For how long? With what consequences?
- Identification of the damage: what is the origin, the cause of the cut? What will be the duration of the cut?
- Analysis of exposure: what is the nature of the roads that may be closed (international, national, regional, departmental, municipal)? What is the nature and volume of traffic (people, freight, volume, number) (Figure 9–a)?
- What are the possible diversions if a section is cut (Figure 9-b)?
- Analysis of the consequences: What will be the lost access, how much will road cut-off increase access time (services, sectors of activity)?

**Figure 9.** Global territorial network analysis: traffic and possible diversion paths.

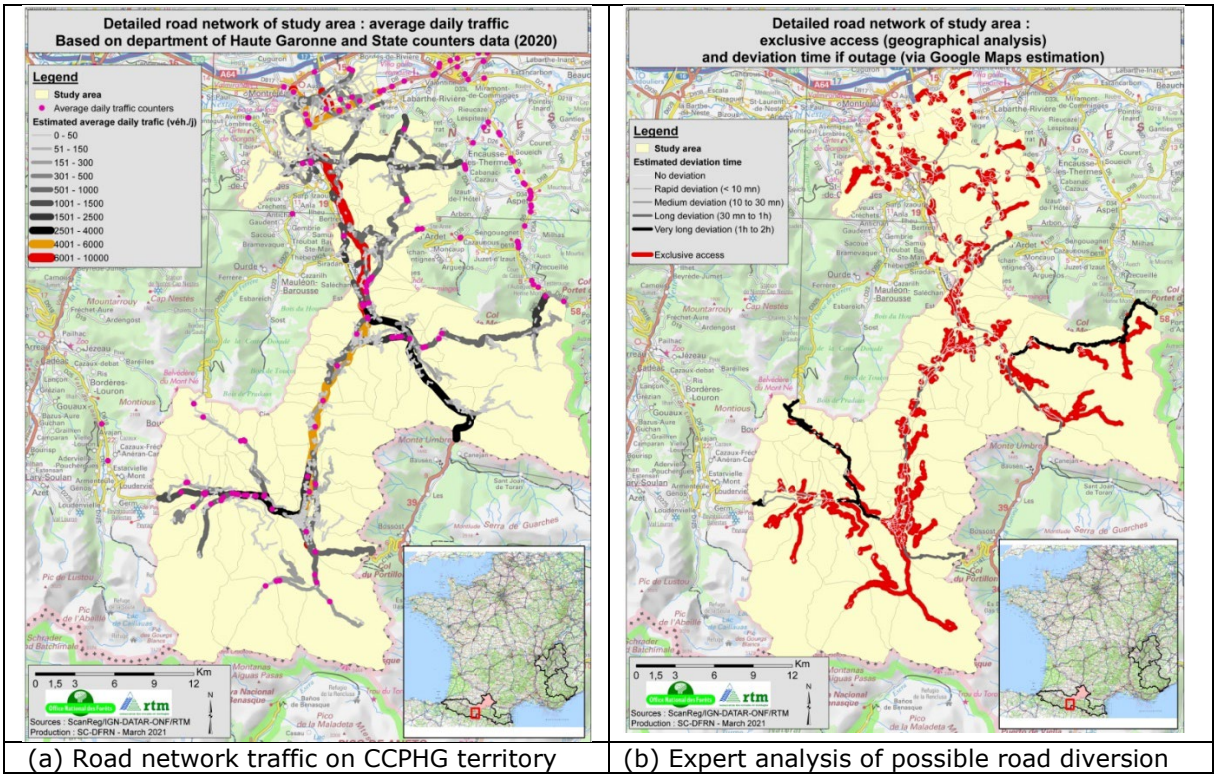


(a) Road network traffic on CCPHG territory | (b) Expert analysis of possible road diversion

In practice, this translates into the following implementation phases:

- Identification and location of the phenomena and their effects (e.g. flooding, scouring, etc.) likely to cut the road. For each phenomenon, effect, for a given frequency level, determination of the intensity of the phenomenon (or of one of its effects);
- For a given phenomenon (effect) and intensity level, estimate the duration of the cut-off $\mathbf{D_c}$ .It depends on the type of road, the nature of the phenomenon and its intensity

(magnitude). A table based on expert assessment is proposed (Table 1). It defines the selected duration ratios according to the nature of the phenomenon and its magnitude;
- The equivalent indicator for damage is the lost time resulting from increase in travel time. For a road cut-off section removing access to an exposed area, determination of the lost time ($\mathbf{t_{lost}}$) compared to the normal situation. $\mathbf{T_{normal}}$ represents the travel time without any traffic disruption, $T_{\mathbf{diversion}}$ represents the travel time when using the diversion An expert analysis is done on each main road to identify the diversion road, its features (length, main speed) and then calculate the duration of travel with diversion $T_{\mathbf{diversion}}$ ;
- Estimated value of damage to exposed covered areas issues determined through lost time ($\mathbf{C_{tlost}}$) following cost-benefit analysis economic approach. Cost in € for each hour of lost travel time is estimated according to the principles of CBA/Multicriteria analysis method (16);
- Assessment of the exposure through the volume and nature of disrupted traffic (**traf**). In practice, traffic information can be obtained on main roads from infrastructure managers (Figure 8-a) ;

**Table 1.** Evaluation of the road cut-off time based on expert assessments.

| | | Snow avalanche | Torrential flood | Landslides | Rockfalls |
|---|---|---|---|---|---|
| **High** phenomenon intesnty | Condition of the roadway (after event) | Snow deposit greater than 1 m over several dozen metres in length | Scouring and/or covering by more than 0.5 m solid material thickness ; gullying and ripping of road pavement | Covering by more than 1 m solid material thickness, road displacement ; road drop or shearing greater than 0.5 m | Stopping and impact of isolated ou grouped blocks greater than 0.5 m³; aerial trajectory height of the blocks greater than 1 m |
| | Accessibility | Road out of order (closed) | | | |
| | Rehabilitation and maintenance operations | Rehabilitation during several days with important means | Decluttering, debris removal ; unclogging of bridges, hydraulic pipes and works | Rehabilitation time of several days with important means and/or reconstruction of roadway, drainage works | Rehabilitation time of several days with important means |
| | Road closure duration (Ds) | 48 hours (2 days) | 24 hours | 168 hours (7 days) | 48 hours (2 days) |
| **Medium** phenomenon intensity | Condition of the roadway (after event) | Snow deposit between 0.5 m and 1 m over several dozen metres in length | Scouring and/or covering by more than 0.5 m solid material thickness ; gullying of road pavement | Covering by more than 0.5 m solid material thickness or road displacement | Stopping and impact of isolated ou grouped blocks greater than 0.5 m³; aerial trajectory height of the blocks lower than 1 m |
| | Accessibility | Road out of order (closed) | | | |
| | Rehabilitation and maintenance operations | Rehabilitation during one day with important means | Decluttering, debris removal ; unclogging of bridges, hydraulic pipes and works | clearing of obstructive materials from the roadway, spot repair works, management of water inputs to the roadway | Blocks removal and residual risk assessment |
| | Road closure duration (Ds) | 24 hours (1 day) | 12 hours (half day) | 12 hours (half day) | 24 hours (1 day) |
| **Low** phenomenon intensity | Condition of the roadway (after event) | Partial snow deposit under 0.5 m | Dispersion and spreading of flows | Covering by less than 0.5 m solid material thickness | Stopping and impact of isolated ou grouped blocks lower than 0.5 m³; aerial trajectory height of the blocks lower than 1 m |
| | Accessibility | Traffic disruption (transport and travel delays) | | | |
| | Rehabilitation and maintenance operations | Roadway clearance with possibly reduced traffic or very temporary road closure | | | |
| | Road closure duration (Ds) | 0 hour | 0 hour | 0 hour | 0 hour |

*Source:* adapted from ONF/RTM, 2022, STePRiM, CCPHG Risk diagnosis report .

Finally, for each frequency, the indirect damage (loss due to traffic disruption, access cut-off) is equal to $\mathbf{D_c}$ (hours) x $\mathbf{t_{lost}}$ (hours) x **traf** (vehicles/hour). On this basis, the cost of loss in € due to traffic disruption could be calculated by $\mathbf{D_c}$ (hours) x $\mathbf{t_{lost}}$ (hours) x **traf** (vehicles/hour) x $\mathbf{C_{tLost}}$ (€/hours.vehicle).

There are indeed two possible cases, depending on whether a diversion is possible or not: 1) without diversion, the time lost is the traffic outage duration (including event triggering, detection and repair time: $\mathbf{t_{lost}} = \mathbf{D_c}$ ; 2) with diversion, the lost time is the minimum between the additional time related to the deviation and the outage time: $\mathbf{t_{lost}} = \text{Min}\ [\ D_c\ ;\ T_{diversion} - T_{normal}\ ]$. This calculation is, of course, a simplified vision of reality since a natural phenomenon affecting a road network can lead to a total cut-off or a reduction in traffic (reduction in speed, number of vehicles). The total lost time is indeed for each part of traffic using them, the sum of the time lost due to traffic reduction on the disrupted road and the time lost due to the use of the diversion.

### 2.3.3 Main results

Table 3 shows the results of direct material and human damage for exposed people on roads for each category of phenomenon. Table 4 represents a synthesis of the direct damage over the whole territory given the asumptions and simplifications described above. Figure 10 shows the lost time in vehicle.days on each section. Those results do not replace precise, local risk analysis but allow to have a quick overview on main threats on a large area and therefore to imagine and choose risk reduction strategies. Cut-off zones and duration have been identified for all phenomena on specific sections (Figure 10) using asumptions of Table 1) and show that tourist accesses at the bottom of the valley are highly exposed. It may provide useful information for infrastructures managers. A first estimation of the effect (lost of activity time) on remote activities is estimated on the basis of an arbitrary expert based cut-off duration as shown on table 2. However the whole operational, simple assessment of indirect damage due to activity losses, somehow useful in a wide land-use planning vision extendinf results of Table 4, is still challenging.

**Table 2.** Proposed expert assessment of the economic activity disruption (to be used for indirect damage assessment).

| | | Snow avalanche | Torrential flood | Landslides | Rockfalls |
|---|---|---|---|---|---|
| **High** phenomenon intensity | Impact on empoyement areas | Covering of facilities, technical zones with important amount of material, important structural damage to buildings, equipment preventing the continuation of the activity | | | |
| | Economic activity continuity | **Interrupted activity** | | | |
| | Nature of the operations necessary for a resumption of activity | Clearance and rehabilitation last several days with important means ; Repair of structural damage | | | |
| | Duration of interruption of activity | +/- 168 hours (7 days long) | +/- 168 hours (7 days long) | +/- 168 hours (7 days long) | +/- 168 hours (7 days long) |
| **Medium** phenomenon intensity | Impact on empoyement areas | Covering of facilities, technical zones with important amount of material, important structural damage to buildings, equipment preventing the continuation of the activity | | | |
| | Economic activity continuity | **Interrupted activity** | | | |
| | Nature of the operations necessary for a resumption of activity | Clearance and rehabilitation last several hours with important means ; Repair of structural damage<br>Mandatory residual risk assessment (duration of expert assessment for the reopening, evaluated at 12 to 24 hours depending on the ease of access for the different phenomena) | | | |
| | Duration of interruption of activity | 12 hours (half day) | 12 hours (half day) | 12 hours (half day) | 24 hours (one day) |
| **Low** phenomenon intensity | Impact on empoyement areas | Covering of facilities, technical zones with limited amount of material, no structural damage to buildings, equipment | | | |
| | Economic activity continuity | **Disrupted activity** | | | |
| | Nature of the operations necessary for a resumption of activity | Clearance and rehabilitation last few hours<br>Mandatory residual risk assessment for rockfalls (duration of expert assessment for the reopening, evaluated at 12 to 24 hours depending on the ease of access for the different phenomena). | | | |
| | Duration of interruption of activity | 0 hour | 0 hour | 0 hour | 24 hour |

*Source:* adapted from ONF/RTM, 2022, CCPHG STePRiM, Diagnosis report

**Table 3.** Assessment results of human exposure and damage (letality) on the roads.

| | | No hazard | Exposed to phenomena: Snow avalanches | Landslides | Floods (plain) | Rockfalls | Torrent floods | Total | |
|---|---|---|---|---|---|---|---|---|---|
| **Departemental roads** | | | | | | | | | |
| Roads length | | 172 km | 14 km | 90 km | 3 km | 40 km | 33 km | **179 km** | |
| Human exposure | | | 7 | 68 | 9 | 39 | 64 | **187** | person(s) |
| Human damage | *Frequent* | | 0.04 | | | 0.10 | 0.03 | **0.16** | person(s) |
| | *Rare* | | 0.20 | | | 0.84 | 0.17 | **1.21** | person(s) |
| **National roads** | | | | | | | | | |
| Roads length | | 29 km | | 3 km | | 2 km | 1 km | **6 km** | |
| Human exposure | | | | 21 | | 9 | 8 | **38** | person(s) |
| Human damage | *Frequent* | | | | | 0.22 | 0.01 | **0.23** | person(s) |
| | *Rare* | | | | | 0.25 | 0.07 | **0.32** | person(s) |
| **Communal, private roads** | | | | | | | | | |
| Roads length | | 242 km | 8 km | 53 km | 10 km | 15 km | 43 km | **129 km** | |
| Human exposure | | | 1 | 2 | 1 | 1 | 5 | **10** | person(s) |
| Human damage | *Frequent* | | 0.00 | 0.00 | 0.00 | 0.00 | 0.01 | **0.01** | person(s) |
| | *Rare* | | 0.02 | 0.00 | 0.00 | 0.01 | 0.02 | **0.05** | person(s) |
| **Total of all exposed roads** | | | | | | | | | |
| Roads length | | 442 km | 22 km | 145 km | 14 km | 58 km | 76 km | **314 km** | |
| Human exposure | | | 8 | 91 | 10 | 49 | 77 | **235** | person(s) |
| Human damage | *Frequent* | | 0.04 | 0.00 | 0.00 | 0.32 | 0.05 | **0.41** | person(s) |
| | *Rare* | | 0.22 | 0.00 | 0.00 | 1.11 | 0.25 | **1.57** | person(s) |

*Source:* adapted from ONF/RTM, 2022, CCPHG STePRiM, Diagnosis report

**Table 4.** Assessment results of direct damage (material and human letality )

**DMD** — **Direct Material Damage** (whole territory, classified by exposure types)

| Type of exposure | Whole territory Nb | Value | % Val | Exposed elements Nb | Value | %Ter. | Direct material damage Frequent | %Val. | Rare | %Val. |
|---|---|---|---|---|---|---|---|---|---|---|
| Individual dwelling building | 11 680 | 2 335 M€ | 79% | 2 697 | 536 M€ | 23% | 9.4 M€ | 2% | 38.9 M€ | 7% |
| Collective dwelling building | 7 728 | 555 M€ | 19% | 4 695 | 155 M€ | 28% | 8.5 M€ | 5% | 17.8 M€ | 11% |
| Economic activity building | 244 | 20 M€ | 1% | 85 | 4 M€ | 18% | 0.0 M€ | 1% | 0.9 M€ | 25% |
| Building open to public | 252 | 19 M€ | 1% | 86 | 2 M€ | 13% | 0.0 M€ | 1% | 0.4 M€ | 16% |
| Public infrastructure | 924 | 11 M€ | 0% | 300 | 4 M€ | 33% | 0.3 M€ | 9% | 1.7 M€ | 48% |
| **Total** | **20 828** | **2 940 M€** | **100%** | **7 825** | **701 M€** | **24%** | **20 €** | **3%** | **63.4 M€** | **9%** |

**DHD** — **Direct Human Damage** (whole territory, classified by exposure types)

| Human exposure | Nb | Occup. | Frequent | Rare |
|---|---|---|---|---|
| (in) Individual dwelling building | 11 680 | 23 360 | 1.80 | 15.59 |
| (in) Collective dwelling building | 7 728 | 13 910 | 1.15 | 2.99 |
| (in) Economic activity building | 244 | 11 574 | 0.00 | 1.93 |
| (in) Building open to public | 252 | 11 769 | 0.02 | 0.54 |
| (on) Roads (passengers…) | 760 km | 597 | 0.41 | 1.57 |
| **Total** | | | **3.37** | **24.89** |

**DMD** — **Direct Material Damage** -> for each phenomenon)

| Hazard | Scénario Frequent | Rare |
|---|---|---|
| Torrential T | 9 600 782 € | 36 939 089 € |
| Flood I | 10 121 379 € | 15 807 451 € |
| Avalanche A | 13 671 € | 5 576 960 € |
| Landslide G | 48 350 € | 4 473 685 € |
| Rockfall P | 235 862 € | 562 717 € |
| **Total** | **20 020 044 €** | **63 359 901 €** |

**DHD** — **Direct Human Damage** -> for each phenomenon)

| Hazard | Scénario Frequent | Rare |
|---|---|---|
| Avalanche A | 0.05 | 12.46 |
| Torrential T | 1.70 | 6.45 |
| Rockfall P | 1.61 | 5.98 |
| Landslide G | 0.00 | 0.00 |
| Flood I | 0.00 | 0.00 |
| **Total** | **3.37** | **24.89** |

**Available** — Extended analysis and location of all possible cut-off zones for all phenomenons

**Remaining challenges**

**ID** — **I**ndirect **D**amage (access cut-off): Estimation of duration of traffic disruption for all paths, considering all phenomena

**IED** — **I**ndirect **E**conomic **D**amage(business interruption): Estimation of cost of traffic disruption for activities all paths, considering all phenomena

*Source:* adapted from ONF/RTM, 2022, CCPHG STePRiM, Diagnosis report

# 3 Conclusions

The STePRiM framework is a new and original tool for mountain risk integrated management and resilience for two reasons. First, the objective of the STePRiM framework is dedicated to promote an integrated vision of risk management (from risk awareness to protection works) which somehow allows to be better prepared at a territorial scale to event management. Secondly, The analysis introduces a temporal aspect by looking at the delayed consequences of network outages. While risk assessment is done statically at a given time, indirect damage due to road networks disruption is characterized using practical expert assessment of effects and time to recover and repair.

**Figure 10.** Global territorial network analysis: indirect damage (lost time in vehicles.days).

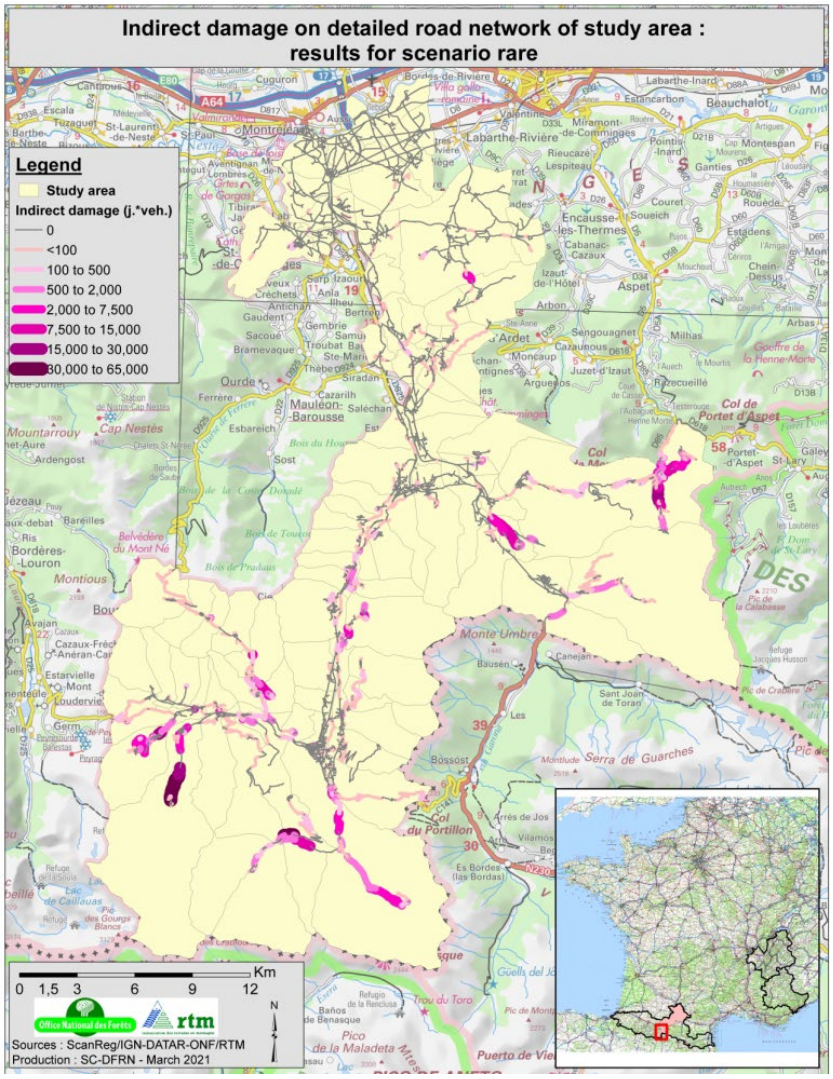


*Source:* ONF/RTM, 2022, CCPHG StePRiM, Diagnosis report

The STePRiM also innovates in mixing both risk analysis and decision-making steps. Its territorial features emphasizes needs to combine assessment methods with specific decision support frameworks designed and adapted to various contexts in terms of actors, solutions, spatial and temporal scales. This constitutes a promising challenge for development of new progressive, integrated resilience assessment frameworks for critical infrastructures exposed to natural (or technological) threats mixing quantitative, qualitative assessment and decision-aiding methods. From a more general point of view, this kind of approach demonstrates gaps between theory and practice. The challenge will always consist in finding the best compromise between performance, precision, complexity and simplification, speed, imprecision (Figure 11) when choosing and applying assessment methods.

**Acknowledgements**: we thank the services of DDT (Departmental Directorate of Territories) of Haute-Garonne, DDT of Alpes de Haute-Provence, DREAL (Regional Directorate for Environment) of Provence Alpes Cote d'Azur and also the French National Forest Office/RTM of Hautes-Alpes for our fruitful discussions and collaboration.

**Figure 11.** Coping with complexity, accuracy and usabilty, the challenge of transfer from science to real decision-making contexts.

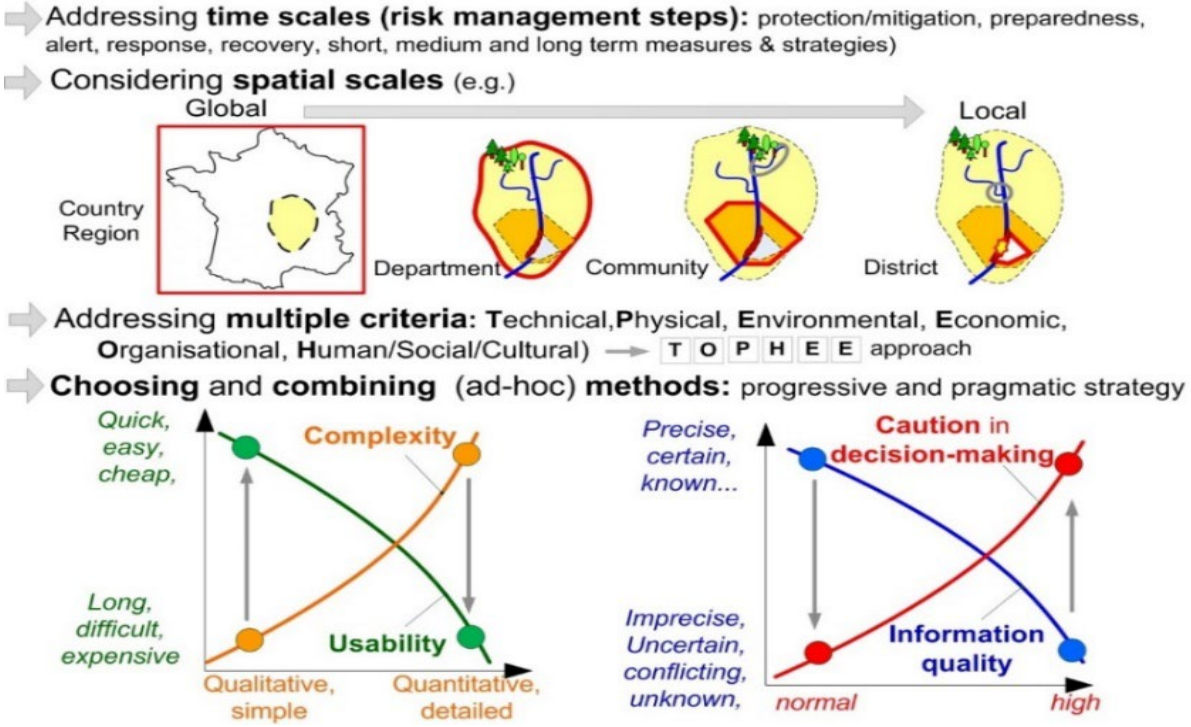


## References


1. MTES. Appel à projet STePRiM (Stratégie de Protection contre les Risques en Montagne) - Cahier des charges. Ministère de la Transition Ecologique et Solidaire (MTES), Direction Générale de la Prévention des Risques (DGPR), Service des Risques Naturels et Hydrauliques (SRNH), Bureau des Risques Naturels Terrestres (BRNT); 2019.
2. IPCC. Climate Change 2021: The Physical Science Basis. Contribution of Working Group I to the Sixth Assessment Report of the Intergovernmental Panel on Climate Change. Masson-Delmotte V, Zhai P et al, editors. Cambridge University Press. In Press.; 2021.
3. Commission E. Council Directive 2008/114/EC of 8 December 2008 on the identification and designation of European critical infrastructures and the assessment of the need to improve their protection [Internet]. 2008. Available from: https://eur-lex.europa.eu/legal-content/EN/TXT/?uri=CELEX:32008L0114&qid=1649840359995
4. Tacnet J-M, Forestier E, Mermet E, Curt C, Berger F. Résilience territoriale : du concept à l'analyse d'infrastructures critiques en montagne. La Houille Blanche. 2018;5-6:20–28.
5. Gallina V, Torresan S, Critto A, Sperotto A, Glade T, Marcomini A. A review of multi-risk methodologies for natural hazards: Consequences and challenges for a climate change impact assessment. Journal of Environmental Management. 2016;168:123–132.
6. Marzocchi W, Garcia-Aristizabal A, Gasparini P, Mastellone ML, Di Ruocco A. Basic principles of multi-risk assessment: a case study in Italy. Natural Hazards. 2012;62(2):551–573.
7. ESREDA. Modelling the Resilience of Infrastructure Networks: an ESREDA (European Safety, Reliability & Data Association) project group report. Remenyte-Prescott R, Kopustinkas V, editors. Norway: Det Norske Veritas AS; 2021.
8. Hackl J, Lam JC, Heitzler M, Adey BT, Hurni L. Estimating network related risks: A methodology and an application in the transport sector. Natural Hazards and Earth System Sciences. 2018;18(8):2273–2293.
9. Mermet E. Aide à l'exploration des propriétés structurelles d'un réseau de transport. Conception d'un modèle pour l'analyse, la visualisation et l'exploration d'un réseau de transport. Thèse de doctorat. [Marne-la-Vallée, France]: Université Paris-Est; 2011.
10. Tacnet J-M, Mermet E, Zadonina K, Deschatres M, Humbert P, Dissart J-C, et al. Road network management in the context of natural hazards: a decision-aiding process based on multi-criteria decision making methods and network structural properties analysis. Proceedings of the International Snow Science Workshop (ISSW 2013), 7-11 october 2013, Grenoble, France. Grenoble, France; 2013. p. 95–106.

11. Tacnet J-M (coord. . Decision Support Guidelines - Methods, procedures and tools developped in PARAmount (WP7 report) - hal-03639896. European Regional Development Fund - Alpine Space Progam - Intereg IV - PARAmount projet : imProved Accessibility: Reliability and safety of Alpine transport infrastructure related to mountainous hazards in a changing climate. http://www.paramout-project.eu/; 2012.
12. Carladous S, Tacnet J-M. Stratégie Territoriale de Prévention des Risques en Montagne (STePRiM) - Guide méthodologique pour la mise en œuvre - version de travail. Ministère de la Transition Ecologique et Solidaire (MTES), Direction Générale de la Prévention des Risques (DGPR), Service des Risques Naturels et Hydrauliques (SRNH), Bureau des Risques Naturels Terrestres (BRNT); 2022.
13. European Commission D-G for R, Innovation. Evaluating the impact of nature-based solutions: A handbook for practitioners - doi:10.2777/244577. Wendling L, Dumitru A (Eds), editors. Luxembourg: Publications Office of the European Union; 2021.
14. ONF/RTM. Stratégie de prévention des risques en montagne. Diagnostic de risque de la Communauté des communes Pyrénées Haut Garonnaises. Rapport provisoire. Avril 2022. 2022.
15. CCPHG. Candidature de la Communauté de CommunesPyrénées Haut-Garonnaises (CCPHG) à l'appel à projets« Stratégie territoriale pour la prévention des risques en montagne ». 2017.
16. MTES/CGDD. Analyse multicritères des projets de prévention des inondations - guide et annexes techniques. Ministère de la Transition Ecologique et Solidaire, Commissariat général au développement durable; 2018.

# Decision-Aiding Towards Improved Resilience of a Deteriorating Debris Retention System Subject to Maintenance Strategies

Nour CHAHROUR
Univ. Grenoble Alpes, INRAE, ETNA, 38000 Grenoble, France.
Univ. Grenoble Alpes, CNRS, Grenoble INP, GIPSA-lab, 38000 Grenoble, France.
Nour.chahrour@grenoble-inp.fr

Guillaume PITON, Jean-Marc TACNET
Univ. Grenoble Alpes, INRAE, ETNA, 38000 Grenoble, France.
Guillaume.piton@inrae.fr, jean-marc.tacnet@inrae.fr

Christophe BÉRENGUER
Univ. Grenoble Alpes, CNRS, Grenoble INP, GIPSA-lab, 38000 Grenoble, France.
Christophe.berenguer@grenoble-inp.fr

## Abstract

*Protection systems against natural phenomena in mountains are critical infrastructures that deteriorate over time and necessitate regular maintenance. Debris retention systems, for example, are one type of protection systems that aim to mitigate natural phenomena such as torrential floods and debris flows by storing a specific volume of solid materials and by regulating the passage of the flows. They thus reduce negative consequences and provide protection to downstream exposed assets. The deterioration of a retention system overtime, including its filling by debris, reduces its efficacy in achieving the desired objectives. One key issue in natural risk context is that budgets provided by State or local authorities for the management of protection structures will always be somewhere limited. Consequently, it is essential and expected to develop models that facilitate ensuring the resilience of such critical structures while respecting available human, material and financial resources. This paper proposes a maintenance decision-aiding model that makes it possible to assess and prioritize different maintenance strategies applied to a retention system over its lifetime. The overall framework involves a (1) physical deterioration model, which contributes in building degradation trajectories of the system; (2) a stochastic deterioration surrogate model learnt from the degradation trajectories, developed using stochastic Petri nets and (3) a maintenance model, which is constructed as an additional layer in the stochastic Petri nets degradation model and which contributes in figuring out the most cost-effective maintenance strategy. A numerical analysis is performed using the data from a real retention system located in the Claret torrent in France and subjected to debris flows over a period of 50 years*.

## 1 Introduction

Modern societies highly rely on infrastructure systems that provide the economy and well-being with essential utilities and services. The consequences of infrastructure malfunction or failure can be significant (e.g., evacuations, economic loss, environmental impacts). However, the complexities involved in the design of these critical systems make it difficult for the managers to predict when the system could fail. On the other hand, the rehabilitation of such complex systems requires high monetary budgets, which could not be always affordable by the State or by local authorities.

Infrastructure systems resilience is among the main concerns of those managing complex systems. In the context of critical infrastructures, resilience is defined according to four different principles: anticipation, absorption, adaptation and recovery [1]. These principles refer respectively to the ability of the system to resist and manage a crisis, to maintain its functioning during its lifetime, to cope with changing conditions and to return rapidly back to normal conditions after disruption [2]. It is therefore, essential to have a comprehensive knowledge concerning the mechanisms of the system (efficacy, deterioration, maintenance) associated with each principle, seeking for a high resilient system. Indeed, understanding when and how the system could fail make it possible to know when to apply preventive maintenance operations instead of carrying out corrective maintenance operations, which are much more expensive than preventive ones.

Protection systems in mountains can be considered as one type of critical infrastructures. They aim in reducing the causes or the consequences of natural phenomena (e.g. torrential floods, debris flows, etc.) thus protecting people, assets and properties that are exposed to these events [3]. These systems (e.g. check dams series, debris retention system) are supposed to attain high efficacy levels that permit them to fulfil their assigned functions over time. However, over their lifetime, their efficacy is reduced because of aging or because of structural and/or functional failures that occur due to the impacts and consequences of natural phenomena on the system itself. This could in turn prevents them from providing the desired protection level to elements at risk.

Debris Retention systems, are usually implemented in downstream areas of torrential watersheds. They aim in storing specific volume of solid materials transported by debris flows. Therefore, their main objective is to prevent huge volumes of sediments and big boulders to be transferred to areas where vulnerable elements are located. The system is composed of several components that functions collaboratively in order to provide high level of protection [4]. These components could differ from one system to another depending on the desired functions. However, a debris basin, retention dam and a maintenance access track should at least be present in every debris retention system regardless their type, shape and sizes (fig. 1). The debris basin is a deposition area where solid materials are stored (boulders, woody debris, gravel and mud). It has a specific storage capacity. The retention dam is the outlet of the debris basin. It has openings (top weir and eventual orifices) that allow it to moderate the flow by reducing its intensity and to trap large debris materials. The maintenance access track permits technicians, trucks and engines to reach the system in order to carry out maintenance operations (e.g. cleaning the basin). A recent study provides a thorough review concerning the design (structural, hydraulic), functions (e.g., flow moderation, debris storage), malfunctions (e.g., excess trapping, flow lateral bypass) and maintenance (e.g. cleaning) of retention systems constructed in French torrents of the Alpes and Pyrénées [5].

In France, the level of degradation of retention systems is estimated either by field inspection or on expert predictions. Maintenance operations are then made on these bases.

**Figure 1.** Claret retention system: (1) retention basin, (2) retention dam, (3) lateral dykes, (4) access track and (5) downstream counter dam. Upstream view (left panel) and downstream view (right panel) © ONF-RTM/S. Carladous May, 23rd 2018.

According to historical experience, the managers of these systems adopt a specific maintenance policy for each system depending on its components and on the features of the torrent at which it is located. For example, for the retention system located in the Claret torrent in France, cleaning operations are carried out after each debris flow event whatever is the debris volume stored in the basin. The problem is that in the Claret torrent, debris flows are frequent (one event every two years on average). This requires frequent maintenance operations, which in turn necessitates high budgets. However, limited monetary budgets are provided by the French State for the management of protection systems. This sheds the light on the importance of developing decision-aiding models that use and analyse available information in order to choose the most cost-effective maintenance strategy to be applied on deteriorating protection systems.

A very recent decision-aiding model was developed in order to support maintenance-decision-making of check dams subjected to clear water floods [6]. In this paper, the objective is to develop further the model by considering the case of retention systems because these structures increase in number and managers should take informed decision before to select and design such systems [5]. For this purpose, a holistic approach integrating several stages is developed. The approach starts by physically modelling the filling of the debris basin when subjected to a series of debris flows over its lifetime. The obtained deterioration trajectories are then used in order to estimate the probability laws corresponding to the transition times between the states of the basin. These laws are then used in a stochastic Petri net model (SPN) in order to model the stochastic behaviour of the system when subjected to different maintenance strategies implemented based on a condition-based maintenance (CBM) policy. Finally, the outputs of the SPN model are used to compare the modelled maintenance strategies in terms of the total cost of each strategy. The main contributions behind this approach is to (1) define and implement a maintenance policy that can efficiently improve the resilience of retention systems and (2) support risk managers to make optimal decisions thus contributing to a safer and better world.

Section 2 thoroughly describes the global developed modelling approach that can be used for analysing the behaviour of any retention system. In section 3, the approach is adopted in order to analyse the behaviour of a real case retention system located in the Claret torrent in France. Conclusions and perspectives are provided in Section 4.

# 2 Methodology

Improving the resilience of retention systems necessitates understanding first their deterioration mechanisms when subjected to debris flows over time. However, knowledge concerning the deterioration trajectories of these systems is often partially or totally missing. This section proposes an integrated approach that combines several sources of information (expert assessments, historical data and numerical simulations) in order to estimate these trajectories over the lifetime of the system and then to implement a CBM policy that makes it possible to optimize maintenance strategies. The approach considers only the functional failure of retention systems and does not consider the failure of the system from a structural point of view. It models the filling of the debris basin over time, which could lead to insufficient storage capacity. The different modelling stages of the overall approach are detailed in the following subsections.

## 2.1 Building Deterioration Trajectories of a Debris Basin

Retention systems are implemented in mountains aiming to reduce the risk level induced due to debris flows by trapping a specific volume of the flow. However, the trapping of low magnitude events that do not pose harm to vulnerable issues increases the stored volume and thus reduces the capacity of the debris basin. Indeed, the jamming of the retention dam's openings by big boulders transported by the flow will prevent small events to pass through the dam. In this section, a physical model routing debris flows through a retention system is proposed. The model results in the final volume stored in the basin after each debris flow event. The steps involved in the physical model are explained below.

### 2.1.1 Random Generation of Debris Flow Events

The first step of the physical model is to generate series of debris flow events occurring over a period of 50 years. This requires data concerning the frequency and the magnitude of the events that really occurred in the studied torrent. Indeed the frequency-magnitude curve of a given torrent makes it possible to generate random debris flow events with random volumes $V_{event}$ and random dates of occurrence $D_{event}$.

The routing of a generated debris flow series through the retention system will result in one deterioration trajectory corresponding to the filling of the debris basin over 50 years. However, the end purpose of the physical model is to have a set of these trajectories in order to attain a stochastic vision of the system's dynamic behaviour. Therefore, a satisfactory number $n$ of debris flow series that allow having a good vision of the resulted trajectories should be generated. Each generated debris flow series will be referred to as "a scenario".

Each debris flow event in a scenario is represented by a hydrograph, which provides the inlet discharge as a function of time over the whole duration of the event. In this study, triangular hydrographs are assumed. Therefore, the hydrograph is characterized by three parameters: peak discharge, time to peak and duration of the event. The peak discharge $Q_{peak}$ is estimated as follows [7]:

$$Q_{peak} = 0.0188 \cdot V_{event}^{0.79} \quad (1)$$

The time to peak $t_{peak}$ is assumed to 5 seconds based on monitoring data. It corresponds to the time at which the flow reaches its peak discharge. The duration of the event $t_{end}$ is estimated using the following equation:

$$t_{end} = 2 \cdot \frac{V_{event}}{Q_{peak}} \quad (2)$$

### 2.1.2 Stochastic Arrival of Boulders to the Retention Dam's Openings

The second step of the physical model is to randomly sample the number of boulders in a given debris flow volume that approaches towards the dam's openings. The jamming of the retention dam's openings by boulders during a debris flow is a very recent field of study. Indeed, a recent model that studies the stochastic arrival of boulders to the dam and whether each arriving boulder is blocked in the dam's opening has been proposed by [8]. The developed model assumes that the stochastic arrival of boulders to the dam follows a binomial distribution. The model starts by classifying the boulders transported by the flow into classes of different diameters. Each class $j$ corresponds to a range of diameters [$D_{j,min}$; $D_{j,max}$]. For each class $j$, the average diameter $D_j$ and the volume $V_j$ of the boulders is computed assuming that boulders are spherical on average.

In a given event of reference whose whole volume of the debris flow is $V_{event}$, one can count the number $n_j$ of boulders of each classes. For each class $j$, the same volume can be split in $N_j$ elementary volumes $V_j$:

$$N_j = \frac{V_{event}}{V_j} = \frac{V_{event}}{\pi \cdot D_j^3/6} \quad (3)$$

These "packets" of debris might be boulders of class $j$ or something else (boulders of another class or mud). The binomial law telling us how many packets in a given volume of debris are true boulders of class $j$ can be calibrated by its probability $p_j$:

$$p_j = n_j/N_j \quad (4)$$

If replacing $V_{event}$ in Eq. (3) by a volume $V(t)$ reaching the retention dam at a given time step, $N_j$ corresponds to the number of "packets" of debris that could be a boulder of class $j$ at this time step. The number of successes on the aforesaid binomial law gives the number of boulders $n_j$ of class $j$ involved in $V(t)$. However, when randomly sampling $n_j$ of all the boulder classes, $V(t)$ should be progressively reduced by the volume of boulders of larger classes that have already been identified at a given time step (k = 1, 2, …, $\sum n_{j-1}$). Consequently, Eq. (3) becomes:

$$N_j = \frac{V(t) - \sum_{k=1}^{n_{j-1}} V_k}{V_j} = \frac{V(t) - \sum_{k=1}^{n_{j-1}} \pi \cdot D_k^3/6}{\pi \cdot D_j^3/6} \quad (5)$$

Finally, the dimensions of the jamming of the retention dam's openings by boulders arriving to the dam are estimated based on classical jamming conditions that depend on the configuration of jamming (horizontal, vertical or both) and on the size of boulders relative to the size of the openings [8]. The width and base level of the opening, noted respectively $w_i$ and $y_i$ are thus updated over time depending of the obstruction related to the boulders.

### 2.1.3 Discharge Capacity of the Retention dam's Openings

The third step of the physical model is to calculate the total discharge that is released through the retention dam at each time step. The openings of the dam are the elements responsible for releasing a specific volume of the flow to the downstream. The discharge capacities through the dam's openings (spillway, orifices) are estimated based on the following stage-discharge equations provided in literature [9]:

$$Q_i^{spillway}(t) = 0.385\, w_i\,(t)\sqrt{2g\big(h(t) - y_i(t)\big)^3} + 0.308\frac{1}{\tan(\varphi)}\sqrt{2g\big(h(t) - y_i(t)\big)^5} \quad (6)$$

$$Q_i^{orifice} = 0.65 * w_i\,(t) * \frac{2}{3} * \sqrt{2 * g} * \big((h(t) - y_i(t))^{3/2} - (h(t) - y_i(t) - a_i)^{3/2}\big) \quad (7)$$

where $Q$ *(m³/s)* is the discharge through opening $i$, $t$ *(s)* is the time, $w_i\,(t)$ *(m)* is the width of the opening including the obstruction by boulders (free width), $g$ *(~ 9.81 m/s²)* is the gravitational acceleration, $h(t)$ *(m)* is the depth of the flow over the dam's base level, $y_i(t)$ *(m)* is the base level of orifice $i$ including the obstruction by the boulders, $\varphi$ *(°)* is the angle between the spillway's wing and the horizontal and $a_i$*(m)* is the orifice's height. The total discharge capacity $Q_{out}$ of a retention dam is equal to the sum of the discharge capacities of all its openings.

### 2.1.4 Buffering Capacity of the Debris Basin

Retention systems aim to regulate debris flows by reducing their peak discharges. This means that the volume stored in the debris basin during a debris flow event is expected to be released gradually through the openings of the retention dam. This phenomenon is referred to as "buffering". However, the jamming of the dam's openings by boulders reduces the total discharge capacity of the dam. Therefore, the stored volume in the basin will progressively increase not being able to escape through the jammed dam. In other words, the buffering capacity of the debris basin will be reduced. The retention dam will thus no more be able to self-clean a filled basin. In this case, the debris basin has to be cleaned by performing maintenance operations.

The fourth step of the physical model is to estimate the buffering capacity of a debris basin using the following mass conservation equation:

$$\big(\, Q_{in}(\mathrm{t}) - Q_{out}\big(\mathrm{h(t)}\big)\,\big) \cdot \Delta t = \Delta V_b\big(h(t)\big) \quad (8)$$

Where $Q_{in}$ *(m³/s)* is the inlet discharge provided by the hydrograph of the event, $Q_{out}$ *(m³/s)* is the discharge capacity of the retention dam estimated according to section 2.1.3, $\Delta t$ *(s)* is the time step, h *(m)* is the flow level and $\Delta V_b$ *(m³)* is the variation of the volume stored in the basin. In order to use Eq. (8), data concerning the input hydrograph of the event, retention dam's outlet discharge capacity, storage capacity of the debris basin, deposition slope and the stage - volume capacity curve (*h* versus $V_b$) should be acquired.

### 2.1.5 Computational Analysis and Expected Outputs

The physical model is implemented in an R code that makes it possible to solve all the previously mentioned steps. The developed model is general and can be used to analyse any retention system just by changing input data concerning the features and characteristics of the system (basin storage capacity, deposition slope, and dimensions of the dam's openings, number of boulders of all classes for a given volume of event). Concerning the first step, presented in section 2.1.1, each scenario will be simulated separately. The steps represented in sections 2.1.2, 2.1.3 and 2.1.4 should be performed at each time step, covering the whole duration of each debris flow event involved in a scenario. The jamming of the openings and the simultaneous filling of the basin is thus explicitly modelled during the event and therefore the outlet discharge of the dam will also vary in time. This in turn provides time-evolving indicators that makes it possible to plot their time-series.

The model results in several outputs such as the times series of the inlet discharge $Q_{in}(t)$ *(m³/s)* outlet discharge $Q_{out}(t)$ *(m³/s)* vertical and horizontal jamming rate *(%)* of the dam's openings by boulders, flow level *Z(t) (m)* at the dam and the cumulative volume stored in the basin $V_b$ *(t) (m³)*. In this study, the focus will be on the change of $V_b$, which is already dependent on the other indicators. Therefore, the main interest will be to extract, from the R code results, the final stored volume in the basin attained at the end of each event. This will help to build the deterioration trajectories of the stored volume in the debris basin over the studied period (50 years).

## 2.2 Surrogate Deterioration Model using SPNs

A stochastic Petri net (SPN) degradation model is composed of four different elements: places, tokens, transitions and arcs [10]. A place represents the state (level of deterioration) of the deteriorating system. The presence of a token in a place means that the system is residing in the state corresponding to this place. Transitions permit the token to move from one place to another according to the stochastic firing time assigned to each transition. Arcs link between places and transitions thus showing the possible paths between the states of the system. Consequently, in order to build a deterioration model using SPNs, two main steps described below should be achieved.

### 2.2.1 States Definition of a Deteriorating Retention Basin

The first step required for building a SPN deterioration model is to define different states of the studied system reflecting different levels of deteriorations. In this study, four different states at which the debris basin can reside are considered. It is assumed that the stored volume in the basin $V_b$ evolves progressively from an initial state (empty basin) to a completely failed state, reaching the maximum storage capacity of the basin $C_b$. Therefore, each of the defined states corresponds to a range of stored volume in the basin as follows:

- State 1: $0 \leq V_b \leq V_{b1}$ (good condition)
- State 2: $V_{b1} < V_b \leq V_{b2}$ (poor condition)
- State 3: $V_{b2} < V_b \leq V_{b3}$ (very poor condition)
- State 4: $V_{b3} < V_b \leq C_b$ (almost totally failed condition)

The choice of thresholds $V_{b2}$, $V_{b2}$ *and* $V_{b2}$ can be based on expert assessments. Moreover, the deterioration process is not necessarily gradual. In other words, the state of the debris basin could either evolve gradually between the states (e.g. evolution from state 1 to state 2 to state 3 to state 4) or could be rapid (e.g. direct evolution from state 1 to state 3, from state 2 to state 4, etc.). Fig. 2, (a) represents the SPN deterioration model, which better illustrates all the possible transitions between the states of the basin.

### 2.2.2 Estimation of Transition Probability Laws

The stochastic transitions that link between the states of a system are the main elements responsible for the functioning of a deterioration SPN model. In literature, the probability laws of these transitions are either assumed by experts to follow a specific distribution (e.g. Exponential, Gamma, Weibull) or estimated using available real data about time to failure. In the case of torrent protection structures, such data are either totally missing or are imperfect [11]. Moreover, this imperfection makes conflicts between experts' judgments. Consequently, Chahrour et al. recently proposes a surrogate deterioration SPN model that uses the physical modelling of the system in order to estimate empirical non-parametric transition probability laws [6].

In this study, the physical modelling concerning the filling of the debris basin as presented above is used in order to estimate non-parametric probability laws of the stochastic transitions involved in the SPN model of fig. 2a. Indeed, after defining four states of the debris basin, the simulation of the *n* generated scenarios makes it possible to have several estimates of the transition times between the states. The transition probability laws are therefore built based on the deterioration trajectories obtained from the physical model using non-parametric estimations.

## 2.3 Maintenance SPN Model Implementing a CBM Policy

The developed surrogate deterioration SPN model makes it possible to extend the model so that it integrates a maintenance model by easily implementing a CBM policy. Different CMB maintenance policies can be used. However, in the present study, the following policy is adopted:

- If the debris basin is in state 1, no maintenance operation is carried out.
- If the debris basin is in state 2, minor maintenance operations are carried out.
- If the debris basin is in state 3, major maintenance operations are carried out.
- If the debris basin is in state 4, corrective maintenance operations are carried out.

The maintenance operations in all cases are cleaning operations. The only difference between minor, major and corrective operations is in the volume of debris to be cleaned. Moreover, when a maintenance operation is carried out, all the stored debris volume in the basin should be cleaned. In other words, upon maintenance, the debris basin returns back to its initial state (empty basin). Fig. 2b represents the CBM policy implemented in the SPN model. Each maintenance operation is linked to a deterministic transition of a constant firing time reflecting the time required for the operation to be performed. The figure also shows an inspection process that is necessary for detecting the state of the system over time. Inspection is assumed to take periodically every one year.

When Monte-Carlo simulation starts, the token present initially in place $P_1$ (state 1) starts to move between the states based on the assigned probability laws to the stochastic transitions thus revealing the evolution of the volume present in the debris basin over time. Every year, an inspection is performed in order to detect the state of the basin. According to the detected state, the assigned maintenance operation is carried out. After the time needed for the operation to be accomplished, the token returns back to place $P_1$ revealing that the basin is restored back to a good state and the evolution starts again. When the

simulation duration (50 years) is attained, the SPN model results in the number of maintenance operations carried out over a period of 50 years.

In order to compare the results provided by the SPN model for different maintenance strategies, four strategies are proposed:

- Strategy 1: all maintenance operations are allowed.
- Strategy 2: minor operations are inhibited.
- Strategy 3: major operations are inhibited.
- Strategy 4: minor and major operations are inhibited.

Knowing the cost of each maintenance operation, the results of the SPN model permits computing the total cost of each proposed maintenance strategy. This in turn support risk managers and decision-makers to be aware of the most cost-effective strategy.

**Figure 2.** SPN model showing the stochastic deterioration model and the implemented CBM policy: (a) deterioration process, (b) inspection and maintenance processes (Adapted from [6]).

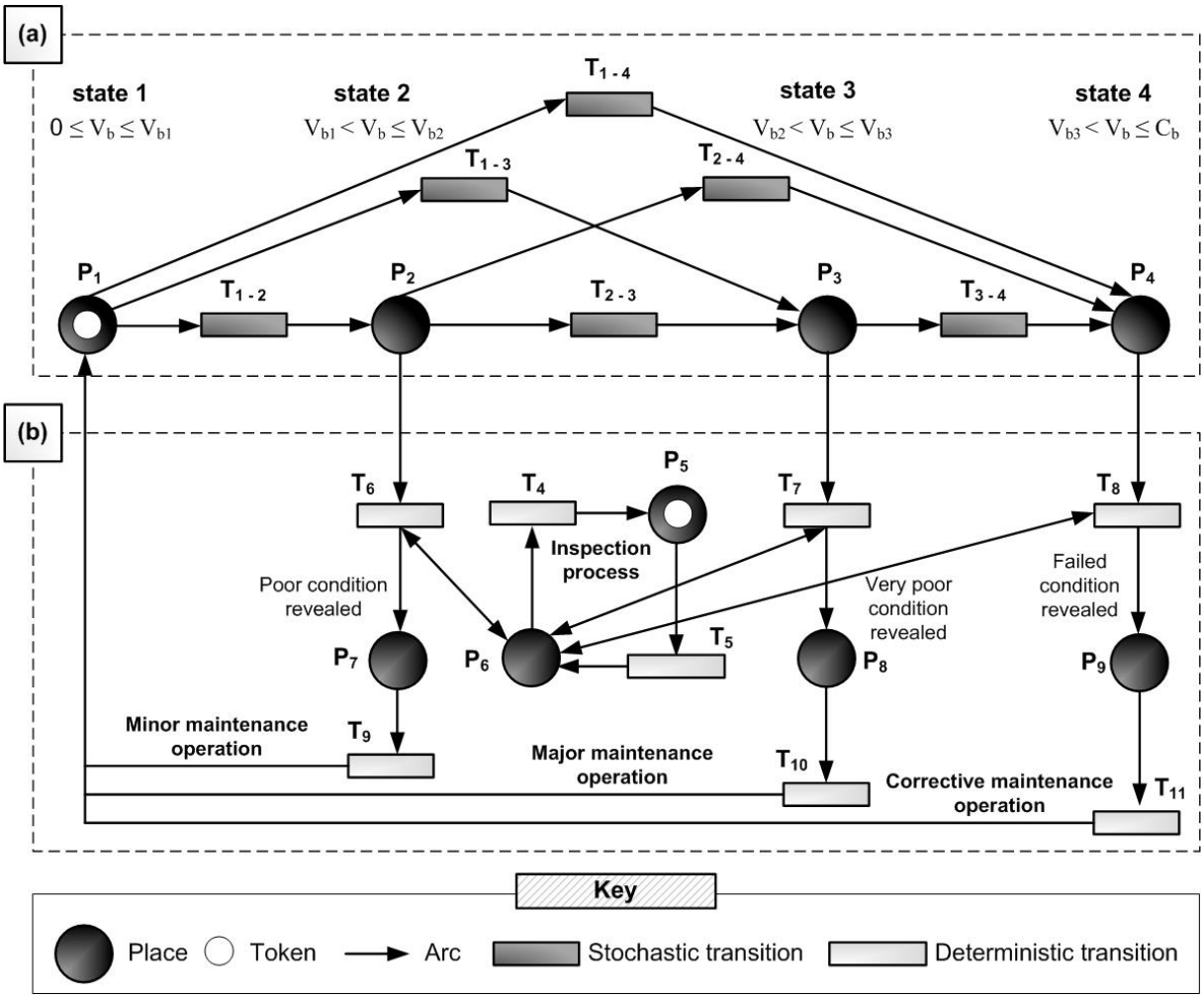

# 3 Case Study: Modelling of the Claret Retention System

The Claret torrent in France is very active in producing destructive debris flow events. Fig. 3 provides the Claret's Frequency - Magnitude curve resulted after the adjustment of real observations of debris flow events using Generalized Pareto distribution (GPD) [12]. In 1991, a retention system was built in the torrent in order to protect vulnerable exposed issues. The capacity of the debris basin is 22,000 m³. The retention dam is made of reinforced concrete and has three openings: a spillway and two orifices as shown in fig. 4. Since the construction of the system, it was noticed that the dam is trapping large volumes of debris materials even those corresponding to small debris flow events. Therefore, excessive volumes rapidly fill the debris basin. The managers of the Claret adopt an event-based maintenance policy, in which after each debris flow event, they carry out cleaning operations whatever is the stored volume in the basin. However, this policy requires very high monetary budgets. The aim of this section is to use the developed approach presented in section 2 in order to (1) model the progressive filling of the Claret debris basin when subjected to debris flow scenarios over a period of 50 years, (2) compare the costs of different maintenance strategies by adopting a CBM policy and (3) support the managers of the Claret to make cost-effective maintenance decisions.

**Figure 3.** Frequency – Magnitude curve of debris flow events in the Claret torrent [12].

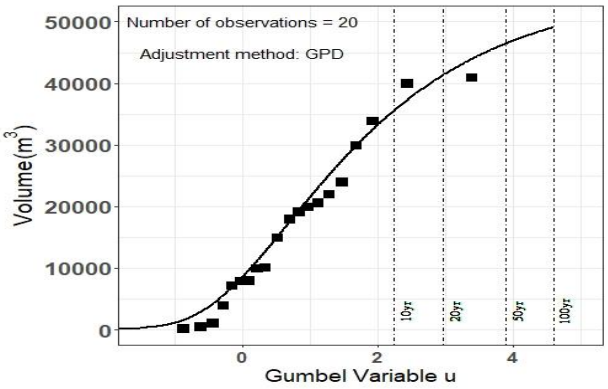


**Figure 4.** Dimensions of the Claret retention dam (m).

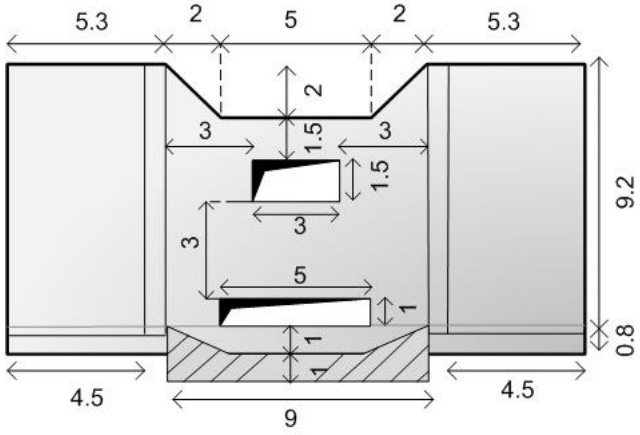


## 3.1 Physical Modelling Results and Discussions

In order to reach the desired objectives, 100 scenarios of debris flow series are generated. The number of boulders of each class were defined by expert knowledge based on pictures of the last cleaning operation. Data concerning the monthly distribution of the recorded torrential flood events in the Claret are given by [13]. On average, three storms per year hit the Claret catchment, but not all trigger debris flows [12]. Therefore, the dates of three torrential events are extracted, every year, from the provided monthly distribution of events. This means that for each scenario, the dates of 150 storms are obtained over a period of 50 years. A binomial distribution is then used in order to specify which event indeed triggered a debris flow events. Knowing that a debris flow occurs once every two years, the success probability in the binomial distribution is considered as $p = 1/6$ (one debris flow event every six storms on average). Random volumes of the revealed debris flow events are finally generated from the Frequency-Magnitude curve of fig. 3.

In order to start simulations, an initial configuration of the retention system should be set up. Therefore, before the simulation of the first event of each scenario, the openings of the retention dams are assumed to be initially empty from boulders and the debris basin is assumed to be initially empty ($V_b = 0\ m^3$). Fig. 5 shows the results obtained for the first two debris flow events involved in scenario 1. The first event has a volume $V_{event} = 19{,}422\ m^3$ and the second event has a volume $V_{event} = 24{,}873\ m^3$. The difference in the

dates of occurrence of both events is approximately 1 year. The final stored volume in the basin attained after the second event is $V_b = 21{,}900\ m^3$, which is approximately equals to the maximum storage capacity of the basin $C_b = 22{,}000\ m^3$. It is also clear from the figure that the final stored volume in the basin is not the maximum attained stored volume during the event. Indeed, the maximum stored volume is usually greater than the final stored volume due to self-cleaning. In other words, within a short duration (< *12 min*), the basin stores a maximum volume and then starts to release some materials through the dam's openings. This example also shows the rapid deterioration (in 1 year), in which the basin is almost completely filled after the second debris flow event in a scenario, which consists of 29 debris flow events occurring over a period of 50 years. Similar results are obtained for the rest of events involved in the scenario and for the others generated scenarios.

**Figure 4.** Results showing the volume stored in the debris basin at the end of the first and the second debris flow events involved in the first generated scenario.

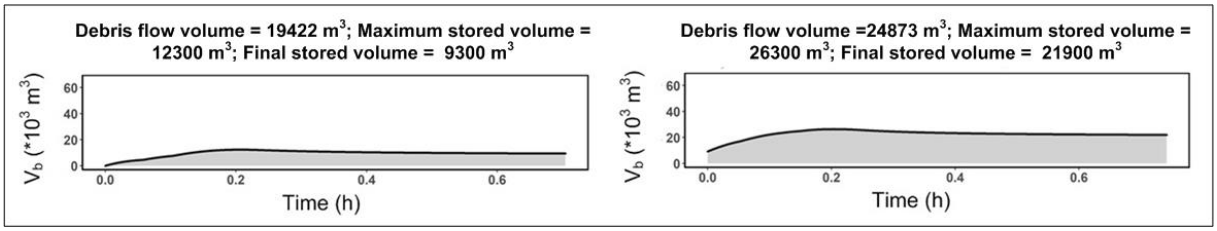


The obtained final stored volume after each debris flow event involved in a scenario permits building deterioration trajectories of the debris basin. Fig. 5 shows the evolution of the volume stored in the debris basin over time for the 100 generated scenarios. It is revealed that in most scenarios, the debris basin is completely filled within 5 years (after two or three debris flow events). Moreover, in all scenarios, the basin reaches its maximum storage capacity before 20 years. Consequently, cleaning maintenance operations are required at very early stages. The simulations are coherent with the field observation available so far [8].

**Figure 5.** Deterioration trajectories showing the evolution of the stored volume in the basin over time. Dashed lines: chosen thresholds defining the states of the basin.

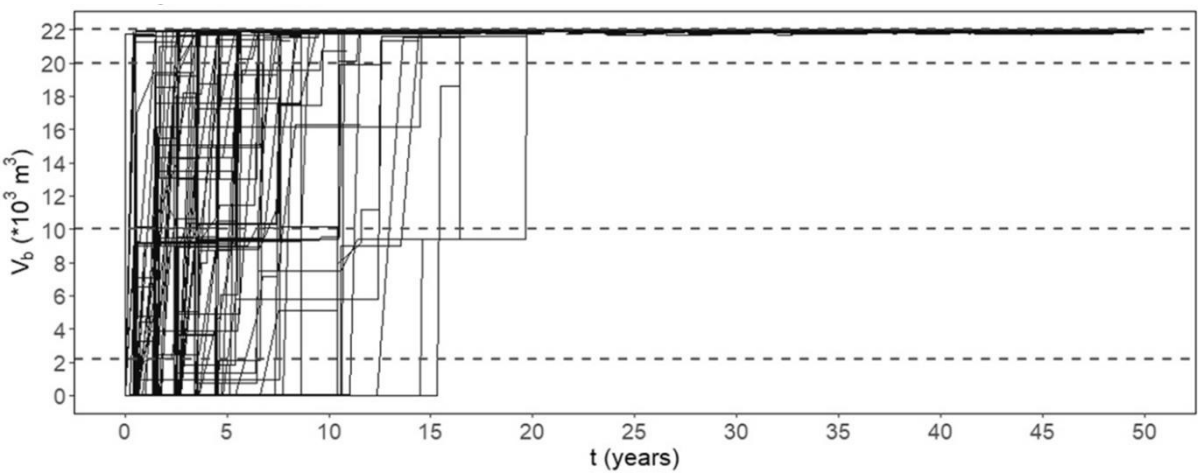


## 3.2 SPN Model Results and Discussions

As mentioned in section 2.2.1, four states of the debris basin should be defined. The thresholds representing these states are chosen, based on expert assessment as follows:

— State 1: $0 \leq V_b \leq 2{,}200\ m^3$ (until *10%* of the basin's capacity)

— State 2: $2{,}200\ m^3 < V_b \leq 10{,}000\ m^3$ (before reaching *50%* of the basin's capacity)

— State 3: $10{,}000\ m^3 < V_b \leq 20{,}000\ m^3$ (before reaching *90%* of the basin's capacity)

— State 4: $20{,}000\ m^3 < V_b \leq 22{,}000\ m^3$ (until the basin is completely filled)

Based on the deterioration trajectories provided in fig. 5, the time spent in each of the defined states can be computed for all the scenarios. The achieved results allow estimating a probability law for each transition. Indeed, an empirical cumulative distribution function (CDF) is obtained for each transition using Kaplan-Meier estimator. These distributions are used then as an input to the SPN deterioration model. After inserting all the necessary inputs to the SPN model (e.g. time to inspection, maintenance duration), Monte-Carlo simulations are executed. In the studied case, 200 simulations were enough to reach convergence in results. Table 1 provides the results of the SPN model obtained after simulating each of the proposed maintenance strategies. Results reveal that almost in all the strategies, corrective cleaning operations are the most performed. This reassures the issue revealed by the physical model that the basin reaches almost its storage capacity within a short duration.

In order to estimate the total cost of each maintenance strategy, the cost of each maintenance operation should be specified. Real data dedicated to Claret retention system shows that the cost of cleaning operations is 2.83 €/$m^3$ [13]. Assuming mean cleaning operations, the costs of minor, major and corrective operations are respectively 17,000 €, 42,000 € and 59,000 €. Table 2 reveals that all le proposed maintenance strategies have more or less the same average total cost. However, strategy 4 seems slightly more cost effective and strategy 2 more expensive. Consequently, from the strict point of view of maintenance costs, for the Claret retention system, it is better to wait until the debris basin is almost completely filled and then to carry out corrective cleaning operations.

**Table 1.** Average number of maintenance operations performed over a period of 50 years.

| Strategy | Minor | Major | Corrective |
|---|---|---|---|
| **1** | 4.84 | 3.66 | 4.14 |
| **2** | 0 | 4.09 | 5.29 |
| **3** | 4.09 | 0 | 6.44 |
| **4** | 0 | 0 | 7.48 |

**Table 2.** Average total cost of each maintenance strategy.

| Strategy | Total cost (K€) |
|---|---|
| **1** | 480 |
| **2** | 484 |
| **3** | 449 |
| **4** | 441 |

# 4 Concluding remarks

In this paper, a surrogate deterioration model that benefits from the physical modelling of a retention system is developed using SPNs. The model makes it possible to implement easily a CBM policy concerning cleaning operations of the system. Indeed, the physical modelling results in deterioration trajectories that show the evolution of the volume stored in the debris basin. These trajectories are then used in order to estimate the transition probability laws to be used in the SPN model. The overall developed approach provides a better understanding of the trapping process governed by the retention dam and the debris. It also supports the managers of retention systems in making cost-effective maintenance decisions by avoiding unnecessary cleaning costs. The model can be developed further by considering not only the cost of the proposed maintenance strategies, but also their efficiency in increasing the protection level provided by the system.

## Acknowledgements

This work has been partially supported by MIAI@Grenoble Alpes, (ANR-19-P3IA-0003).

## References

1. Hosseini, S., Barker, K. and Ramirez-Marquez, J.E. (2016) A review of definitions and measures of system resilience. *Reliability Engineering & System Safety*, Volume 145, Pages 47-61. https://doi.org/10.1016/j.ress.2015.08.006
2. Connelly, E., Allen, C.R., Kirk, H., José, P.-O., David, W. and Linkov, I. (2017) Features of resilience. *Environment Systems and Decisions*. Volume 37. https://doi.org/10.1007/s10669-017-9634-9
3. Tacnet, J.-M. and Degoutte G. (2013) Principes de conception des ouvrages de protection contre les risques torrentiels. In *Torrents et Rivières de Montagne: dynamique et aménagement*. Recking, A.; Richard, D.; Degoutte, G. (ed.), Quae, Pages 267-331. ⟨hal-02605935⟩
4. Hübl, J., Suda, J. (2008) Debris flow mitigation measures in Austria. In: *Debris Flows: Disaster, Risk, Forecast, Protection.* Pyatigorsk, Russia. p. 27-30.
5. Carladous, S., Piton, G., Kuss, D., Charvet, G., Paulhe, R., Morel, M. and Quefféléan, Y. (2021) French Experience with Open Check Dams: Inventory and Lessons Learnt Through Adaptive Management. In *Check Dam Construction for Sustainable Watershed Management and Planning*. Chapter 13. Wiley Online Library.
6. Chahrour, N., Nasr, M., Tacnet, J.M. and Bérenguer, C. (2021) Deterioration modeling and maintenance assessment using physics-informed stochastic petri nets: Application to torrent protection structures. *Reliability Engineering System Safety* 210, 107524. https://doi.org/10.1016/j.ress.2021.107524
7. Mizuyama, T., Kobashi, S. and Ou, G. (1992) Prediction of debris flow peak discharge, in: INTERPRAEVENT, Vol. 4, *International Research Society INTERPRAEVENT*, Bern, Switzerland. p. 99–108.
8. Piton G, Goodwin SR, Mark E, Strouth A. 2022. Debris flows, boulders and constrictions: a simple framework for modeling jamming, and its consequences on outflow. Journal of Geophysical Research: Earth Surface. https://doi.org/10.1029/2021JF006447
9. Piton, G. and Recking, A. (2015) Design of Sediment Traps with Open Check Dams. I: Hydraulic and Deposition Processes. *Journal of Hydraulic Engineering* 142, 1–16. https://ascelibrary.org/doi/10.1061/%28ASCE%29HY.1943-7900.0001048
10. Signoret, J.P., 2009. Dependability & safety modeling and calculation: Petri nets. *IFAC Proceedings* Volumes 42, 203 – 208. https://doi.org/10.3182/20090610-3-IT-4004.00040
11. Chahrour, N., Tacnet, J.-M and Bérenguer, C. (2021) Integrating Imperfect Information in the Deterioration Modeling of Torrent Protection Measures for Maintenance and Reliability Assessment. ESREL 2021 - *31st European Safety and Reliability Conference*, Sep 2021, Angers, France. pp.2630-2637. https://doi.org/10.3850/978-981-18-2016-8_670-cd
12. Morel M, Piton G, Evin G and Le Bouteiller C (2022) Projet HYDRODEMO : Évaluation de l'aléa torrentiel dans les petits bassins versants des Alpes du Nord - Action 3 : Caractériser la production sédimentaire. *Research Report*. https://hal.archives-ouvertes.fr/hal-03549827
13. ONF-RTM, 2013. Études de bassin versant: Torrent du Claret. *Research report*. Office National des Forêts, Service de Restauration des Terrains en Montagne du Département de l'Isère, Grenoble.

# A Simulation-driven Tool for Supporting Risk and Resilience Assessment in Cities

Stefan Schauer, AIT Austrian Institute of Technology, stefan.schauer@ait.ac.at

Thomas Hiebl, ACP CUBIDO Digital Solutions GmbH, t.hiebl@cubido.at

Benjamin Doppler, ACP CUBIDO Digital Solutions GmbH, b.doppler@cubido.at

Wolfgang Mayr, ACP CUBIDO Digital Solutions GmbH, w.mayr@cubido.at

Stefan Rass, Johannes Kepler University Linz, Alpen-Adria University Klagenfurt, stefan.rass@jku.at

Sandra König, AIT Austrian Institute of Technology, sandra.koenig@ait.ac.at

Martin Latzenhofer, AIT Austrian Institute of Technology, martin.latzenhofer@ait.ac.at

## Abstract

*We present a tool-based method, i.e., the ODYSSEUS approach, to support cities' risk and crisis managers on evaluating the cascading effects of an incident occurring in their metropolitan areas. The presented tool is set up with structural and operative information of CIs from various sectors within a metropolitan area, focusing in particular on different concepts for dealing with diverse quality and sources of the available information such as integrating expert opinions or neural networks. Further, ODYSSEUS utilizes an abstract model to represent the CIs' assets and their interrelations; the simulation capabilities are based on that model and provide a detailed overview on the propagation of cascading effects in the CI network. To showcase the functionality of the ODYSSEUS approach, we will present the evaluation of a use case scenario, describe the instantiation process of the abstract CI model, demonstrate how resulting cascading effects are simulated and how the results can be used to support crisis managers to assess counter measures.*

## 1 Introduction

In large cities and metropolitan areas, Critical Infrastructures (CIs) from different sectors are located in a geographically narrow space. They are required to maintain essential services like supply with power, water, food or communication and thus represent the backbone of social life in that area. Due to the high interdependencies among each other, a single incident within one CI can have wide-ranging cascading effects among the entire CI network and thus affect society in that area to a large degree. Cyber-attacks from the past years such as the hacking of the Colonial pipeline in 2021 [1], the ransomware attack on the Irish national health system (NHS) in 2021 [2] or the shutdown of Moeller-Maersk container terminal operating systems by the (Not)Petya malware in 2017 [3] have underlined that. However, also technical failures or natural hazards lead to, e.g., major blackouts as in Venezuela [4] and Argentina [5] in 2019, indicating that the cascading effects affect multiple CI domains on a metropolitan and national level. Therefore, crisis managers in cities need a consistent overview on these potential consequences a serious incident might have to estimate the city's resilience and coordinate necessary risk measures appropriately.

In the literature, many approaches to identify and structurally analyse these cascading effects have been proposed for decades, such as the Cross Impact Analysis (CIA) [6], the Hierarchical Holographic Model (HHM) [7] or the Input-output Interoperability Model (IIM) [8] just to name a few. More recent approaches focus on stochastic processes such as Interdependent Markov Chains (IDMCs) [9]–[11], Bayesian networks [12], [13] or Mealy automata [14], [15] to model the uncertainty of these cascading effects and integrate it into a risk assessment. Co-simulations [16], [17] and cross-domain simulations [18] bring

two or more CI sectors together into one comprehensive analysis. However, only a few of those methods have been integrated into tools that can be used by city administration or crisis mangers to improve their analysis of cascading effects of such complex scenarios. For example, Schaberreiter et al. have described a tool [19] that implements the Bayesian network approach for simulating cascading effects from [12], but this tool focuses mainly on critical information infrastructures and the services they provide; the physical aspects or other CI networks are not covered by this tool. Similarly, the 3Di simulation tool [20] provides a detailed view on a city's water management system together with ground water and overland flows to model the cascading effects of flooding events; nevertheless, the focus of the 3Di tool lies only on this network and does not consider cascading effects on other CI networks or domains. Another approach is the coupled grid simulation tool CAESAR [21] developed by Fraunhofer EMI, which follows a flow-based method and is also able to integrate existing simulation tools for the individual networks. However, CAESAR integrates only three network types, namely the power, water and mobile phone network, and thus cannot indicate effects on any other network or the society itself, i.e., the people living in the city.

In this paper, we introduce the ODYSSEUS Cascading Effects Simulator, a novel tool that simulates the effects an incident can have across different CI sectors located within a metropolitan area. The simulation software supports the ODYSSEUS Risk Management Framework [22] to structurally describe and analyse the cascading effects among the CIs. Therefore, it implements a risk model for interdependent CIs [23] together with a cross-domain simulation approach [18]. Further, the simulator contains a dedicated Model Generator Component to set up and instantiate the CIs in the metropolitan area. Based on a simplified showcase scenario, we demonstrate how the simulation tool can describe the effects of a terrorist attack in the city centre and how other infrastructures and the city population is affected.

The remainder of the paper is structured as follows: Section 2 provides a brief overview on the individual steps of the ODYSSEUS Risk Management Process and Section 3 characterises the general structure of the simulation tool, including the cross-domain simulation and the Model Generator. Section 4 describes a terrorist attack scenario, how it can be modelled and analysed using the simulation tool and discusses the main results from the analysis. Section 5 concludes the paper and provides an outlook on the further improvement of the tool.

# 2 ODYSSEUS Risk Management Framework

The ODYSSEUS Risk Management Framework integrates several solutions developed in the ODYSSEUS project and provides a step-by-step approach to model a metropolitan area with different CI domains, analyse various threat scenarios in this metropolitan area and their respective effects on the CIs from different domains (cf. Figure 1).

As a first step in the framework, a cross-domain geographic information system (GIS) model is set up. Therefore, infrastructure data from multiple CI sectors and domains, either coming from publicly available sources, e.g., OpenStreetMap or OpenInfrastructureMap, or from within the CI operators, is integrated into a single GIS model. This GIS model serves as a basis for all subsequent analysis processes directly provides geo-referenced information on CIs and their subsystems for the analysis results.

Subsequently, the information from the GIS model is translated into a directed graph representation, where the individual critical entities and infrastructures correspond to the nodes and their interdependencies correspond to the edges the graph, with edge directions encoding the direction of dependency between CIs. This representation shall further differentiate the critical entities and CIs according to their domains, resulting in a multi-layered representation that visually separates domains (e.g., electrical grid vs. water pipe network vs. communication networks, etc.; cf. Figure 1), and manifests in the graph model as attributes attached to the graph's nodes. Each node has several operational states characterising the functionality of the respective critical entities (cf. Section 3.1 for detailed

information on the cross-domain simulation). The edges are created based on the exchange of resources, data or information among the critical entities and can be created manually or following a set of predefined rules (cf. Section 3.3 for more details). The resulting graph is the basis for the cross-domain simulation, which represents the core feature of the ODYSSEUS Risk Management Framework.

**Figure 1.** General overview of the ODYSSEUS approach

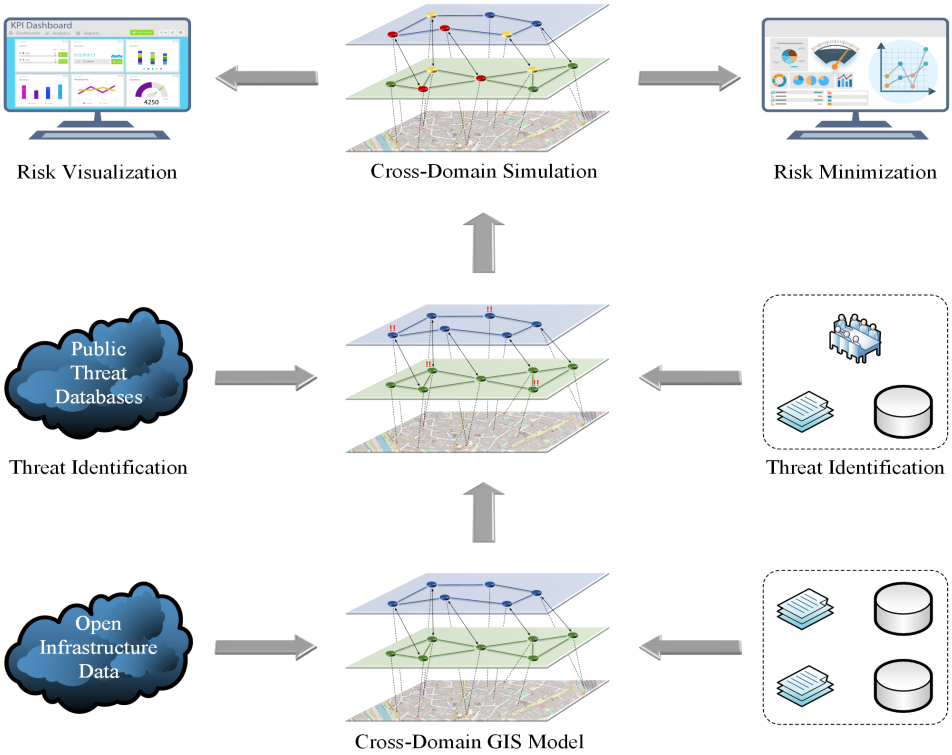


Based on the GIS data and the graph representation, the relevant threats are analysed and collected. These threats can originate from public threat databases and threat catalogues or from CI internal data based on historic data and expert knowledge. The most relevant threats are further translated into threat scenarios in which specific critical entities (i.e., nodes in the graph) across all domains can be affected; those scenarios are then analysed by the cross-domain simulation.

The simulation results are then visualised on the one hand using the GIS data and map view, highlighting which critical entities and infrastructures are affected to which degree, and on the other hand using charts and numerical results, describing the resulting state and thus the impact of the simulated scenario. Additionally, the results also support risk minimisation activities as the entities and CIs with the highest damage are displayed but also the most crucial entities, i.e., the ones creating the largest cascading effects, can be identified from the simulation steps. Usually, those are the entities that require the most protection to minimise the overall damage to the entire metropolitan area.

# 3 ODYSSEUS Cascading Effects Simulator

## 3.1 Cross-Domain Simulation Model

The ODYSSEUS Cascading Effects Simulator implements large parts of the risk management framework described in Section 2 with an important part being the visualisation of the GIS model and the implementation of the cross-domain simulation approach. As already mentioned above, the simulation builds upon an abstract graph model [18] in which the CIs from different domains or the critical entities therein, e.g., individual

components, their control systems or classic IT systems and relevant actors in the domains, are represented as nodes (cf. Figure 2). The dependencies between the individual entities are represented as edges in the graph and are based on the exchange of resources, data, or information between the critical entities of the infrastructure networks that can also range across the individual domains (cf. Figure 2).

**Figure 2.** Illustration of the Cross-Domain Simulation Model

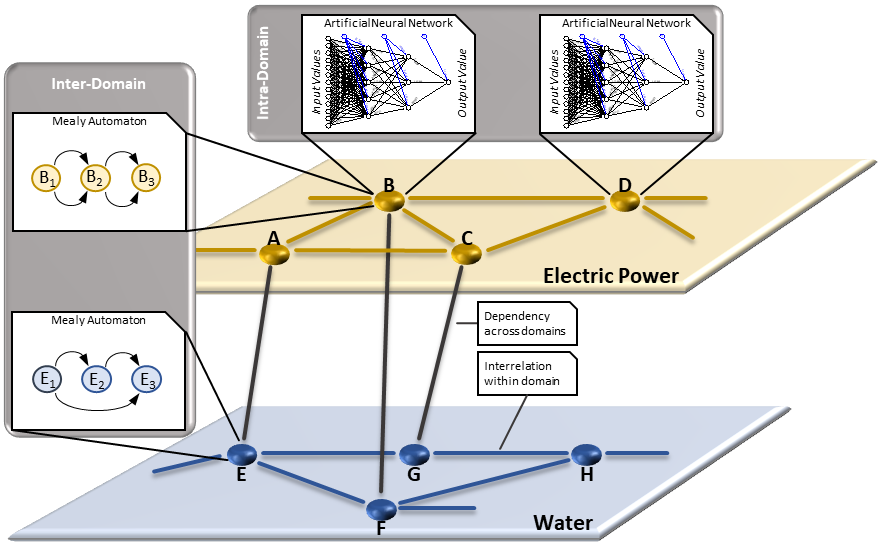


A core focus of the model is the description of the response behaviour of a CI upon an incident occurring in a supplier CI. For example, a power grid outage may not instantly affect a connected hospital, but may do so with a certain temporal delay, once the emergency power supply runs out of fuel. The mathematical models for the general stochastic processes to describe such time-dependent dynamics are based on deep neural networks. We train them to be simplified digital twins of individual domains, which learn the behaviour of the underlying CIs or critical entities, provided that the required data are made available by the operators of the respective infrastructures. These neural networks thus form a realistic representation of the individual entities to facilitate the analysis of the effects and resulting impacts of incidents on them. Having all CIs under such a common representation significantly simplifies their assembly into a joint co-simulation framework, in which potential cascading effects can become visible for decision makers and a strategic defence planning.

For the description of the dynamics across the individual domains, an approach is applied in which the behaviour and functionality of the respective systems is represented by a probabilistic Mealy automaton with multiple states [14]. Each state of an automaton represents its degree of functionality. The ODYSSEUS Simulator uses five such degrees, ranging from "normal operation" (State 1) to "complete breakdown" (State 5). The central aspect to describe the dynamics are the transitions between the different states. They characterise how a system reacts due to an incident taking place in another system or domain. A change of working state can then either occur (i) internally as dictated by the specific neural network describing the CI's behaviour over time (intra-domain model in Figure 2), or (ii) externally, if a supplier node changes its state, and communicates this information as a signal through the Mealy automaton (inter-domain model in Figure 2). The external influences of the incident together with the current state (the current functionality) of the critical entity determine the new state of the entity. In contexts where the temporal response behaviour of a CI does not lend itself to a training of its dynamics, for example, if the data is too scarce to allow machine learning, or if the dynamics is highly uncertain, the Mealy automaton can also do state changes based on randomness, with specified probabilities to change its state from one to the other, and does not need to use

a neural network. This adds flexibility to include a large variety of domains, combining areas where the physical dynamics are well known (such as water, energy, etc.), with others, where the dynamics does not admit an accurate mathematical description (such as people's risk response, social media/press reception, and others).

## 3.2 Simulator Architecture

The ODYSSEUS Cascading Effects Simulator implements the cross-domain simulation approach for different CI networks within a city. It is a web application and is based on the web technologies JavaScript, HTML and CSS. It is supported by the framework Angular 12, which is one of the standard tools for the development of modern single-page applications. In addition, a Model Generator was created as a .NET console application, which processes the GIS data of the nodes and accesses a Microsoft SQL server database for this purpose.

**Figure 3**. Data-flow diagram of the ODYSSEUS Cascading Effects Simulator

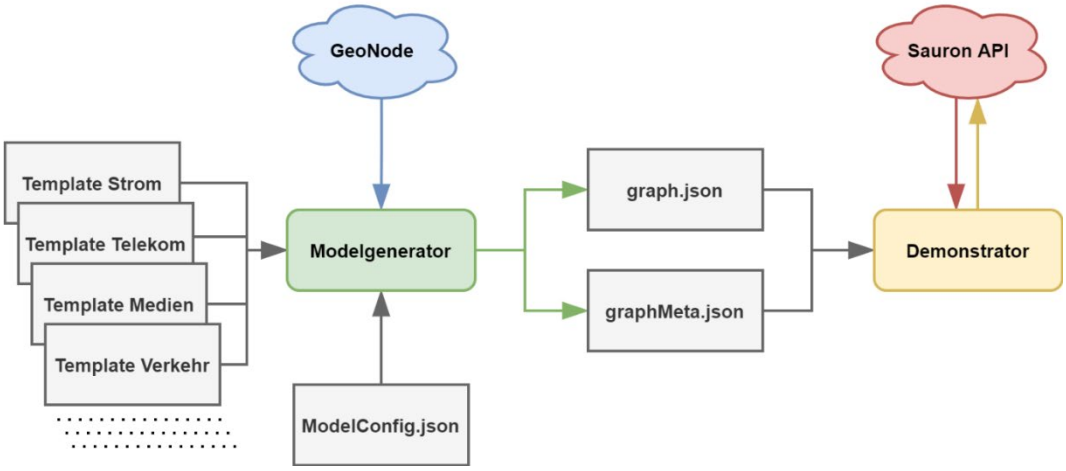


Although it can be shown that data trained into a machine learning model will, in an information-theoretic sense, not leak out from the model [24], we refrained from using any real-life data of any city or CIs, to avoid data protection issues. Instead, a fictional city was created in the project based on the publicly available GIS-Data of the German city of Hamburg. Therein, several artificial CI networks have been created, representing classical CI network structures like the power, telecom or water network but also more abstract infrastructures like the city administration, crisis management or the population itself.

To model the CI networks properly, their behaviour was discussed with experts from the field throughout several workshops in the project involving domain experts from real-life infrastructure provider companies (water supply, electric power grid, and others). Based on the information gathered therein, infrastructure templates were generated, which described the infrastructures' reaction in the case of an incident. This was realised using five different states, labelled as 1…5 and represented in the demonstrator with the colours green, light green, yellow, orange, and red to indicate increasing severity. The templates include the decrease (failure process) as well as the increase (repair functions) of the operational states together with the probabilistic transitions in both directions.

The Demonstrator uses these templates to instantiate the individual nodes in the overall CI network (cf. Figure 1). This is achieved using the Model Generator Component, which initially reads the templates and describes in a configuration file how the nodes and edges are to be generated. In this step, GIS data that is required for specific layers is loaded from a GeoNode server. The Model Generator then creates the CI interdependency graph and saves it as a JSON file. A second file contains additional meta information such as the geolocation, layer, events, and layer membership.

The ODYSSEUS Demonstrator now reads the JSON files and displays the corresponding data in a georeferenced form (based on OpenStreetMap). Since an ODYSSEUS Simulation is scenario based, the next step is the definition of the particular incident to let occur in the model. This incident is specified as a sudden transition on one or more nodes from their working states 1 into a worse state 2, 3, 4 or 5. The simulation then starts by initially letting all nodes be in their normal conditions (state 1), and, according to the specified incident scenario, puts some CIs into bad conditions, to let the cascading effects run when the user starts a simulation. This triggers the Threat Propagation API is accessed, the requested scenario is simulated, and the results are recorded as time-lines showing the state of each CI, as long as the incident(s) percolate or the simulation terminates after a fixed time horizon. Finally, these simulation results are displayed in the demonstrator.

## 3.3 Model Generator

As a core part of the ODYSSEUS Demonstrator, the Model Generator was designed to prepare the data (nodes and edges) that will eventually be displayed in the demonstrator. The Model Generator supports the representation of all layers as geo-located nodes, creates the connections between the interdependent nodes and stores all this information in an easily processable format. Figure 4 shows a schematic representation of the layers and their connections. For example, it shows that power nodes are related to power nodes in adjacent sectors, as well as to mobile, population, and heating nodes. The demonstrator currently offers 14 different layers that can be roughly divided into four groups:

- **Global Nodes**: they exist only once in the model, have no geo-location and represent a citywide status of their subject area. Nevertheless, in order to be able to select the nodes on the demonstrator's map and intuitively display their connections, they are arranged outside of the city, comparable to a heading. An example would be the media, the traffic network or public transport.
- **Sector Nodes**: they represent critical infrastructure that is widespread within a city but is not modelled in further detail (e.g., due to lack of data) and thus is represented in each one of the predefined sectors. Usually, a Sector Node depends on other nodes of the same type but in different sectors. An example would be the power grid nodes that influence each other in case of a problem. To simulate these nodes, the virtual city was divided into $n$ rectangular sectors (with $n$=4 in our example case) and one central node is generated per sector. Depending on the type, a central node connected to all sector nodes can also be generated.
- **Building Nodes**: they are a group of nodes representing an inhabited building, i.e., they are related to housing units and population. A Building Node contains one node for population, one for heating, and one for water supply. The GIS data also provides information on the height of the houses; thus, the water supply high (> 4 stories) or low (<= 4 stories) can be placed accordingly. This division is important in cases where the water supply makes use of the city's surrounding geography, for example, if the water comes from higher regions and therefore has enough pressure to get up to a certain level of buildings without extra pumping.
- **Geo-located Nodes**: they are obtained directly from GIS data, i.e., they are based on real geo-information. In principle, all of the above nodes could be geo-located as well but, due to the large amount of data and the sensitivity of the information, it is often not feasible to do that.

The initial setup of the fictional city is predefined and based on the results coming from the Model Generator (cf. Section 3.3). Due to reasons of simplicity, the fictional city is divided in four main sectors, with each one having a power network node, a Telecom Network node as well as a City Administration and a Crisis Management node. Furthermore, the mobile network towers are geo-reference with data coming from OpenStreetMap, the

Traffic is geo-referenced with the political districts and the Population is inserted according to the population density in the respective regions. Public Transport, Press and Media are global nodes set on the upper left corner.

**Figure 4.** Schematic Illustration of the Model Generator concept

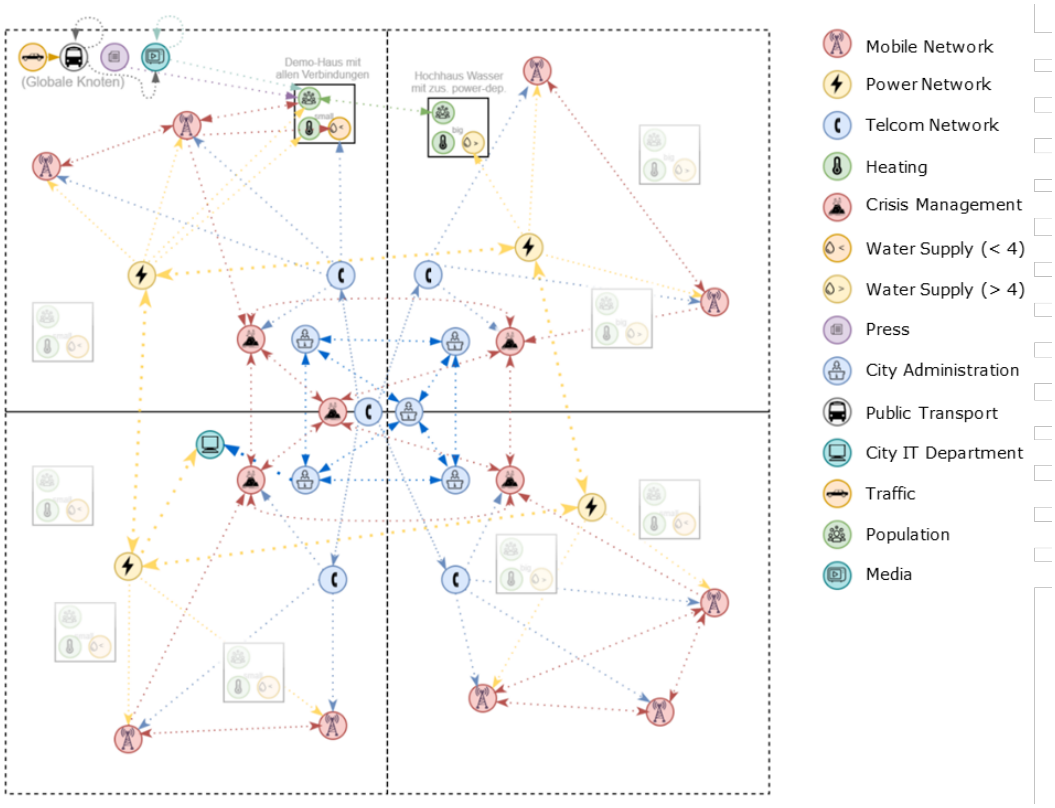


# 4 Showcase Scenario: Terrorist Shooting

## 4.1 Scenario Description

One use case scenario in the ODYSSEUS project deals with a terrorist shooting at a market in the centre of the fictional city. In detail, several rifle shot can be heard at the Christmas market in the late afternoon, resulting in a general panic escape movement away from the scene. People flee into the surrounding streets and alleys or seek shelter in the nearby stores and subway station. Immediately after the shots were fired, the police's and ambulance's emergency phones receive numerous calls reporting the incident and that an unknown number of visitors has been severely injured.

When police officers arrive at the scene, they are informed about several armed persons fleeing from the scene. Some of them have run down to the subway station, others allegedly dived into the crowd of people fleeing from the scene. While police and ambulance are still on the scene taking care of the injured for the time being, first postings about the incident as well as videos of the crime scene are already appearing on social media platforms. First speculations that it was a terrorist attack hit the web and are spread on countless channels within a few minutes.

As reports on the incident are also covered by TV channels, uncertainty is spread among the population in the vicinity of the centre and a high number of calls leads to an overload of the mobile phone network; this results in telephone calls being temporarily disconnected and mobile use of the Internet failing. Since the population's need for information can no longer be satisfied for some time, an increased number of direct inquiries to police stations, hospitals and the public transport operators in the city.

To delay the further movements of the attackers, the public transport lines are suspended in the entire centre. Subway trains, streetcars and buses traveling in the centre at that time only go to the next station, let passengers get off there and stop operating. As a result, thousands of passengers crowd the streets which directly causes obstructions of the road traffic and within a few minutes to traffic jams in the centre's main streets. This sectoral shutdown of public transport leads to massive impediments, traffic jams and cancellations within a very short period of time, even in the connecting areas to the outskirts of the city.

Duplicated videos posted online from the crime scene and the panic scenes on social media creates a false timeline, and people who are in the centre find it difficult to distinguish whether something has just recently happened or happened some time ago. This leads to the continuation in different locations and to continuous resurgence of the panic, escape scenes and violent confrontations.

After about two hours, the police can arrest the attacker and this fact is communicated via television. However, emergency call centres are still busy until the early morning of the next day with processing alleged further crime scenes.

**Figure 5.** Initial setup of the scenario.

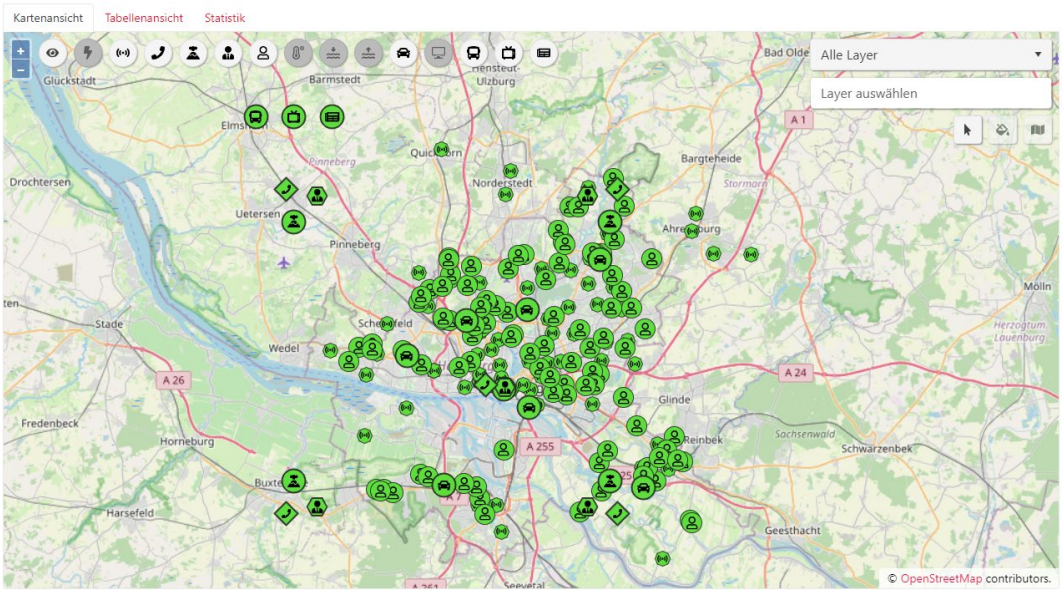


## 4.2 Scenario Simulation

The above-described scenario can be modelled in the ODYSSEUS demonstrator [25] by generating the initial event ("Shooting at the Market") together with the subsequent events regarding the Media such as the TV reports and the false timeline communicated in social media together with disinformation about other crime scenes.

The initial event is targeted to three "Population" nodes in the city centre where the shooting takes place (see Figure 6), putting them from normal state 1 into panic state 5 when the scenario begins. Starting from that, the Cross-Domain Simulation engine in the demonstrator calculates the cascading effects on the Traffic (as people are flooding the streets), the Public Transport (as subways and streetcars are halted), the Mobile Network (as the number of calls is increasing) and so on. The additional events regarding the media are targeted at the Media node to indicate the announcements therein. These events cause additional cascading effects, influencing the Population even more.

Already after a few steps into the simulation, the Population nodes around the area where the shooting has occurred are heavily affected by the event, indicated by the orange colour (see Figure 7); the Mobile Network node closest to the event is already failing, indicated

by the red colour. More distant Population nodes also get more and more affected (indicated by the light green, yellow and orange colours) due to the news in the Media and social media posts. At this point, the global Public Transport node in the upper left corner also reflect the severe interruptions by the orange colour. The number of affected Population nodes grows over after 12 steps (see Figure 8) and reaches its maximum after 18 steps (see Figure 9). However, after the 14th step, the propagation has almost reached its maximum and the situation does not get worse that much.

**Figure 6**. Start of the shooting scenario

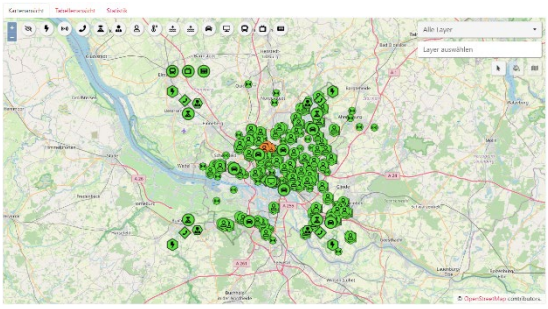

**Figure 7**. Cascading effects after 7 steps

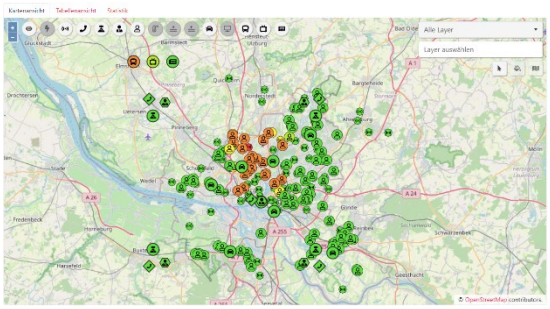

**Figure 8**. Cascading effects after 14 steps

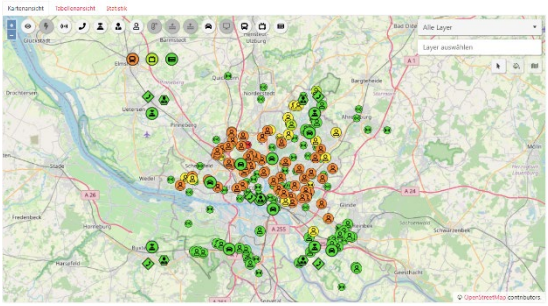

**Figure 9**. Cascading effects after 21 steps

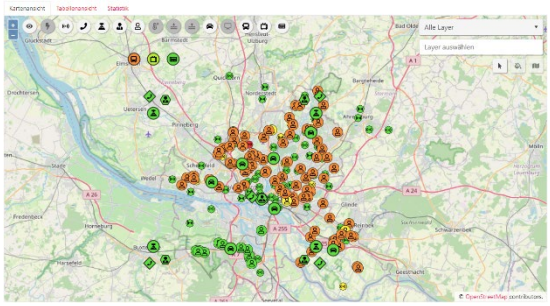

## 4.3 Results Discussion

Overall, the model of the fictional city consists of 396 nodes and 1883 edges. Looking at the worst-case simulation, about 74% stay unaffected by the scenario, i.e., remain in green colour. About 22% change into a severe state, i.e., orange colour, and only about 4% change into an intermediate state, i.e., yellow colour, due to the events happening. Looking at the best-case simulation, only 5% of the nodes end up in a severe state and about 88% remain in their initial state. This might indicate that the fictional city is not that much affected by the consequences of the scenario.

**Figure 10.** Worst-case simulation results in relative (Left) and absolute (right) numbers

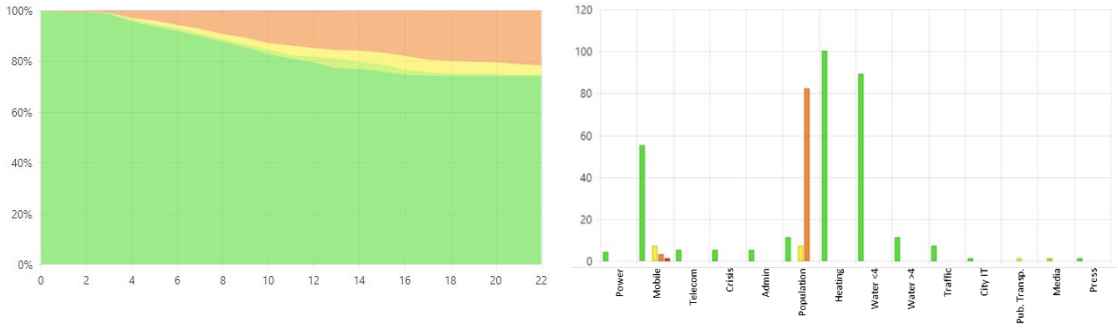


However, if we look at the details of the simulations we see, that a large number of nodes is part of the Heating and Water networks, which are per definition not affected at all by

this kind of scenario. Additionally, there are lot of Mobile Network nodes located in the city but only a few are located in the vicinity of the initial incident and are affected by it. If we reduce the number of nodes from these unaffected networks and evaluate the overall results for the worst-case simulation again, then only about half of the nodes (51%) remain in their initial state and 41% go into a severe state, i.e., are heavily affected by the incident. For the best-case simulation, about three quarters (76%) remain in their initial state and only roughly 10% end up in a severe state, with 6% of the nodes ending up in a light green and 6% in a yellow state.

**Figure 11.** Best-case simulation results in relative (Left) and absolute (right) numbers

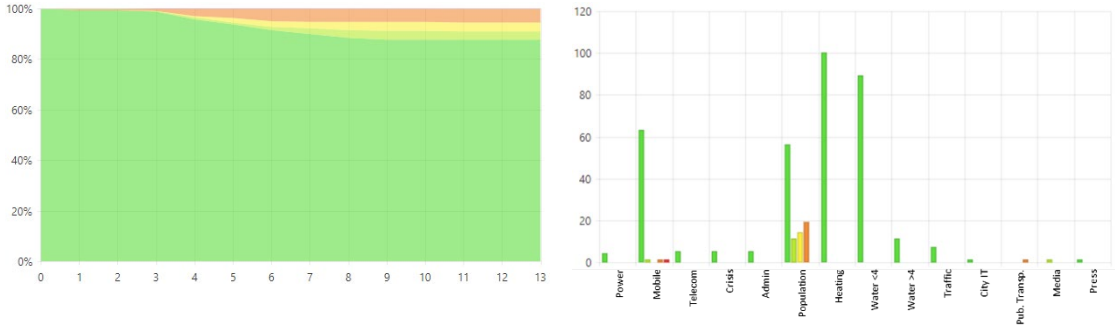


A large part of the nodes in a severe state are coming from the Population, which indicates that this is the part of the city that is most affected in this scenario. This is not surprising since the attack is targeted towards the people in the city centre and not specifically to any infrastructure. Accordingly, if the city administration wants to prepare for such a scenario, on the one hand, the communication with the public will be an important factor to avoid a lot of uncertainties and a large panic. In that context, it will be necessary to follow social media and be aware of the information spread therein. On the other hand, the city administration will need to prepare for the breakdown of the public transport (which was a deliberate act in the simulated scenario) and the traffic (which was a direct consequence) and prepare their measure accordingly.

# 5 Conclusion and Outlook

ODYSSEUS leverages machine learning for a double advantage of (i) converting domain-specific simulator and therefore incompatible simulators into domain-agnostic and hence compatible emulations, and (ii) proposing an interaction layer using automata theory that allows a flexible inclusion of different domain-specific emulations into an overall co-simulation environment for the analysis of cascading effects in critical infrastructures. This generality comes at the price of being model-based (only), and hence is as accurate as the underlying data and simulation models are that provide the data. The combination as proposed by ODYSSEUS is herein advantageous over self-implemented simulations in designated frameworks like the high level architecture standards for distributed simulation (federations) [26]. The benefits of the ODYSSEUS method are threefold: First, it can run as a distributed simulation, since each node can run independently of the others, and thereby implement any complex or sensitive dynamics, ranging from pure probabilistic state transitions in absence of dynamical models, to emulations based on pre-recorded empirical data, up to full-featured domain simulators that interface with the ODYSSEUS nodes (an aspect that we did not touch in the project, but which is conceptually not difficult to implement). This also facilitates security precautions, since sensitive information to base a simulation on do not need to leave the security domain, except for signalling other nodes numbers in the range 1…5 (but nothing beyond this information). Second, the inter-domain model is designed to work with only few parameters to be specified, and directly relates to different kinds of dependency, such as geographic proximity, community adoption of different services (for example, not all social media are equally well used by all groups in the population), and others. Finally, ODYSSEUS admits template-based models that can

be re-used in several application scenarios and simulations. For example, a water provider that has been modelled already is easy to duplicate and adapt to scale up the basic building blocks into large and complex simulation environments, without substantially slowing down the simulation itself.

## Acknowledgements

This work was supported by the research project ODYSSEUS (Project-Nr. 873539), which is funded by the Austrian National Security Research Program KIRAS (http://www.kiras.at/).

## References

[1] C. Bing and S. Kelly, 'Cyber attack shuts down U.S. fuel pipeline "jugular," Biden briefed', *Reuters*, May 08, 2021. Accessed: Mar. 19, 2022. [Online]. Available: https://www.reuters.com/technology/colonial-pipeline-halts-all-pipeline-operations-after-cybersecurity-attack-2021-05-08/

[2] 'Cyber attack "most significant on Irish state"', *BBC News*, May 14, 2021. Accessed: Mar. 19, 2022. [Online]. Available: https://www.bbc.com/news/world-europe-57111615

[3] PTI, 'New malware hits JNPT operations as APM Terminals hacked globally', *The Indian Express*, 2017. http://indianexpress.com/article/india/cyber-attack-new-malware-hits-jnpt-ops-as-apm-terminals-hacked-globally-4725102/ (accessed Jul. 06, 2017).

[4] R. Dube and M. Castro, 'Venezuela Blackout Plunges Millions Into Darkness', *Wall Street Journal*, Washington, DC, USA, Mar. 08, 2019. Accessed: Dec. 04, 2019. [Online]. Available: https://www.wsj.com/articles/venezuela-blackout-stretches-across-country-closing-schools-and-businesses-11552053011

[5] A. Nordrum, 'Transmission Failure Causes Nationwide Blackout in Argentina - IEEE Spectrum', *IEEE Spectrum: Technology, Engineering, and Science News*, 2019. https://spectrum.ieee.org/energywise/energy/the-smarter-grid/transmission-failure-causes-nationwide-blackout-in-argentina (accessed Jun. 30, 2021).

[6] M. Turoff, 'An alternative approach to cross impact analysis', *Technol. Forecast. Soc. Change*, vol. 3, pp. 309–339, 1971, doi: 10.1016/S0040-1625(71)80021-5.

[7] Y. Y. Haimes, 'Hierarchical Holographic Modeling', *IEEE Trans. Syst. Man Cybern.*, vol. 11, no. 9, pp. 606–617, 1981, doi: 10.1109/TSMC.1981.4308759.

[8] J. R. Santos and Y. Y. Haimes, 'Modeling the demand reduction input-output (I-O) inoperability due to terrorism of interconnected infrastructures', *Risk Anal. Off. Publ. Soc. Risk Anal.*, vol. 24, no. 6, pp. 1437–1451, 2004, doi: 10.1111/j.0272-4332.2004.00540.x.

[9] Z. Wang, A. Scaglione, and R. J. Thomas, 'A Markov-Transition Model for Cascading Failures in Power Grids', in *2012 45th Hawaii International Conference on System Sciences*, Maui, HI, USA, Jan. 2012, pp. 2115–2124. doi: 10.1109/HICSS.2012.63.

[10] M. Rahnamay-Naeini, Z. Wang, N. Ghani, A. Mammoli, and M. M. Hayat, 'Stochastic Analysis of Cascading-Failure Dynamics in Power Grids', *IEEE Trans. Power Syst.*, vol. 29, no. 4, pp. 1767–1779, Jul. 2014, doi: 10.1109/TPWRS.2013.2297276.

[11] M. Rahnamay-Naeini and M. M. Hayat, 'Cascading Failures in Interdependent Infrastructures: An Interdependent Markov-Chain Approach', *IEEE Trans. Smart Grid*, vol. 7, no. 4, pp. 1997–2006, Jul. 2016, doi: 10.1109/TSG.2016.2539823.

[12] T. Schaberreiter, P. Bouvry, J. Röning, and D. Khadraoui, 'A Bayesian Network Based Critical Infrastructure Risk Model', in *EVOLVE - A Bridge between Probability,*

*Set Oriented Numerics, and Evolutionary Computation II*, vol. 175, Berlin, Heidelberg: Springer Berlin Heidelberg, 2013, pp. 207–218. doi: 10.1007/978-3-642-31519-0_13.

[13] R. Ojha, A. Ghadge, M. K. Tiwari, and U. S. Bititci, 'Bayesian network modelling for supply chain risk propagation', *Int. J. Prod. Res.*, vol. 56, no. 17, pp. 5795–5819, Sep. 2018, doi: 10.1080/00207543.2018.1467059.

[14] S. König, S. Rass, B. Rainer, and S. Schauer, 'Hybrid Dependencies Between Cyber and Physical Systems', in *Intelligent Computing*, vol. 998, K. Arai, R. Bhatia, and S. Kapoor, Eds. Cham: Springer International Publishing, 2019, pp. 550–565. doi: 10.1007/978-3-030-22868-2_40.

[15] S. Schauer, T. Grafenauer, S. König, M. Warum, S. Rass, and S. Rass, 'Estimating Cascading Effects in Cyber-Physical Critical Infrastructures', in *Critical Information Infrastructures Security*, Linköping, Sweden, 2020, pp. 43–56.

[16] Y. Cao, X. Shi, Y. Li, Y. Tan, M. Shahidehpour, and S. Shi, 'A Simplified Co-Simulation Model for Investigating Impacts of Cyber-Contingency on Power System Operations', *IEEE Trans. Smart Grid*, vol. 9, no. 5, pp. 4893–4905, Sep. 2018, doi: 10.1109/TSG.2017.2675362.

[17] B. Camus *et al.*, 'Co-simulation of cyber-physical systems using a DEVS wrapping strategy in the MECSYCO middleware', *SIMULATION*, vol. 94, no. 12, pp. 1099–1127, Dec. 2018, doi: 10.1177/0037549717749014.

[18] S. Schauer and S. Rass, 'Creating a Cross-Domain Simulation Framework for Risk Analyses of Cities', in *Critical Infrastructure Protection XIV*, Cham, 2020, pp. 307–323. doi: 10.1007/978-3-030-62840-6_15.

[19] T. Schaberreiter, P. Bouvry, J. Röning, and D. Khadraoui, 'Support Tool for a Bayesian Network Based Critical Infrastructure Risk Model', in *EVOLVE - A Bridge between Probability, Set Oriented Numerics, and Evolutionary Computation III*, vol. 500, Heidelberg: Springer International Publishing, 2014, pp. 53–75. doi: 10.1007/978-3-319-01460-9_3.

[20] Nelen & Schuurmans, '3Di – Water Management', 2022. https://3diwatermanagement.com/ (accessed May 30, 2022).

[21] Fraunhofer EMI, 'Analysis of the cascade effects in supply networks – software tool CAESAR', *Fraunhofer Institute for High-Speed Dynamics, Ernst-Mach-Institut, EMI*, 2022. https://www.emi.fraunhofer.de/en/business-units/security/research/analysis-of-the-cascade-effects-in-supply-networkssoftwaretool-c.html (accessed May 30, 2022).

[22] S. Schauer, S. Rass, S. König, S. Klaus, T. Schaberreiter, and G. Quirchmayr, 'Cross-Domain Risk Analysis to Strengthen City Resilience: the ODYSSEUS Approach', in *ISCRAM 2020 Conference Proceedings – 17th International Conference on Information Systems for Crisis Response and Management*, Blacksburg, VA (USA), May 2020, pp. 652–662.

[23] S. Schauer, S. Rass, and S. König, 'Simulation-driven Risk Model for Interdependent Critical Infrastructures', in *Proceedings of the 18th ISCRAM Conference - Blacksburg, VA, USA May 2021*, Blacksburg, USA, 2021, pp. 404–415.

[24] S. Rass, S. König, J. Wachter, M. Egger, and M. Hobisch, 'Supervised Machine Learning with Plausible Deniability', *Comput. Secur.*, vol. 112, p. 102506, 2022, doi: https://doi.org/10.1016/j.cose.2021.102506.

[25] 'ODYSSEUS Demonstrator', 2022. https://risk-mgmt.ait.ac.at/odysseus/ (accessed Jun. 01, 2022).

[26] IEEE Standards Association (IEEE-SA), 'IEEE Standard for Modeling and Simulation (M&S) High Level Architecture (HLA)-- Framework and Rules', IEEE, 2010. doi: 10.1109/IEEESTD.2010.5553440.

# Risk Management with Multi-categorical Risk Assessment

Sandra König and Stefan Schauer, AIT Austrian Institute of Technology, sandra.koenig@ait.ac.at, stefan.schauer@ait.ac.at

Mona Soroudi, Ili Ko, Meisam Gordan, Paraic Carroll and Daniel McCrum, University College Dublin, mona.soroudi@ucd.ie, ili.ko@ucd.ie, meisam.gordan@ucd.ie, paraic.caroll@ucd.ie, daniel.mccrum@ucd.ie

## Abstract

*Risk assessment and risk management often has to deal with uncertainty, especially in the context of critical infrastructure networks with manifold interdependencies and cascading effects. This uncertainty is not only due to the unpredictability of incidents, e.g., due to zero-day exploits or stealthy attacks such as Advanced Persistent Threats, but also consequences of an incident are challenging to predict. The traditional one-dimensional risk assessment is therefore not always sufficient and should be extended, e.g., to multiple impact categories (such as effects on humans, economic impact, etc.) Uncertainty should be explicitly considered during the entire risk management process. This paper illustrates how to adapt the classical risk management process to such generalized risk assessments, i.e., how to deal with risks that are assessed in multiple categories, within the context of a Serious Game approach to critical infrastructure protection.*

## 1 Introduction

Risk management often needs to deal with complex risks that can hardly be measured with a single number. The classical approach of understanding risk as the product of likelihood and (one-dimensional) impact seems to be insufficient in situations where risks have indirect consequences. This is particularly the case in the context of critical infrastructures (CIs) which are highly interconnected and influence one another. Here, one of the main challenges lies in understanding the risk, including identification of potential cascading effects. Another core issue is understanding the manifold impacts an incident has. Due to the vital role CIs play in society, the consequences of an incident cannot be measured in financial loss only but may also affect people's health (mental or and/or physical) or even influence the environment, for example in terms of resilience.

In the context of an Austrian project focusing on critical infrastructure protection (Odysseus), we proposed to use multiple risk categories to increase the quality of risk assessment and subsequently the risk management. In many discussions, experts confirmed the need of such an extension showed interest in the proposed approach. However, they also asked how this generalization should actually be put in practice, i.e., how to integrate it in a classical risk management process. This paper answers this question by describing the generalized framework step by step and illustrating it with an example from the H2020 funded PRECINCT project (www.precinct.info).

This paper is organized as follows. Section 2 describes a risk assessment that considers multiple categories. Section 3 shows how to incorporate this generalized assessment in the classical risk management process and how serious games may support the assessment. Section 4 illustrates the idea with an approach from the PRECINCT project and Section 5 provides concluding remarks.

# 2 Multi-categorical risk assessment

Incidents that affect one or more CIs have far-reaching consequences and impact society in many ways. It is therefore hardly adequate to measure the impact in a single (one-dimensional) quantity. Rather, we recommend considering multiple impact categories and measure the impact in each of these to get a richer picture of the consequences of an incident.

## 2.1 Multi-categorical impact

Existing guidelines in the context of critical infrastructure protection [BMI] and discussion with experts showed that 5 categories capture the most relevant effects [1]:

(A) Humans affected

(B) Property damage

(C) Economic damage

(D) Environmental damage

(E) Political-social effects

A multi-dimensional impact assessment now estimates the impact of the considered incident in each category. This estimate should use the same scale to assure comparability. Qualitative estimates are recommended [2] e.g., ranging from 1 (minimal impact) to 5 (massive impact). The interpretation of these categories is CI-specific, see Table 1.

**Table 1.** Qualitative impact scale with different interpretations (cf. [1]).

| Score | Interpretation | General description | City traffic | Hospital |
|---|---|---|---|---|
| 1 | Minimal | Insignificant impact | Normal operation | Normal operation |
| 2 | Minor | Reversible impact | Minor congestion | Special treatment may not be possible |
| 3 | Moderate | Slight effects | Delays possible in some areas | Treatment assured, but maybe delayed |
| 4 | Major | Irreversible effects | Some roads blocked, significant delays | Reduced resources, less urgent treatment postponed |
| 5 | Massive | Extensive irreversible effects | Impossible to transfer inner city | Intensive care limited or unavailable |

This multi-categorical impact assessment is then a vector of assessments, denoted by $I = (I_A, I_B, I_C, I_D, I_E)$, where $I_K$ is the impact in category $K$. It is best illustrated through a histogram.

## 2.2 Multi-categorical risk

As often in risk management, a risk level is determined based on likelihood and impact. Even though it is possible to also have multi-dimensional likelihood assessments [1], we recommend to use a one-dimensional qualitative measure. For example, the likelihood of occurrence can be measured on a 5-tier scale ranging from 1 (very unlikely) to 5 (very likely) with intermediate values representing unlikely, possible, and likely events.

An established way to do this is to work with a risk matrix that assigns to each combination of likelihood (column) and impact (row) category a risk value, usually represented through colours ranging from green (lowest risk) to red (highest risk). An example of a risk matrix is shown below in **Figure 1** (taken form [1]).

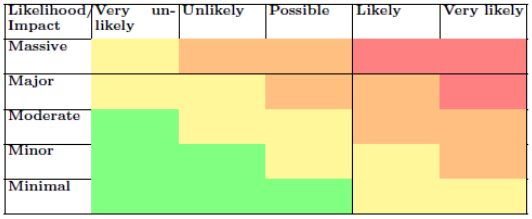


**Figure 1.** Risk matrix

Experts should here choose their own risk matrix corresponding to their understanding of their specific risks. The colour of the cell is mapped to a *risk score*, e.g., ranging from 1 (green cell) to 4 (red cell). Applying this to all impact categories yields a vector of risks scores that can again be illustrated through a histogram.

# 3 Risk management under uncertainty

Risk management has to deal with uncertainty in many regards. Consequences of a threat are uncertain due to cascading effects, but also due to external influencing factors (e.g., extreme weather, changes in legal restrictions, etc.). Further, new threats may occur (e.g., zero-day attacks) or multiple incidents may happen at the same time and influence one another (either by chance or intentionally as in the case of an APT). This intrinsic uncertainty should be explicitly considered during risk management.

## 3.1 Adapted risk Management process

An adapted risk management process that can capture uncertainty to some degree has been developed in course of the HyRiM project ('Hybrid Risk Management for Utility Networks') [3] and is therefore called HyRiM-RM process [4]. It is based on the ISO 31000 risk management process [5] and consists of the following steps:

1. Establishing the context: collection of information on internal and external relevant factors, understand relevant components and dependencies
2. Risk Identification: relevant threats and vulnerabilities are identified
3. Risk Analysis: the identified risks are analysed to better understand the consequences (and ideally also likelihood of occurrence)
4. Risk Evaluation: based on the analysis, risks are compared, and priority is assigned according to criteria defined in the first step
5. Risk Treatment: identification of an optimal set of controls such that the chance for the worst-case damage is minimized, based on a game-theoretic model

A case study following these steps has been conducted in course of the HyRiM project to investigate advanced persistent threats on a water utility network [6].

Uncertainty is captured through:

- a probabilistic or multidimensional risk analysis, i.e., the consequences are described either through a (discrete) probability distribution over all possible consequences or through multiple consequences (as in the case of multiple impact categories, see Section 2.1)
- a generalized risk evaluation: two risks are compared based on the probability of the worst-case damage (the one with lower probability for maximal damage is preferred) or with a lexicographic ordering where the most important category has most influence
- a game-theoretic risk treatment: different strategies to reduce the risk are compared and a recommendation of which to choose is returned

The game-theoretic model used in the risk treatment considers an attacker who tries to cause as much harm as possible, i.e., the operator of the CI and this (abstract) attacker play a zero-sum game. The identified optimal choice of controls is such that the players have no incentives to deviate. If the considered risk is not due to an intentional attacker but rather due to natural disaster, the chosen framework provides an upper bound to the expected damage because the attacker deviates from his optimal strategy (that causes most harm due to the zero-sum assumption). The approach can therefore be considered as conservative but can also be used in situations where we do not have any knowledge about the attacker.
A crucial difference to traditional game-theoretic models is that the games considered here, sometimes called security games, are able to handle vector-valued payoffs, e.g., payoffs that represent discrete probability distributions [7].

## 3.2 Insights from serious games

Infrastructure systems are known as the foundation of cities nowadays. They are considered as complex socio-technical systems that assist in transporting, supplying and distributing people, services and materials to individuals, businesses, and organizations. If infrastructure failure has the potential to cause dramatic consequences in terms of a disruption of vital services, the term Critical Infrastructure (CI) is often used [8]. CIs symbolize system-of-systems, which are large-scale concurrent and distributed systems whose components are complex systems themselves [9]. In other words, the components of CIs are networked, where the connectivity as well as the topology of these networks have enormous impact on their functionalities [10]. Therefore, the protection of CIs is considered as the main concern for decision makers and urban planners around the world. In order to resolve this challenging issue, Serious Games are a promising approach that have been receiving much attention in recent decades [11]. Serious Games are a simplified version of reality that enable players to experience decision-making and evaluate the results. Serious Games are primarily used for training purposes as a form of experiential learning that employ simulation techniques as a cost-effective alternative to often high risk and costly real-life activities. In Serious Games, players interact to gain understanding of how complex social–technological systems are and learn from their decision-making experience [12]. Moreover, the interaction of players who play certain stakeholder roles may lead to a better understanding of the system, including the real-world consequences of the players' decisions [13]. Serious Games are capable of combining game technology with science in real-world applications, with the explicit aim of a serious game being, for instance, the analysis of human behaviour/decisions, a training effect in the players' skills, or the development of a better understanding and increased awareness of challenging problems and interdependencies in complex systems such as CIs [14]. Game theory provides a framework to model the confrontations in CIs between the strategic attackers and defenders [15]. Ultimately, Serious Games create targeted learning objectives and encourage the player to make strategic decisions, define priorities and solve a given problem interactively.

Within this paper, a multiplayer turn-based attacker-defender game dynamic is presented. The Serious Game concept is presented in **Figure 2**. This game dynamic will achieve the goal of the Serious Game to provide an environment whereby CI operators and cybersecurity specialists can engage their area-specific skills and knowledge to ultimately discover the unknown threats that exist in cyber-physical infrastructure, to aid vulnerability assessments. Examples of the summary statistics collected from attacking gamers' actions include; percentages of budget spent on bribery, explosives, gun/knife attacks, hacking, etc., and percentages of budget spent by the emergency response sector. In the scenario of a cyber-attack (e.g., distributed denial-of-service (DDoS)), a Game Director will be assigned a role to specify the attackers' budgets and other attack and controlling parameters – the scenarios that will emerge will come from the attackers and the defenders' responses to them. Whereas, for natural disaster scenarios (which could be caused by an attack), the Game Director will define the natural event parameters and monitor the interaction with the attackers and defenders.

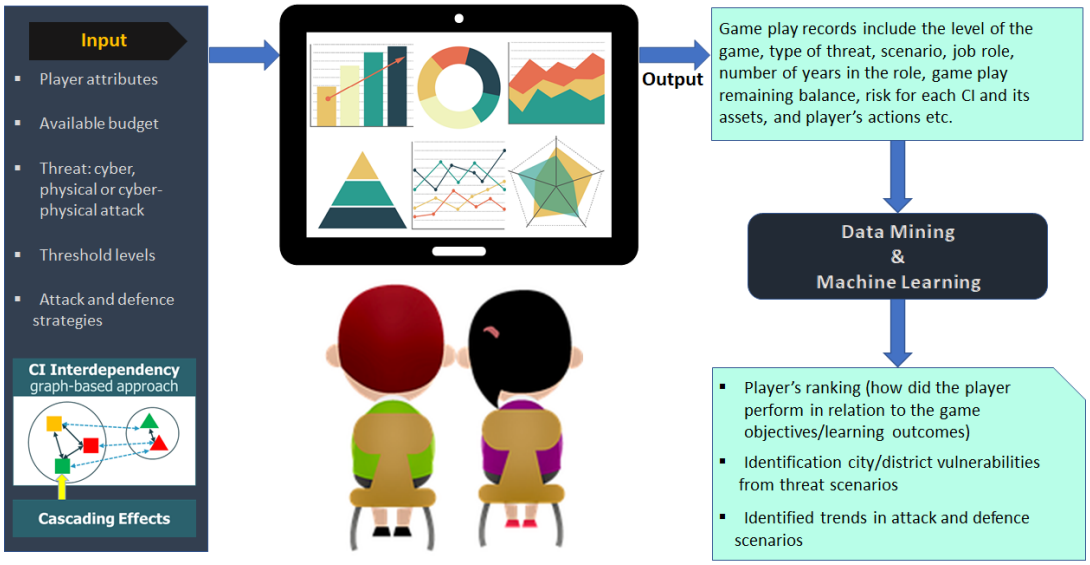


**Figure 2.** Serious Game design concept

While the game-theoretic framework assures optimal selection of countermeasures to protect a system against a threat, assumptions about players preferences and behaviours may be incorrect. A good way to validate or improve the chosen model is to collect data on how people react in the considered scenario by evaluating their decision-making. A data mining algorithm will be deployed on the server of the Serious Game, tracking defined interactions of the user and the system (see **Figure 3**). These trends will highlight potentially unidentified interdependencies, vulnerabilities and cascading effects as well as measures taken by the players to mitigate them and facilitate the updating of conditional probabilities.

Vulnerabilities to previously unanticipated combinations of threats or cascading effects will be identified through the novel Serious Games approach. The ingenuity of the game players (CI operators, emergency responders, etc) will be exploited by data mining (involving machine learning techniques) the Serious Games' gameplay records to pre-empt the potential for successful attacks and inform defence strategies. The Serious Game environment will provide a powerful experiential learning and training tool for staff involved in the defence of CIs. The game simulation will set out desired learning objectives via prompting the player to make various decisions to cyber-physical treat scenarios. The backend simulation of the game will then model the consequential effects of the cyber and physical attacks on the performance of transport/ energy/ communications networks. Records from playing the Serious Game will contain valuable data on how people behave and which actions they take. Comparing this with the

hypothetical behaviour of players will allow the refinement of the game theoretic model and therefore adjust the optimal choices, where necessary.

# 4 Illustrative example

One of the threats considered in the ongoing PRECICNT project [16] is a flash flood due to heavy rainfall affecting a city of approx. 500,000 inhabitants. Historical data and discussions with experts showed that such an event first and foremost affects city traffic. Strong limitations of city traffic affect other CIs, in particular it is difficult for emergency services to reach the city centre to help people or to take people to the hospital. In case of strong and long-lasting disruptions, electricity and gas supply may be affected, which in turn affects other CIs, e.g., the sewer system or a hospital. The consequences depend on many external factors that are unknown or can't be controlled, e.g., the traffic situation in the city or availability of emergency stuff and equipment. The adapted risk management process from Section 3.1 is applied step by step.

1. Establishing the context

Relevant components and dependencies are identified in discussion with experts. This can be represented in a diagram as shown in **Figure 3**

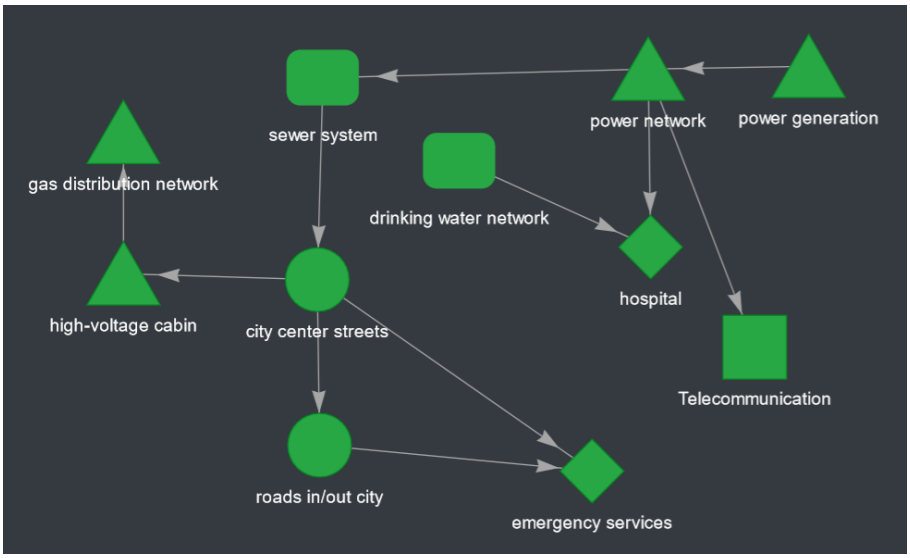


**Figure 3.** Dependency graph for flooding scenario

2. Risk Identification
   Information on the relevant threats is collected (e.g., from historical data) and vulnerabilities are identified. Vulnerabilities can be technical (e.g., supported by tools such as OpenVAS or Nessus), organisational (e.g., lack of awareness of social engineering attacks that may be reduced through trainings). In the considered example the focus is on the flooding threat as such events have been observed with increased frequency in recent years.

3. Risk Analysis
   The identified risks are analysed to get a better understanding. For the considered flooding scenario, the likelihood of occurrence may be estimated from recent data (due to ongoing climate changes it is recommended to refrain from old data as it may be biased). We assume that a flooding is possible, i.e., the level is 3.

The impact is estimated based on experience where the assessments in different categories can come from different experts. For the flooding example we expect minimal damage for humans, environment, and minimal political-social effects, minor damage for the environment and moderate economic damage, so the impact assessment is $I = (1,2,3,1,1)$ as shown in **Figure 4**.

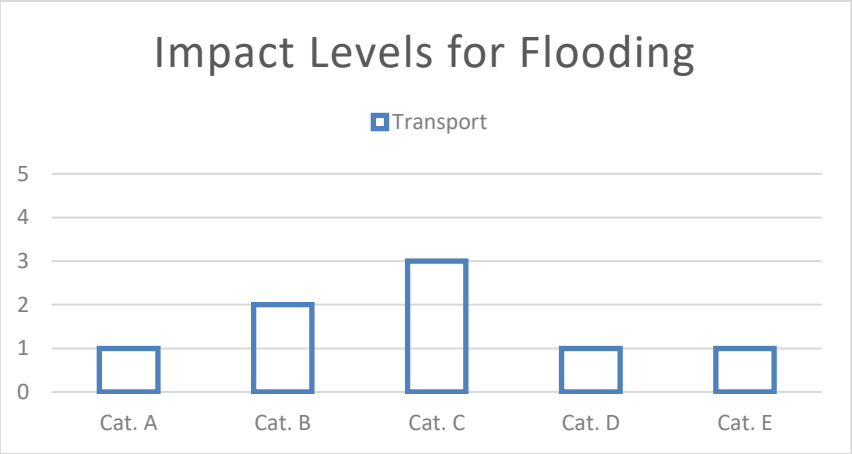


**Figure 4.** Illustrative multi-categorical impact assessment for CI transportation in case of a flooding

Assuming a likelihood of occurrence of 3 (i.e., assumed that a flood is possible) and a risk matrix as shown in Section 2.2 yields risk levels as shown in **Figure 5**.

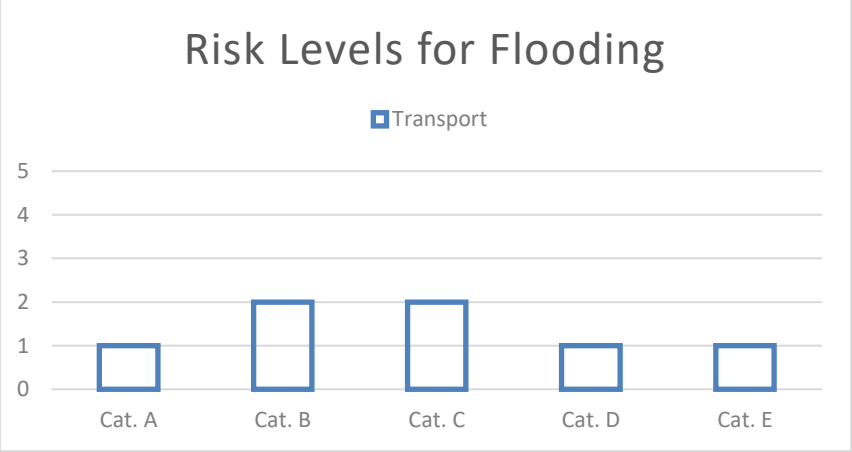


**Figure 5.** Multi-categorical risk assessment for CI transportation in case of a flooding

4. Risk Evaluation
   In this general framework, risks are compared through lexicographic ordering. For that sake, the different categories may be rearranged such that the assessments of the most important category are compared first. For example, if A (humans) is the most important category, then a risk with assessment $R_1 = (1,2,3,1,1)$ is 'better' than $R_2 = (2,1,3,1,1)$ since the level in category A (first entry) is smaller.

5. Risk Treatment
   Finally, the question is how to deal with the analysed risks. The answer can be found in two steps. First, a set of possible counteractions is identified. Such a set contains options to protect critical points or reduce the impact. For the flooding example, this could include improved protection of strongly affected points (e.g.,

narrow roads or tunnels) or building of an additional protection wall. Second, the question is which of these should be chosen to provide maximal protection with limited resources. Even for a small set of counteractions it is recommended to approach this problem systematically, e.g., by applying game theory. To do so, the payoffs for each combination of threat and counteraction need to be estimated – in our setting, this results in a histogram of expected damage for each scenario. The best combination of counteractions can then be identified through an optimization algorithm [17]. The implemented algorithm prefers situations where the worst-case damage (i.e., the risk level of the most relevant category) is lower. Optimization of multiple quantities is possible (e.g., minimize damage and maximize availability), but in this case it is necessary to measure all quantities on the same scale.

# 5 Conclusions

In situations where risk assessment and risk management face uncertainty, as in the case of networks of CIs, it is recommended to use multi-dimensional risk assessments. This general form can be incorporated in a classical risk management process and can be supported from both game theory and serious games. However, there are also several challenges, including the individual risk assessments and the identification of countermeasures. These issues will be discussed in more detail in the course of the PRECINCT project.

## Acknowledgements

The PRECINCT project has received funding from the European Union's HORIZON 2020 research and innovation program under Grant Agreement No 101021668.

## References

1. König S, Schauer S, Rass S. Multi-categorical Risk Assessment for Urban Critical Infrastructures. In: Percia David D, Mermoud A, Maillart T, editors. Critical Information Infrastructures Security [Internet]. Cham: Springer International Publishing; 2021 [cited 2022 Apr 7]. p. 152–67. (Lecture Notes in Computer Science; vol. 13139). Available from: https://link.springer.com/10.1007/978-3-030-93200-8_9

2. BSI. IT-Grundschutz-catalogues 13th version 2013 [Internet]. Bonn, Germany: Bundesamt für Sicherheit in der Informationstechnik - Federal Office for Information Security; 2013. Available from: https://www.bsi.bund.de/EN/Topics/ITGrundschutz/ITGrundschutzCatalogues/itgrundschutzcatalogues_node.html

3. HyRiM Consortium. Hybrid Risk Management for Utility Providers [Internet]. 2015. Available from: https://hyrim.net/

4. Schauer S. A Risk Management Approach for Highly Interconnected Networks. In: Rass S, Schauer S, editors. Game Theory for Security and Risk Management [Internet]. Cham: Springer International Publishing; 2018 [cited 2018 Sep 19]. p. 285–311. Available from: http://link.springer.com/10.1007/978-3-319-75268-6_12

5. ISO, editor. ISO 31000:2009 Risk management - Principles and guidelines. Geneva: ISO; 2009. (ISO).

6. Gouglidis A, König S, Green B, Rossegger K, Hutchison D. Protecting Water Utility Networks from Advanced Persistent Threats: A Case Study. In: Rass S, Schauer S, editors. Game Theory for Security and Risk Management: From Theory to Practice. Cham: Springer International Publishing; 2018. p. 313–33.

7. Rass S, König S, Schauer S. Uncertainty in Games: Using Probability Distributions as Payoffs: 346–357. In: Khouzani M, Panaousis E, Theodorakopoulos G, editors. Decision and Game Theory for Security, 6th International Conference, GameSec 2015. Springer; 2015. (LNCS 9406).

8. Chowdhury N, Gkioulos V. Cyber security training for critical infrastructure protection: A literature review. Computer Science Review. 2021 May;40:100361.

9. Bocchini P, Frangopol DM, Ummenhofer T, Zinke T. Resilience and Sustainability of Civil Infrastructure: Toward a Unified Approach. Journal of Infrastructure Systems. 2014;20(2):04014004.

10. Li Y, Qiao S, Deng Y, Wu J. Stackelberg game in critical infrastructures from a network science perspective. Physica A: Statistical Mechanics and its Applications. 2019 May;521:705–14.

11. Yamin MM, Katt B, Nowostawski M. Serious games as a tool to model attack and defense scenarios for cyber-security exercises. Computers & Security. 2021 Nov;110:102450.

12. van Riel W, Post J, Langeveld J, Herder P, Clemens F. A gaming approach to networked infrastructure management. Structure and Infrastructure Engineering. 2017 Jul 3;13(7):855–68.

13. Wehrle R, Wiens M, Schultmann F. Application of collaborative serious gaming for the elicitation of expert knowledge and towards creating Situation Awareness in the field of infrastructure resilience. International Journal of Disaster Risk Reduction. 2022 Jan;67:102665.

14. Lukosch HK, Bekebrede G, Kurapati S, Lukosch SG. A Scientific Foundation of Simulation Games for the Analysis and Design of Complex Systems. Simulation & Gaming. 2018 Jun;49(3):279–314.

15. Xu H, Windsor M, Muste M, Demir I. A web-based decision support system for collaborative mitigation of multiple water-related hazards using serious gaming. Journal of Environmental Management. 2020 Feb;255:109887.

16. PRECINCT consortium. PRECINCT Website [Internet]. PRECINCT project. 2022. Available from: https://www.precinct.info/

17. Rass S, König Sandra, Alshawish A. HyRiM: Multicriteria Risk Management using Zero-Sum Games with vector-valued payoffs that are probability distributions [Internet]. 2020. Available from: https://cran.r-project.org/package=HyRiM

## List of abbreviations and definitions

| | |
|---|---|
| CI | Critical Infrastructure |

# An Overview of Causes of Landslides and Their Impact on Transport Networks

Kwan Ben Sim, Faculty of Science & Engineering, University of Nottingham Malaysia, Jalan Broga 43500 Selangor, evxks8@nottingham.edu.my

Min Lee Lee, Faculty of Science & Engineering, University of Nottingham Malaysia, Jalan Broga 43500 Selangor, MinLee.Lee@nottingham.edu.my

Remenyte-Prescott Rasa, Faculty of Engineering, University of Nottingham, University Park, Nottingham NG7 2RD, United Kingdom, r.remenyte-prescott@nottingham.ac.uk

Soon Yee Wong, Faculty of Science & Engineering, University of Nottingham Malaysia, Jalan Broga 43500 Selangor, SoonYee.Wong@nottingham.edu.my

## Abstract

*Landslide is one of the major geohazards threatening human life and economy. Landslides have claimed tens of thousands of lives in the new millennium worldwide and an estimated economic loss of $20 billion annually. Information on causes and impacts of landslide hazards can be found abundantly, however, studies on impacts of landslide on transport networks, particularly on the quantification methods of the landslide impact are still relatively scarce. This paper aims to review the distribution of contributing and triggering factors of landslides around the world and their physical and economic impact on transport networks, including the methods of assessing the impact. A slope can undergo a failure due to numerous contributing factors, i.e. geological, morphological, ground and hydrological conditions, human causes, etc., but there is often only one factor that triggers the landslide at the moment of its failure. Statistics showed that precipitation followed by water level change are the leading triggering factors (58%) of landslides worldwide. In particular, rainfall-induced landslides have resulted in nearly 90% of deaths worldwide. Ground conditions and human causes are the main contributing factors of landslides. 40% of the landslides resulting from human factors come from construction activities in the developing world. Various methods have been deployed to assess the impacts of landslide on transport networks, such as GIS approach, transport network modelling, impact modelling and questionnaires surveys. The impacts of landslides on transport networks include delays in travel time, damage to vehicles and transport infrastructure, serious injuries and fatalities, and increased cost of maintenance. Scarcity of data and the difficulties in obtaining robust database, as well as their associated costs proved to be a hindrance to effective landslide impact assessments on road networks.*

***Keywords:*** *Landslide, resilience, triggering factors, contributing factors, impact assessment, transport network.*

# 1 Introduction

Landslides are one of the major devastating geohazards that claimed tens of thousands of lives in the new millennium worldwide and an estimated economic loss of $20 billion annually [1]–[3]. Centuries prior, many countries worldwide have suffered deaths and economic losses due to landslides and the impact is still on the rise. It was reported in [4] that the greatest economic impact of landslides is on transportation infrastructures. This is especially true in rural regions where the transportation network is sparse, and the availability of alternate routes is minimal. As a result, a minor landslide will bring a great impact on the economic sector over an extensive region [5]. Studies of landslides relating

to deaths of the population can be found abundantly [3], [6], [7], but studies on the impacts of landslide on transport networks are still relatively scarce.

This paper aims to review the factors causing landslides and their impacts on transportation networks. These include triggering factors, as well as contributing factors. This review is useful to help in understanding the reasons of high landslide susceptibility in certain parts of the world. In addition, case studies methods and impacts on transportation networks will also be discussed.

# 2 Factors Affecting Landslides

According to [8], a slope can undergo failure due to many contributing factors, i.e. geological, morphological, human and physical, but there is only one factor that triggers the landslide at the moment of failure. By definition, a trigger is an external stimulus, i.e. extreme precipitation, storm waves, earthquake shaking, volcanic eruption, or rapid stream erosion that result in a near-immediate reaction in the form of a landslide through the rapid rise in the stresses or through the reduction of the strength of slope properties. In certain scenarios, landslides could transpire without any evident attributable trigger due to assortment or combination of causes, such as chemical or physical weathering of materials, that progressively take the slope to failure [9]. By definitions, triggering factors are those extrinsic factors that cause a sudden failure to the slope, while contributing factors are defined as the intrinsic factors that gradually reduce the safety margin of slope over a long period. However, this differentiation is arguable as both contributing and triggering factors are inter-related. For instance, rainfall infiltration is a triggering factor for slope failure. As rainwater infiltrates into the soil, it will weaken the soil strength, while the weakened soil itself is regarded as a contributing factor. Therefore, it is obvious that slope failure involves a very complicated mechanism that sometimes it is not caused by one factor, but a combination of multiple factors. The triggering and contributing factors that cause landslides will be discussed in this section.

## 2.1 Triggering factors

According to [10], the most common landslides triggering factors include extreme rainfall, rapid snowmelt, volcanic eruption, earthquake shaking, change in water level, i.e. rapid drawdown. Other common triggering factors are the change in slope geometry and erosion [11], [12]. The distribution of triggering factors worldwide is plotted in

**Figure 1**. Statistics showed that precipitation followed by water level change are the leading triggering factors (58%) of landslides worldwide [11]. A comprehensive review by [13] found that the majority (54.2%) of landslide studies that can be found on current available literature dealt with rainfall-induced landslide. A documented study by [6] stated that rainfall has always been the main trigger of landslides all around the world, amounting to approximately 3841 landslide disasters worldwide between 2004 to 2016. Globally, rainfall induced landslides have resulted in nearly 90% of deaths [14], [15]. 41% of the rainfall-induced landslides worldwide were contributed by the Asian continent, notably China, Nepal and India.

Extreme precipitation contributed to 73% of all fatal landslides in Latin America and Caribbean [16]. Brazil and Colombia together contribute to 67% of all rainfall triggered landslides in Latin America amounting to 37% and 32%, respectively, with most of the disasters concentrated around south-east Brazil and central region of Colombia. A distribution of triggering factors of landslides in Colombia are as follows: rainfall 87%, human activity 10%, seismic excitation 0.6% and 0.1% for volcano eruption [17].

From the statistics in **Figure 2**, it is clear that China alone has contributed to 81% of all rainfall triggered landslides of the whole East Asia due to the summer Monsoon season. This amounted to about 15% of all the total rainfall induced landslides worldwide [1].

In South Asia, the summer Monsoon has also resulted in a rise in landslide disasters in India, Nepal, Pakistan and Bangladesh. Nepal and India contributed to 26% of the world rainfall-induced landslides at 10% and 16%, respectively. It was stated by [18] that 83% of landslide occurrence in Bangladesh were caused by extreme precipitation.

Most of the rainfall triggered landslide disasters in South East Asia are from Indonesia and Philippines at 46% (42% caused by typhoons) and 32%, respectively. It was further stated by [6] that 22% of the rainfall triggered landslides in the south-east Asian region which is equivalent to 5% worldwide were brought about by typhoons.

Rainfall-induced landslides occur due to the rise in pore water pressure or loss of matric suction in soil [19]. Rainwater that seeps into the soil may cause an increase in soil overburden pressure and a reduction in shear strength, and hence increases the probability of landslides. The rainfall threshold required to initiate a landslide event varies depending on the contributing factors. For example, a rainfall event of 48 hours with a cumulative rainfall amounting to 36.7 mm only was found to have triggered landslides in the Kalimpong Region of the Darjeeling Himalayas [20]. A few conditions that contributed to this low threshold value for that region included improper drainage, toe cutting as well as the rise in construction activities which blocked the water flow. In addition, the geological settings of the region that consisted of moderately to highly weathered chlorite schist, phyllite, phyllitic quartzite had further contributed to its landslide susceptibility [19]. The distribution of contributing factors of landslides worldwide will be discussed in section 2.2.

**Figure 1** Distribution of landslide triggering factors around the world.

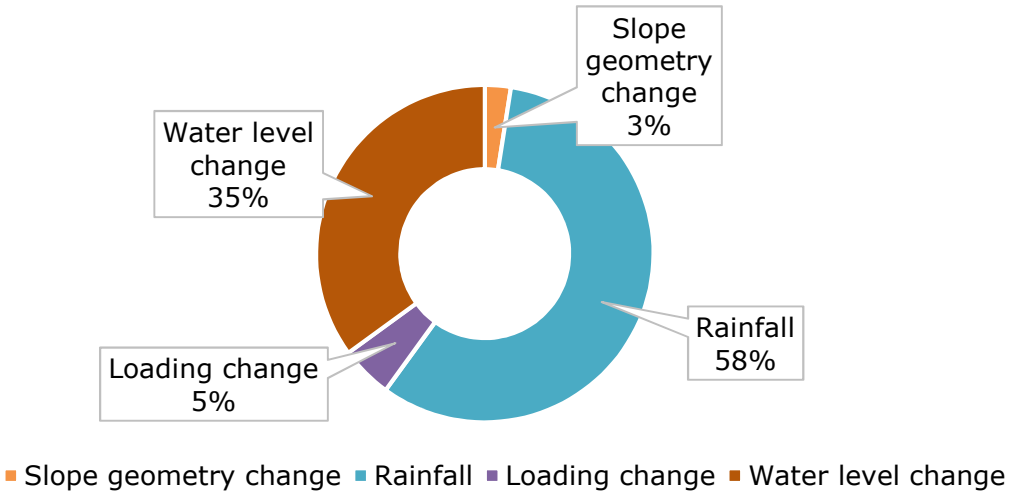


Source: [11]

**Figure 2** Distribution of rainfall induced landslides across different regions.

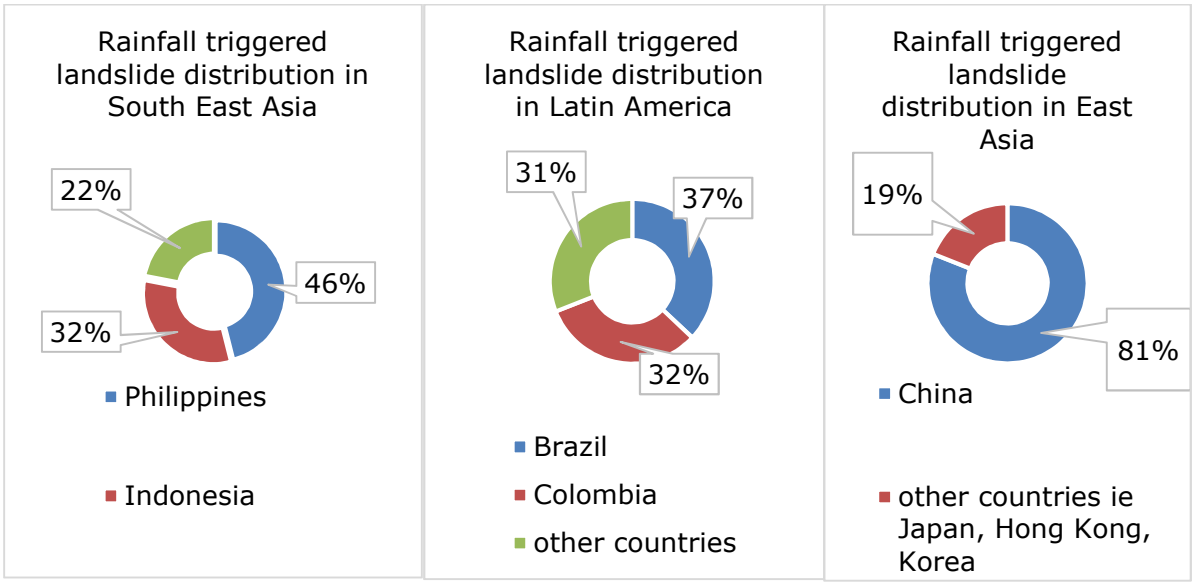


Source: [6]

## 2.2 Contributing factors

Geological conditions, geo-morphological conditions, physical, and manmade factors are the main contributing factors to landslides [8]. According to [11], numerous studies have been conducted to determine the distribution of landslide contributing factors taking into account countries, such as China, Italy, Thailand, Russia, Taiwan, Germany, Korea, Japan, and Australia. **Figure 3** shows the distribution of the contributing factors of landslides worldwide. A similar distribution was found in [12]. It is clearly shown in the chart that ground conditions and human causes are the main contributing factors of landslide failures on a global scale. Furthermore, the landslides disaster also occurs from the mismanagement of land use due to the rise in population and the demand for agricultural activities that consequently force the population to stay in regions susceptible to landslides [21]. A documented study by [1] states that human activities, such as construction and mining, have contributed to approximately 770 landslide disasters with 3725 deaths between 2004 and 2016. **Figure 4** shows the distribution of landslides resulting from human activities worldwide. It is clear that human activities that cause the most landslides come from construction activities followed by illegal mining and illegal hill cutting. Volume of material is not taken as cause of landslides. Globally, majority of the landslides disasters occurring from construction activities in India (28 %), followed by China (9 %), then Pakistan (6 %), the Philippines (5 %), Nepal (5%) and Malaysia (5 %) [1]. On average, construction-induced landslides claimed 3 lives per each landslide. In China, 52% of disasters occurred in urban construction sites, while landslides along roads were scarce (7 %). On the contrary, India and Nepal comprised 30% and 43% of landslide disasters, respectively contributed by road construction. [22], [23] stated that the rise in landslides disasters in the Himalayan region has always been associated with road construction due to the poor engineering design, route choice and poor management [24]. From the chart in **Figure 4** it is seen that landslide disasters due to mining are driven by the rise in illegal or unregulated extraction. Globally, the nations that give rise to landslides from mining activities are India (12 %), followed by Indonesia (11.7 %), China (10 %), Pakistan (7%) and Philippines (7%) [1].

**Figure 3** Distribution of landslide contributing factors around the world.

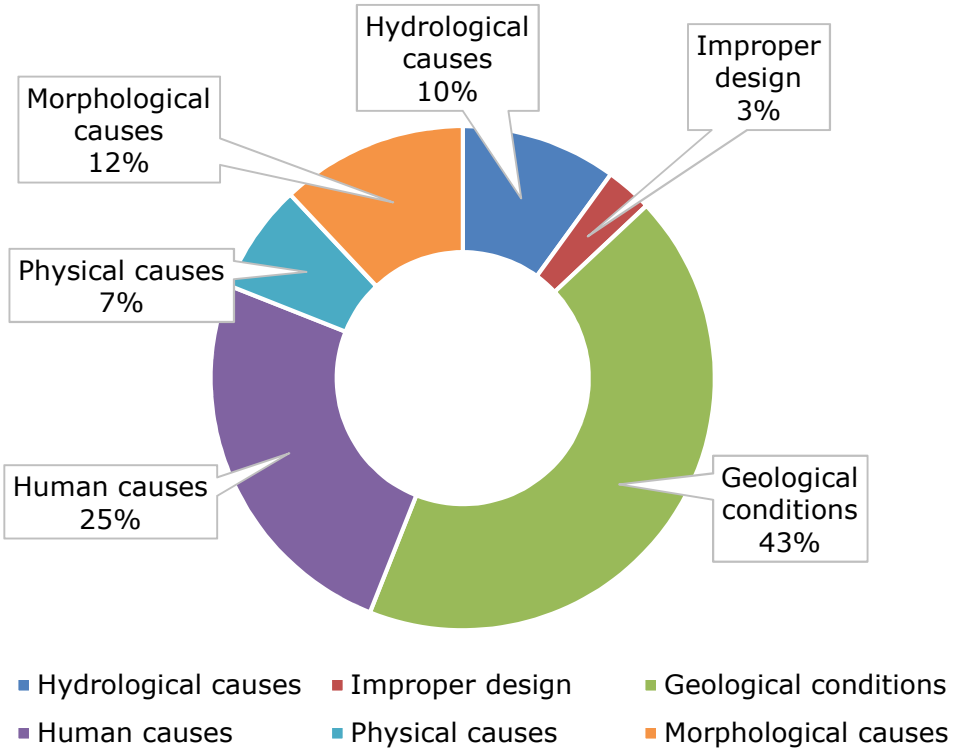


Sources: [11], [12], [25]

**Figure 4** distribution of landslides resulting from human factors worldwide.

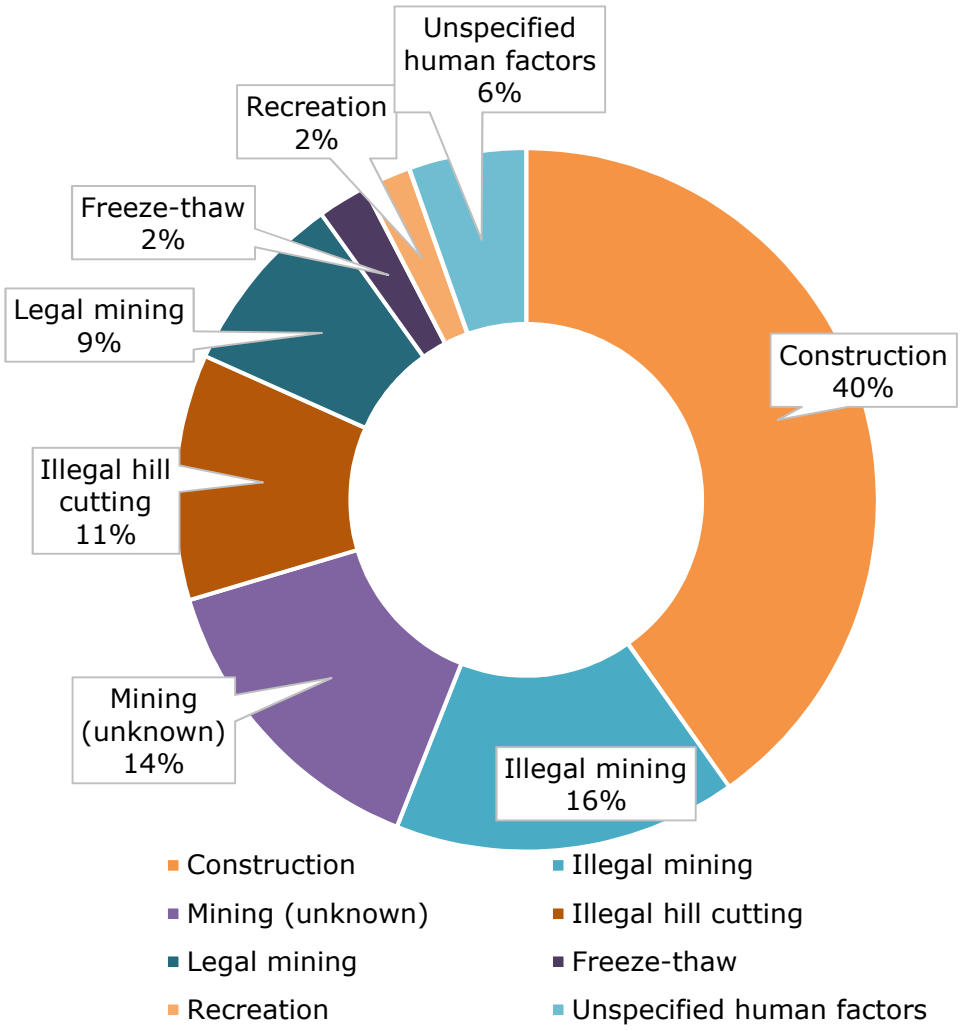


Source: [1]

# 3 Landslide impacts on transport networks

It was stated by [26] that landslides disrupt access to remote rural regions where the economic activities are typically transport-dependent. Extensive areal vulnerability can be attributed to the transport network, instead of the event itself. One can utilize GIS for landslide mapping purposes to determine the area of impact. Slope stability evaluation tools such as Limit Equilibrium Method (LEM) and Finite Element Method (FEM) can be used to predict the landslide susceptibility of a specific study area. The runout distance of a landslide can be evaluated by performing Discrete Element Method (DEM). To perform these assessments, geotechnical field survey such as soil investigations must be carried out in the first place, followed by the modelling of the slope and then accessing its stability and impact.

In real life scenario, a landslide event that occurred at an access road in the Blue Mountains of Jamaica completely cut off the nearest route linking local coffee manufacturers with the international market [5], [26]. A long-term impact following that event would be on the tourism industry, as well as other economic activities. Landslide impacts on transport networks are both qualitative and quantitative and they are generally the largest impact stems from the closure of road networks. Qualitative economic impacts of landslides on transportation networks are such as:

- Loss of utility of parts of the road network
- Road users are forced to make detours to reach their destination
- Cutting off the access to and from rather rural regions to other services i.e. employment, health and educational prospects

Quantitative economic impacts of landslide events that result in road closure are categorized by [27] into three categories:

- **Direct economic impacts -** The direct expenditures involved in cleaning up and repair/replacement of lost / damaged infrastructures, search and rescue operation costs
- **Direct consequential economic impacts –** Typically related to infrastructure disruption and utility losses, i.e. costs for road closures (or implementation of single-lane with traffic lights) for a specific period with a given diversion, costs involving injuries and deaths may also be taken into account
- **Indirect consequential economic impacts –** Generally, access to secluded regions is affected by landslides causing a disruption in economic activities. Hence the vulnerability is widespread and is governed by the transport network rather than the landslide incident itself. If an impacted route is forced to close for an indefinite or a very long period of time, confidence and viability of local economic activities, i.e. business, agriculture and manufacturing on a long term basis will certainly be greatly affected, such as the coffee production of Jamaica example above. Furthermore, tourism industry will be affected as the confidence of visitors / tourists to travel within the landslide prone regions will be lower. This is the hardest cost to compute as they are typically widespread both socially and geographically. A few approaches to compute these costs will be through cost-benefit analysis, cost-effectiveness analysis, willingness to pay, multi-criteria analysis and approaches based on transport assessment.

However, the terms and definition used by [27] may appear to be ambiguous and overlap each other such as the **Direct consequential economic impacts** and **indirect consequential economic impacts.** In light of this uncertainty, another similar set of terms and definitions by [28] will be used in this present study:

- **Direct losses**: Deals with human life and injury as well as physical damage to productive and social assets.

- **Indirect losses**: Related to disruptions to the flow of goods and services stemming from the direct losses. i.e. costs of road closures for a specific period of time.

- **Secondary losses**: Deals with the impacts on socio-economic imbalances and performance of the economy of the affected region. For example, profitability losses in a certain manufacturing or agricultural industry.

## 3.1 Direct losses

In a documented study by [4], data collection was made and the direct economic losses due to landslides affecting the federal road network in the Lower Saxon Uplands of North-West Germany were modelled. The method utilizes the locally obtained data for the purpose of extrapolating direct costs for the study area. A susceptibility assessment and infrastructure exposure model was also used. The study estimated that the average cost per kilometre of highway at risk of landslides in the study area to be US$52,000 per km. It was also mentioned that obtaining landslide restoration costs proved very challenging and, where available, their accuracy and reliability was to be questioned.

Another similar study by [29] dealt with the direct economic impacts of rainfall induced landslides on the road network of two regions of Italy, i.e. Marche and Sicily. Road maps and landslide data were exploited using the GIS method to determine the different metrics which quantify the impact of the landslide events on the natural landscape and on the road networks, by road type. The maps were utilized with cost data obtained from various sources, i.e. local authorities, as well as special legislature, so as to assess the unit cost per metre of damaged road and unit costs per square metre. The result varied in the two study areas. The cost per metre and the cost per square metre in the secondary road of Marche region were computed to be approximately US$ 2215/m and US$55/$m^2$; whereas for the main road of Sicily, costs were estimated at US$18,431/m and US$124/$m^2$.

A related study [30] collected and utilized information on the national road network of the People's Democratic Republic (PDR) of Laos, as well as road maintenance costs to assess the yearly average landslide losses per kilometre. It was reported to be between US$1000–1500 per km.

The direct landslide losses on the road networks as extracted from the studies by [4], [29], [30] are tabulated in **Table 1**. It is seen that there is a huge variation between the landslide costs incurred per metres for the regions. This could be due to a number of reasons such as; (i) both Marche and Sicily computed estimates based on a single huge landslide event where as NW Germany and Laos were based on a longer period of time where numerous landslide events have occurred; (ii) engineering features, as well as maintenance levels for different types of road will surely vary; (iii) different countries will possess different socioeconomic condition, resulting in the variation of remediation and maintenance policies and costs. The studies by [4], [29] however, only focused on direct economic impacts and the degree of extrapolation used by [4] across the road network was deemed inappropriate in regions where landslides occurred rather rarely such as in Scotland. The study by [30] indeed dealt with direct economic costs and consequential impacts. However, the methodology to the indirect losses seemed to assume that all the vehicles that will regularly drive on the road will wait until the period of closure is over. This may be applicable in Laos and reflects on the road network's morphology of the country of study. Diversions and traffic flow restrictions that are common in the European continent is not being considered.

**Table 1** Direct economic impact of landslides on road networks of various regions

| Region | Direct economic cost (US$ per metre) |
|---|---|
| North-West Germany | 52 |
| Sicily | 18,431 |
| Marche | 2,215 |
| Laos | 1 -1.5 |

In August 2004, a series of rainfall-induced landslides occurred in Scotland notably at the A83 between Glen Kinglas and to the north of Cairndow (9 August), the A9 to the north of Dunkeld (11 August), and the A85 at Glen Ogle (18 August) [31]. Although there were no casualties, 57 people have to be evacuated by air from the A85 Glen Ogle road when they were trapped between two huge landslides. The A83 Rest and be Thankful road, while not involved in the series of landslides of August 2004, has been subjected to numerous landslides resulting in road closures notably in 2007, 2008,2009, 2011, 2012, 2014, 2015, 2017 and 2018. The direct costs for 5 Scottish landslides between 2004 and 2014 were assessed by [26] and they fall in between US$ 0.34 million and US$ 2.32 million.

## 3.2 Indirect losses

From the case study in Laos [30], indirect losses regards to road closures (predominantly cost of lost time and vehicle operating costs) were assessed by taking into account parameters such as GDP per head, percentage of population within working age, unemployment rates and estimated working hours per year. Their estimate was around US$50,000 per day for an average annual daily traffic (AADT) of 100 and US$150,000 for AADT of 300. Most of the landslides affecting their national road network seemed to be shallow and localised slope failures in cut slopes. Environmental costs associated with average landslide events were estimated to be at US$8,150. Overall, the impacts of landslides on national road networks of Laos was deemed to be less than some other landslide prone Asian countries such as Nepal [22].

Indirect losses for 5 landslides in Scotland between 2004 and 2014 (which were heavily governed by the traffic volume usage of the road and disruption duration) were estimated to be between US$ 0.25 million and US$ 1.91 million using the QUADRO program [26]. A similar case study by [32] generated a database of possible landslide-prone road segments in Scotland by utilizing landslide susceptibility data with the aids of GeoSure program. It was shown that 34% of Scotland's strategic road networks i.e. 1,500km out of 4,300km were prone to landslides, which would bring about indirect economic losses greater than US$ 43,000 per day of closure (as computed in their SUMO road transport models).

## 3.3 Secondary losses

Questionnaires surveys were used to determine secondary losses for Scotland [26]. Although the costs were not released in the study, it gave valuable qualitative statistics. Interestingly, their survey reported that landslide could yield positive secondary impacts. For example, hotel operators benefited from the landslides at A85 Glen Ogle as the road users who were trapped between the landslides have no choice but to put up in the guest house. Similar scenarios also occurred in various places around Killin which seemed to raise the image of the municipal.

Another report by [33] also analysed thoroughly on the direct economic losses, and, to a certain extent, the indirect losses and secondary losses due to landslides in Colorado, USA. The study conducted on the latter two impacts focussed on the qualitative analysis. Similar to the published paper by [26], secondary losses caused the economic activity of certain area to plummet, and impacts on other areas to rise. For example, the 2010 Glenwood Canyon rockfall event resulted in the rise in the economic activity of aviation, i.e. exponential rise in flight costs and an increase in the usage of chartered aeroplane between key locations on either side of the rockfall event. In addition, many geotechnical engineering firms were also benefited from increased remedial and mitigation projects in relation to the rockfall event.

Secondary losses due to landslides on the highway domain strip of Serada Pelada region of Brazil was forecasted by [34] at a loss of US$ 18,307.28 for the banana plantation. The cost attributed to the loss in the banana plantation was of US$ 0.50/m2 for a 6-year period.

# 4 Conclusion

The review provided in this paper is only a restricted summary of the extensive studies carried out on distributions of the factors causing landslides and the economic impacts of landslides on transport networks. Statistics showed that rainfall and change in water level are the main triggering factors to landslide, while ground condition and human causes are the main contributing factors. The majority of the published works on landslide impacts of transport networks dealt with the direct losses which are rather straightforward; less on the indirect losses and even more scarce on the secondary impacts. Sometimes, a landslide event may not only bring negative impacts but also create some positive impacts such as more businesses for hoteliers in providing temporary shelters to road users who are trapped between the debris flow. The estimates of economic consequences of landslides on transport network are much more complicated than the direct impacts. What is apparent is that the approach to this problem is by no means uniform and standard. Every country has its own approach, solutions and roads with different engineering properties and maintenance levels that result in very different costs worldwide.

The present review study also highlighted the difficulties arise in collecting data for landslide events on transport networks and their associated costs. A robust database is needed for accurate and reliable national economic impact analyses, as well as an effective management of landslide risks, particularly in developing countries. At present, the authors are developing a landslide F-N curve for Malaysia in an effort of quantifying landslide risk and its associated impacts. It was found that data collection is not so straightforward as data have to be mined from multiple sources such as newspapers, reports from relevant government agencies etc. The author also has future plans of carrying out quantitative risk assessment (QRA) on societal risk posed by landslide to road networks in Malaysia and foresee challenges in developing a robust database. As quoted in [26], "*past data for direct economic impacts are generally labour intensive to retrieve. The experience here has been that as people move on both knowledge and experience are lost but, even more critically, as contracts pass to new organizations data and information about events is lost*". Perhaps this is the reason why there is such a scarcity on published studies regarding impacts of landslides on transportation networks. The authors are currently putting in efforts to develop a landslide database for the country of study. In addition, the authors also plan to predict the data which is missing such as using methods of extrapolation. A potential improvement could be for regulatory bodies and authorities to make their data more organized and available so that impact assessments of landslides on transportation networks will be more effective.

## References


[1] M. J. Froude and D. N. Petley, "Global fatal landslide occurrence from 2004 to 2016," *Nat. Hazards Earth Syst. Sci.*, vol. 18, no. 8, pp. 2161–2181, 2018, doi: 10.5194/nhess-18-2161-2018.

[2] M. Klose, P. Maurischat, and B. Damm, "Landslide impacts in Germany: A historical and socioeconomic perspective," *Landslides*, vol. 13, no. 1, pp. 183–199, 2016, doi: 10.1007/s10346-015-0643-9.

[3] K. Ben Sim, M. L. Lee, and S. Y. Wong, "A review of landslide acceptable risk and tolerable risk," *Geoenvironmental Disasters*, vol. 9, no. 1, 2022, doi: 10.1186/s40677-022-00205-6.

[4] M. Klose, B. Damm, and B. Terhorst, "Landslide cost modeling for transportation infrastructures: a methodological approach," *Landslides*, vol. 12, no. 2, pp. 321–334, 2015, doi: 10.1007/s10346-014-0481-1.

[5] M. G. Winter, B. Shearer, D. Palmer, and J. Sharpe, "Assessment of the Economic Impacts of Landslides and Other Climate-Driven Events," *Publ. Proj. Rep. PPR 878. Transp. Res. Lab. Wokingham.*, no. December, 2018.

[6] M. Froude and D. Petley, "Global fatal landslide occurrence 2004 to 2016," *Nat. Hazards Earth Syst. Sci. Discuss.*, no. 2012, pp. 1–44, 2018, doi: 10.5194/nhess-2018-49.

[7] A. K. Turner, "Social and environmental impacts of landslides," *Innov. Infrastruct. Solut.*, vol. 3, no. 1, pp. 25–27, 2018, doi: 10.1007/s41062-018-0175-y.

[8] J. S. Griffiths, "Proving the occurrence and cause of a landslide in a legal context," *Bull. Eng. Geol. Environ.*, vol. 58, no. 1, pp. 75–85, 1999, doi: 10.1007/s100640050070.

[9] G. F. Wieczorek, "Landslide Triggering Mechanisms," *Landslides— Investig. Mitig.*, pp. 76–78, 1996.

[10] L. M. Highland and P. Bobrowsky, "The landslide Handbook - A guide to understanding landslides," *US Geol. Surv. Circ.*, no. 1325, pp. 1–147, 2008, doi: 10.3133/cir1325.

[11] K. Y. Ng, "Rainfall-induced landslides in Hulu Kelang area, Malaysia," *Ecol. Econ.*, vol. 1, no. April, p. 32, 2012, doi: 10.1017/CBO9781107415324.004.

[12] A. Akter, M. J. M. M. Noor, M. Goto, S. Khanam, A. Parvez, and M. Rasheduzzaman, "Landslide Disaster in Malaysia: An Overview," *Int. J. Innov. Res. Dev.*, vol. 8, no. 6, pp. 292–302, 2019, doi: 10.24940/ijird/2019/v8/i6/jun19058.

[13] K. Sassa, S. Tsuchiya, K. Ugai, A. Wakai, and T. Uchimura, "Landslides: A review of achievements in the first 5 years (2004-2009)," *Landslides*, vol. 6, no. 4, pp. 275–286, 2009, doi: 10.1007/s10346-009-0172-5.

[14] N. Sultana, "Analysis of landslide-induced fatalities and injuries in Bangladesh: 2000-2018," *Cogent Soc. Sci.*, vol. 6, no. 1, pp. 2000–2018, 2020, doi: 10.1080/23311886.2020.1737402.

[15] U. Haque *et al.*, "Fatal landslides in Europe," *Landslides*, vol. 13, no. 6, pp. 1545–1554, 2016, doi: 10.1007/s10346-016-0689-3.

[16] S. A. Sepúlveda and D. N. Petley, "Regional trends and controlling factors of fatal landslides in Latin America and the Caribbean," *Nat. Hazards Earth Syst. Sci.*, vol. 15, no. 8, pp. 1821–1833, 2015, doi: 10.5194/nhess-15-1821-2015.

[17] E. Aristizábal and O. Sánchez, "Spatial and temporal patterns and the socioeconomic impacts of landslides in the tropical and mountainous Colombian Andes," *Disasters*, vol. 44, no. 3, pp. 596–618, 2020, doi: 10.1111/disa.12391.

[18] N. Sultana, "Analysis of landslide-induced fatalities and injuries in Bangladesh: 2000-2018," *Cogent Soc. Sci.*, vol. 6, no. 1, pp. 1–26, 2020, doi: 10.1080/23311886.2020.1737402.

[19] A. Dikshit, R. Sarkar, and N. Satyam, "Probabilistic approach toward Darjeeling Himalayas landslides-A case study," *Cogent Eng.*, vol. 5, no. 1, pp. 1–11, 2018, doi: 10.1080/23311916.2018.1537539.

[20] T. S. Teja, A. Dikshit, and N. Satyam, "Determination of rainfall thresholds for landslide prediction using an algorithm-based approach: Case study in the Darjeeling

Himalayas, India," *Geosci.*, vol. 9, no. 7, 2019, doi: 10.3390/geosciences9070302.
[21] S. Soralump, "Rainfall-triggered landslide: From research to mitigation practice in Thailand," *Geotech. Eng.*, vol. 41, no. 1, 2010.
[22] D. N. Petley *et al.*, "Trends in landslide occurrence in Nepal," *Nat. Hazards*, vol. 43, no. 1, pp. 23–44, 2007, doi: 10.1007/s11069-006-9100-3.
[23] S. Chaudhary, G. K. Jimee, and G. K. Basyal, "Trend and geographical distribution of landslides in Nepal based on Nepal DesInventar data," *New Technol. Urban Saf. Mega Cities Asia*, vol. 1, 2017.
[24] G. J. Hearn and N. M. Shakya, "Engineering challenges for sustainable road access in the himalayas," *Q. J. Eng. Geol. Hydrogeol.*, vol. 50, no. 1, pp. 69–80, 2017, doi: 10.1144/qjegh2016-109.
[25] D. Kazmi, S. Qasim, I. S. . Harahap, S. Baharom, M. Imran, and S. Moin, "A Study on the Contributing Factors of Major Landslides in Malaysia," *Civ. Eng. J.*, vol. 2, no. 12, pp. 669–678, 2016, doi: 10.28991/cej-2016-00000066.
[26] M. G. Winter, D. Peeling, D. Palmer, and J. Peeling, "Economic impacts of landslides and floods on a road network," *Acta Univ. Carolinae, Geogr.*, vol. 54, no. 2, pp. 207–220, 2019, doi: 10.14712/23361980.2019.18.
[27] M. G. Winter and E. N. Bromhead, "Landslide risk: Some issues that determine societal acceptance," *Nat. Hazards*, vol. 62, no. 2, pp. 169–187, 2012, doi: 10.1007/s11069-011-9987-1.
[28] C. Benson, "Indirect economic impacts from disasters," *Contin. Cent.*, no. Dec, pp. 1–2, 2012.
[29] M. Donnini *et al.*, "Impact of event landslides on road networks: a statistical analysis of two Italian case studies," *Landslides*, vol. 14, no. 4, pp. 1521–1535, 2017, doi: 10.1007/s10346-017-0829-4.
[30] G. Hearn, T. Hunt, J. Aubert, and J. Howell, "Landslide impacts on the road network of Lao PDR and the feasibility of implementing a slope management programme," *Int. Conf. …*, 2008.
[31] M. G. Winter, B. Shearer, D. Palmer, D. Peeling, C. Harmer, and J. Sharpe, "The Economic Impact of Landslides and Floods on the Road Network," *Procedia Eng.*, vol. 143, no. Ictg, pp. 1425–1434, 2016, doi: 10.1016/j.proeng.2016.06.168.
[32] B. Postance, J. Hillier, T. Dijkstra, and N. Dixon, "Extending natural hazard impacts: An assessment of landslide disruptions on a national road transportation network," *Environ. Res. Lett.*, vol. 12, no. 1, 2017, doi: 10.1088/1748-9326/aa5555.
[33] L. M. Highland, "Landslides in Colorado , USA : Impacts and Loss Estimation for the Year 2010," 2012.
[34] E. F. Batista, L. D. B. Passini, and A. C. M. Kormann, "Methodologies of economic measurement and vulnerability assessment for application in landslide risk analysis in a highway domain strip: A case study in the Serra Pelada region (Brazil)," *Sustain.*, vol. 11, no. 21, 2019, doi: 10.3390/su11216130.

# The prevention of NaTech risks on the Italian territory: the importance of the Safety Management System

Romualdo Marrazzo, ISPRA – Istituto Superiore per la Protezione e Ricerca Ambientale, romualdo.marrazzo@isprambiente.it

Fabrizio Vazzana, ISPRA – Istituto Superiore per la Protezione e Ricerca Ambientale, fabrizio.vazzana@isprambiente.it

## Abstract

*The Seveso III Directive 2012/18/EU imposes an obligation for the site operator, in identifying the hazards and assessing the major risks of the establishment, to take the NaTech risks into account, paying attention to the entire spectrum of natural hazards that may affect the site.*

*The results of the NATECH risks assessment must be considered in the location, design, construction, and operation of the industrial establishment, as well as in the implementation of mitigation measures and emergency planning. In this sense the Safety Management System for the Prevention of the Major Accidents plays an important role to ensure the correct implementation of the prevention and protection measures against major accidents originating from NATECH events.*

*Starting from the main outcomes of the analysis of some industrial accidents, a specific focus is presented on how organizations could manage these problems, through specific procedures, good practices and methods used to assess industry's response to NATECH issues. It is then described an in-depth analysis carried out on the NATECH risk of lightning for industrial plants and equipment, for the identification of the critical elements for safety, as well as the main protection measures for electrical and electronic equipment.*

## 1 Introduction

The Seveso III Directive 2012/18/EU, implemented in Italy by the D.Lgs. 105/2015 [1], imposes an obligation for the site operator, in identifying the hazards and assessing the major risks of the establishment, to take the NaTech risks into account, paying attention to the entire spectrum of natural hazards that may affect the site.

With the acronym NaTech, from the English Natural Hazards Triggering Technological Disasters, the international literature identifies technological accidents, such as fires, explosions and toxic releases that can occur inside industrial establishments and along distribution networks and pipelins following natural disasters events. The evaluation of the effects of natural events on Major Accident Hazard establishments requires a systemic and multidisciplinary approach in relation to the complexity of the contexts to be analysed both from the plant and structural point of view.

Scope of the paper is highlighting the importance of the Safety Management System for the Prevention of the Major Accidents (SMS-PMA), to ensure the correct implementation of the prevention and protection measures against major accidents originating from NATECH events, as derived from the analysis of some industrial accidents occurred in Italy.

## 2 Natural hazards as significant cause of industrial accidents

The incidental data extracted from the e-MARS database of the European Commission [2] show that from 1985 to today in the EU countries there has been an average NaTech accident per year, while on about 7000 accidents that occurred in industrial sites,

collected in the Bank UK-HSE MHIDAS data [3], 3% of accidents are classified as NaTech having been induced by natural events such as earthquakes (8%), floods (16%), landslides (7%), strong winds (13 %) and lightning (56%). Figure 1 is shown below, which represents the number of accidents occurring as a function of extreme natural events [4].

**Figure 1.** Number of accidents occurring as a function of extreme natural events.

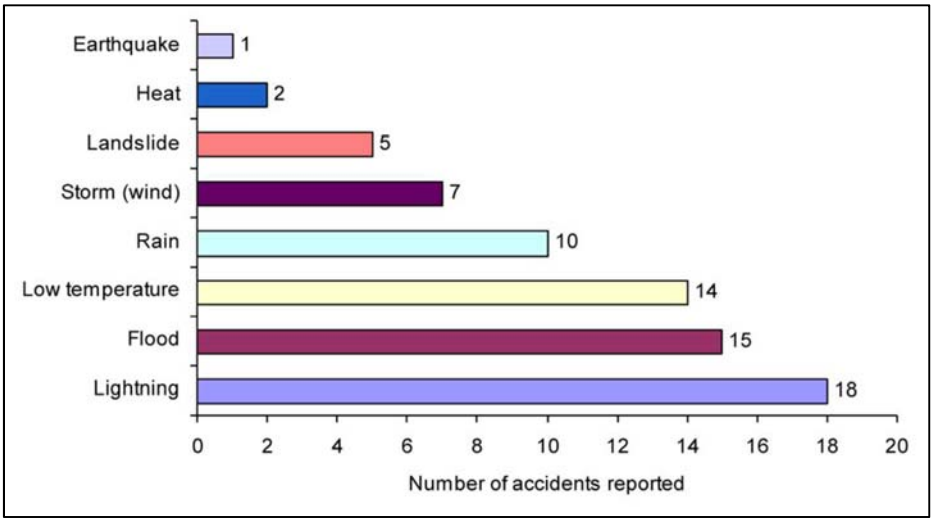


*Source:* JRC, 2014

In the Table 1 below it is possible to summarize the main types of plants, infrastructures and industrial equipment vulnerable to natural hazards in the event of adverse weather conditions.

**Table 1.** Equipment and plants vulnerable to natural hazards.

| **Industrial equipment and plants** | **Natural hazards for adverse conditions** |
|---|---|
| Gas, fuel oil and coal thermoelectric power plants | Floods |
| Pipelines for the transmission and distribution of gas, oil pipelines | Floods (Landslides) |
| LPG depots | Floods |
| Mineral oils depots | Floods, lightning, strong winds, storms |
| Refineries and chemical and petrochemical plants: | |
| • Process columns | Strong winds, storms |
| • Above ground tanks | Strong winds, storms, floods, lightning |
| • Mounded tanks | Floods |
| • Pipelins (also underground) | Floods |
| • Motors, pumps, compressors | Floods |

| | |
|---|---|
| • Control room and instrumentation | Floods, lightning |
| • Warehouses of packed products | Floods |
| Service utilities commonly found in industrial plants whose failure can lead to hazardous situations: boilers; refrigeration systems; cooling towers; power supply; water treatment; torch systems | Strong winds, storms, floods, lightning, changes in water availability, increases in water temperatures and decreases in the availability of cooling water |
| Toxic products depots | Floods |
| Warehouses of phytosanitary products | Floods |
| Coastal depots, plants and terminals | Sea storms, sea level rise |

*Source:* CTI, 2021.

## 2.1 Floods

As indicated in the table 1, floods (with consequent landslides, depending on the terrain) are the most common and widespread natural danger in our country and many productive activities in all sectors are vulnerable in the event of adverse weather conditions.

The danger of floods can never be completely eliminated and therefore every manager of a Seveso establishment must prepare in advance to limit the impact that a flood could have on its activities, through dedicated planning that takes into account that an event of this type could trigger or make a major accident more serious, directly or indirectly. He must therefore provide, through the adaptation of its SMS-PMA, the necessary measures to prevent or limit the consequences for human health and the environment.

Directive 2007/60/EC relating to the assessment and management of flood risks (Floods Directive - FD) [5], provides the elements for the assessment and management of this type of risk which in Italy is implemented with D.Lgs. 49/2010 [6].

### 2.1.1 Industrial accidents following floods

Following continuous torrential rains which lasted several days, the plants of a refinery located in the port area flooded. Production was stopped due to the water level. A violent fire followed, as well as several explosions of tanks, electrical equipment (transformers) and pipes. Four hours later, fires still persisted in the gas and crude oil sectors of the refinery. The fire was extinguished after 20 hours. Two people died and four were injured. Extensive material damage resulting from the accident led to the closure of the refinery and the suspension of all activities.

The sequence of fires was caused by the flood that actually moved the exhausted oil, displacing it from the sewer system. The waste oil that floated on the surface then came into contact with the hot parts of the systems, causing several fires and explosions in the pipes and electrical transformers. From the analysis of the operational experience on the event carried out by the site operator, as detailed during the post-event inspection on SMS-PMA, in accordance with the D.Lgs. 105/2015, it is fundamental to highlight the following technical and organizational factors:

- Implement effective procedures to prevent the rapid distribution of flammable liquids by alluvial waters. This element is critical for the operational control of the protection measures, as reported in the emergency planning of the establishment;

- Good maintenance practice is to make sure the drains are clean so that they do not block the water drain. This element is critical for the operational control activities according to an adequate and scheduled maintenance plan, as reported in the SMS-PMA implementation.

Following an in-depth analysis of the accident occurred, it is possible to focus attention on a series of lessons learned from the event, in order to prevent possible occurrence or, if necessary, limit their consequences.

The site manager, in order to mitigate the impact of a flood, must undertake a series of improvement actions in order to make the perimeter of the plant, buildings or specific areas within buildings or equipment containing hazardous substances (in quantities and conditions such as to cause a major accident), inaccessible to water. These actions include the following types of protection (or combinations thereof), chosen following an adequate balance between critical systems of a technical and managerial nature:

- Construction of defense works;
- Closure of openings and water entry points;
- Waterproofing of walls;
- Seal the penetrations in the walls;
- Installation of pumps for the collection and removal of water (dewatering pumps);
- Installation of non-return valves;
- Ensure a control plan on a periodic basis and also to be carried out afterwards a flood and before an expected flood.

The site manager should also locate fire pumps, sprinklers, suppression systems and other fire suppression systems, with associated electrical equipment, outside of flood hazard areas or above the maximum achievable water level.

If there are critical equipment for process safety, production or operations that are located at a lower level than the maximum achievable by the water, the site manager must ensure they are flood-proof (if their functionality is required during the flood for safety reasons or to ensure continuity of production). In the case of electrical equipment, it must be designed to work even if continuously immersed and have an electrical classification IP X8 (protected by permanent immersion in water - submersible to 3 m depth in continuous immersion and in any case for more than one hour, resistant to a pressure of at least 10 bar exerted in all directions).

## 2.2 Lightning

As indicated in the table 1, lightning is another common and widespread natural danger in our country. In fact, every year Italy is struck on average by about 600,000 lightning (excluding seas), with an average density of lightning on the ground equal to approx. 2 discharges per year per km2. However, the actual lightning density largely depends on geographic conformation.

There are currently no known devices or systems aimed at modifying the natural epilogue of this meteorological phenomenology, in order to prevent its formation: this means that the risk associated with lightning cannot be eliminated in any way.

The CEI 81-30 standard [7] was repealed in 2020 and with it the method of obtaining the average number of lightning strikes to the ground per year and per square kilometre (s.c. “Ng”). This value is a fundamental parameter for calculating the lightning risk of a structure. It is important to remind that the obligation to make this assessment derives from Legislative Decree 81/08 (safety at work legislation) [8]. Now, to calculate the lightning risk, it must refer to the new CEI 81-29 guide [9], which refers to the CEI EN IEC 62858 standard [10].

These data have now been replaced with those of the SIRF (Italian Lightning Detection System) database [11]. The detection system consists of a network of sensors for the detection of lightning throughout the Italian territory, including the neighbouring islands

and seas, capable of providing extremely precise data. This approach is a major innovation in the field of lightning damage prevention as it provides a value of "Ng" based on lightning data collected in over ten years of observations. These data, for the entire Italian territory, have high spatial and temporal precision (identification of the place and instant in which each single lightning strike occurred).

### 2.2.1 Industrial accidents following lightning

Following a thunderstorm, there was a significant interruption in the power supply of a refinery which resulted in the loss of cooling on a distillation column inside the hydrogenation unit. Some control systems were of the manual type: the lack of detection caused an increase in column pressure. Safety valves, designed to protect equipment from overpressure, did not work properly, causing a large volume of gas to be released into the atmosphere.

From the analysis of the operational experience on the event carried out by the site operator, as detailed during the post-event inspection on SMS-PMA, in accordance with the D.Lgs. 105/2015, it is fundamental to highlight the following technical and organizational factors:

- The impact of lightning strikes on the power supply can be an indirect cause of loss of containment due to process anomalies;
- This element should be considered in the risk assessment and the safety critical elements that could be affected should be assessed accordingly.

The elements above are critical for the issue of the hazards identification and risks evaluation, and the subsequent operational control activities on critical technical systems, according to the SMS-PMA implementation.

Another important theme to focus on are the fires involving storage tanks; they are also typical events following lightning in fact, a third of the tank fires are attributable to it. In particular, floating roof tanks are the most vulnerable to the effects of atmospheric discharges.

The American Petroleum Institute (API) has formed a technical committee to study the phenomenon and find solutions to take into account its effects. The result of this work is the publication of API RP 545, for the lightning protection of above ground storage tanks [12].

This kind of events occurs when the lightning current passes between the SHUNTS and the tank shell, with the formation of an electric arc. In fact, when the discharge passes through the connection between the floating roof and the tank shell, if flammable vapours are present, they will probably be triggered. As a result of the work of the commission, the API RP 545 recommendation indicates 3 main changes to be made:

1. Install "submerged" SHUNT between the floating roof and the shell every 3 meters along the entire circumference of the Floating Roof.
2. Electrically insulate all the components of the Sealing System (including Springs, Shields, Seals, etc.).
3. Install connection conductors between the floating roof and the shell every 30 meters, along the entire circumference of the tank.

### 2.2.2 Dangers and main protection measures

From the analysis carried out above, it is possible to summarize the details of the main dangers caused by lightning:

- Fire damage: this is the greatest danger for systems and equipment, starting from storage tanks, up to cables and pipes. A classic example is the burning of the roofs of the tanks, the destruction of electrical lines and equipment with consequent disruption and lack of power supply.

- Damage from overvoltage: it is less known and spectacular than the previous one, but it can cause serious damage to the electrical and electronic control and process management systems. The high stress to which the equipment is subjected compromises its correct functioning during normal operation and during any emergencies.
- Shock Wave Damage: Lightning produces shock waves that can be destructive. These shock waves can severely damage concrete and brick/stone fireplaces and torches.

It is finally important to highlight the main protection measures for electrical and electronic equipment to be considered in the risk assessment for the identification of the critical elements for safety, with the subsequent attention in the phase of operational and maintenance activities, as reported in an adequate scheduled plan for a Seveso establishment:

- Earthing and equipotential bonding: the earth rod system conducts and disperses the lightning current in the ground. The equipotential bonding network minimizes potential differences and can reduce the magnetic field.
- Magnetic shielding and cable routing: local shields attenuate the magnetic field associated with lightning strike (direct, or close to the structure), thereby reducing induced pulses in internal lines.
- Protection with SPD System: the SPD (Surge Protection Device) System limits the effects of impulses within the structure, both of external and internal origin to the structure.
- Insulating Interfaces: insulating interfaces limit the effects of conducted pulses on incoming lines.

# 3 Conclusions

The results of the NATECH risks assessment must be considered in the location, design, construction, and operation of the industrial establishment, as well as in the implementation of mitigation measures and emergency planning. The site operator of industrial establishments under the Seveso directive should develop appropriate measures to address natural hazards, so as to allow the maintenance of control of the plants vital to safety and their safe operation.

Starting from the main outcomes of the analysis of some industrial accidents, where natural hazards have been identified as a significant and triggering cause, it is possible to focus the main types of plants, infrastructures, and industrial equipment vulnerable to extreme weather conditions. These lessons learned are also useful examples on how organizations could manage these problems, through specific procedures, good practices and methods used to assess industry's response to NATECH issues.

In this sense the Safety Management System for the Prevention of the Major Accidents of the establishment, and the relative integration with the issues as operational management, hazards identification and risks evaluation, emergency planning, etc., plays an important role to ensure the correct implementation of the prevention and protection measures against major accidents originating from NATECH events, with specific procedures for extreme weather conditions, such as heavy rainfall, lightning, strong winds and extreme temperatures.

## References


1. DECRETO LEGISLATIVO 26 giugno 2015, n. 105. SO n. 161 del 14 luglio 2015 "Attuazione della direttiva 2012/18/UE relativa al controllo del pericolo di incidenti rilevanti connessi con sostanze pericolose". (GU 14 luglio 2015, n. 161, S.O.).
2. https://emars.jrc.ec.europa.eu/en/emars/content (accessed 26/10/2021).
3. https://www.hse.gov.uk/research/journals/mrn698a.htm (accessed 26/10/2021).

4. https://minerva.jrc.ec.europa.eu/en/shorturl/minerva/6_mahb_bulletin_no6_forthweb_a4 (accessed 26/10/2021).
5. Directive 2007/60/EC of the European Parliament and of the Council of 23 October 2007 on the assessment of flood risks (Text with EEA relevance) Oj L 288, 06/11/2007, p. 27-34.
6. DECRETO LEGISLATIVO 23 febbraio 2010, n. 49. “Attuazione della direttiva 2007/60/CE relativa alla valutazione e alla gestione dei rischi di alluvione”. (GU 02 aprile 2010, n. 77).
7. CEI 81-30 “Protezione contro i fulmini – Reti di localizzazione fulmini (LLS) – Linee guida per l’impiego di sistemi LLS per l’individuazione dei valori Ng (Norma CEI EN 62305-2)”.
8. DECRETO LEGISLATIVO 9 aprile 2008, n. 81. “Attuazione dell’articolo 1 della legge 3 agosto 2007, n. 123, in matria di tutela della salute e sicurezza nei luoghi di lavoro”. (GU Serie Generale n. 101 30 aprile 2008. SO n. 108).
9. CEI 81-29 “Linee guida per l’applicazione delle Norme CEI EN 62305”.
10. CEI EN IEC 62858 (CEI 81-31) “Densità di fulminazione – Reti di localizzazione fulmini (LLS) – Principi generali”.
11. https://www.fulmini.it/ (accessed 26/10/2021)
12. API RP 545 “Recommended Practice for Lightning Protection of Above Ground Storage Tanks for Flammable or Combustible Liquids” (2009)

# Influence of availability transients on network resilience

Christian Tanguy, Orange/INNOVATION/DATA-AI, christian.tanguy@orange.com

## Abstract

*The resilience of networks is a fundamental issue in the telecommunications industry. The disruption of services must be kept at a minimum so that its consequences are not too serious and its duration is as short as possible. Maintenance policies often rely on the steady-state availabilities of each element of the system, given by the well-known ratio MTTF/(MTTF + MTTR).*

*The all-terminal availability — a standard performance index for networks — of a meshed network has recently been addressed by Eid in 2021, who used a topological framework for its description. The time-dependent contributions of links and nodes to the unavailability were computed using exponential failure and repair distributions for both types of (identical) components.*

*In this work we consider the same network as Eid's, but use the standard derivation of the all-terminal reliability. The contributions of links and nodes are given analytically for non-identical elements, leading to the variation with time of the global availability of the system. Furthermore, we rank the links in importance, using well-known performance indices (Birnbaum, Fussell-Vesely, etc.). A few links are definitely more equal than others, and should receive due attention in maintenance.*

*As the steady-state availability may not always be a lower bound to the transient availability in the case of non-exponential failure and repair distributions, we have studied the influence of such configurations on the time-dependent behaviours of all the aforementioned quantities and discuss the results.*

## 1 A brief introduction

The resilience of systems has become an issue of great importance for many industries, all the more so in telecommunications. Networks must recover rapidly after failures, incidents, natural events, cyberattacks, and so on. In order to develop maintenance strategies, it is helpful to determine the weak links of the chain. Usually, calculations consider the steady-state availabilities of the various components of the whole system.

Recent publications have shown important transient variations of the availability in several fields: 5G systems and Network Virtualization Functions studies [1-2], high availability of cluster configurations [3], and communication channels in the European railway industry [4], to cite but a few. They clearly demonstrate that the availability may strongly oscillate for an extended period of time.

Resilience issues have of course initiated a large body of work, and it is worth noticing that, especially in the last two years, time-dependent aspects of resilience have come to the fore in urban and commodities infrastructures [5-7]. The systems investigated in these publications are large, and may thus require a substantial computational effort

Another approach is to consider reasonably small systems, for which the number of parameters is still tractable while allowing to derive possibly general insights regarding the behaviour of larger systems. One such study has been proposed by Eid [8], in which the time-dependent contributions of nodes and links to the global unavailability have been assessed, when these components have exponential failure and repair time distributions.

This approach is very promising for the description of telecommunications networks, and we have decided to apply some of our former results in the case of non-exponential distributions [9-10] to investigate the assessment of potential weak links of the network,

and determine whether the assumptions of exponential distributions are questionable [11]. Our main, new result is that for non-exponential distributions, the blame game has no fixed victim.

The paper is organised as follows. In a first Section, we present the network architecture proposed by Eid [8], and derive the all-terminal reliability of the system, using the standard calculation procedure, which differs from the topological definition of Eid. We then compute several importance indices in Section 3, so as to determine the weak links of the network. Section 4 is devoted to a possible way — specific to networks — to decrease the global unavailability, a solution that should be kept in mind when defining maintenance strategies. Section 5 shows that the weak links are not always either the nodes or the links. We conclude by urging caution about the use steady-state availabilities for the determination of maintenance strategies since in some cases they might lead to wrong assumptions.

## 2 Description of the network

The network considered in this work has been proposed by Eid [8] and is represented in Figure 1. The performance index he considered is the all-terminal reliability (or availability), namely the probability that all nodes are connected to each other. It is well known that the computation of the all-terminal reliability is extremely complex in the general case, and is at least cumbersome even for a small number of nodes in the underlying graph [12]. However, it can be factorized in two terms

$$\mathrm{Rel_A(system)} = \mathrm{Rel_A(edges)}\ \mathrm{Rel_A(nodes)} \tag{1}$$

**Figure 1.** Representation of the network (after Eid [8]).

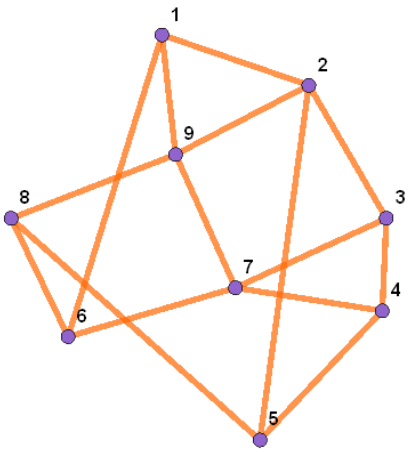


Assuming that all nodes are identical, it is very simple to find (this is a typical series system)

$$\mathrm{Rel_A(nodes)} = \rho^9 \tag{2}$$

The computation of $\mathrm{Rel_A(edges)}$ is more complicated, because the underlying graph (undirected links are assumed) cannot be reduced to a series-parallel graph. Using the standard pivotal decomposition method and the Wolfram software Mathematica, it has been nonetheless possible to express analytically the all-terminal reliability for arbitrary edge reliabilities, which is required for the determination of importance measures. This expression is linear in each of the availabilities $p_{ij}$ corresponding to the link between

nodes *i* and *j*. Since it has 9504 terms, only the result when all edges are identical with the same availability $p$ is given

$$\begin{aligned}\mathrm{Rel_A(edges)} = {} & 2007\,p^8 - 10907\,p^9 + 25796\,p^{10} - 34336\,p^{11} \\ & +27728\,p^{12} - 13565\,p^{13} + 3718\,p^{14} - 440\,p^{15}\end{aligned} \tag{3}$$

**Table 1.** Failure and repair rates for exponential distributions (after Eid [8]).

| | **Failure rate $\lambda$** (hour$^{-1}$) | **Repair rate $\mu$** (hour$^{-1}$) |
|---|---|---|
| Node | 0.001 | 0.040 |
| Edge | 0.025 | 0.100 |

In the following discussion, the exponential distributions of Eid [8], listed in Table 1, will be used as a reference. The availabilities of edges and nodes are then given by

$$p(t) = \frac{4}{5} + \frac{1}{5}\,e^{-t/8} \tag{4}$$

$$\rho(t) = \frac{40}{41} + \frac{1}{41}\,e^{-41\,t/1000} \tag{5}$$

Their asymptotic values are therefore $\frac{4}{5}$ and $\frac{40}{41}$, respectively. One can then deduce the asymptotic availabilities of the edge and node subsystems,

$$\mathrm{Rel_A(nodes)}_\infty = \left(\frac{40}{41}\right)^9 \approx 0.80072836 \tag{6}$$

$$\mathrm{Rel_A(edges)}_\infty = \frac{5728567296}{6103515625} \approx 0.93856847 \tag{7}$$

so that

$$\mathrm{Rel_A(system)}_\infty = \frac{5728567296}{6103515625}\left(\frac{40}{41}\right)^9 \approx 0.75153839 \tag{8}$$

Alternatively, one might be interested in the unavailabilities of each element, of the nodes and edges subsystems, and of the total system. Let the unavailabilities be described by $U$. The value for the edges differ from that of Eid [8], because of his different, topological definition of the availability of the edges' subsystem.

$$U(\mathrm{nodes})_\infty = 1 - \left(\frac{40}{41}\right)^9 \approx 0.19927164 \tag{9}$$

$$U(\mathrm{edges})_\infty = \frac{374948329}{6103515625} \approx 0.06143153 \tag{10}$$

$$U(\mathrm{system})_\infty \approx 0.24846161 \tag{11}$$

Let us now turn to the calculation of the importance measures that determine the elements whose improvement deserves scrutiny in resilience and maintenance policies.

# 3 Performance indices

Since the contribution of nodes is that of a series system, the more important nodes are those of lower availabilities. As elements are assumed identical in the present discussion, all nodes have the same importance. In this section, we shall therefore consider links only, and use the availability of each link to represent the link. The aim of this section is to rank all these links, using various importance measures [13]. The first elements of this list are those requiring extra attention when operating the system.

## 3.1 Birnbaum importance measure

This coefficient is simply defined by the derivative of the system availability with respect to the availability of the component. The exact knowledge of $\mathrm{Rel_A(edges)}$ allows to compute every Birnbaum factor $I^{(B)}$. Assuming identical elements, one finds

$$\begin{aligned} I^{(B)}(p_{45}) = {} & 1193p^7 - 7168p^8 + 18523p^9 - 26687p^{10} \\ & +23150p^{11} - 12089p^{12} + 3518p^{13} - 440p^{14} \end{aligned} \quad (12)$$

$$\begin{aligned} I^{(B)}(p_{58}) = {} & 1184p^7 - 7129p^8 + 18456p^9 - 26630p^{10} \\ & +23126p^{11} - 12085p^{12} + 3518p^{13} - 440p^{14} \end{aligned} \quad (13)$$

…

$$\begin{aligned} I^{(B)}(p_{79}) = {} & 992p^7 - 6180p^8 + 16499p^9 - 24473p^{10} \\ & +21785p^{11} - 11639p^{12} + 3456p^{13} - 440p^{14} \end{aligned} \quad (14)$$

$$\begin{aligned} I^{(B)}(p_{29}) = {} & 900p^7 - 5681p^8 + 15372p^9 - 23116p^{10} \\ & +20866p^{11} - 11307p^{12} + 3406p^{13} - 440p^{14} \end{aligned} \quad (15)$$

It is then straightforward to compute the fifteen factors, and assess their order. Note that $p$ might vary with time. For $p > 0.7$, the order is always the following: $\{p_{45}, p_{58}, p_{68}, p_{16}, p_{34}, p_{67}, p_{23}, p_{25}, p_{89}, p_{47}, p_{12}, p_{37}, p_{19}, p_{79}, p_{29}\}$. For instance, if $p = 0.8$, one finds $I^{(B)}(p_{45}) = 0.018471$, while $I^{(B)}(p_{29}) = 0.0046815$.

## 3.2 Other importance measures

The Improvement Potential, Risk Achievement Worth, Risk Reduction Worth, and Criticality Importance [13] have also been computed (some are very closely related, so that their ranking are identical). For identical edges, we recover exactly the same order as in the preceding subsection, namely

$$\{p_{45}, p_{58}, p_{68}, p_{16}, p_{34}, p_{67}, p_{23}, p_{25}, p_{89}, p_{47}, p_{12}, p_{37}, p_{19}, p_{79}, p_{29}\} \quad (16)$$

## 3.3 Fussell-Vesely index

This importance measure is more complicated to obtain since it relies on the probability of the failure occurring in at least one minimum cut set containing the element under consideration, provided that the system is failed [13]. Because of the meshed nature of the system, the determination of the minimum cut sets is rather tedious. The total number of minimum cut sets is 110, and their numbers for each link also vary: 38 for $p_{58}$, 39 for $p_{45}$, … , 51 for $p_{19}$, and 55 for $p_{29}$. One must then compute the corresponding probability for each particular set of minimum cut sets. In the original definition of the

Fussell-Vesely factor [13], this probability is divided by the total unavailability of the (sub-)system $U(p) = 1 - \mathrm{Rel_A(edges)}$. Since this term is identical for all the edges under consideration, it is more convenient to provide the aforementioned probability. Finally,

$$I^{(FV)}(p_{45}) \propto (1-p)^3(1 + 2p + 3p^2 + 3p^3 - p^4 - 10p^5 - 18p^6 \\ -2p^7 + 47p^8 + 51p^9 - 160p^{10} + 111p^{11} - 25p^{12}) \quad (17)$$

$$I^{(FV)}(p_{58}) \propto (1-p)^3(1 + 2p + 3p^2 + 3p^3 - p^4 - 11p^5 - 19p^6 \\ +p^7 + 48p^8 + 48p^9 - 159p^{10} + 111p^{11} - 25p^{12}) \quad (18)$$

$$\dots$$

$$I^{(FV)}(p_{79}) \propto (1-p)^4(1 + 3p + 6p^2 + 7p^3 + p^4 - 14p^5 - 27p^6 \\ -7p^7 + 37p^8 + 49p^9 - 78p^{10} + 25p^{11}) \quad (19)$$

$$I^{(FV)}(p_{29}) \propto (1-p)^4(1 + 3p + 5p^2 + 5p^3 - p^4 - 14p^5 - 21p^6 \\ -5p^7 + 37p^8 + 41p^9 - 74p^{10} + 25p^{11}) \quad (20)$$

The variation of these terms has been evaluated for different values of $p$ and is displayed in Figure 2. The ranking provided by the Fussell-Vesely index is exactly the same as that of Birnbaum and the other coefficients, given in equation (16).

**Figure 2.** Variations of $I^{(FV)}(p_i)\, U(p)/(1-p)^3$ for the fifteen links (see eq. (16) for the ranking).

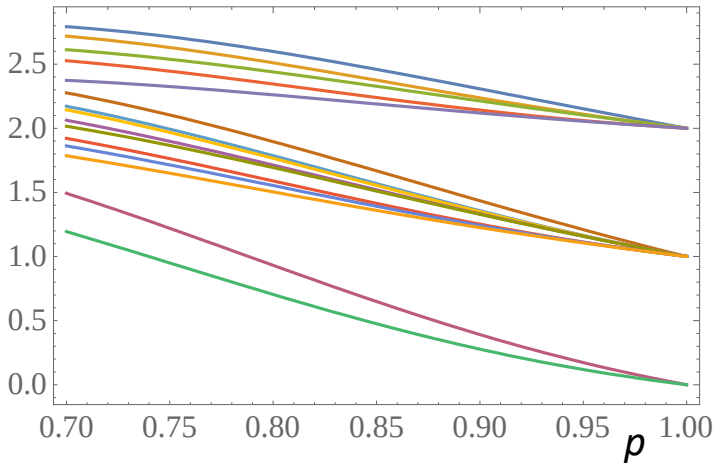


## 3.4 Time variation of performance indices, and a word of caution

Since the various expressions of the performance indices do not exhibit crossings for $0.7 \leq p \leq 1$ one cannot expect a possible influence of transient availabilities on the ranking of all the links for identical elements.

In the preceding subsections, an important assumption was made for the sake of simplicity: all links are identical. It is however possible to evaluate the ranks of each of the fifteen links when their availabilities are not identical, but follow a uniform distribution centred on $p = 0.8$, for instance in the interval [0.7,0.9]. In that case, ranks may change, as shown in Figure 3, which displays the result for a simulation of 50 000 samples. This may also happen if the transient behaviours of elements having the same asymptotic availability are different. Even then, the group of links $\{p_{45}, p_{58}, p_{68}, p_{16}, p_{34}\}$ is

ranked higher than the group $\{p_{23}, p_{25}, p_{89}, p_{47}, p_{12}, p_{37}, p_{19}\}$, while $\{p_{79}, p_{29}\}$ comes last. This comforts the conclusions derived from Figure 2. It is not surprising for the last pair, because of the $(1-p)^4$ factors appearing in equations (19) and (20) only.

**Figure 3.** Ranks of various links when the availabilities are uniformly distributed in [0.7,0.9] (size of the sample: 50 000).

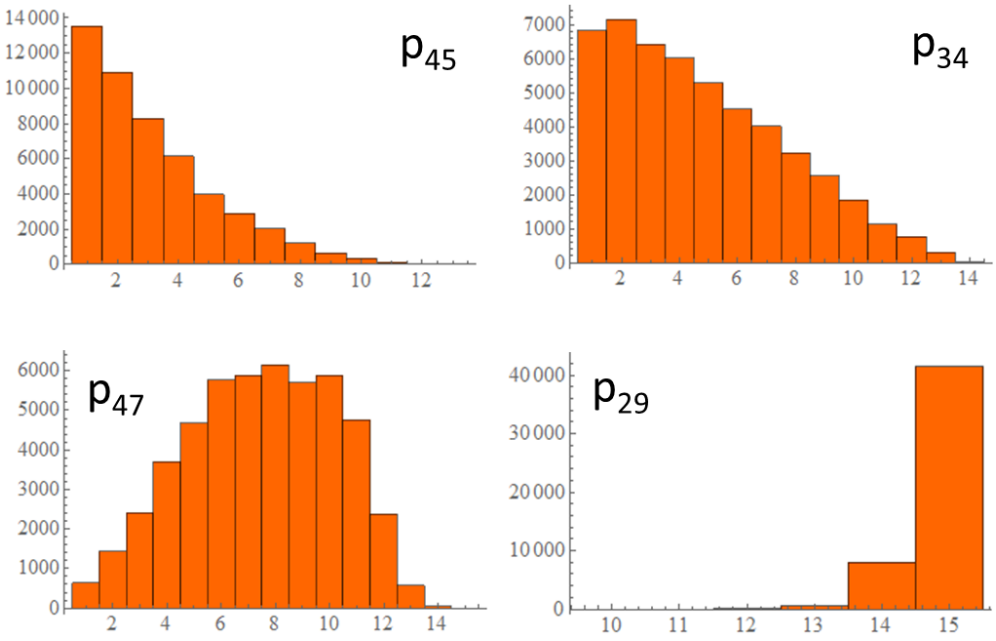


## 4 Performance improvement by edge adjunction

Improving the availability of elements is not the only way to increase the performance of a network. Adding a link may be quite beneficial since it increases the variety of possible connections for each pair of nodes. Starting from the network represented in Figure 1, the all-terminal availability $\mathrm{Rel_A}(+p_{ij})$ has been obtained when a new edge $p_{ij}$ (among the 21 remaining ones) is added to the graph. A few expressions are listed below, ranked in decreasing order for $p = 0.8$.

$$\mathrm{Rel_A}(+p_{46}) = 3707p^8 - 22933p^9 + 63083p^{10} - 100524p^{11} + 101302p^{12} - 66009p^{13} + 27127p^{14} - 6422p^{15} + 670p^{16} \quad (21)$$

$$\mathrm{Rel_A}(+p_{48}) = 3674p^8 - 22677p^9 + 62214p^{10} - 98838p^{11} + 99257p^{12} - 64421p^{13} + 26356p^{14} - 6208p^{15} + 644p^{16} \quad (22)$$

...

$$\mathrm{Rel_A}(+p_{69}) = 3222p^8 - 19612p^9 + 53123p^{10} - 83431p^{11} + 82938p^{12} - 53359p^{13} + 21670p^{14} - 5074p^{15} + 524p^{16} \quad (23)$$

$$\mathrm{Rel_A}(+p_{27}) = 3161p^8 - 19296p^9 + 52472p^{10} - 82804p^{11} + 82766p^{12} - 53566p^{13} + 21890p^{14} - 5158p^{15} + 536p^{16} \quad (24)$$

Numerically, this leads to $\mathrm{Rel}_A(+p_{46}) = 0.95608334$ and $\mathrm{Rel}_A(+p_{27}) = 0.94384526$ for $p = 0.8$; the relative improvement of the first solution is more than 3.3 times that of the second one. This can be interpreted very simply: it is more profitable to link two three-connected nodes instead of already four-connected nodes. The best and worst solutions of adding one link are represented in Figure 4. One should keep in mind, though, that the previous remarks at the end of Section 3 still apply. Considering identical elements does not necessarily give the full picture of what is actually the best solution for a performance increase of the network.

**Figure 4.** The added links providing the largest (green) and smallest (magenta) improvement for the all-terminal reliability of the network .

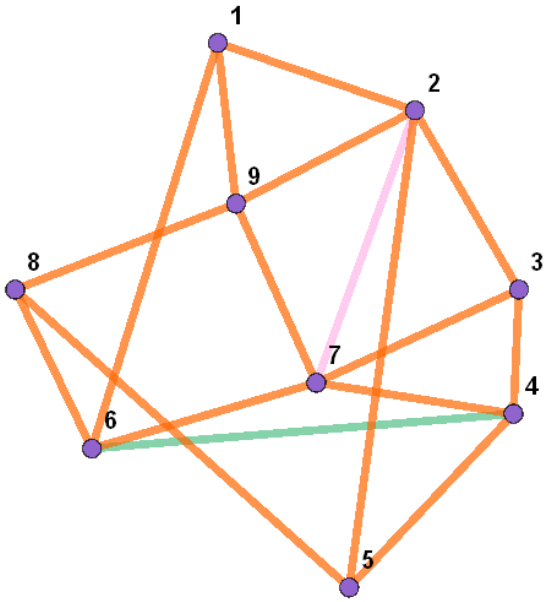


## 5 Relative influence of edges and nodes on the total unavailability

We have seen in the preceding section that the ranking of nodes, or that of edges of the network is the same for all the performance indices. The main reason for this is that we assumed identical elements. For this reason, it could be worthwhile to assess the relative importance of edges and nodes, and investigate, as performed by Eid [8], if such a behaviour varies with time. In this section, we shall first consider the asymptotic values derived in Section 2, before turning to time-dependent availabilities $p(t)$ and $\rho(t)$. In a first step, we shall consider the simple case of exponential failure and repair time distributions. We shall then proceed by using gamma failure time distributions, characterized by a shape factor $\alpha$ for which it is possible to compute the exact availability while keeping the same asymptotic value [9-10]. The criterion studied in this Section is the ratio of the unavailability of the nodes (respectively, edges) to the total unavailability, as previously investigated by Eid [8].

## 5.1 Steady-state regime

One might solely consider the asymptotic availabilities to decide which type of components, edge or nodes, is the prevailing source of unavailability. In that case, equations (9) to (11) lead to

$$\frac{U(\text{nodes})_\infty}{U(\text{system})_\infty} \approx 0.80202184 \tag{25}$$

$$\frac{U(\text{edges})_\infty}{U(\text{system})_\infty} \approx 0.24724759 \tag{26}$$

Note that the contribution of nodes is more than three times that of edges, and maintenance should be mostly devoted to nodes. The sum of the ratios is larger than unity, since $U(\text{system}) = U(\text{nodes}) + (1 - U(\text{nodes}))\, U(\text{edges})$.

## 5.2 Exponential distributions

Let us recall that for general failure and repair rate $\lambda$ and $\mu$ of exponential distributions (which both correspond to the special case $\alpha = 1$), the time-dependent availability $A(t)$ is simply given by

$$A(t) = \frac{\mu}{\lambda+\mu} + \frac{\lambda}{\lambda+\mu}\, e^{-(\lambda+\mu)\, t} \tag{25}$$

Using the values of Table 1, one recovers equations (4) and (5). The variation with time of the total unavailability is represented in Figure 5. One can observe that the asymptotic limit is reached rather quickly, from below.

The contributions of nodes and edges to the total unavailability are displayed in Figure 6 as a function of time. The conclusion that can be drawn is that nodes contribute mostly to the total unavailability, as in Section 5.1.

**Figure 5.** Variation with time of the total unavailability for exponential distributions ($\alpha = 1$).

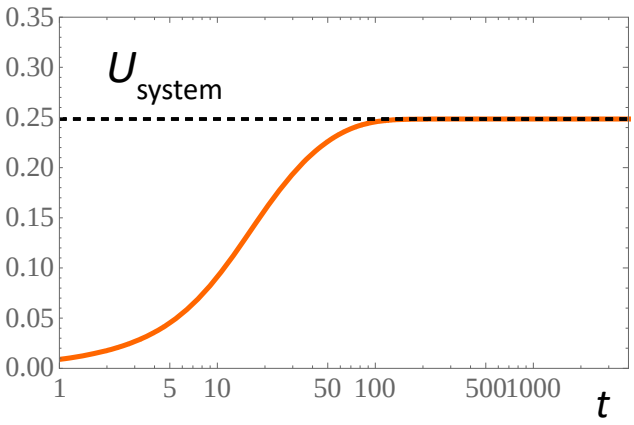

**Figure 6.** Variation with time of the contributions of nodes (blue) and links (magenta) to the total unavailability for exponentials ($\alpha = 1$). The steady-state values are represented by dashed lines.

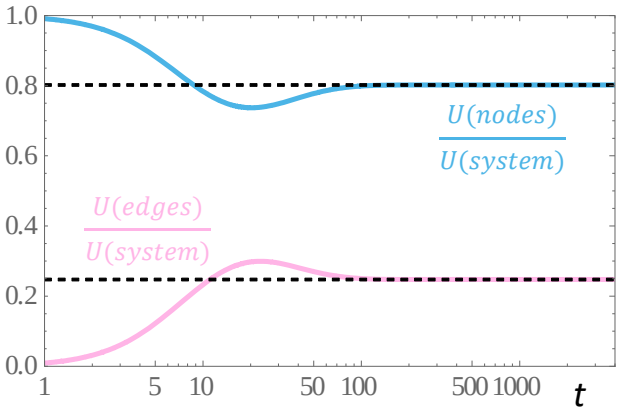


## 5.3 Gamma failure distributions with $\alpha = 2$

Let us now consider failure distributions of both edges and nodes obeying a gamma distribution with $\boldsymbol{\alpha = 2}$ so that the steady-state value stays the same as in the precedent subsection. The time-dependent availabilities are given by

$$p(t) = \frac{4}{5} + \frac{1}{5}\, e^{-t/10} \left[\cos\left(\frac{t}{20}\right) + 2\ \sin\left(\frac{t}{20}\right)\right] \tag{7}$$

$$\rho(t) = \frac{40}{41} + \frac{1}{820}\, e^{-11\,t/500} \left[20\ \cosh\left(\frac{\sqrt{5}\,t}{125}\right) + 11\,\sqrt{5}\ \sinh\left(\frac{\sqrt{5}\,t}{125}\right)\right] \tag{8}$$

The variation with time of the total unavailability is displayed in Figure 7, and the contributions of nodes and edges in Figure 8. The asymptotic limit is reached after a much longer time with respect to the case of pure exponential distributions, even if the limit is still reached from below. More importantly, the roles of nodes and edges are transiently swapped as regards their contributions to the total unavailability.

**Figure 7.** Variation with time of the total unavailability (violet) for $\alpha = 2$ for links and nodes. The result for the exponential case (orange) is kept for comparison.

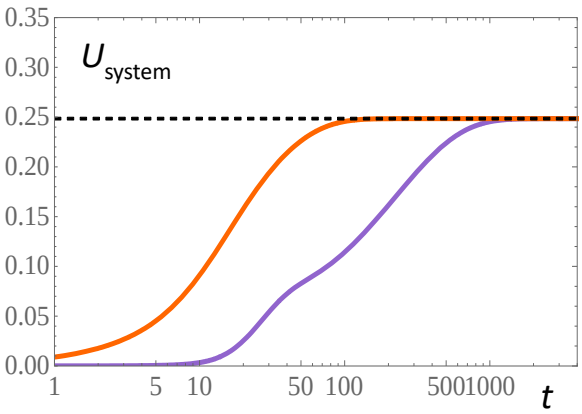

**Figure 8.** Variation with time of the contributions of nodes (blue) and links (magenta) to the total unavailability for $\alpha = 2$ .

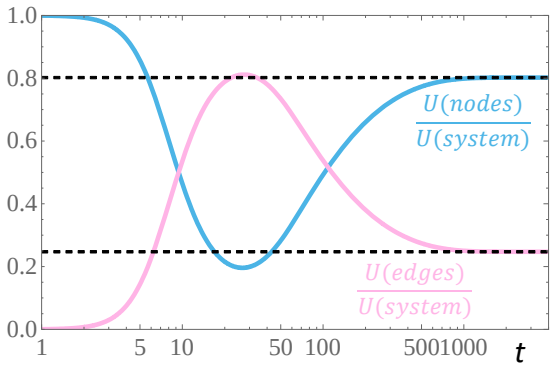


## 5.4 Gamma failure distributions with larger values of $\alpha$

We now assume that $\alpha = 10$ for nodes and $\alpha = 20$ for edges. The variations of the total unavailability and the respective contributions of edges and nodes are plotted in Figures 9 and 10, respectively. Obviously, the transient total unavailability does not exhibit a smooth increase toward its asymptotic value; it may even exceed it. The level performance of the system is far from constant, contrary to what is generally admitted in resilience studies. One might consider changing an equipment, not necessarily for its steady-state availability, but its smoother transient availability.

Likewise, the behaviours displayed in Figure 10 are also markedly different from the previous cases. These results should make one cautious about relying only on the steady-state availabilities of various components, when defining maintenance policies or resilience procedures. Transient effects are not always negligible. One should keep in mind that for larger systems, a greater error in the assessment of the global availability might be committed, unless the deviation from the exponential assumption results is somehow smeared out because of different time scales pertaining to subsystems or components.

**Figure 9.** Variation with time of the total unavailability for $\alpha = 10$ (nodes) and for $\alpha = 20$ (edges) (violet). The result for the exponential case (orange) is displayed for comparison.

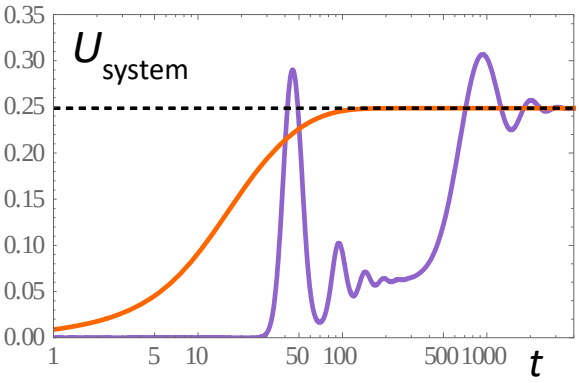

**Figure 10.** Variation with time of the contributions of nodes (blue) and links (magenta) to the total unavailability for $\alpha = 10$ (nodes) and for $\alpha = 20$ (edges).

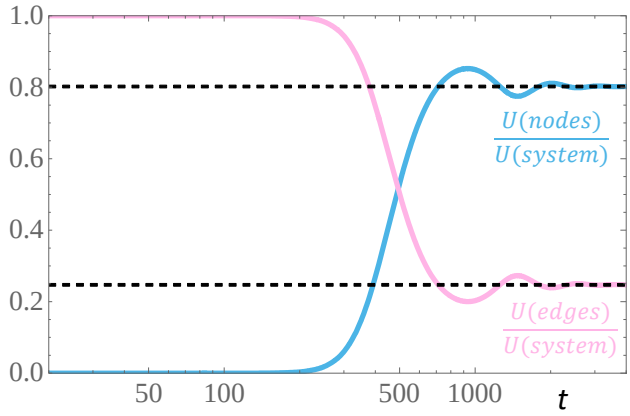


# 6 Conclusion

In this work, we have considered a meshed network first proposed by Eid [8], for which the performance index is the all-terminal reliability. We have computed exactly this availability and been able to derive analytical expressions for several performance indices such as Birnbaum, Fussell-Vesely, etc. Using various non-exponential failure and repair time distributions, we have shown that the relative contributions of nodes and links to the total unavailability may vary markedly with time, to such an extent that wrong assumptions about the weak links of the system can be made by considering the steady-state regime or the case of exponential distributions for failure and repair times.

## Acknowledgements

It is a great pleasure to thank Dr. M. Eid for useful discussions.

## References

1. Mauro M.D., Galatro G., Longo M., Postiglione F., and Tambasco M. (2018) Availability modeling of a virtualized IP multimedia subsystem using non-Markovian stochastic reward nets. In: Haugen S. et al. (eds.) *Safety and Reliability — Safe Societies in a Changing World, Proceedings of ESREL 2018, June 17–21, 2018, Trondheim, Norway*. Taylor & Francis Group; 2018, paper 305. https://doi.org/10.1201/9781351174664
2. Mauro M.D., Galatro G., Longo M., Postiglione F., and Tambasco M. (2017) Availability evaluation of a virtualized IP multimedia subsystem for 5G network architectures. In: Čepin M. et al. (eds.) *Safety and Reliability — Theory and Applications, Proceedings of ESREL 2017, June 18–22, 2017, Portorož, Slovenia*. CRC Press/Balkema — Taylor & Francis Group; 2017. p. 2203-10.
3. Distefano S., Longo F., and Scarpa M. (2010) Availability Assessment of HA Standby Redundant Clusters. In: *29th IEEE Symposium on Reliable Distributed Systems*. The Institute of Electrical and Electronics Engineers, Inc., pp. 265-74.

4. Carnevali L., Flammini F., Paolieri M., and Vicario E. (2015) Non-Markovian Performability Evaluation of ERTMS/ETCS Level 3. In: Beltrán M. et al. (eds.) *Computer Performance Engineering*. Springer International Publishing, pp. 47-62.
5. Chengqian Li, Qi Fang, Lieyun Ding, Yong K. Cho, and Ke Chen (2020) Time-dependent resilience analysis of a road network in an extreme environment. *Transportation Research Part D: Transport and Environment*, vol. 85, article 102395. https://doi.org/10.1016/j.trd.2020.102395.
6. Ouyang M. and Dueñas-Osorio, L. (2012) Time-dependent resilience assessment and improvement of urban infrastructure systems. *Chaos,* vol. 22, paper 033122 https://doi.org/10.1063/1.4737204.
7. Szu-Yun Lin and Sherif El-Tawil (2020) Time-Dependent Resilience Assessment of Seismic Damage and Restoration of Interdependent Lifeline Systems. *J. Infrastruct. Syst.*, vol. 26 (1), article 04019040. https://doi.org/10.1061/(ASCE)IS.1943-555X.0000522.
8. Zhiguo Zeng, Shijia Du, and Yi Ding (2021) Resilience analysis of multi-state systems with time-dependent behaviors. *Applied Mathematical Modelling*, vol. 90, pp. 889-911. https://doi.org/10.1016/j.apm.2020.08.066.
9. Eid, M. (2021) Network connectivity dynamic modelling. In: Kołowrocki, K. et al. (eds.) *Safety and Reliability of Systems and Processes, Summer Safety and Reliability Seminar 2021*. Gdynia Maritime University, 2021. https://doi.org/10.26408/srsp-2021.
10. Tanguy C., Buret M., and Brinzei N. (2019) Is it safe to use MTTF/(MTTF + MTTR) for the availability? In: Beer M. et al. (eds.), *Safety and Reliability — Theory and Applications, Proceedings of the 29th European Safety and Reliability Conference*. Research Publishing, Singapore, pp. 925-929. https://doi.org/10.3850/978-981-11-2724-3_0250-cd.
11. Tanguy C. (2020) When considering the asymptotic availability is not a safe bet. In: Baraldi P. et al. (eds.) *Proceedings of the 30th European Safety and Reliability Conference and the 15th Probabilistic Safety Assessment and Management Conference*. Research Publishing, Singapore, pp. 3091-3098. https://doi.org/10.3850/978-981-14-8593-0.
12. Albert M. and Dorra M. (2018) Industry 4.0 and complexity: Markov and Petri net based calculation of PFH for designated architectures and beyond. In: Haugen S. et al. (eds.) *Safety and Reliability | Safe Societies in a Changing World, Proceedings of ESREL 2018, June 17-21, 2018, Trondheim, Norway*. Taylor & Francis Group, paper 303.
13. Beichelt, F. and Tittmann, P. (2012) *Reliability and Maintenance: Networks and Systems*. CRC Press, Taylor & Francis Group.
14. Rausand, M. and Høyland, A. (2004) *System Reliability Theory, Models, Statistical Methods and Applications (2nd ed.)*. Wiley.

# Resilience and Capacity in Networks- a comparative investigation of rail transport networks and electric power grids

Pierre Dersin,Ph.D., Eumetry sas and Luleå University of Technology , pierre.dersin@ltu.se

## Abstract

*Rail transport networks ( particularly urban ones) ) and electric power grids share some important characteristics. First, they both have an intrinsic network structure , although nodes and edges have very different physical meanings in both cases. Second, their function is to deliver a service, i.e. to serve a demand which can be subject to sudden fluctuations; third, they can undergo sometimes substantial disruptions. Resilience should therefore be a core characteristic of those systems, but at the same time an essential attribute is capacity, i.e. roughly, the amount of demand they are able to serve; and the two properties are in fact antagonistic.*

*In view of the above considerations, it seems that the study of those two types of networks could benefit from methodological cross-fertilization. Work in progress in that direction, specifically the use of graph theory, is reported here , and further directions are outlined.*

## 1 Introduction

Resilience is a property that characterizes a system's ability to absorb external disruptions and to recover from those disruptions [1].

On the other hand, many complex systems, such as electric power grids or urban rail transport networks, are characterized by metrics, or key performance indicators(KPI), which measure their ability to meet the demand. Such metrics can generally be described by a capacity .For instance, the capacity of an urban rail transport network can be measured by the throughput, or number of passengers per hour per direction, which can flow through the system. The capacity of an electric power network can be characterized by the total active electric load, in MW, or by the set of distributed loads ( at various locations) that can be served by the network in steady state. Although this is not always emphasized, there is a trade-off between capacity and resilience, which is easily understood through the notion of margin. For instance, in an urban rail transport network [2], the headway, or time interval between two successive trains, determines the capacity, i.e. the average number of trains that can flow through the network per unit of time. If the headway is increased, the capacity is reduced, but the system is made more resilient since disruptions can be absorbed by the so-called time margins, i.e. a local delay is less likely to be propagated throughout the network. On the other hand, if the trains run in a tight mode, i.e. close to the minimum theoretical headway, the slightest local perturbation will propagate; therefore, in actuality, the theoretical maximal capacity is difficult to achieve if at the same time a punctuality or regularity clause [3] is imposed; in other words, the system is not very resilient. Likewise, for electric power grids, there is a notion of security margin which measures the gap between the total load ( or electrical power demand) which can be theoretically met with given generation and transmission capacities and the real load that can be handled in view of inevitable fluctuations in demand, voltage surges, etc., as well as equipment failures. Consequently, the closer the actual load is to total theoretical capacity, the less resilient the system.

To complete this brief overview, it it is worth mentioning that both urban rail transport networks and electric power grids are actually systems of systems , i.e.

they are made up of heterogeneous systems which are technically and operationally independent but have to coordinate somehow to meet the demand (let one think for instance of the communication networks which are essential to the operation of large power grids).

# 2 Characterizing Demand and Supply

We turn to a brief characterization of demand and supply in the two categories of networks.

## 2.1 Urban Transport Networks.

Demand in urban transport networks can undergo important and sometimes sudden fluctuations, due to a number of reasons : typical causes are timings of events or other large gatherings that cause sudden surges in passenger flows, or disruption in feeder lines, such as bus traffic feeding into rail lines, or antenna lines feeding into a central line.

It is therefore desirable to be able to update passenger demand in real time ; today's machine learning methods can be used to that end [4], for instance by utilizing data on vehicle weight, ticketing data or smartphone data.

Supply can be impacted by technical failures but also by passenger use (the typical example being passengers blocking access doors), by weather ( flooding, poor adhesion conditions) or by external systems ( such as power supply or telecommunications).

Supply is adapted to demand through traffic management ( "regulation") , which essentially consists of acting on station dwell times or speed between stations, and sometimes rerouting traffic.

In conclusion, resilience must be studied in the joint context of supply and demand.

Failing to meet demand is expressed in "lost passenger-kilometers" or in" ratio of cancelled trips to planned trips" or in other measures such as ratio of cumulated delays over theoretical travel time; and of course, time needed to recover normal operation ( e.g. nominal headway) after a perturbation is a key resilience indicator.

## 2.2 Electric Power Grids

Demand in electric power grids is characterised by peak and off-peak cycles which are well predictable but sudden fluctuations may occur , in particular due to intermittent loads. Also , power imports from neighbouring grids through tie lines can be substantial.

Power supply is impacted, not only by technical failures, but also by intermittent sources subject to uncertainty such as hydro-power or solar energy.

With the advent of the Internet of Things, the monitoring of electrical load in real time has become easier, and machine learning techniques make demand prediction easier and more precise.

Real-time adaptation of supply to demand is needed since electric power can in general not be stored: supply must match demand at all times. Imperfect balance between demand and supply results in frequency fluctuations, which are only transient when control is exercised adequately but may otherwise have adverse effects.

When the mismatch is too important, load shedding is needed; extensive power outages may occur, some of which have been abundantly featured in the news and documented in the literature |6].

Performance measures include Loss-of-load probability (LOLP) and expected unserved energy (EUE), for instance; and of course, a key resilience indicator is the time needed to recover normal operations after a disruption.

# 3 Modelling Flows in Networks

Every model entails simplifications. An electric power network is an extremely complex structure ([5], (7]) but, at the cost of sometimes excessive simplification, it can be conveniently represented by a graph: the nodes ( or vertices) represent the busses ( where electric power is injected, at generation plants, or consumed by the loads); and the transmission lines and transformers are represented by edges.

A useful simplification of the full AC ( alternating current) power flow model is the DC (direct current) model. In that model, the constraints on the power flows are summarized by the Kirchhoff laws [7]: the sum of incoming and outgoing flows at a node is zero; and a weighted sum of active power flows along a mesh is zero.

Sometimes, an even coarser model is used: the so-called 'transportation flow' model, which expresses the constraint that the total load should not exceed the sum of the generating capacities and the transmission line and transformer capacities ; or, in graph terms, the sum of the node demands should not exceed the sum of the node generations and of the edge capacities.

In rail transportation networks, the physical constraints are flow conservation at nodes and, and dynamic edge constraints ( on speed, acceleration) linked to safety and geometry; as well as operational constraints on theoretical time schedules or headways and the time spent in stations (dwell time). An accurate simplified representation can also match the graph formalism.

Now, flows in networks have been studied since the middle of last century, notably in the context of commodity shipments .

For instance, the well-known Ford-Fulkerson theorem [8] states that the maximal flow through a network is equal to the minimal cut, i.e. the minimal sum, over all cuts, of capacities of all the edges in the cut. This theorem is convenient in order to characterize how close a given demand is to the maximum 'service capacity' of the network, and therefore how much margin exists and how close the system is to congestion.

In the electric power grid context, with the DC load flow model, the Ford-Fulkerson theorem was generalized [10] by means of mathematical duality and graph duality :Kirchhoff mesh constraints correspond to node flow constraints on the dual graph. The 'feasibility set', i.e. the set of bus load combinations ( 'vectors') that can be served in steady state, given generation and transmission capacities, is described by a set of linear inequalities on the loads, i.e. by a convex polyhedron in the space of ' load vectors' . Those inequalities include those which correspond to the simplified 'transportation model '( the Gale inequalities [9]).

Two related useful features of that model are :

1) Its potential usefulness as a tool for measuring resilience, i.e. through the distance of a given ' load vector" to the boundary of the set;
2) Sensitivity analysis, i.e. studying the impact of a change in generation or transmlssion capacity on load feasibility. For instance, the "transportation flow" problem is formulated as a linear programming problem and the optimal dual variables are equal to 0 or 1 depending whether constraints are active or not. When making the presence of edges probabilistic , the expectation of those dual variables ( between 0 and 1) provide a sensitivity measure of the LOLP with respect to the corresponding edge capacities. it is interesting that, in the more realistic ' DC load flow' model, an increase in some transmission capacities may have a detrimental effect on resilience, i.e. it may reduce the margin; or sometimes , when a local load increases, it may be easier to serve it .This is an example of counterintuitive nonlinear effect.

In the rail transport context, the equivalent of Kirchhoff laws does not exist ( except for the first one: flow conservation). But additional rights-of-way or additional node capacity, defined as parking spaces ( sidings) for trains also impacts performance measures, all other things being equal, by increasing the margins, and therefore improving resilience.

To our knowledge, the assessment of the corresponding impact is mostly performed through simulations ( Monte Carlo simulation of disruptions and modelling of dynamic traffic management following each disruption).

It is felt however that room exists for more use of graph theory to assess such questions in the aggregate and derive some qualitative and quantitative insights. For instance, a link was established [11] between the topological characteristics of the graph ( its connectedness) and the ability to eliminate the effect of a disruption further down the line; in control-theoretic terms, this is a controllability property.

# 4 Connectivity, Capacity and Resilience

It has been argued [12] that , in general, the impact of connectivity on resilience is illustrated by an " inverted U" curve: no connectivity makes for poor resilience, while too much connectivity destroys resilience, and therefore there is an intermediate, optimal degree of connectivity.

We find this line of thinking interesting, and propose to use some of the tools described in order to test it; but resilience alone is not sufficient: capacity must be brought into the picture as well.

For instance, in the electric power grid case, it seems clear that a set of unconnected island networks is not very resilient, since a disruption in one of the islands cannot be compensated by energy importation from the other islands. And, at the other extreme, the more meshed the network is, the more opportunities for cascading failures.

The study referred to in Section 3 confirms indeed that in some instances ( not systematically), additional connections may impair resilience, i.e. reduce margins.

In the rail transport example similar situations occur: having several connected components ( essentially several non-communicating networks) will not favor resilience; on the other hand, it is not clear that a very connected network will necessarily favor cascading delays: all depends on the precise topology and operating program. An important factor is also communication, including information to the users ( the passengers or the electric power grid customers) as it facilitates demand adaptation to supply and thus can speed up recovery. Therefore the concept of connectivity should subsume user communication.

# 5 Conclusions and Further Research

It seems to us that the study of resilience in networks stands to benefit more from the very rich body of graph theory, at least in the cases of electric power grids and rail transport networks. Some hints of how that could be accomplished have been given.

Cross-fertilization between those two areas could arise as a result.

In addition, recent advances in machine learning, and particularly graph neural networks, will most likely enable the application of the full strength of that discipline to realistic complex models while taking full advantage of the graph structure [5].

## Acknowledgements

The author is grateful to colleagues from Luleå University of Technology, former colleagues from Alstom, and scientific partners from Hydroquébec, for useful discussions.

## References

1. Cassottana,B.,Shen, L. and Tang, L.C.,'Modeling the Recovery Process: a key Dimension of Resilience" *Reliability & System Safety' Engineering & Design*, vol. 190, 2019 ( Elsevier).
2. Dersin, P., Péronne, A., 'Building Resiience into Urban Transport Systems', ASPECT 2019 Conference, Institute of Railway Signal Engineers, Delft, October 2019
3. UITP Core Brief - Metro service performance indicators, UITP, April 2011
4. Moskowicz, D., Gutierres, B., Kleine, M.",Mastria: Mobilitätsorchestrierung im digitalen Zeitalter", SIGNAL+DRAHT 7+8/202
5. Donon.B., Deep statistical solvers & power systems applications. Artificial Intelligence [cs.AI]. Université Paris-Saclay, 2022. English. NNT : 2022UPASG016
6. Komljenovic, D. (2021). Engineering Asset Management at Times of Major, Large-Scale Instabilities and Disruptions. In: Crespo Márquez, A., Komljenovic, D., Amadi-Echendu, J. (eds) 14th WCEAM Proceedings. WCEAM 2019. Lecture Notes in Mechanical Engineering. Springer, Cham. https://doi.org/10.1007/978-3-030-64228-0_22
7. Elgerd, O.J., Electric Energy Systems Theory: an Introduction, McGraw Hill, 1971
8. Ford, L.K., and Fulkerson, D.K, Flows in Networks, Princeton University Press, Princeton, NJ, 1962.
9. Gale,D., The Theory of linear economic Models, Mc Graw-Hill, NY, 1960.
10. Dersin, P., and Levis, A.H., , 'Feasibility Sets for Steady-State Loads in Electric Power Networks", IEEE Transactions on Power Apparatus and Systems, Vol. PAS-101, No. 1 January 1982
11. Gerswhin, S.B., Dersin, P., and Athans, M.," Perturbation Strategies for optimal Traffic Reassignment" " IEEE Transactions on Automatic Control, Volume AC-2, Issue 6, 1977, p. 985-987
12. Homer-Dixon, T. Complexity Science. Oxford Leadership Journal, Jan.2011, Vol.2, Issue 1.

AC Alternating Current

DC Direct Current

| | |
|---|---|
| LOLP | Loss-of-Load Probability |
| EUE | Expected Unserved Energy |
| KPI | Key Performance Indicator |

# Interdependencies of infrastructures in Smart Cities and advanced topological approach for the resiliency of coupled systems - example of Power and ICT systems

Raphael Caire, Univ. Grenoble Alpes, CNRS, Grenoble INP[1], G2Elab, 38000 Grenoble, France, raphael.caire@grenoble-inp.fr

## Abstract

*The paper is about the interdependencies between various infrastructures existing in a Smart Cities. Indeed, many important systems are on line and interacting to serve our modern societies. Increasing interdependencies between those infrastructures are leading to larger complexity for a risk analysis task. The paper is at first presenting example of interdependencies of infrastructures in Smart Cities. It then presents advanced topological approaches to increase the resiliency of coupled systems. It then finished with an example of Power and ICT systems interacting together in a Smart Grid. In that infrastructure, it is obvious that a decrease of service in the ICT infrastructure will lead to a potential decrease of service from electrical grid and vice-versa.*

## 1 Introduction

Critical infrastructures as defined by EU [1] or USA [2] are vital in a sense that if harmed or attacked, it leads to a large (economical but not only) loss for the entire society. Unfortunately, many of those infrastructures are interdependent.

The interdependency can be related to one of the three following axes. At first, the interdependency can lead to cascading failures. It is the case of the 2003 blackout in the United State and in Canada. It was one of the most catastrophic as it impacted more than 50 million of customers and was evaluated to UD$ 7 to 10 Billion [3]. It has been caused by several line faults but the major problem was the alarm system (state estimator processing the sensor data) bug. Because of it, the operator was blind and unable to react to the following failures. This was one of the first and major cascading failure between critical infrastructure (ICT and Power Systems). At second, the interdependency can lead to a common mode failure, e.g. whenever some key components are hit together such as for a fire in a station, usually hosting control, communication and power system equipment's. At third, the interdependency can lead to an increasing failure. It is the case of the 2003 blackout [4] in Italy where the initial Power System blackout led was worsen because of the inability to remotely access to some of the remote disconnectors. Some of the reconnection were not possible and the operator had to rely on field crew to do classical remote connections.

In the Power System world, and especially in the Smart Grid area, the interdependencies are increasing and more and more important thanks to the large amount of automation functions. The current trend of research and development in most of the utilities leads to a larger coordination of local energy resources with grid components. This operational evolution (more control) is related to the structural evolution of the grid itself [5].

In order to secure critical infrastructures, some advanced methodologies must be setup to analyse the coupled infrastructure components. Finding the ability to isolate critical components in between the architecture is of major importance. Presented methods are included in the thesis of José-Libardo Sanchez-Torres [6]

(1) * Institute of Engineering Univ. Grenoble Alpes

# 2 Summary of the technical content to be presented

A comparison between advanced graph theory methods (betweenness centrality from complex network theory) and spectral analysis will be presented in order to compare proficiency of both methods. This comparison will be applied on a specific test case of a real reduced case distribution network hosted in PREDIS center (Grenoble INP platform).

## 2.1 Test case

The test system is a modification of the typical French Distribution Network presented in [7]. The network has 14 power-bus, 17 lines, 7 distributed generation, 9 loads, and 3 transformers HTB/HTA (63/20 kV), as shown in Fig. 1. The communications network involves several routers connected by Optic Fiber, 1 WiMax BS several multiplexers, and ICT links including ADSL, PSTN/ISDN, Optic Fiber, and Ethernet technologies. On the left-hand side, the black lines represent normally closed lines. The red dotted lines represent normally open lines. The blue lines are communication links.

**Figure 1.** Single line diagram of the electrical power system test case and ICT connections.

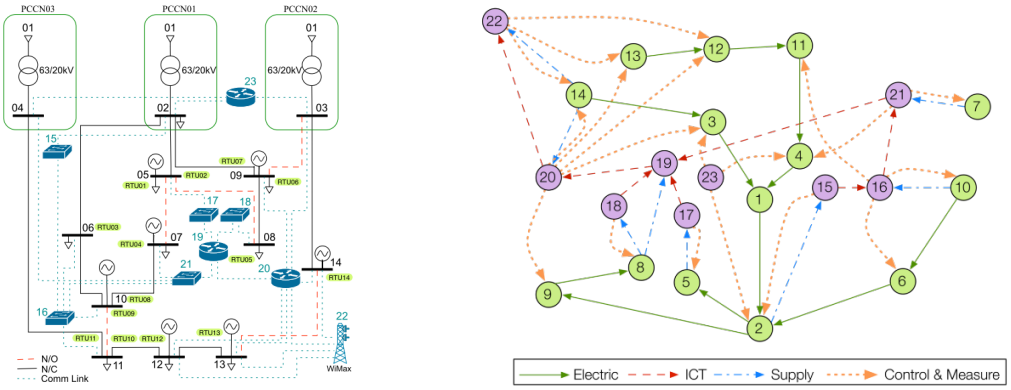


## 2.2 Results

### 2.2.1 Results on the side of Betweenness Centrality

**Figure 2.** Single line diagram of the electrical power system test case and ICT connections.

| Node | $b_e$ | $b_c$ | $b_{global}$ |
|---|---|---|---|
| 1 | 48 | 0 | 48 |
| 2 | 63 | 0 | 63 |
| 3 | 9 | 0 | 9 |
| 4 | 27 | 0 | 27 |
| 5 | 10 | 0 | 10 |
| 6 | 8 | 0 | 8 |
| 7 | 0 | 0 | 0 |
| 8 | 22 | 0 | 22 |
| 9 | 30 | 0 | 30 |
| 10 | 0 | 0 | 0 |
| 11 | 20 | 0 | 20 |
| 12 | 11 | 0 | 11 |
| 13 | 0 | 0 | 0 |
| 14 | 0 | 0 | 0 |
| 15 | 0 | 0 | 0 |
| 16 | 0 | 14 | 14 |
| 17 | 0 | 0 | 0 |
| 18 | 0 | 0 | 0 |
| 19 | 0 | 35 | 35 |
| 20 | 0 | 36 | 36 |
| 21 | 0 | 20 | 20 |
| 22 | 0 | 0 | 0 |
| 23 | 0 | 0 | 0 |

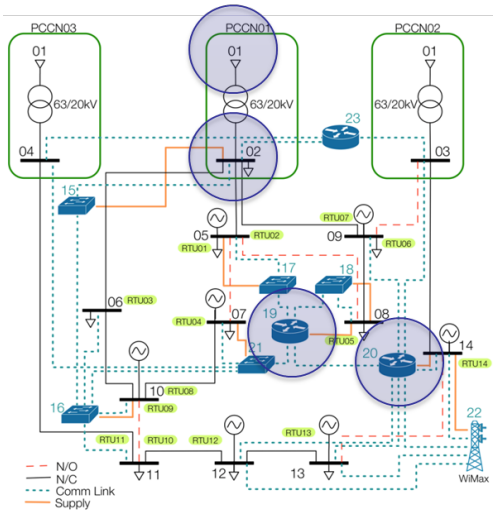


The figure 2 represents the results with the evaluation of betweenness centrality

### 2.2.2 Results on the side of Spectral Analysis

**Figure 3.** Results with spectral analysis combined with Hermitian matrix.

Electric Layer

| Node | \|x\| | Φ |
|---|---|---|
| 2 | 0.60 | 0.00 |
| 1 | 0.39 | 2.36 |
| 9 | 0.31 | -2.36 |
| 6 | 0.29 | 2.36 |
| 5 | 0.28 | -2.36 |

Comm. Layer

| Node | \|x\| | Φ |
|---|---|---|
| 20 | 0.56 | 0.00 |
| 22 | 0.43 | 0.00 |
| 12 | 0.32 | 0.00 |
| 13 | 0.32 | 0.00 |
| 19 | 0.31 | 0.00 |

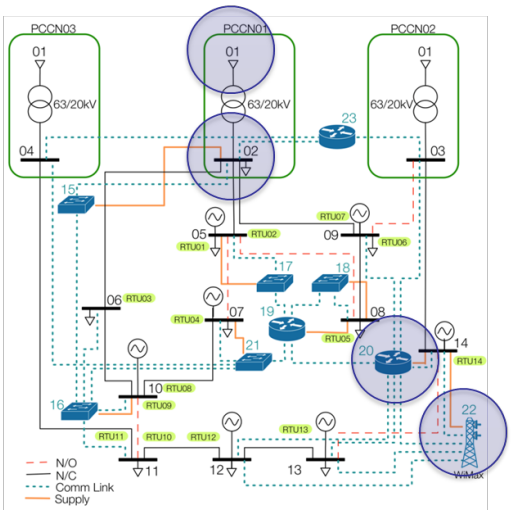


The figure 3 represents the results with the spectral analysis.

## 3 Conclusions

Both methods, relying on different topological approaches, are able to assess the most important components while doing risk analysis study. Classically, Electrical and ICT experts are able to find critical ones on the diagonal of the Fig 4. Adding such representation (representing the links with the energy service and the communication service) allows to track classical components at the far end of graphs and thus with classical lower importance.

**Figure 4.** Betweenness Centrality and the cross infrastructure key components.

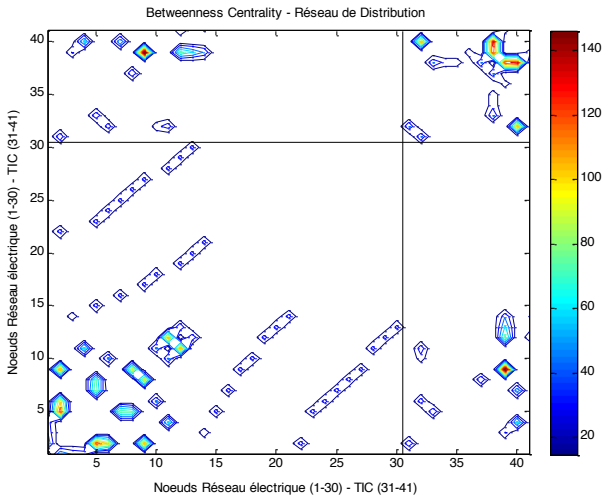


## Acknowledgements

The author wishes to thank the ESReDA organising committee for the invitation. This work is from the PhD thesis of [6] José Libardo Sanchez Torres and had been translated to a lecture for the students of the University Grenoble Alpes belonging to advanced modelling in Electrical Engineering.

## References


1. CISA – Cybersecurity & Infrastructure Security Agency which leads the national effort to understand, manage, and reduce risk to USA cyber and physical infrastructure - https://www.cisa.gov/critical-infrastructure-sectors
2. European Programme for Critical Infrastructure Protection (EPCIP) Directive 2008/114 and new version available https://ec.europa.eu/home-affairs/system/files/2020-12/15122020_proposal_directive_resilience_critical_entities_com-2020-829_en.pdf
3. Electricity Consumers Resource Council (ELCON) "The Economic Impacts of the August 2003 Blackout" February 9, 2004, available https://elcon.org/wp-content/uploads/Economic20Impacts20of20August20200320Blackout1.pdf
4. UCTE "FINAL REPORT of the Investigation Committee on the 28 September 2003 Blackout in Italy", April 2004, available https://eepublicdownloads.entsoe.eu/clean-documents/pre2015/publications/ce/otherreports/20040427_UCTE_IC_Final_report.pdf
5. Nouredine Hadjsaïd, Jean-Claude Sabonnadière « Smart Grids » Publisher ISTE Ltd and John Wiley & Sons Inc, edition January 2013, ISBN-13 9781848212619
6. José Libardo Sanchez Torres. "Vulnerability, interdependencies and risk analysis of coupled infrastructures : power distribution network and ICT". Electric power. Université de Grenoble, 2013. English. ⟨NNT : 2013GRENT104⟩. ⟨tel-01201802⟩
7. B. Stahl, L. Le Thanh, R. Caire, and R. Gustavsson, "Experimenting with Infrastructures," 5th International CRIS Conference on Critical Infrastructures, Beijing, 2010, available http://www.integral-eu.com/fileadmin/user_upload/downloads/Presentations/IEEE%20Experimenting%20with%20infrastuctures.pdf


## List of abbreviations and definitions

| | |
|---|---|
| EU | European Union |
| USA | United States of America |
| ICT | Information and Communication Technologies |

# A Study on Resilience Index for Transport Infrastructure in China

Chao Yang, Associate Professor, China Transportation Institute in Tongji, Tongji University, China, yangchaozmv@163.com

Rasa Remenyte-Prescott, Associate Professor, School of Civil Engineering, University of Nottingham, UK, R.Remenyte-Prescott@nottingham.ac.uk

Xukuan Hao, Senior Engineer, Dalian Institute of Transport Planning Investigation and Design Co. Ltd, China, haoxukuan@126.com

## Abstract

*Over the last decades and after the opening up reforms, achievements in the large-scale construction of China's transport infrastructure worldwide attention. In the "Outline for Building China's Strength in Transport", issued by the CPC Central Committee and the State Council, it is proposed to build modern and high-quality transportation networks, enhance system's flexibility, improve the ability to prevent and withstand disasters, in particular, establish a traffic prevention and a control system in case of natural disasters. This paper aims to propose a resilience index for transport infrastructure in China, which can be used to evaluate and improve the resilience of transportation.*

***Keywords:*** *Resilient transport infrastructure, transportation risks, Safety and security, resilience index.*

## 1 Aims and Objectives

This research aims to develop a resilience index for highways with an ambition to use it for evaluation of current resilience and then evaluation of any improvements in terms of resilience in China. The objectives are listed as follows:

- To investigate the concept and characteristics of highway resilience.
- To understand the current methods for building the resilience of highway infrastructure.
- To develop a resilience index and specific indicators for highway infrastructure in China.

## 2 Methodology

This research is conducted in four steps, shown in Figure 1:

- To define the concept of the highway resilience and to identify the main features of resilience.
- To find out about the state-of-the-art methods in resilience evaluation, such as work by World Bank, USA and UK.
- To realize what has been done in China already. It is worth noting that resilience is a quite new concept in China, but a number of related areas have been developed in the past, such as high planning, construction, maintenance, reconstruction, risk evaluation, safety and security.
- To propose the highway resilience index applied to China, which specifies the main structure of resilience, the specific indicators, and how to evaluate a network or an asset.

**Figure 1.** Methodology


## 3 Proposed Highway Resilience Index

Reliable transportation services are universally considered to be essential for increasing the quality of life. Resilient transportation infrastructure takes account of roads, bridges and tunnels that can withstand disturbances, such as more frequent or stronger floods and earthquakes. This research focusses on a comprehensive sustainability framework and a rating index that enables a thorough examination of resilience of different types of transportation infrastructure. The resilience index for transport infrastructure focusses on six main areas, as shown in Figure 2:

- Leadership: To have the continued ability to meet resilience goals and carry out designated functions of service;
- Network availability: To calculate the serviceability of transportation network (without and with disruptions);
- Risk exposure: To identify and evaluate risks to the network due to climate change and natural hazards;
- Project vulnerability: To analyse the vulnerability of the network and individual infrastructure;
- Safe and secure response security: To provide an emergency response when a disruption occurs;
- Service delivery: To provide travel information and provision of transport service delivery.

**Figure 2.** The proposed Highway Resilience Index

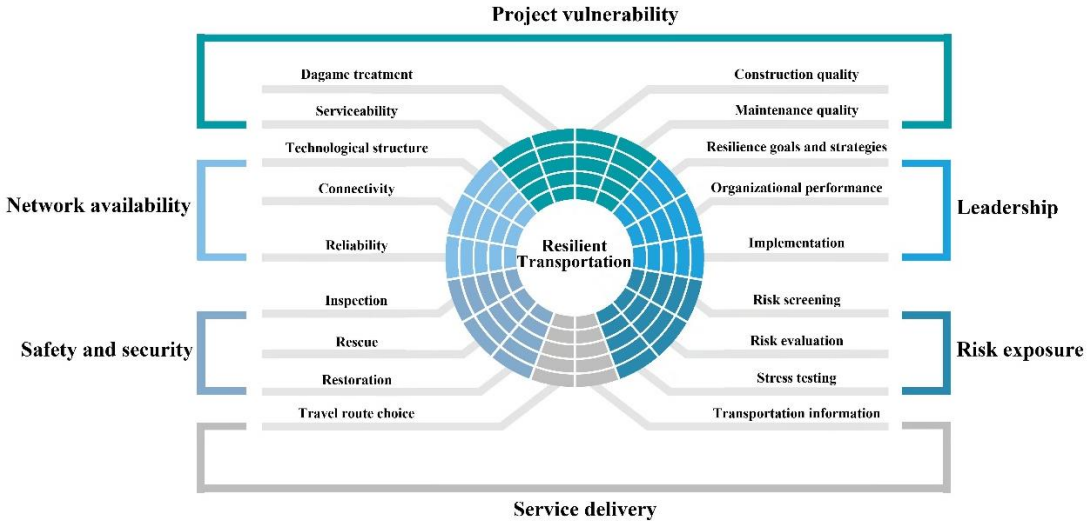


## References


1. World Bank Group (2021). Resilience Rating System : A Methodology for Building and Tracking Resilience to Climate Change. World Bank, Washington, DC. © World Bank.
2. Institute for Sustainable Infrastructure (2018), ENVISION Sustainable Infrastructure Framework, Version 3, USA.
3. Hallegatte, Stephane; Rentschler, Jun; Rozenberg, Julie. (2019). Lifelines : The Resilient Infrastructure Opportunity. Sustainable Infrastructure;. Washington, DC: World Bank.
4. World Bank Group (2019), From a rocky road to smooth sailing, Building Transport Resilience to Natural Disasters, World Bank.
5. Rozenberg, Julie; Espinet Alegre, Xavier; Avner, Paolo; Fox, Charles; Hallegatte, Stephane; Koks, Elco; Rentschler, Jun; Tariverdi, Mersedeh. (2019). From A Rocky Road to Smooth Sailing : Building Transport Resilience to Natural Disasters. Background paper for Lifelines;. World Bank, Washington, DC.
6. UN office for Disaster Risk Reduction (2020), Global Assessment Report on Disaster Risk Reduction 2020, UN.
7. Federal Highway Administration (2018), Integrating Resilience into the Transportation Planning Process, USA.
8. Weilant, Sarah, Aaron Strong, and Benjamin M. Miller (2019), Incorporating Resilience into Transportation Planning and Assessment, Santa Monica, Calif.: RAND Corporation, RR-3038-TRB.
9. Gina Filosa, Amy Plovnick, Leslie Stahl, Rawlings Miller, Don H. Pickrell (2017), Vulnerability Assessment and Adaptation Framework, Third Edition, Office of Planning, Environment, and Realty, Federal Highway Administration. USA.
10. Transportation Research Board, National Academies of Sciences, Engineering, (2018), Resilience in Transportation Planning, Engineering, Management, Policy, and Administration, USA.
11. National Institute of Building Sciences (2018), Natural Hazard Mitigation Saves: 2018 Interim Report, USA.

12. National Academies of Sciences, Engineering, and Medicine, (2019). Freight Transportation Resilience in Response to Supply Chain Disruptions. Washington, DC: The National Academies Press.
13. Department for Transport (2014), Transport Resilience Review: A review of the resilience of the transport network to extreme weather events, UK.
14. Mayor of London (2011), Managing risks and increasing resilience, The Mayor's climate change adaptation strategy, UK.
15. Kent County Council (2017), Definition of Kent's Resilient Highway Network, UK.
16. Ministry of Infrastructure and Water Management (2019), Delta Programme 2019: Continuing the work on the delta: adapting the Netherlands to climate change in time, Netherlands.
17. JF Hughes and K Healy, (2014), Measuring the resilience of transport infrastructure, NZ Transport Agency research report 546, AECOM New Zealand Ltd, New Zealand.

# Gas network modelling to support pipeline hub area risk assessment study

Vytis Kopustinskas, European Commission, Joint Research Centre (JRC), Ispra, Italy
vytis.kopustinskas@ec.europa.eu

Bogdan Vamanu, Horia Hulubei National Institute of Physics and Nuclear Engineering
bvamanu@nipne.ro

Sebastian Ganter, Jörg Finger, Ivo Häring, Fraunhofer Institute for High-Speed Dynamics
sebastian.ganter@emi.fraunhofer.de; Joerg.Finger@emi.fraunhofer.de;
ivo.haering@emi.fraunhofer.de

Ivars Zalitis, Laila Zemite, Riga Technical University, Institute of Power Engineering

ivars.zalitis@rtu.lv; laila.zemite@rtu.lv

## Abstract

The paper presents a risk assessment study of a gas transmission system pipeline hub area of 1km radius including a gas compressor station. The study was supported by the results of gas network modelling task, performed within a framework of SecureGas project under Horizon 2020 research programme. The study adopted all-hazards all-threats approach and developed a risk matrix of 59 elements. The study identified a number of findings and recommendations for further action.

## Extended abstract

The paper presents a risk assessment study of a pipeline hub and a compressor station with particular focus on gas network modelling activity. Due to sensitivity of the data used and findings obtained, we cannot disclose all the details of the study and therefore provide only limited information. The pipeline hub included an area of about 1km radius with a compressor station and over 20 interconnecting pipelines inside (Figure 1).

The study adopted all-hazards, all-threats approach by analysing in detail natural hazards likely to happen in the area (e.g. forest fire, extreme cold, hurricane), external events (loss of power), technical failures (e.g. pipeline corrosion, compressor failure, valve inadvertent closure), human errors (e.g. operators' actions, unauthorized ground works), intentional human malicious actions on site (terrorist acts) and cyber-attacks. The methodological basis for the study was HAZID type process [1]. The study used the results from gas network modelling for quantification of consequences in terms of security of supply in the whole gas network and in particular the pipelines inside the hub.

In the risk assessment study, the following methodological steps were performed:

- Step 1: Identification of hazards and threats
- Step 2: Screening of hazards and threats for the area under study and historical failure data analysis
- Step 3: HAZID process with input from the modelling task; Consequence (severity) and likelihood estimation
- Step 4: Risk matrix build-up
- Step 5: Findings and recommendations

**Figure 1.** Layout of the pipeline hub.

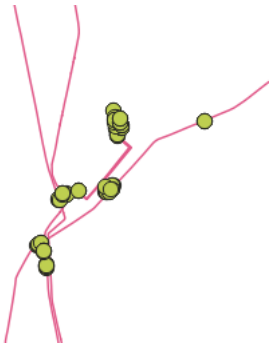

*Source:* SecureGas project, 2021.

The hydraulic gas network models developed were based on steady state gas flow conditions. Two models were developed and both models were using similar, but not the same computational engines that allowed better and more precise analysis as well as cross-check of the obtained results. All data were obtained directly from the network operator. Calculations were performed at extreme scenarios, unfavourable for the gas supply situations in order to test the preparedness of the network for critical disruptions. Therefore, the result interpretation must consider the approach taken. The major extreme conditions are the following:

- Peak demand in the network
- Peak demand at export points
- Minimum contractual inlet pressure at entry points

The network used for simulations contains 430 pipeline segments, 69 gas consumer nodes, 3 gas sources, 9 pressure reducers and 2 compressor stations. The network complexity is demonstrated by a section of the gas network graph in Figure 2.

**Figure 2.** Network graph illustration.

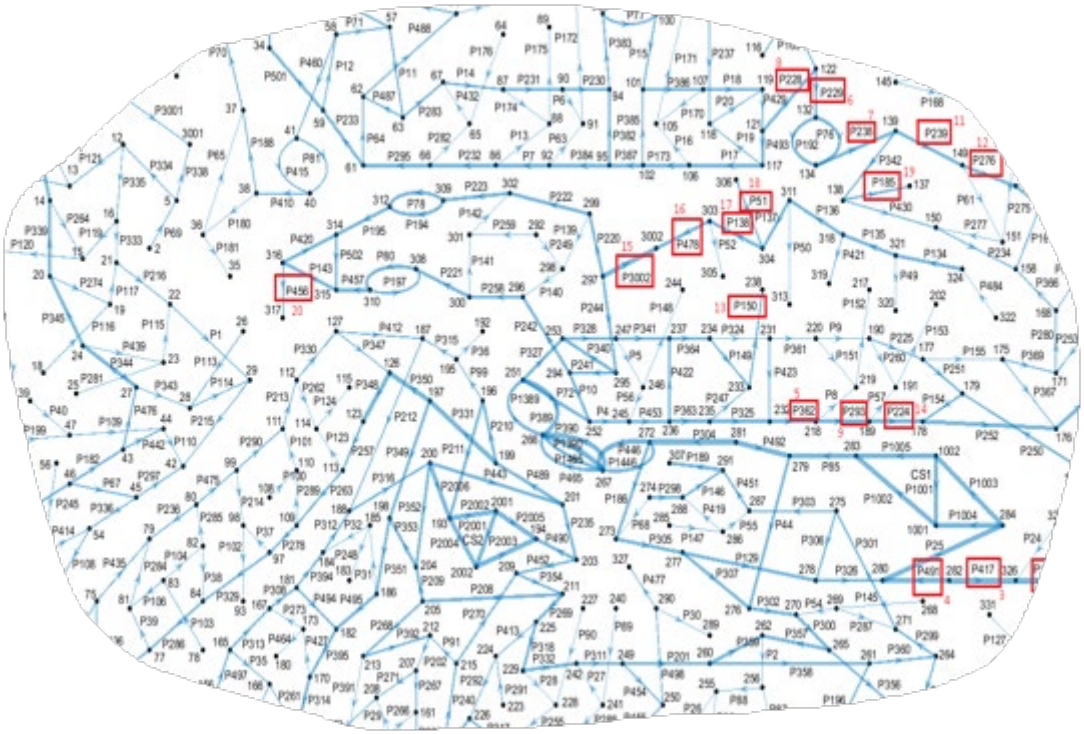

*Source:* SecureGas project, 2021.

The computational engine of the modelling tool is described in SecureGas project deliverables and open references [2, 3]. The pipeline importance ranking was obtained by computing non-supplied gas volume in the whole network (local consumers and exports) in case of the following two disruptions scenarios:

- Disconnecting from the network each single pipeline segment (427 total cases, called N-1 cases)
- Disconnecting from the network two pipeline segments (181902 total cases, called N-2 cases)

Computationally this task is very heavy; therefore, some simplifications were applied.

The modelling results identify the most important pipeline sections of the hub for the security of supply in the whole network. Six single segments were identified under N-1 disruption scenario (unsupplied gas volume ranging from 39 to 5%) and eight double segment disruptions were identified from N-2 disruption scenarios (unsupplied gas volume ranging from 76 to 22%). The unsupplied gas is computed as a total peak maximum demand in the whole network. The maximum demand is a rather conservative number; therefore, all estimates must be considered as conservative, i.e. the situation can hardly become more critical than estimated by the calculations.

The final step in the process of risk assessment was to construct a risk matrix which is based on the hazard evaluation table (not presented in the paper). The risk matrix for the pipeline hub is shown as illustration in Figure 3.

**Figure 3.** Risk matrix visualisation of a pipeline hub.

| Severity of consequence | | | | | | |
|---|---|---|---|---|---|---|
| Very High | VH | | | | | |
| High | H | | N27, P1 | | | |
| Medium | M | N6, N30 | N1, N14, H3, I1, I7, I8 | | N12, E1, E5 | |
| Low | L | N22, N29, E7 | N2, N10, N11, N21, N24, N26, P3, P4, P5, P6, P7, P8, H1, H2, H4, H5, I2, I3, I4, I5, I6, I9 | N7, N8, N9, N15, N18, N23, N25, E2, E4 | N19, N28 | N4, N5, N16, N17 |
| Very low | VL | E6, P2 | E3 | | N3, N13, N20 | |
| | | Likelihood | | | | |
| | | VL | L | M | H | VH |
| | | Rare | Unlikely | Credible | Probable | Frequent |

The study concluded with 10 findings and 13 recommendations for the operator for further improvements.

## Acknowledgements

The work was funded by SecureGas project (grant agreement number No. 833017, https://www.securegas-project.eu/) under EU Horizon 2020 research programme.

## References


1. Lees, F., Lees' Loss Prevention in the Process Industries: Hazard Identification, Assessment and Control: 4th Edition, Butterworth-Heinemann, 2012.
2. Zalitis, I., Dolgicers, A., Zemite, L., Ganter, S., Kopustinskas, V., Vamanu, B., Bode, I. and Kozadajevs, J. "A Linearized Numerical Solution for Steady-State Simulations of Gas Networks", Latvian Journal of Physics and Technical Sciences, 58(3), 2021, pp.137-153. https://doi.org/10.2478/lpts-2021-0022.
3. Ganter, S., Srivastava, K., Vogelbacher, G., Finger, J., Vamanu, B., Kopustinskas, V., Haering, I. and Stolz, A. "Towards Risk and Resilience Quantification of Gas Networks based on Numerical Simulation and Statistical Event Assessment", In: Baraldi, P., et al. (eds.) *Proceedings of the 30th European Safety and Reliability Conference and the 15th Probabilistic Safety Assessment and Management Conference*, Research Publishing, Singapore. ISBN 978-981-14-8593-0, pp. 3971-3978.

# 3 Conclusions

The 60th Seminar served as a closing event for the ESReDA project group, entitled 'Resilience Engineering and Modelling of Networked Infrastructure'. Since the start of its activities in 2018, the project group has organised a number of meetings and delivered a book, Modelling the Resilience of Infrastructure Networks, published by DNV in 2021. The book can be purchased by contacting ESReDA at www.esreda.org

Although this Seminar was the closing event of the project group, research in infrastructure resilience needs to continue. The recent EC proposal of the Directive on resilience of critical entities indicates that the term "resilience" becomes a part of legislation. This will foster the need to develop a methodological framework in which resilience plays the key role.

We believe that the work done in resilience so far marks only the beginning of a new field of research, tightly linked to reliability and risk analysis, assessment and management. In fact, resilience goes beyond the scope of risk assessment and touches the field of self-repairable and non-stop service systems. As when the first time the term resilience was used in ecology, it is about survivability under changing environmental conditions and variety of shocks and threats. This paradigm perfectly captures the times that we are living in today.

We envisage the need to continue this work on resilience within another ESReDA project group. We expect to launch a new project group in the second half of 2022 at the latest. Therefore we invite all interested institutions to contact us to develop a joint plan for future work in resilience.

## Annexes

### Annex 1. Seminar Programme

*Tuesday 3rd May 2022*
*Project Group Meetings, plus ESReDA Board of Directors Meeting*

| Day 1 – Wednesday 4th May 2022 | | | Day 2 – Thursday 5th May 2022 | |
|---|---|---|---|---|
| 08h45 - 09h15 | Coffee and registration | | 08h45 – 09h15 | Welcome coffee |
| 09h15 - 10h00 | Welcome | | 09h15 – 10h00 | Keynote Lecture 2 |
| 10h00 - 10h45 | Keynote Lecture 1 | | 10h00 – 11h00 | Session 4 |
| 10h45 - 11h20 | Coffee break | | 11h00 – 11h30 | Coffee break |
| 11h20 - 12h20 | Session 1 | | 11h30 – 12h30 | Session 5 |
| 12h20 - 14h00 | Lunch | | 12h30 – 14h00 | Lunch |
| 14h00 - 15h40 | Session 2 | | 14h00 – 15h00 | Session 6 |
| 15h40 - 16h00 | Coffee break | | 15h00 – 15h20 | Seminar close |
| 16h00 - 17h00 | Session 3 | | | |
| 17h00 - 18h30 | ESReDA General Assembly | | | |
| 20h00 | Seminar dinner | | | |

*Location:*
**GreEN-ER Building**
21 Avenue des Martyrs
38031 GRENOBLE CEDEX 1
*Access : Tramway B, direction "Oxford", station Marie-Louise Paris CEA.*


# Scope of the seminar

In resilience engineering, failure is an inability to adapt to disruptions rather than a breakdown or malfunction, as is commonly the case in traditional risk analysis. Resilience encompasses the phases of avoiding (being proactive against the occurrence or consequences), absorbing (withstanding without reconfiguration), adapting to (reconfiguring) and recovering from disruptions (restoring the pre-disruption state as closely as possible).

Modern engineering systems continually increase in size and complexity, whilst also becoming more distributed, integrated, and autonomous, all of which can lead to many safety and risk management challenges. There is a constant, relentless pursuit of cheaper, more efficient, optimised performance, which can inadvertently introduce system vulnerabilities and potentially erode safety margins. Threats constantly evolve and emerge, with recent years seeing numerous failures of aging infrastructure, catastrophic events following natural disasters or due to the effects of climate change, and major disruption caused by deliberate acts such as terrorism and cyber or hybrid attacks. Increasingly automated and software-intensive infrastructure can struggle to adapt to unanticipated situations and can hence be extremely vulnerable to emergent threats. Coupling this with the growing complexity and interdependencies between infrastructure assets, it is clear that there is an urgent need for new approaches to protect these critical systems.

Many of the critical infrastructure systems on which modern society is so dependent are networks. These include transport networks (rail, metro, highway, air traffic and shipping routes), utilities (electricity, gas, water) and communications (mobile phone, land line phones, internet). The disruption of such systems can have a big impact on the communities that they serve. Such critical systems must be resilient. It is important to understand the characteristics of such networks and the methods that exist to model their resilience and to identify their weaknesses so that efforts are targeted at those places that will most protect network performance.

The 60th ESReDA seminar will be a forum for exploring these and other related issues. We aim to discuss theories, concepts, and experiences of methods for improved network resilience. Authors are invited to present their research and experience and discuss challenges in enhancing resilience through modelling. We are encouraging new ideas, case studies and cross-sectoral and inter-disciplinary research on the theme of network resilience. This seminar will bring together researchers, practitioners, specialists and decision-makers to discuss strategies and practical experiences.

## Target groups and domains of application

Papers or extended abstracts for the seminar have been invited from various stakeholders, from practitioners to researchers (industrialists, regulators, safety boards, universities, R&D organisations, engineering contractors and consultants, training specialists) and address different sectors:

- Transport: rail, road, air and maritime
- Critical infrastructure: electricity, water, telecommunications, information systems
- Urban planning and management
- Public sector and government.

This seminar is aimed at addressing resilience due to different threats, such as failures of aging infrastructure, natural disasters and climate change, intentional attacks (cyber-security and terrorism), and emerging threats, met by different industries, critical infrastructures and urban settlements.


# Day 1: Wednesday 4th May, 2022

| | |
|---|---|
| 08h45-09h15 | **Registration and welcome coffee** |
| 09h15-10h00 | Welcome to participants from:<br>**Mohamed Eid** - President of ESReDA<br>**Julien Baroth** - Université Grenoble Alpes,<br>**Delphine Riu** – Head of Grenoble-INP Ense³ Engineering School<br>**Didier Georges** – Head of cross-disciplinary project RISK@UGA<br>**Rasa Remenyte-Prescott** – ESReDA Resilience PG Lead &Chairperson of the Conference |
| 10h00-10h45 | **Keynote lecture:**<br>**"Risk and Resilience of Infrastructure Systems"**<br>by Anne Barros, CentraleSupélec, France<br>Chair: Stefan Schauer |
| 10h45-11h20 | **Coffee Break** |
| 11h20-12h20 | **Session 1: Resilience of Electrical Networks**<br>Chair: Vytis Kopustinskas |
| *1h*<br><br>*(20' each including questions)* | **"Improved Modeling of Fault Propagation, Isolation, and Fast Service Restoration in Smart Grids",** (paper 8)<br>by Youba Nait Belaid, Yiping Fang, Zhiguo Zeng, Anne Barros; CentraleSupélec, France |
| | **"Bayesian Updating and Reliability Analysis for Nuclear Containment Buildings",** (paper 5)<br>by Donatien Rossat*, Julien Baroth*, Frédéric Dufour*, Matthieu Briffaut*, Benoît Masson**, Alexandre Monteil**, Sylvie Michel-Ponnelle**; *Grenoble INP, France; **EDF, France. |
| | **"Improving Power System Frequency Response with a Novel Load Shedding Method",** (paper 2)<br>by Andrejs Utans*, Antans Sauhats*, Laila Zemite*, Dimitrijs Guzs**; *RTU, Latvia; **AST, Latvia (Virtual Presentation) |
| 12h20-14h00 | **Lunch** |
| 14h00-15h40 | **Session 2: Infrastructure Resilience to Natural Hazards**<br>Chair: Christophe Berenguer |
| *1h40mn (20' each including questions)* | **"A Simulation Approach for Evaluating Interventions to Improve the Resilience of Transport Networks Against Climate-Induced Hazards",** (paper 1)<br>by Hossein Nasrazadani*, Bryan Adey*, Saviz Moghtadernejad* and Alice Alipour**; *ETH Zurich, Switzerland; **Iowa State University, USA |

| | |
|---|---|
| | **"The prevention of NATECH risks on the Italian territory: the importance of the Safety Management System",** (paper 16)<br>by Romualdo Marrazzo, Fabrizio Vazzana; Ispra, Italy *(Virtual Presentation)* |
| | **"An Overview of Causes of Landslides and Their Impacts on Transport Networks",** (paper 14)<br>by Kwan Ben Sim*, Min Lee Lee*, Rasa Remenyte-Prescott**, Soon Yee Wong*; *University of Nottingham, Malaysia; **University of Nottingham, UK |
| | **"Risk and Resilience in Practice: A Methodology for Implementation of Mountain Risk Management and Prevention Strategy (StePRiM)"**, (paper 10)<br>by Jean-Marc Tacnet*, Simon Carladous**, François Sassus**, Eva Ripert***, Patrick Lagleize***, Ariane Stephan****, Catherine Calmet**** *Grenoble INRAE, France; **Office National des Forêts, France; ***Communauté de Communes Pyrénées Haut Garonnaises, France; ****Ministère de la Transition Ecologique, France |
| | **"Decision-Aiding Towards Improved Resilience of a Deteriorating Debris Retention Dam Subject to Maintenance Strategies"**, (paper 11)<br>by Nour Chahrour*, Guillaume Piton**, Jean-Marc Tacnet**, Christophe Bérenguer*; *Grenoble INP, France; **Grenoble INRAE, France |
| 15h40-16h00 | **Coffee Break** |
| 16h00-17h00 | **Session 3: Resilience Evaluation**<br>Chair: Anne Barros |
| *1h*<br>*(20' each including questions)* | **"Definition and Nature of Resilience"**, (paper 3)<br>by Yves Merian; IMdR, France |
| | **"Study of a degrading system with stochastic arrival intensity subject to CBM",** (paper 9)<br>by Lucia Bautista Bárcena, Inmaculada T. Castro, Luis Landesa Porras; University of Extremadura, Spain |
| | **"A Simulation-driven Tool for Supporting Risk and Resilience Assessment in Cities",** (paper 12)<br>by Stefan Schauer*, Thomas Hiebl**, Stefan Rass***, Sandra König*, Martin Latzenhofer*; *AIT, Austria; **Cubido Business Solutions, Austria; ***Universitaet Klagenfurt, Austria. |
| 17h00-18h30 | **ESReDA General Assembly** |
| 19h00 | **Seminar Dinner – Access by cable car and a short walk**<br>Meeting point at the Bastille cable car, Quai Stéphane Jay, 38000 Grenoble<br>*Tramway B station Hubert Dubedout-Maison du Tourisme; take the direction on foot of the place Grenette, pass under the porch at the beginning of the street Montorge and cross the park of the Jardin de Ville towards the river Isere and the cable car station*).<br><br>Restaurant at *Le Pèr'Gras*<br>90, Chemin de La Bastille<br>38700 La Tronche<br>Mail: restaurant@pergras.fr<br>T. 04 76 42 09 47 |


# Day 2: Thursday 5th May 2022

| | |
|---|---|
| 08h45-09h15 | **Welcome coffee** |
| 09h15-10h00 | **Keynote lecture:**<br>**"The Resilience Performance Assessment (RPA): A Framework and Decision-Making Tool to Evaluate and Follow the Resilience of Infrastructures and Territories"**<br>by Philippe Sohouenou, Resalliance, France<br>Chair: Mohamed Eid |
| 10h00-11h00 | **Session 4: Resilience of Transport Networks and Smart Cities**<br>Chair: Bryan Adey |
| *1h*<br>*(20' each including questions)* | **"Resilience and Capacity in Networks - A comparative Investigation of Rail Transport Networks and Electric Power Grids",** (paper 18)<br>by Pierre Dersin; Luleå University of Technology, Sweden |
| | **"Simulation Supported Bayesian Network Approach for Performance Assessment of Complex Bridge Network Systems"**, (paper 6)<br>by Mohsen Songhori, Claudia Fecarotti, Geert-Jan van Houtum; Eindhoven University of Technology, The Netherlands |
| | **"A Study on Resilience Index for Transport Infrastructure in China"**, (paper 20)<br>by Chao Yang*, Rasa Remenyte-Prescott**; *China Transportation Institute, Tongji University, China; **University of Nottingham, UK |
| 11h00-11h30 | **Coffee Break** |
| 11h30-12h30 | **Session 5: Resilience of Utility Networks**<br>Chair: Julien Baroth |
| *1h*<br>*(20' each including questions)* | **"Real-time Monitoring of Gas Pipelines with Leak Detection and Localization via a Receding Horizon Observer",** (paper 4)<br>by Didier Georges; Grenoble INP, France |
| | **"Gas Network Modelling to Support Pipeline Hub Area Risk Assessment",** (paper 21)<br>by Vytis Kopustinskas*, Bogdan Vamanu**, Sebastian Ganter***, Jörg Finger***, Ivo Häring***, Ivars Zalitis****, Laila Zemite****; *European Commission, Joint Research Centre (JRC), Ispra, Italy; **Horia Hulubei National Institute of Physics and Nuclear Engineering, Romania; ***Fraunhofer Institute for High-Speed Dynamics, Germany; ****Riga Technical University, Institute of Power Engineering, Latvia |
| | **"Influence of Availability Transients on Network Resilience"**, (paper 17)<br>by Christian Tanguy; Orange Labs, France |
| 12h30-14h00 | **Lunch** |

| | |
|---|---|
| 14h00-15h00 | **Session 6: Resilience of Infrastructure Networks**<br>Chair: Jean-Marc Tacnet |
| *1h*<br>*(20' each including questions)* | **"Applying Deep Reinforcement Learning to Improve the Reliability of an Infrastructure Network",** (paper 7)<br>by Jose Carlos Hernandez Azucena, Haitao Liao, Henley Wells, Kelly Sullivan, Ed Pohl; University of Arkansas, USA. (Virtual Presentation) |
| | **"Interdependencies of Infrastructures in Smart Cities and Advanced Topological Approach for the Resiliency of Coupled Systems - Example of Power and ICT systems",** (paper 19)<br>by Raphael Caire; Grenoble INP, France. |
| | **"Risk Management with Multi-Categorical Risk Assessment"**, (paper 13)<br>by Sandra König*, Stefan Schauer*, Mona Soroudi**, Ili Ko**, Paraic Caroll**, Daniel McCrum**; *AIT, Austria; **University College Dublin, Ireland |
| 15h00-15h20 | **Conference Closure** |

**Book of abstracts**
**Link to abstracts**

…or scan the QR code:

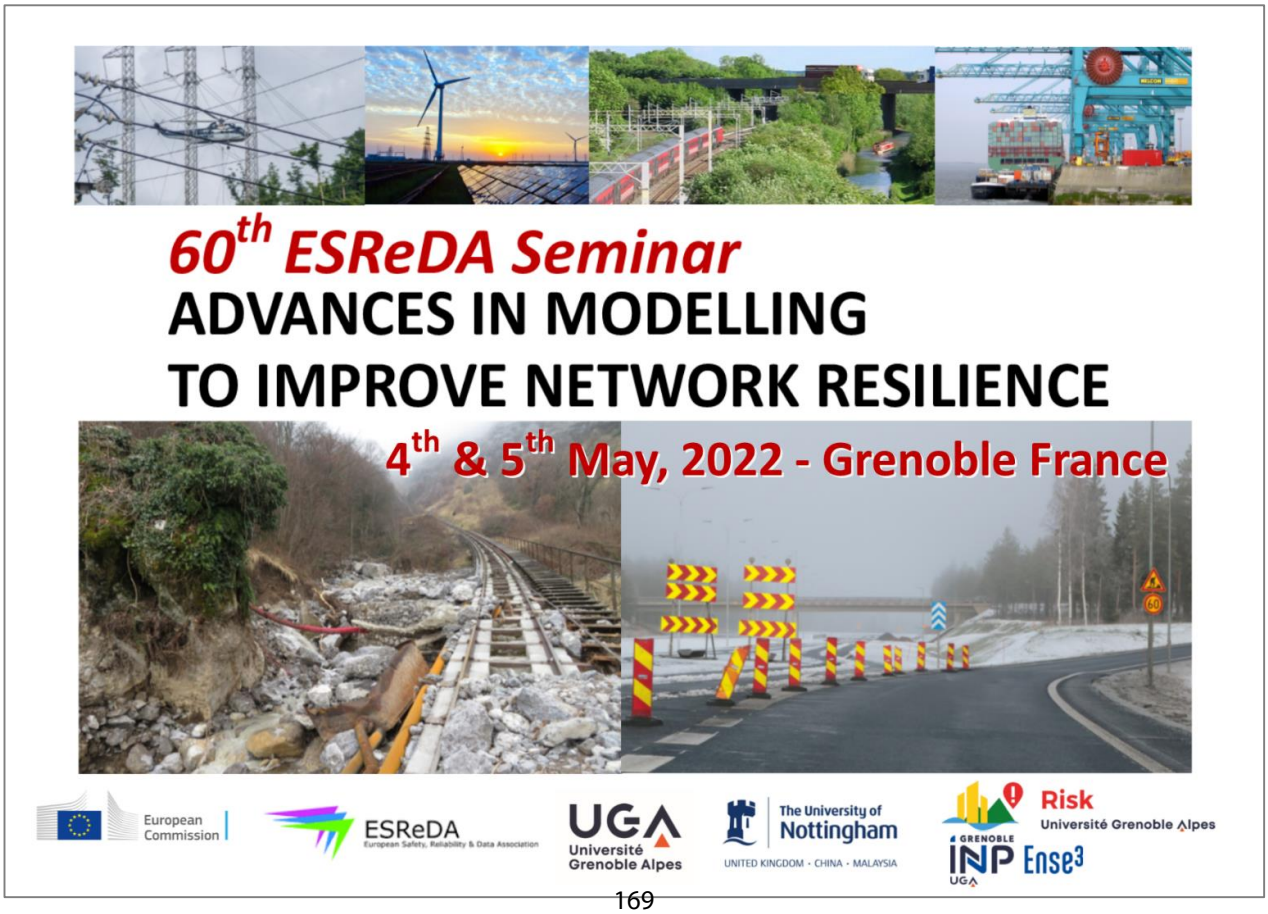


**Seminar Organization**
The Seminar is jointly organised by ESReDA and University Grenoble Alpes

**Location**
Grenoble, GreEn-ER building

**Chairperson of the Seminar**

| | |
|---|---|
| REMENYTE-PRESCOTT Rasa | (University of Nottingham, UK) |

**Technical Programme Committee (TPC)**

| | |
|---|---|
| ANDREWS John | (University of Nottingham, UK) |
| BAROTH Julien | (Université Grenoble Alpes, 3SR, France) |
| BASTEN Rob | (Eindhoven University of Technology, Netherlands) |
| BERENGUER Christophe | (Université Grenoble Alpes, GIPSA-lab, France) |
| DUNNETT Sarah | (Loughborough University, UK) |
| EID Mohamed | (ESReDA President, Consultant at RiskLyse, France) |
| FECAROTTI Claudia | (Eindhoven University of Technology, Netherlands) |
| JACKSON Lisa | (Loughborough University, UK) |
| JUDEK Clement | (IMDR, France) |
| KOPUSTINSKAS Vytis | (European Commission, Joint Research Centre – Ispra, Italy) |
| LANNOY Andre | (IMDR, France) |
| LIU Yiliu | (Norwegian University of Science and Technology, Norway) |
| OTTENBURGER Sadeeb Simon | (Karlsruhe Institute of Technology - KIT, Germany) |
| POHL Ed | (University of Arkansas, USA) |
| SARUNIENE Inga | (Lithuanian Energy Institute, LEI) |
| SCHAUER Stefan | (Center for Digital Safety & Security, Austrian Institute of Technology, Austria) |
| TACNET Jean Marc | (Université Grenoble Alpes, INRAE, ETNA, France) |
| TUBIS Agnieszka | (Wroclaw University of Science and Technology, Poland) |
| UTANS Andrejs | (Riga Technical University, Latvia) |
| VAN HOUTUM Geert-Jan | (Eindhoven University of Technology, Netherlands) |
| YUSTA Jose Maria | (University of Zaragoza, Spain) |

**Opening of the Seminar:** **4th May 2022**
**Closing of the Seminar:** **5th May 2022**

**Local Organization Committee:**

| | |
|---|---|
| BAROTH Julien | (UGA) – Local Organizing Committee chairperson |
| BERENGUER Christophe | (GINP) |
| CHAHROUR Nour | (INRAE) |
| TACNET Jean-Marc | (INRAE) |
| PERRIER Sylvie | (UGA) |

**Annex 2. Authors' list**

**GETTING IN TOUCH WITH THE EU**

**In person**

All over the European Union there are hundreds of Europe Direct centres. You can find the address of the centre nearest you online (european-union.europa.eu/contact-eu/meet-us_en).

**On the phone or in writing**

Europe Direct is a service that answers your questions about the European Union. You can contact this service:

— by freephone: 00 800 6 7 8 9 10 11 (certain operators may charge for these calls),

— at the following standard number: +32 22999696,

— via the following form: european-union.europa.eu/contact-eu/write-us_en.

**FINDING INFORMATION ABOUT THE EU**

**Online**

Information about the European Union in all the official languages of the EU is available on the Europa website (european-union.europa.eu).

**EU publications**

You can view or order EU publications at op.europa.eu/en/publications. Multiple copies of free publications can be obtained by contacting Europe Direct or your local documentation centre (european-union.europa.eu/contact-eu/meet-us_en).

**EU law and related documents**

For access to legal information from the EU, including all EU law since 1951 in all the official language versions, go to EUR-Lex (eur-lex.europa.eu).

**Open data from the EU**

The portal data.europa.eu provides access to open datasets from the EU institutions, bodies and agencies. These can be downloaded and reused for free, for both commercial and non-commercial purposes. The portal also provides access to a wealth of datasets from European countries.

## The European Commission's science and knowledge service

Joint Research Centre

### JRC Mission

As the science and knowledge service of the European Commission, the Joint Research Centre's mission is to support EU policies with independent evidence throughout the whole policy cycle.

**EU Science Hub**
joint-research-centre.ec.europa.eu

@EU_ScienceHub

EU Science Hub - Joint Research Centre

EU Science, Research and Innovation

EU Science Hub

EU Science

Publications Office
of the European Union